20536502

MICHIGAN STATE UNIVERSITY LIBRARIES

3 1293 00536 3910

LIBRARY
Michigan State
University

This is to certify that the

dissertation entitled

Geochemical Gradients in the Topopah
Spring Member of the Paintbrush Tuff:
Evidence for Eruption Across
a Magmatic Interface

presented by

Benjamin Charles Schuraytz

has been accepted towards fulfillment
of the requirements for

Doctoral degree in Geology

Thomas A. Vogel
Major professor

Date 9/16/87

MSU is an Affirmative Action/Equal Opportunity Institution O-12771

MSU
LIBRARIES

RETURNING MATERIALS:
Place in book drop to remove this checkout from your record. FINES will be charged if book is returned after the date stamped below.

GEOCHEMICAL GRADIENTS IN THE TOPOPAH SPRING MEMBER OF THE PAINTBRUSH TUFF: EVIDENCE FOR ERUPTION ACROSS A MAGMATIC INTERFACE

By

Benjamin Charles Schuraytz

A DISSERTATION

Submitted to
Michigan State University
in partial fulfillment of the requirements
for the degree of

DOCTOR OF PHILOSOPHY

Department of Geological Sciences

1988

ABSTRACT

GEOCHEMICAL GRADIENTS IN THE TOPOPAH SPRING MEMBER
OF THE PAINTBRUSH TUFF:
EVIDENCE FOR ERUPTION ACROSS A MAGMATIC INTERFACE

By

Benjamin Charles Schuraytz

The Topopah Spring Member of the Paintbrush Tuff, southern Nevada, is a classic example of a compositionally zoned ash-flow sheet that is inferred to have resulted from eruption of a compositionally zoned magma body. Geochemical and petrographic analyses of whole-rock tuff samples indicate that the base of the ash-flow sheet and the dominant volume of erupted material is composed of crystal-poor high-silica rhyolite, with a gradational transition into overlying crystal-rich quartz latite. These compositional variations are consistent with a model of progressive eruption of a stratified magma body in which relatively cooler, crystal-poor high-silica rhyolitic magma overlay hotter, crystal-rich quartz latitic magma.

Major and trace element chemical analyses of glassy pumice samples and microprobe analyses of coexisting silicate and oxide phenocrysts from within the pumice samples provide closer approximations to the chemical and thermal gradients within the inferred magma body. The magmatic gradients inferred from these data indicate that the transition from high-silica rhyolitic to quartz latitic magma within the chamber was abrupt, rather than gradational, with a distinct liquid-liquid interface separating the contrasting magmas.

Benjamin C. Schuraytz

Compositionally and texturally distinct pumice types are present throughout the ash-flow sheet. The degree of heterogeneity within and among the pumice samples increases with increasing stratigraphic height, and becomes most pronounced in the uppermost quartz latite, where the chemical variability among the pumice samples is as great as that of the entire ash-flow sheet.

The observed heterogeneities among the pumice samples of the Topopah Spring Member are consistent with predictions of fluid dynamic models in which the velocity field developed near the entrance region of the vents results in simultaneous withdrawal of magma from a progressively greater lateral and vertical extent within the chamber, thereby forming a pyroclastic deposit that becomes increasingly heterogeneous with increasing stratigraphic height. The abrupt transition to chemically variable pumice types, dominated by those of quartz latitic composition, implies that the interface between the magma layers remained relatively stable until drawdown breached the interface and preferentially erupted higher temperature, more mafic magma along with subordinate amounts of the incompletely exhausted high-silica rhyolitic magma.

ACKNOWLEDGMENTS

I thank my supervisor, Thomas Vogel, who is largely responsible for initiating my interest in igneous processes and my commitment to geologic research, and to whom I owe a debt of gratitude for his continued encouragement and support as a teacher, a colleague, and a friend. Special thanks are extended to Kazuya Fujita who spared no effort in his guidance and support, and whose enthusiasm for science and teaching, even in the wee hours of the morning, will always be remembered and appreciated. I am especially grateful to my committee members, Thomas Vogel, Kazuya Fujita, John Wilband, and David Long, for their helpful reviews and criticisms of this manuscript. I also wish to thank William Cambray for his support through the Department of Geological Sciences at Michigan State University and for sharing his keen field observations during my undergraduate years.

Financial support for this research was provided by the Nevada Nuclear Waste Storage Investigation Project and the Nuclear Test Containment Program at Lawrence Livermore National Laboratory. This was made possible through the efforts and interest of Leland Younker, to whom I am particularly grateful for his insightful discussions throughout this research project. I also wish to acknowledge the following LLNL personnel: Frederick Ryerson and Kevin Knauss for assistance with the electron microprobe analyses, Robert Heft for providing INAA, and Jan Brown for assistance with sample preparation.

I am especially grateful to Frank Byers, Jr. for convincing me to focus my dissertation research on the Topopah Spring Tuff, and for sharing his vast experience during several excursions to the southwestern Nevada volcanic field during my tenure as research assistant at Los Alamos National Laboratory. I also wish to thank LANL scientists David Broxton and Richard Warren, and Robert Scott of the U.S.G.S. for many stimulating and helpful discussions in the field, and Wayne Morris of LANL for financial support during the summer of 1985.

Many people were extremely helpful to me during my studies at Michigan State: I am indebted to John Wilband and Bill Monaghan for their expert assistance with computer software; I thank Loretta Knutson, Cathy Caswell, and Mona Kindell for their skill in cutting through red tape, and Diane Baclawski for assistance in the library. I benefited greatly from discussions with my fellow petrologists, Tim Flood, Jim Mills, Tim Rose, Carolyn Rutland, and in particular, Steve Mattson, to whom I owe many thanks. I also benefited from interactions with my fellow students and friends over the years, in particular, Susan Bullen, Bud Moyer, Jim Newberry, Dave Cook, Cindy McMullen, and Soo-Meen Wee. I extend my deepest appreciation to my dear friend Frederick Kaplan.

I am grateful to Dan and Sue Steinberg for their warm hospitality during my visits to Livermore, and to Debra Steinberg for her inspiration at critical moments.

Most of all I thank my parents, Irving and Aline Schuraytz, and my family, for their unfailing encouragement and support, and for instilling in me the importance of a good education.

TABLE OF CONTENTS

LIST OF TABLES

LIST OF FIGURES

INTRODUCTION

The common occurrence of systematic compositional and mineralogical zonations within ash-flow sheets provides strong evidence that their source magma bodies were chemically and thermally zoned (for reviews see Smith, 1979; Hildreth, 1981; Mahood, 1981; Bacon et al., 1981; Crecraft et al., 1981; Baker and McBirney, 1985). Recently, interest in how zoned magmas evolve and erupt has focused on the fluid dynamic aspects of magma chambers. The results of scaled laboratory experiments using aqueous solutions have been used to suggest that the interfacial effects of compositionally and thermally contrasting fluid layers may be important in the differentiation of magmas (Huppert and Sparks, 1984; Sparks et al., 1984; Huppert et al., 1984; McBirney et al., 1985; Baker and McBirney, 1985). Theoretical studies of magma withdrawal during eruption indicate that magma from different depths within the chamber will erupt simultaneously and that ash-flow stratigraphy will not simply represent the inverse of the zonations within the magma body (Blake, 1981; Spera, 1984). The purpose of this study is to evaluate key assumptions and predictions of these fluid dynamic models using geochemical data obtained from pumice samples collected from a well known zoned ash-flow sheet -- the Topopah Spring Member of the Paintbrush Tuff. The specific questions addressed herein are: (1) To what degree does the compositional zonation in the Topopah Spring Member represent the inverse of the compositional zonation in the magma body? (2) Was the zonation in the magma body characterized by continuous gradients within a single liquid or by discontinuous gradients within discrete liquid layers separated by a distinct interface. A major emphasis of this study is placed on the heterogeneities among pumice samples that have been observed within all stratigraphic horizons throughout the ash-flow sheet. With few exceptions (Lipman, 1967; Byers et al., 1968; Noble et al., 1969; Rose et al., 1979; Wright and Walker, 1977; Fridrich and Mahood, 1987), this important feature has received sparse attention in previous studies.

It has long been realized that ash-flow tuffs and associated calderas result from the explosive eruption and partial evacuation of large volumes of magma at single points in time (Williams, 1941; Smith, 1960) and that the chemical and mineralogical variability of these tuffs may be used to infer pre-eruptive magmatic conditions. Among the first to establish this premise was the study by Lipman et al. (1966) of the Topopah Spring Member of the Paintbrush Tuff. A notable feature of this voluminous ash-flow sheet is the systematic variation in composition with stratigraphic height. The zonation from nearly aphyric high-silica rhyolite upward into phenocryst-rich quartz latite was first described by Lipman et al. (1966) and interpreted by them to reflect the compositional zonation of magma in the source chamber prior to eruption.

Subsequent studies of this (Noble and Hedge, 1969; Lipman, 1971; Lipman and Friedman, 1975) and other compositionally variable ash-flow sheets have provided a considerable base of chemical, isotopic, and mineralogical data (for reviews see Hildreth, 1981; Baker and McBirney, 1985). This information has been used to estimate compositional and thermal gradients inferred to be present in the magma chambers. It is these inferred gradients that are fundamental in evaluating various magmatic differentiation mechanisms thought to operate in high-level magmatic systems. The importance of precise reconstruction of the eruptive sequence (and the inferred thermo-chemical gradients) cannot be overemphasized if quantitative tests of differentiation and eruptive mechanisms are to lead to meaningful conclusions.

It is axiomatic that a stratigraphic sequence preserves depositional order. This fact combined with the progressive compositional variation observed in ash-flow sheets promotes the tacit assumption that "These systems are normally tapped from the top down." (Smith, 1979, p. 18). That is, the lowermost portions of the erupted sequence are derived from the upper part of the magma chamber and overlying products are derived from successively deeper levels. For example, Cox et al. (1979) state that "It is essential, in order that the evidence be preserved, that the eruption is not accompanied by excessive mixing of magma from different parts of the chamber. That zoned magma chamber sequences exist at all implies also a lack of convection in the chamber." (Cox et al., 1979, p. 273). This is undoubtedly true with regard to large scale convection, and it should be noted that the authors of the above statement were aware of additional complexities and limitations (Cox et al., 1979, p. 275).

The complexities and limitations referred to above are discussed in a detailed study of an ash-flow sheet from the Aso caldera, Japan (Lipman, 1967). Lipman demonstrated that bulk compositions of these tuffs deviate significantly from original magmatic compositions due to eruption, emplacement, and post-emplacement processes. He cited as evidence both chemical and mineralogical heterogeneities within and among individual pumice samples and noted that similar complexities characterize ash-flow tuffs in southwestern Nevada and are probably widespread in other ash-flow fields as well. These features, and the conclusions Lipman drew from them, clearly indicate the need to understand the dynamic processes involved in ash-flow eruptions in order to properly assess the primary character of their quenched products.

Recent interest in the fluid-dynamical processes involved in high-level magmatic systems has prompted research and the development of models dealing with input and replenishment of magma (Eichelberger, 1980; Huppert and Sparks, 1980; Huppert and Turner, 1981; Huppert et al., 1982b, 1984), internal magmatic differentiation processes (Chen and Turner, 1980; Huppert et al., 1982a; McBirney and Noyes, 1979; Sparks et al., 1984; Turner and Gustafson, 1981; Turner et al., 1983; McBirney et al., 1985; Baker and McBirney, 1985), and dynamics associated with eruption and magma withdrawal (Wilson et al., 1980; Blake, 1981; Schuraytz et al., 1983; Blake and Ivey, 1986a, b; Spera, 1983, 1984; Spera et al., 1986; Wohletz et al., 1984). The applicability and refinement of these experimental and theoretical models to real systems, however, will require continual geological observation and testing with field evidence.

The Topopah Spring Member of the Paintbrush Tuff is a classic example of a compositionally zoned ash-flow sheet for which the field relations are well constrained and for which substantial documentation of characteristic features is available. This study presents new major and trace element chemical analyses and microprobe phenocryst analyses, primarily from samples of glassy pumice. The purpose of these analyses is to determine if there were continuous gradients or discrete, discontinuous zones in the magma body that erupted the Topopah Spring Member. A recurring theme throughout this thesis is the nearly ubiquitous occurrence of chemical heterogeneities among individual pumice samples. While this feature may be a hindrance in that it may obscure primary magmatic variations, it also provides information that can be used to evaluate dynamic processes associated with petrogenesis.

GENERAL GEOLOGIC RELATIONS

The Topopah Spring Member (Figure 1) is the lowermost formal unit of the Paintbrush Tuff, a major effusive sequence associated with the Timber Mountain-Oasis Valley caldera complex in southern Nye County, Nevada (Byers et al., 1976). This caldera complex is a major part of the southwestern Nevada volcanic field which was active during the upper Tertiary period. Eruptive activity occurred contemporaneously with extensional basin-range normal faulting (Christiansen et al.,1965; Lipman et al., 1966; Ekren et al., 1968; Christiansen et al., 1977). The Timber Mountain-Oasis Valley caldera complex is comprised of four overlapping and superposed volcanic centers (Byers et al., 1976), recording evidence of repeated eruptive activity of a high-level magmatic system from 16 to 9 m.y. ago (Kistler, 1968; Marvin et al., 1970).

The Paintbrush Tuff consists of genetically related bedded tuff and ash-flow tuff sheets that were erupted 13.2-12.5 m.y. ago from the Claim Canyon cauldron center,* the southernmost part of which is exposed in an arcuate segment along the south side of the Timber Mountain-Oasis Valley caldera complex (Byers et al., 1976). In ascending stratigraphic order, the four major units of the Paintbrush Tuff are the Topopah Spring, Pah Canyon, Yucca Mountain, and Tiva Canyon Members. Both the Topopah Spring and Tiva Canyon Members, which

---

* Christiansen et al. (1977) present the alternative view that the Yucca Mountain and Tiva Canyon Members may have been erupted from an overlapping area including the Oasis Valley cauldron segment, centered slightly northwest of the Claim Canyon segment; however, the Claim Canyon segment did subside during eruption of the Tiva Canyon Member.

are the most voluminous ash-flow sheets, are compositionally zoned from high-silica rhyolite to quartz latite.* In contrast, the Pah Canyon and Yucca Mountain Members are volumetrically smaller by several orders of magnitude and lack extensive compositional zoning. The Pah Canyon Member is lithologically similar to the quartz latitic caprock of the Topopah Spring Member, and the Yucca Mountain Member consists of uniform high-silica rhyolite similar to that at the base of the overlying Tiva Canyon Member. These four ash-flow sheets and associated lavas are thought to record repeated volcanic activity of a single evolving magma chamber that was part of a larger high-level magmatic system. In this context, the Topopah Spring Member represents the tapping of this chamber during a relative "instant", early in its evolution.

The Topopah Spring Member is a multiple-flow compound cooling unit that is inferred to have originally covered an area of 1,800 km^2, with an extracauldron volume of 170 km^3 (Lipman et al., 1966). An unknown volume of tuff, inferred to be buried beneath the Claim Canyon cauldron, led Byers et al. (1976) to suggest that the total eruptive volume was probably greater than 250 km^3. Estimate of the total eruptive volume, however, has been recently revised upward to 1,200 km^3 (Scott et al., 1984; F. M. Byers, Jr., personal communication,

---

* The compositional designation of quartz latite and the term caprock synonymously refer to the uppermost subunit of the eruptive sequence, that is more mafic and crystal-rich than the underlying subunits, and commonly forms an erosion resistant ledge (Lipman et al., 1966; Byers et al., 1976). However, Christiansen et al. (1977) point out that this uppermost subunit contains a much lower Ca/(Na+K) ratio than typical quartz latites and plots in the rhyolite field of the classification scheme of O'Connor (1965).

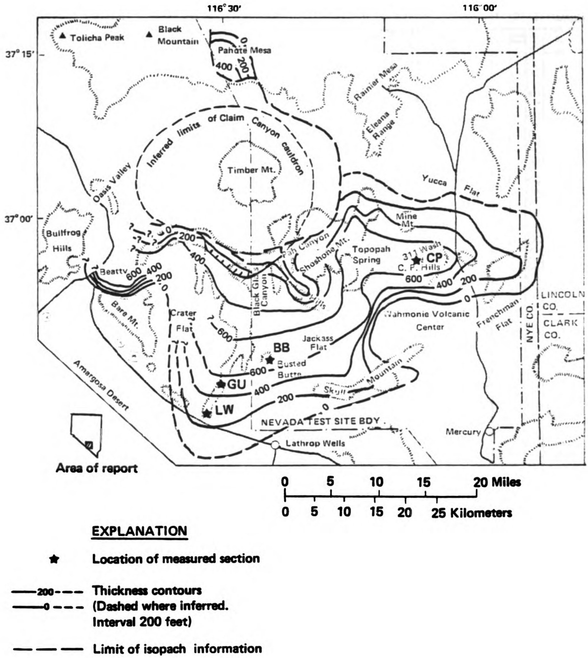

Figure 1. Distribution and thickness of the Topopah Spring Member of the Paintbrush Tuff (Lipman et al., 1966). Locations of measured sections and chemically analyzed samples indicated by two letter ID's as follows: BB = Busted Butte; CP = 311 Wash; LW = Lathrop Wells; GU = USW-GU3 drill hole.

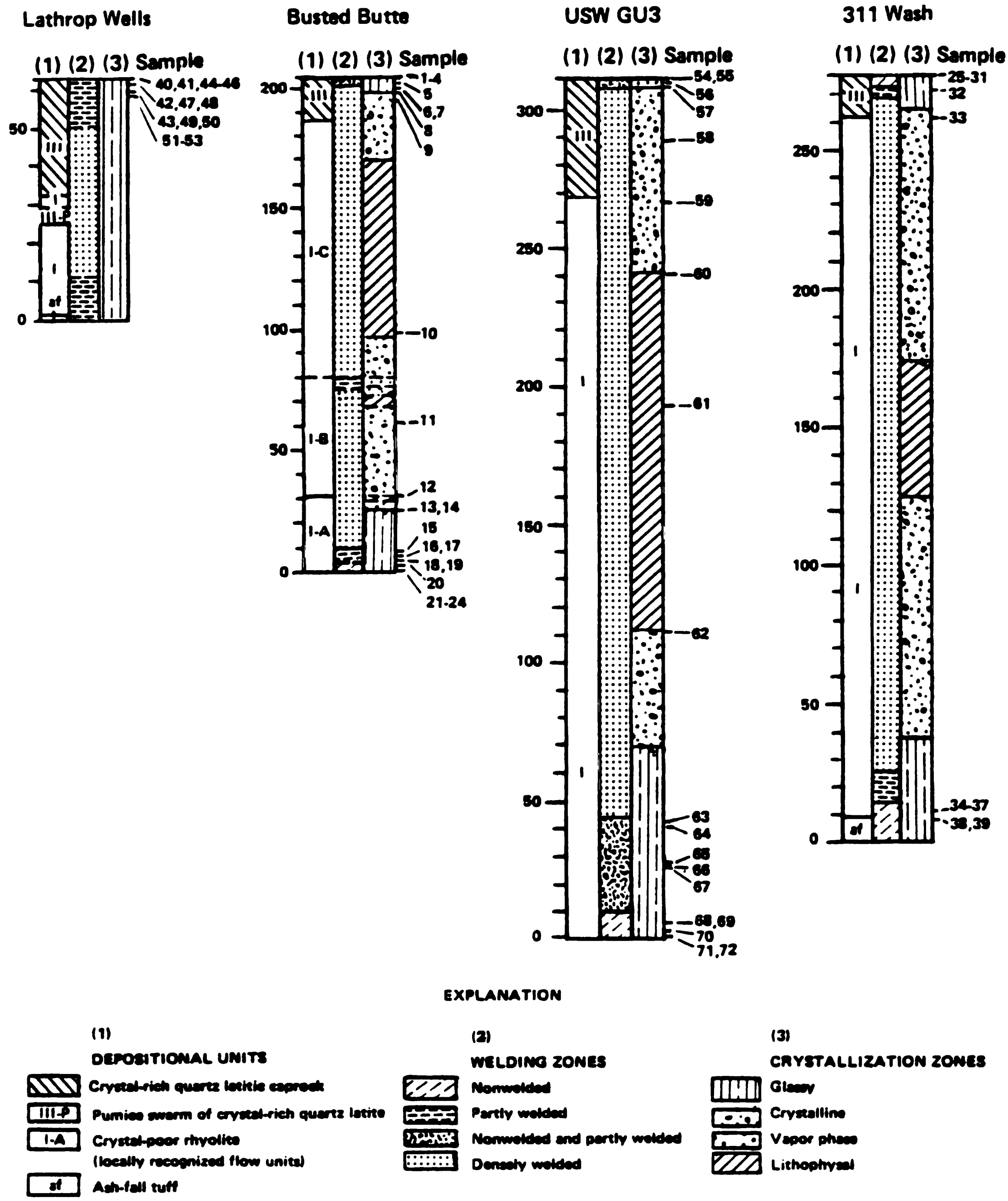

Figure 2. Measured sections of the Topopah Spring Member, showing variations in depositional units, welding zones, and crystallization zones (Lipman et al., 1966). Numbers on the right of each section correspond to the sample number of chemically analyzed specimens in Table 2.

1985), making the Topopah Spring Member the most voluminous ash-flow sheet of the Paintbrush Tuff. Figure 1 includes the inferred distribution and thickness of the Topopah Spring Member.

Field relations and characteristic lithologic and petrographic features of the Topopah Spring Member have been thoroughly described by Lipman et al. (1966). Because the majority of samples analyzed in the present study were collected from outcrops that have been previously described, only a brief summary of the characteristic features noted by Lipman et al. (1966, p. F5-11) is presented here. The Busted Butte section (Figures 1 and 2) is representative of the Topopah Spring Member and serves to illustrate the zonal variations in composition, welding, and crystallization.

At Busted Butte, the base of the ash-flow sheet directly overlies genetically related bedded ash-fall material and consists of a 3-m-thick zone of light colored nonwelded pumice and ash. Above this zone, there is a gradational increase in the degree of welding with increasing stratigraphic height which is evident by the presence of collapsed pumice fragments and darkening of the shard matrix. This zone grades upward into a 15-m-thick densely welded vitrophyre in which the pumice fragments, occurring as black fiamme, contrast against the dark grey shard matrix. There is an abrupt transition at the top of this lower vitrophyre into overlying densely welded crystalline (devitrified) tuff. Above this transition is approximately 145 m of densely welded devitrified tuff that contains several lithophysal zones and in which two depositional contacts between flow units have been identified. The 170-m thickness of tuff described thus far constitutes approximately 90% of the total thickness of the Busted Butte section.

This entire thickness is composed of high-silica rhyolite (77-74% SiO_2) which contains a major phenocryst assemblage of alkali feldspar, plagioclase, biotite, and opaque oxides that increases uniformly upward from approximately 1 to 6%. Within the next 5 m, there is a progressive change from rhyolite to quartz latite along with a considerable increase in the percentage of phenocrysts. In the remaining 15 m, the total phenocryst assemblage increases to about 21% with the addition of minor amounts of clinopyroxene, quartz, and hornblende, and the whole-rock silica content decreases to approximately 69 wt%. Approximately 4 m above the transition to quartz latite, there is an abrupt change from devitrified tuff to a 3-m-thick upper vitrophyre. The upper vitrophyre grades upward into partly welded and nonwelded tuff, where the upper contact of the Topopah Spring Member is sharply overlain by ash-fall material.

The thicknesses of these various subunits vary laterally throughout the ash-flow sheet and several distinct subunits that are recognized at other localities (e.g., the xenolithic subunit at Black Glass Canyon) are absent from the Busted Butte section (Lipman et al., 1966). As noted by Lipman et al. (1966), these variations are probably due to both the progressive change in the composition of the erupted magma and the mechanical processes of eruption and emplacement.

In this study, an attempt was made to evaluate the vertical and lateral compositional variations within the Topopah Spring Member by sampling sections that were widely separated and that spanned the entire range in thickness. However, for reasons discussed in the following section, chemical analyses were performed primarily on samples from the upper and lower margins of measured sections.

METHODS

Sample Selection

Because precise reconstruction of thermo-chemical gradients inferred to be present within the magma chamber is crucial to the evaluation of differentiation mechanisms, two primary considerations guided the sampling scheme in this study. First and foremost was the desire to sample individual glassy pumice fragments, based on the assumption that these samples most closely preserve the composition of the magma, with the exception that volatiles have been lost. In contrast, whole-rock tuff samples represent composite mixtures that are subject to sorting and xenolithic contamination during eruption, transportation, and deposition. Although glassy samples were preferred over samples which have undergone vapor phase crystallization and devitrification, it has been shown that even glassy samples have usually been chemically modified as a result of secondary ground water hydration and no longer strictly represent the composition of magmatic liquids (Aramaki and Lipman, 1965; Lipman, 1965; Noble, 1965; 1967). Second was the desire to obtain samples from sections where the entire eruptive sequence was preserved and close stratigraphic control could be maintained, so that the relative position of samples in the magma chamber could be more readily inferred. This consideration was based on the assumption that the compositional zonation of magma within the source chamber is preserved in inverted sequence in the ash-flow sheet.

It is usually difficult to satisfy the above criteria within the same measured section. The nature of the densely welded devitrified interior of thick sections precludes obtaining glassy pumice samples from the central portion of the eruptive sequence in sections where the entire sequence is present. Glassy pumice fragments are generally confined to the nonwelded to partly welded margins and densely welded vitrophyres. The abundance and size of the pumice fragments also vary vertically in the section (Lipman et al., 1966); however, this is partly due to the effects of welding and devitrification which often obscure the compacted pumice lenses. Although pumice fragments are readily distinguishable in vitrophyres, their compacted nature makes removal quite tedious and sometimes futile.

In the theoretical, ideal case, where a given stratigraphic horizon of the ash-flow sheet corresponds to a single stratigraphic level in the magma chamber, the thermo-chemical gradients in the pre-eruptive magma may be reconstructed by randomly sampling individual pumice fragments, vertically throughout the eruptive sequence. However, in the Topopah Spring Member, it is evident that more than one type of pumice is present within a small volume of tuff at any given stratigraphic horizon. The variability among pumice types is readily distinguishable by textural characteristics, most notably those of color, phenocryst content, and vesicular structure. At the base of the ash-flow sheet, at least five distinct pumice types can be recognized within an area of 200 cm^2 and several other pumice fragments with textural characteristics intermediate to these occur within close proximity. None of the pumice fragments observed show distinct compositional banding or display other macroscopic features indicative of commingling. With increasing stratigraphic height, fewer distinct pumice types are recognizable, as welding tends to obscure the primary textural features. However, individual pumice fragments clearly display a differential response to welding that, in some cases, appears to be independent of size or orientation. At the top of the ash-flow sheet, the number of pumice types is similar to that at the base, although the nature of the textural distinctions are more clearly attributable to differences in phenocryst abundance and vesicularity, as well as color.

This pumice heterogeneity has important implications that necessarily influenced the sampling strategy. On the basis of megascopic textural differences among pumice fragments, without addition of chemical and mineralogical data, it is only possible to conclude that the various pumice types have had different histories. Because these differences may or may not correspond to compositional differences (primary or secondary), discussion of hypotheses for the origin of the pumice heterogeneity is deferred until the chemical analyses of the individual pumice samples have been presented. In order to evaluate the heterogeneity among pumice samples, each pumice type must be considered separately. Therefore, each section was measured at vertical intervals of 1.5 m, beginning at clearly defined contacts with underlying ash-fall material. At each sampled interval, all in situ, macroscopically distinct pumice types were collected, in addition to a large block of whole-rock tuff that contained the various pumice types. For reasons previously noted, the preponderance of individual glassy pumice samples selected for analyses were collected within 3 m of the upper and lower margins of the ash-flow sheet. Several glassy fiamme and whole-rock tuff samples were also analyzed in order to achieve some degree of continuity throughout the eruptive sequence and to compare the compositions of individual pumice samples with their whole-rocktuff composite mixtures. Every effort was made to perform all analyses on single pumice fragments. In some cases, this was not possible because there was insufficient mass from the small sized pumice fragments to perform ICP, INAA, and heavy mineral separation on a single pumice fragment. However, it is possible to distinguish the various pumice types by textural features such as structure of vesicles, glass color, and phenocryst content. Only pumice fragments that were texturally identical were combined. Eighteen of the 50 pumice samples represent composites of texturally identical pumice fragments and these samples are indicated in the data tables. The data base comprises samples collected from outcrops at the Busted Butte, 311 Wash, and Lathrop Wells sections, and from drill hole USW-GU3, the locations of which are shown in Figure 1. The stratigraphic positions of individual samples and their relation to zones of bulk composition, crystallization, and welding are illustrated in Figure 2.

Analytical Procedure

Fifty whole pumice and 22 whole-rock tuff samples were analyzed in this study. After coarse crushing, the fine fraction was examined petrographically for secondary carbonate, and if calcite was observed, the samples were leached in a mixture of sodium acetate and glacial acetic acid. The samples were then pulverized by hand in an agate mortar. All samples were analyzed by instrumental neutron activation analysis (INAA) at Lawrence Livermore National Laboratory and by inductively coupled plasma emission spectroscopy (ICP) at Barringer Magenta, LTD. Results of analyses of U.S.G.S. standards BCR-1 and

GSP-1, which were analyzed as unknowns, are reported alongside their published values in Table 1.

There was sufficient material from 52 samples to concentrate phenocrysts for microprobe analysis. Heavy minerals from the -60+140 sieve size fraction were separated in bromoform and mounted in epoxy. Analyses of Fe-Ti oxide and silicate phenocrysts from selected pumice samples were collected using a JEOL 733 automated electron microprobe at Lawrence Livermore National Laboratory. Oxide and silicate standards were used for quantitative analysis with the Bence-Albee correction procedure (Bence and Albee, 1968).

TABLE 1. Precision and Accuracy of Chemical Analyses. U.S.G.S. standards analyzed as unknowns compared with published concentrations (Abbey, 1978).

A. Concentrations of U.S.G.S. standard GSP-1 determined by inductivly coupled plasma emission spectroscopy (ICP).

(Wt. %)	Abbey (1978)	ICP	% difference
SiO_2	67.31	67.7	-0.58
Al_2O_3	15.19	15.2	-0.07
Fe_2O_3(T)	4.33	4.23	2.31
CaO	2.02	2.05	-1.49
MgO	0.96	1.07	-11.46
TiO_2	0.66	0.59	10.61
MnO	0.04	0.04	0.00
Na_2O	2.80	2.96	-5.71
K_2O	5.53	5.06	8.50
P_2O_5	0.28	0.35	-25.00
(ppm)			
Be	1.5	1.1	26.67
V	49	51	-4.08
Ni	9	10	-11.11
Cu	35	33	5.71
Zn	98	107	-9.18
Sr	230	247	-7.39
Ba	1300	1220	6.15
Pb	53	50	5.66

B. Concentrations of U.S.G.S. standard BCR-1 determined by instrumental neutron activation analysis (INAA).

(ppm)	Abbey (1978)	INAA	% difference	% stand. dev.	n
Sc	34	34	0.00	4.24	7
Cr	16	17	-6.25	6.84	7
Co	37	39	-5.41	4.18	7
Rb	47	54	-14.89	5.93	7
Zr	185	169	8.65	14.60	6
Sb	0.6	0.7	-16.67	6.78	7
Cs	0.95	0.98	-3.16	7.21	7
La	25	27	-8.00	3.54	7
Ce	54	54	0.00	6.59	7
Nd	29	27	6.90	12.85	4
Sm	6.6	6.4	3.03	6.77	7
Eu	1.9	2.0	-5.26	3.19	7
Tb	1.0	1.0	0.00	6.63	7
Yb	3.8	3.6	5.26	9.14	7
Lu	0.6	0.5	16.67	8.23	6
Hf	4.5	5.4	-20.00	5.55	7
Ta	0.88*	0.78	11.36	6.09	7
Th	6.0	5.7	5.00	6.99	7
U	1.8	1.9	-4.56	22.30	7

*Flanagan (1969).

Table 2. Chemical Analyses of Whole Pumices and Whole-rock Tuffs.

Sample No.	1	2	3	4	5	6
Field No.	BB9-1WR	BB9-1A*	BB9-1B*	BB9-1C*	BB9-5C*	BB9-10A*
<u>wt%</u>						
SiO_2	70.5	75.9	69.6	70.7	69.2	76.2
Al_2O_3	13.8	12.6	15.9	15.7	15.8	12.2
Fe_2O_3	1.60	1.48	2.12	1.99	2.20	0.90
CaO	4.07	0.10	0.56	0.50	1.27	0.65
MgO	0.31	0.07	0.40	0.42	0.42	0.12
TiO_2	0.30	0.10	0.47	0.44	0.47	0.11
MnO	0.08	0.05	0.13	0.11	0.09	0.02
Na_2O	3.28	3.47	4.09	4.03	4.43	3.35
K_2O	5.98	6.22	6.52	6.01	5.91	6.42
P_2O_5	0.09	0.02	0.13	0.11	0.13	0.03
<u>ppm</u>						
Be	2.2	1.9	2.7	3.1	1.8	2.4
Sc	5	2	7	7	7	3
V	11	10	17	16	13	3
Cr	-	-	3	-	4	-
Co	0.4	0.1	0.5	0.6	0.5	0.2
Ni	<1	<1	<1	<1	2	<1
Cu	5	10	3	4	4	4
Zn	78	19	121	124	82	31
Rb	154	171	148	151	138	175
Sr	116	15	179	149	203	28
Zr	391	138	699	603	732	143
Sb	0.3	0.4	0.4	0.3	0.1	0.3
Cs	3.96	4.61	3.14	3.39	2.62	4.02
Ba	1390	117	2910	2230	2350	160
La	113	31	200	185	217	48
Ce	170	70	320	321	360	101
Nd	61	31	104	93	100	37
Sm	9.2	5.8	12.5	11.8	13.2	6.3
Eu	1.6	0.2	3.2	2.7	3.6	0.4
Tb	0.8	0.7	0.9	0.9	0.9	0.8
Yb	2.8	3.1	3.2	3.3	3.1	2.9
Lu	0.6	0.6	0.5	0.5	0.5	0.6
Hf	8.8	5.0	14.9	11.9	14.9	5.8
Ta	0.98	1.35	0.77	0.87	0.80	1.29
Pb	30	25	40	40	15	5
Th	19.7	22.7	19.9	18.9	20.3	25.1
U	4.6	4.7	2.9	5.0	2.8	5.0

* Major element oxides have been recalculated to 100% anhydrous. Locations of samples (see Figs. 1 & 2) indicated by two letter prefix: BB = Busted Butte; Cp = 311 Wash; LW = Lathrop Wells; GU = Drill Hole USW-GU3. "WR" suffix in field no. indicates whole-rock tuff. An asterisk indicates a combined sample of texturally identical pumices. All other samples are of individual whole pumice.

Table 2 (cont'd.).

Sample No.	7	8	9	10	11	12
Field No.	BB9-10C*	BB9-15WR	BB9-25WR	BB8-320WR	BB8-200WR	BB8-100WR
wt%						
SiO_2	67.7	68.6	68.5	75.6	76.2	76.7
Al_2O_3	16.0	15.9	16.2	12.8	12.3	12.3
Fe_2O_3	2.34	2.26	2.11	0.99	0.93	1.00
CaO	1.63	1.31	1.68	0.58	0.63	0.55
MgO	0.44	0.40	0.62	0.09	0.15	0.07
TiO_2	0.49	0.47	0.37	0.10	0.09	0.09
MnO	0.10	0.09	0.09	0.06	0.11	0.06
Na_2O	4.49	4.66	4.98	4.08	3.94	3.98
K_2O	6.75	6.19	5.39	5.59	5.63	5.18
P_2O_5	0.15	0.12	0.12	0.03	0.01	0.02
ppm						
Be	1.8	1.7	1.9	3.2	3.1	3.1
Sc	7	7	7	2	2	2
V	14	13	10	4	4	5
Cr	-	-	-	-	-	-
Co	0.6	0.6	0.7	0.2	0.2	0.2
Ni	98	16	34	7	<1	33
Cu	7	4	5	7	3	4
Zn	116	63	58	47	43	44
Rb	135	126	123	180	190	202
Sr	224	207	161	22	27	22
Zr	675	656	639	151	126	160
Sb	0.2	0.1	0.2	0.3	0.4	0.4
Cs	2.79	2.68	1.92	3.78	4.44	3.86
Ba	2840	2420	1380	192	80	50
La	215	201	181	34	35	34
Ce	322	349	314	72	83	69
Nd	108	114	97	27	26	24
Sm	13.0	11.8	11.2	5.7	6.2	5.7
Eu	3.7	3.4	2.9	0.3	0.3	0.2
Tb	0.9	0.9	0.9	0.8	0.8	0.7
Yb	2.8	3.0	3.0	3.1	3.3	2.2
Lu	0.5	0.6	0.6	0.5	0.6	0.4
Hf	14.4	14.4	13.0	4.9	5.1	4.7
Ta	0.80	0.84	0.92	1.31	1.38	1.38
Pb	10	20	25	45	40	25
Th	19.5	19.6	20.2	22.1	23.8	21.0
U	3.4	2.1	4.5	4.5	5.0	3.8

Table 2 (cont'd.).

Sample No.	13	14	15	16	17	18
Field No.	BB8-85BWR	BB8-85B*	BB8-20	BB8-15B	BB8-15C	BB8-10WR
<u>wt%</u>						
SiO_2	76.4	76.9	77.0	77.0	78.2	77.9
Al_2O_3	13.0	12.9	12.9	13.4	12.2	12.5
Fe_2O_3	0.98	0.97	0.93	0.99	0.90	0.94
CaO	0.67	0.66	0.58	0.45	0.52	0.64
MgO	0.07	0.06	0.17	0.21	0.12	0.12
TiO_2	0.10	0.11	0.12	0.14	0.10	0.11
MnO	0.07	0.08	0.08	0.13	0.07	0.07
Na_2O	4.49	3.58	3.23	2.90	3.23	3.04
K_2O	4.12	4.67	4.96	4.68	4.63	4.66
P_2O_5	0.03	0.01	0.02	0.03	0.03	0.03
<u>ppm</u>						
Be	3.0	3.1	2.8	2.7	2.8	2.8
Sc	2	2	2	2	2	2
V	3	-	2	2	2	2
Cr	-	-	6	5	1	3
Co	0.2	0.1	0.2	0.8	0.3	0.4
Ni	<1	-	6	8	6	6
Cu	3	20	5	13	10	20
Zn	45	50	46	59	49	46
Rb	203	235	195	194	187	186
Sr	39	36	14	16	17	21
Zr	137	140	164	177	131	144
Sb	0.3	0.4	0.3	0.4	0.3	0.4
Cs	11.37	10.14	5.39	5.53	5.15	5.10
Ba	42	132	27	49	27	<25
La	38	41	34	36	33	28
Ce	71	88	79	83	66	54
Nd	29	35	26	26	28	26
Sm	5.2	7.2	5.4	5.7	5.5	5.1
Eu	0.2	0.3	0.2	0.3	0.2	0.2
Tb	0.7	0.9	0.7	0.7	0.7	0.7
Yb	3.0	3.4	3.0	3.1	3.1	2.8
Lu	0.4	0.6	0.5	0.5	0.5	0.4
Hf	4.8	6.0	5.4	6.4	4.9	4.9
Ta	1.32	1.52	1.37	1.57	1.36	1.30
Pb	20	20	25	45	25	25
Th	20.8	26.4	22.5	27.3	23.1	21.3
U	4.2	6.1	4.5	5.3	5.1	5.2

Table 2 (cont'd.).

Sample No.	19	20	21	22	23	24
Field No.	BB8-10	BB8-5	BB8-3A	BB8-3B	BB8-2	BB8-1
wt%						
SiO_2	76.8	79.3	78.0	76.8	78.2	78.3
Al_2O_3	13.1	11.8	12.5	13.3	12.4	12.3
Fe_2O_3	0.96	0.83	0.87	0.94	0.86	0.83
CaO	0.85	0.47	0.46	0.46	0.49	0.46
MgO	0.31	0.05	0.10	0.14	0.07	0.14
TiO_2	0.12	0.09	0.12	0.17	0.09	0.11
MnO	0.07	0.07	0.08	0.06	0.09	0.06
Na_2O	2.81	2.76	2.87	2.91	2.91	2.78
K_2O	4.94	4.60	5.03	5.20	4.85	5.02
P_2O_5	0.04	0.02	0.02	0.02	0.02	0.01
ppm						
Be	2.8	2.8	2.8	2.8	2.9	2.8
Sc	2	2	2	2	2	2
V	2	1	1	2	1	1
Cr	2	2	1	2	1	1
Co	0.9	0.2	0.3	0.2	0.2	0.2
Ni	6	6	6	6	6	6
Cu	19	6	15	22	40	36
Zn	49	40	51	61	47	61
Rb	192	187	205	216	188	198
Sr	30	15	13	24	15	15
Zr	154	108	160	207	120	136
Sb	0.4	0.7	0.3	0.3	0.4	0.3
Cs	5.61	5.09	5.89	6.05	5.07	5.24
Ba	27	27	<25	<25	27	27
La	32	35	31	45	31	30
Ce	63	82	65	92	66	57
Nd	25	29	24	32	26	25
Sm	5.2	5.9	5.2	6.0	5.4	5.1
Eu	0.2	0.2	0.2	0.3	0.2	0.2
Tb	0.7	0.8	0.7	0.8	0.7	0.6
Yb	2.8	3.3	2.8	3.1	3.1	2.6
Lu	0.5	0.3	0.5	0.5	0.6	0.4
Hf	5.3	4.5	5.4	7.1	4.5	4.7
Ta	1.36	1.31	1.37	1.43	1.31	1.23
Pb	30	25	30	15	30	20
Th	22.2	22.0	21.8	24.2	21.6	20.3
U	4.7	5.2	4.8	5.0	4.8	4.6

Table 2 (cont'd.).

Sample No.	25	26	27	28	29	30
Field No.	CP3-2A	CP3-2B	CP3-1WR	CP3-1A	CP3-1B	CP3-1C
<u>wt%</u>						
SiO_2	70.7	70.8	72.3	78.4	79.1	76.8
Al_2O_3	15.0	16.0	14.6	11.6	11.2	12.6
Fe_2O_3	2.27	2.12	1.69	0.85	0.84	0.97
CaO	1.02	0.31	0.90	0.47	0.48	0.49
MgO	0.71	0.49	0.38	0.08	0.07	0.14
TiO_2	0.48	0.48	0.35	0.09	0.09	0.11
MnO	0.09	0.04	0.09	0.04	0.03	0.06
Na_2O	3.85	3.58	3.94	3.30	3.11	3.34
K_2	5.78	6.11	5.69	5.11	5.03	5.49
P_2O_5	0.12	0.11	0.07	0.03	0.02	0.03
<u>ppm</u>						
Be	1.6	1.7	2.0	2.8	2.7	2.8
Sc	7	7	5	2	2	3
V	12	12	8	2	1	3
Cr	6	5	4	4	41	5
Co	0.7	0.8	0.5	0.2	0.6	0.3
Ni	10	12	8	8	8	9
Cu	8	15	7	6	15	8
Zn	134	390	56	40	40	49
Rb	126	141	143	181	175	184
Sr	188	53	61	15	14	14
Zr	717	621	463	119	125	147
Sb	0.2	0.6	0.2	0.4	0.4	0.4
Cs	4.18	4.20	3.68	5.13	4.78	5.39
Ba	2880	574	574	<25	27	<25
La	224	208	137	35	31	39
Ce	372	325	233	70	58	76
Nd	115	103	77	26	25	28
Sm	13.2	12.4	9.7	5.5	5.1	5.8
Eu	3.8	2.7	1.9	0.3	0.2	0.3
Tb	0.9	0.9	0.9	0.7	0.7	0.7
Yb	3.2	2.8	3.0	2.9	2.7	3.0
Lu	0.7	0.6	0.6	0.5	0.5	0.5
Hf	14.8	13.0	10.1	4.6	4.7	5.1
Ta	0.78	0.84	1.02	1.35	1.33	1.34
Pb	80	575	25	25	10	35
Th	19.0	20.8	21.1	22.2	20.0	23.5
U	2.3	2.2	3.6	6.1	4.6	4.5

Table 2 (cont'd.).

Sample No.	31	32	33	34	35	36
Field No.	CP3-1D	CP4-20BWR	CP4-60WR	CP1-3WR	CP1-3A	CP1-2E
wt%						
SiO_2	71.0	71.9	73.8	77.3	77.9	78.0
Al_2O_3	15.3	15.0	14.2	12.8	12.4	12.4
Fe_2O_3	1.74	1.81	1.32	0.94	0.84	0.90
CaO	0.86	0.87	0.69	0.49	0.50	0.45
MgO	0.51	0.21	0.32	0.18	0.10	0.19
TiO_2	0.38	0.27	0.19	0.11	0.10	0.09
MnO	0.09	0.09	0.08	0.07	0.07	0.07
Na_2O	3.57	4.44	4.43	3.43	3.37	3.03
K_2O	6.48	5.32	4.98	4.71	4.68	4.85
P_2O_5	0.08	0.05	0.01	0.02	0.02	0.02
ppm						
Be	1.9	2.5	2.5	2.8	2.8	2.8
Sc	5	4	3	3	2	3
V	7	8	5	2	1	2
Cr	10	-	-	2	4	3
Co	0.6	0.3	0.2	0.2	0.2	0.3
Ni	17	157	30	8	7	16
Cu	8	7	4	6	12	6
Zn	52	51	41	52	53	52
Rb	145	164	166	202	204	206
Sr	43	46	35	15	14	15
Zr	431	305	220	122	121	117
Sb	0.2	0.3	0.0	0.4	0.4	0.4
Cs	3.50	4.42	2.81	6.69	6.83	6.37
Ba	314	252	152	27	<25	27
La	163	111	70	37	33	31
Ce	278	213	136	82	60	68
Nd	90	67	39	30	28	23
Sm	10.7	9.8	6.6	5.8	5.6	5.4
Eu	2.1	1.4	0.7	0.3	0.2	0.3
Tb	0.9	0.8	0.8	0.8	0.7	0.7
Yb	3.0	3.2	2.8	3.3	2.7	3.2
Lu	0.6	0.7	0.4	0.6	0.5	0.6
Hf	10.6	9.2	6.8	5.2	4.8	5.0
Ta	1.04	1.11	1.18	1.48	1.37	1.45
Pb	30	25	20	30	30	20
Th	21.6	23.0	20.2	24.5	22.7	22.7
U	2.6	4.8	1.2	4.9	4.9	4.3

Table 2 (cont'd.).

Sample No.	37	38	39	40	41	42
Field No.	CP1-1G	CP1-AFB	CP1-AFWR	LW1-A	LW2-A	LW2-5
<u>wt%</u>						
SiO_2	77.1	77.5	77.6	70.6	70.8	73.2
Al_2O_3	12.9	12.6	12.4	15.1	15.0	13.9
Fe_2O_3	0.90	0.91	0.92	1.86	1.85	1.36
CaO	0.46	0.44	0.52	1.24	0.75	0.84
MgO	0.10	0.12	0.06	0.38	0.38	0.22
TiO_2	0.09	0.10	0.11	0.43	0.43	0.31
MnO	0.07	0.08	0.07	0.10	0.09	0.09
Na_2O	3.19	2.99	3.34	3.95	4.00	3.53
K_2O	5.13	5.19	4.93	6.25	6.66	6.50
P_2O_5	0.02	0.02	0.02	0.10	0.08	0.06
<u>ppm</u>						
Be	2.8	2.8	2.8	1.7	1.8	2.0
Sc	2	2	3	6	6	4
V	1	2	-	9	9	4
Cr	1	2	2	9	6	4
Co	0.2	0.3	0.2	1.1	0.5	0.5
Ni	6	6	6	17	12	10
Cu	5	5	6	12	8	19
Zn	49	51	52	65	63	53
Rb	204	216	213	129	139	156
Sr	14	12	19	61	50	31
Zr	127	126	146	564	515	397
Sb	0.4	0.4	0.4	0.2	0.2	0.2
Cs	7.43	8.38	7.71	3.31	2.96	3.46
Ba	<25	27	27	391	360	102
La	32	34	46	175	172	111
Ce	66	80	91	264	310	202
Nd	25	27	31	101	94	68
Sm	5.6	6.0	6.1	11.7	11.8	9.4
Eu	0.2	0.3	0.3	2.2	2.3	1.2
Tb	0.7	0.8	0.8	0.8	0.9	0.8
Yb	3.0	3.4	2.8	2.9	2.8	3.0
Lu	0.5	0.6	0.5	0.5	0.5	0.3
Hf	5.0	5.6	5.2	12.0	12.0	9.8
Ta	1.41	1.47	1.43	0.85	0.92	1.08
Pb	25	20	25	20	15	15
Th	23.4	24.3	23.9	20.7	21.8	21.0
U	4.9	5.7	3.8	2.6	3.3	3.7

Table 2 (cont'd.).

Sample No.	43	44	45	46	47	48
Field No.	LW2-10	LW4-1A	LW4-1B*	LW4-1C	LW4-5A*	LW4-5B
<u>wt%</u>						
SiO_2	78.7	77.6	73.1	70.7	78.2	71.3
Al_2O_3	11.4	12.0	13.9	15.0	11.6	13.9
Fe_2O_3	0.82	0.92	1.38	2.18	0.86	1.65
CaO	0.50	0.45	1.13	1.13	0.68	1.55
MgO	0.16	0.12	0.24	0.20	0.07	0.39
TiO_2	0.09	0.11	0.27	0.47	0.09	0.39
MnO	0.05	0.06	0.07	0.08	0.05	0.09
Na_2O	3.14	3.39	3.37	3.85	3.26	3.75
K_2O	5.14	5.32	6.38	6.22	5.18	6.82
P_2O_5	0.03	0.04	0.07	0.19	0.04	0.11
<u>ppm</u>						
Be	2.8	2.8	2.3	1.6	2.8	1.7
Sc	2	2	3	7	2	5
V	2	3	7	13	3	9
Cr	9	1	2	4	1	5
Co	0.3	0.2	0.6	1.1	0.3	0.7
Ni	13	8	9	10	8	8
Cu	8	12	22	12	8	30
Zn	39	45	57	66	37	60
Rb	189	183	161	134	190	136
Sr	13	27	42	90	20	64
Zr	112	137	279	618	149	501
Sb	0.3	0.4	0.3	0.3	0.4	0.4
Cs	5.06	4.83	4.08	3.99	5.19	2.77
Ba	<25	<25	107	1030	25	316
La	30	39	93	215	33	152
Ce	60	73	163	324	61	268
Nd	26	29	50	110	26	82
Sm	5.3	5.7	8.0	13.0	6.0	10.3
Eu	0.2	0.4	1.0	2.8	0.2	2.1
Tb	0.7	0.7	0.8	0.9	0.7	0.8
Yb	2.9	2.9	3.1	3.2	2.9	3.0
Lu	0.4	0.5	0.6	0.6	0.5	0.6
Hf	4.6	4.9	8.4	12.8	4.6	11.3
Ta	1.35	1.29	1.10	0.82	1.34	0.87
Pb	35	25	20	25	30	25
Th	22.0	21.7	20.9	20.5	22.0	19.7
U	5.2	5.1	4.0	2.1	4.9	2.5

Table 2 (cont'd.).

Sample No.	49	50	51	52	53	54
Field No.	LW4-10A	LW4-10B	LW4-15A	LW4-15B	LW4-15C	GU3-31BWR
<u>wt%</u>						
SiO_2	77.1	70.9	77.5	77.8	70.1	74.9
Al_2O_3	11.6	14.6	11.0	11.6	15.0	13.6
Fe_2O_3	0.83	1.59	0.78	0.81	2.01	1.41
CaO	1.40	1.58	2.07	0.93	1.55	0.61
MgO	0.31	0.34	0.41	0.15	0.46	0.19
TiO_2	0.11	0.36	0.09	0.10	0.43	0.23
MnO	0.05	0.09	0.04	0.06	0.09	0.08
Na_2O	3.39	4.34	3.24	3.34	4.57	4.54
K_2O	5.12	6.15	4.80	5.24	5.68	4.37
P_2O_5	0.05	0.09	0.05	0.05	0.14	0.04
<u>ppm</u>						
Be	2.5	1.8	2.5	2.7	1.6	1.7
Sc	3	5	2	2	6	5
V	3	8	3	2	9	4
Cr	4	-	3	3	2	-
Co	0.4	0.6	0.5	0.4	0.7	0.3
Ni	8	8	24	8	8	<1
Cu	20	23	14	9	18	3
Zn	46	64	40	39	74	58
Rb	172	156	163	181	123	195
Sr	47	86	50	30	203	87
Zr	145	487	120	153	659	447
Sb	0.4	0.3	0.4	0.4	0.2	0.7
Cs	4.63	3.07	4.79	4.93	2.73	3.12
Ba	80	214	<25	<25	2690	805
La	43	138	28	37	196	10
Ce	82	247	56	74	291	190
Nd	31	80	23	23	111	71
Sm	5.5	10.3	4.8	5.3	12.3	9.2
Eu	0.5	1.8	0.2	0.3	3.3	1.5
Tb	0.7	0.9	0.7	0.7	0.9	0.9
Yb	2.8	3.0	2.8	3.1	3.1	3.6
Lu	0.5	0.5	0.5	0.5	0.5	0.8
Hf	5.2	11.3	4.5	5.0	13.8	9.7
Ta	1.26	0.94	1.25	1.30	0.78	1.35
Pb	25	20	20	25	25	65
Th	20.6	20.4	20.8	22.0	18.4	25.8
U	4.6	3.1	4.7	5.2	2.8	2.4

Table 2 (cont'd.).

Sample No.	55	56	57	58	59	60
Field No.	GU3-31AWR	GU3-29WR	GU3-28WR	GU3-23WR	GU3-21WR	GU3-20WR
wt%						
SiO_2	75.0	76.0	75.4	74.8	71.9	78.4
Al_2O_3	13.8	12.7	13.4	13.0	15.0	12.0
Fe_2O_3	1.36	1.41	1.42	1.57	1.83	1.02
CaO	0.65	0.84	0.77	0.75	0.70	0.49
MgO	0.20	0.19	0.19	0.24	0.34	0.13
TiO_2	0.23	0.22	0.21	0.28	0.37	0.11
MnO	0.07	0.08	0.08	0.08	0.10	0.06
Na_2O	4.35	4.26	4.40	4.60	4.76	4.07
K_2O	4.23	4.24	4.05	4.69	4.88	3.71
P_2O_5	0.06	0.05	0.06	0.06	0.07	0.01
ppm						
Be	2.1	2.4	2.5	2.1	1.8	2.9
Sc	5	4	4	5	6	3
V	4	5	5	7	9	3
Cr	-	-	-	-	-	-
Co	0.4	0.3	0.3	0.3	0.4	0.1
Ni	<1	2	<1	<1	<1	<1
Cu	3	3	2	2	3	2
Zn	59	42	59	55	122	46
Rb	192	173	177	154	155	192
Sr	78	79	71	47	58	19
Zr	363	339	357	411	541	109
Sb	0.5	0.3	0.3	0.0	0.4	0.3
Cs	3.04	5.66	3.63	2.72	4.40	3.74
Ba	697	647	782	304	472	50
La	124	98	93	107	167	42
Ce	239	158	174	188	327	83
Nd	83	61	44	62	83	36
Sm	11.2	8.7	7.5	8.8	12.0	6.1
Eu	1.7	1.4	1.2	1.5	2.3	0.4
Tb	1.0	0.8	0.8	0.8	0.8	0.7
Yb	4.3	2.9	2.8	3.0	3.4	2.2
Lu	1.0	0.6	0.5	0.6	0.5	0.3
Hf	11.1	8.6	8.7	9.5	12.3	4.2
Ta	1.43	1.15	1.29	1.12	0.95	1.42
Pb	45	30	50	15	20	20
Th	28.0	21.8	20.8	21.6	22.3	22.7
U	3.3	3.1	3.6	4.3	3.3	3.7

Table 2 (cont'd.).

Sample No.	61	62	63	64	65	66
Field No.	GU3-17WR	GU3-14WR	GU3-12	GU3-11*	GU3-10*	GU3-9*
wt%						
SiO_2	78.9	78.9	76.6	75.9	76.1	75.5
Al_2O_3	12.3	12.2	12.7	13.1	13.1	13.4
Fe_2O_3	0.97	1.00	0.95	0.97	0.91	1.02
CaO	0.45	0.48	0.51	0.54	0.55	0.55
MgO	0.13	0.11	0.06	0.06	0.07	0.06
TiO_2	0.09	0.10	0.09	0.09	0.09	0.09
MnO	0.05	0.05	0.10	0.07	0.07	0.06
Na_2O	3.92	4.25	3.51	3.51	3.62	3.78
K_2O	3.18	2.94	5.51	5.80	5.50	5.52
P_2O_5	0.01	0.03	0.01	0.01	0.01	0.01
ppm						
Be	3.0	3.1	3.1	3.1	3.1	2.9
Sc	2	2	2	2	2	3
V	3	3	2	2	3	3
Cr	-	-	-	-	-	-
Co	0.2	0.2	0.2	0.2	0.2	0.2
Ni	<1	5	<1	<1	16	<1
Cu	2	4	3	5	10	2
Zn	46	50	55	56	57	50
Rb	201	187	217	215	197	232
Sr	18	18	20	17	22	23
Zr	123	167	122	146	100	181
Sb	0.4	0.4	0.7	0.4	0.3	0.4
Cs	4.27	4.40	5.48	5.58	5.66	7.17
Ba	32	30	160	35	42	67
La	32	38	30	30	29	29
Ce	72	70	65	28	70	81
Nd	23	35	26	24	-	30
Sm	4.5	5.7	5.3	5.4	5.0	5.2
Eu	0.3	0.3	0.2	0.2	0.2	0.3
Tb	0.6	0.7	0.7	0.7	0.7	0.8
Yb	2.9	2.8	2.9	2.0	3.3	3.4
Lu	0.5	0.5	0.6	0.5	0.3	0.6
Hf	5.1	5.2	4.6	4.4	4.6	5.4
Ta	1.43	1.36	1.35	1.32	1.35	1.53
Pb	20	20	30	35	30	25
Th	23.1	23.3	21.7	22.3	21.5	26.0
U	4.4	4.4	4.5	4.4	3.5	4.3

Table 2 (cont'd.).

Sample No.	67	68	69	70	71	72
Field No.	GU3-8*	GU3-7*	GU3-6*	GU3-5*	GU3-2*	GU3-1*
wt%						
SiO_2	76.4	75.8	76.7	77.6	76.3	76.3
Al_2O_3	13.1	13.3	12.8	12.4	12.8	13.3
Fe_2O_3	1.03	0.96	0.99	0.95	1.00	1.00
CaO	0.57	0.59	0.54	0.56	0.58	0.70
MgO	0.09	0.11	0.06	0.08	0.06	0.09
TiO_2	0.10	0.11	0.08	0.09	0.08	0.09
MnO	0.10	0.12	0.07	0.09	0.06	0.09
Na_2O	3.52	3.78	3.93	3.67	3.99	4.02
K_2O	5.13	5.15	4.84	4.54	5.08	4.47
P_2O_5	0.02	0.02	0.02	0.01	0.02	0.01
ppm						
Be	3.1	3.2	2.9	2.8	2.9	3.1
Sc	3	2	2	2	3	2
V	3	3	2	3	<.5	1
Cr	-	1	-	-	-	2
Co	0.2	0.2	0.2	0.0	0.1	0.2
Ni	<1	<1	<1	<1	3	11
Cu	5	3	2	4	1	6
Zn	77	77	51	64	43	67
Rb	241	182	163	203	196	184
Sr	34	44	22	31	21	35
Zr	141	147	117	-	136	147
Sb	0.5	0.3	0.3	0.5	0.4	0.5
Cs	7.89	5.07	5.64	6.24	5.57	6.50
Ba	42	42	60	90	47	42
La	33	32	32	31	31	38
Ce	79	71	58	56	72	66
Nd	36	30	23	-	29	249
Sm	5.9	4.3	5.1	5.5	5.2	5.4
Eu	0.3	0.2	0.2	0.0	0.2	0.2
Tb	0.9	0.6	0.6	0.0	0.7	0.7
Yb	3.7	2.7	2.5	2.7	2.6	3.0
Lu	0.4	0.5	0.2	0.0	0.2	0.5
Hf	5.9	4.3	4.0	0.0	4.1	4.6
Ta	1.60	1.25	1.10	0.00	1.38	1.33
Pb	25	30	25	25	20	25
Th	26.1	20.7	19.0	22.0	20.4	22.1
U	5.1	4.8	4.6	5.1	3.8	5.3

RESULTS

Major Element Chemistry

The major element oxide analyses are reported in Table 2. For purposes of discussion and graphical presentation, all values have been recalculated to 100 weight percent excluding loss on ignition (LOI), to facilitate comparison between variably hydrated glassy and devitrified samples. The overall range and trend in major element composition of the Topopah Spring Member was first reported by Lipman et al. (1966), based on 13 whole-rock tuff samples and one densely welded crystallized pumice sample. The additional analyses reported in this study are consistent with those provided by Lipman et al. (1966), and also help to clarify the previously addressed question regarding an apparent compositional gap. More important, these additional analyses demonstrate that the textural heterogeneity of pumice samples observed in the field corresponds to chemical heterogeneities among the pumice samples, with a systematic variation in their compositional range with stratigraphic position in the ash-flow sheet.

Figure 3 illustrates the variation of the major elements with stratigraphic height in the ash-flow sheet at each sample location. Considering only the whole-rock tuff samples from the Busted Butte section (Figure 3a), SiO_2 displays a total variation from 77.9 wt. % near the base to 68.5 wt. % near the top, with a pronounced chemical change to lower values of SiO_2 coincident with the transition from crystal-poor tuff to crystal-rich caprock (Lipman et al., 1966). However, the various pumice samples occurring at a given stratigraphic level display a range in SiO_2. At the base of the ash-flow sheet,

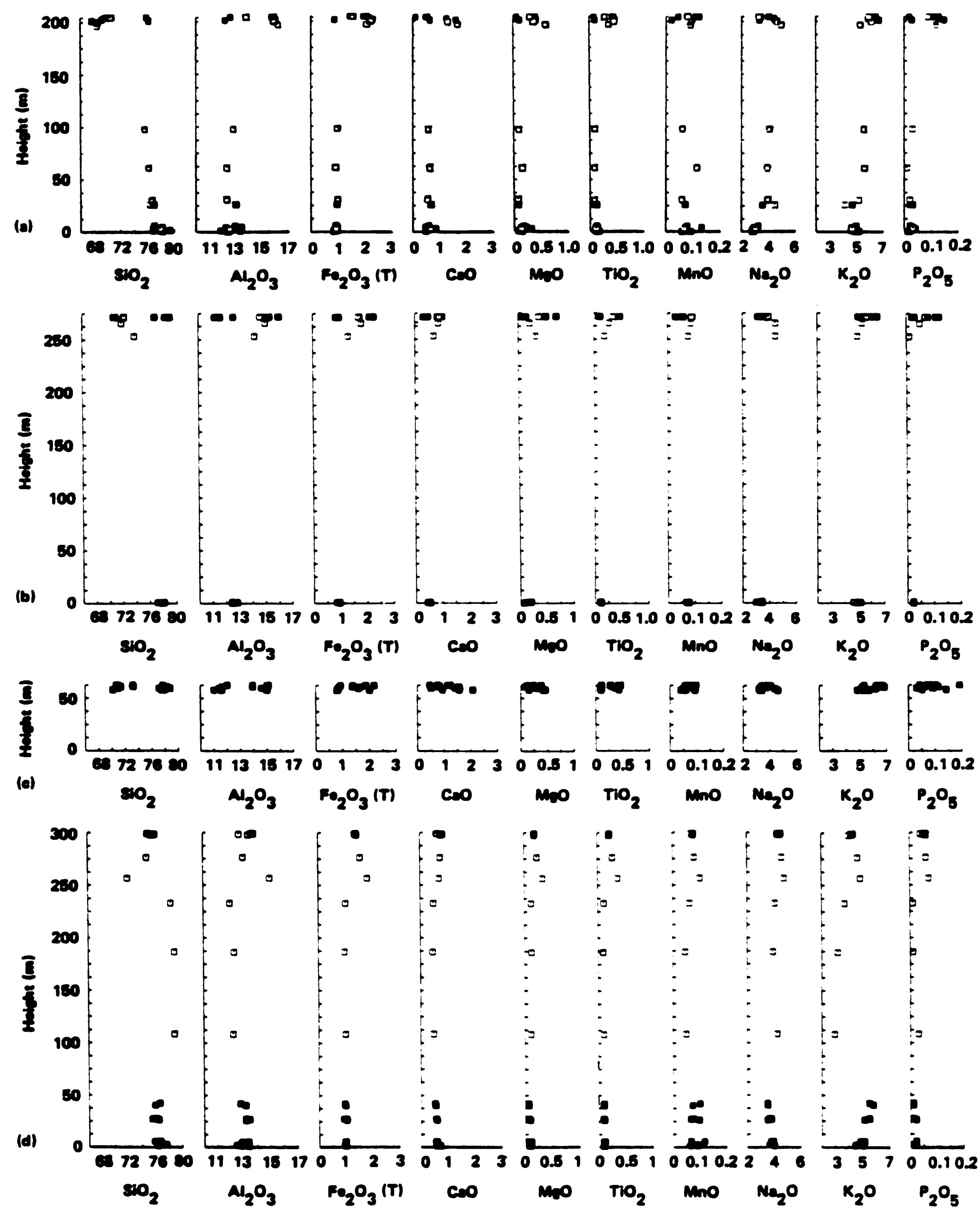

Figure 3. Variation of major element oxides with stratigraphic height. Analytical data from Table 2. Solid symbols = whole pumice; open symbols = whole-rock tuff. (A) Busted Butte; (B) 311 wash; (C) Lathrop Wells; (D) USW-GU3.

all the pumice fragments are high-silica rhyolites, and although individual pumice samples have marked textural variations, they display only a modest range in SiO_2 content. In contrast, the range in SiO_2 for pumice samples at the top of the ash-flow sheet is nearly as great as that of the entire section. At this stratigraphic level, there is a compositional variation among pumice samples ranging from high-silica rhyolite to quartz latite (76.2-67.7 wt%). Although no attempt was made to quantify the proportions of the different pumice types at a given stratigraphic level, comparison of the compositions of the various pumice samples with their associated whole-rock tuff composites gives a first approximation of their relative abundances. It must be noted, however, that while sufficiently large whole-rock tuff samples were taken and their lithic fragments removed before powdering, only one whole-rock tuff sample was taken at a given stratigraphic level.

Unfortunately, due to the difficulty of removing pumice fragments from the densely welded central portion of the ash-flow sheet, it was not possible to fully evaluate the degree of chemical heterogeneity at every stratigraphic level within the entire eruptive sequence. Although the textural variations of pumice lenses in the densely welded devitrified horizons are less extreme, careful observations allow subtle distinctions among pumice fragments to be made at most stratigraphic levels. Based on data from other pumice samples and the overall chemical similarity of whole-rock tuff samples within the crystal-poor rhyolite, any compositional differences corresponding to these textural differences are likely to be modest as well.

The relationship described for SiO_2 at the Busted Butte section has corresponding variations for all the major oxides and at all sample localities. Figure 3 clearly shows that the chemical compositions of individual pumice samples within a given stratigraphic level are not unique, but display a range in composition. Moreover, pumice samples with compositions similar to those deposited during the early phase of the eruption are present throughout the eruptive sequence. The range in pumice compositions increases with increasing stratigraphic height; however, due to the paucity of pumice analyses from the central portion of the ash-flow sheet, the progressive nature of this increase in range is uncertain. This chemical heterogeneity has profound implications for the reconstruction of inferred chemical gradients in the magma chamber based on ash-flow stratigraphy.

The interelement variation of the major oxides with weight percent silica is depicted in Figure 4. The solid symbols represent analyses of pumice samples whereas the open symbols represent whole-rock tuff samples. The overall trends are consistent with the data reported by Lipman et al. (1966). In these previously published analyses (diamond shaped symbols), no data points occur in the interval from 71.8 to 74.7% SiO_2. This apparent gap was thought to be real (Hildreth, 1981) and has been interpreted to indicate the existence of a sharp compositional interface or a narrow transition zone within the magma chamber. The additional analyses reported in this study show an overall continuity in the variation of SiO_2, although compositions in this aforementioned interval are significantly under represented. The paucity of compositions in this interval may be due to inadequate sampling of the central portion of the eruptive sequence, because three

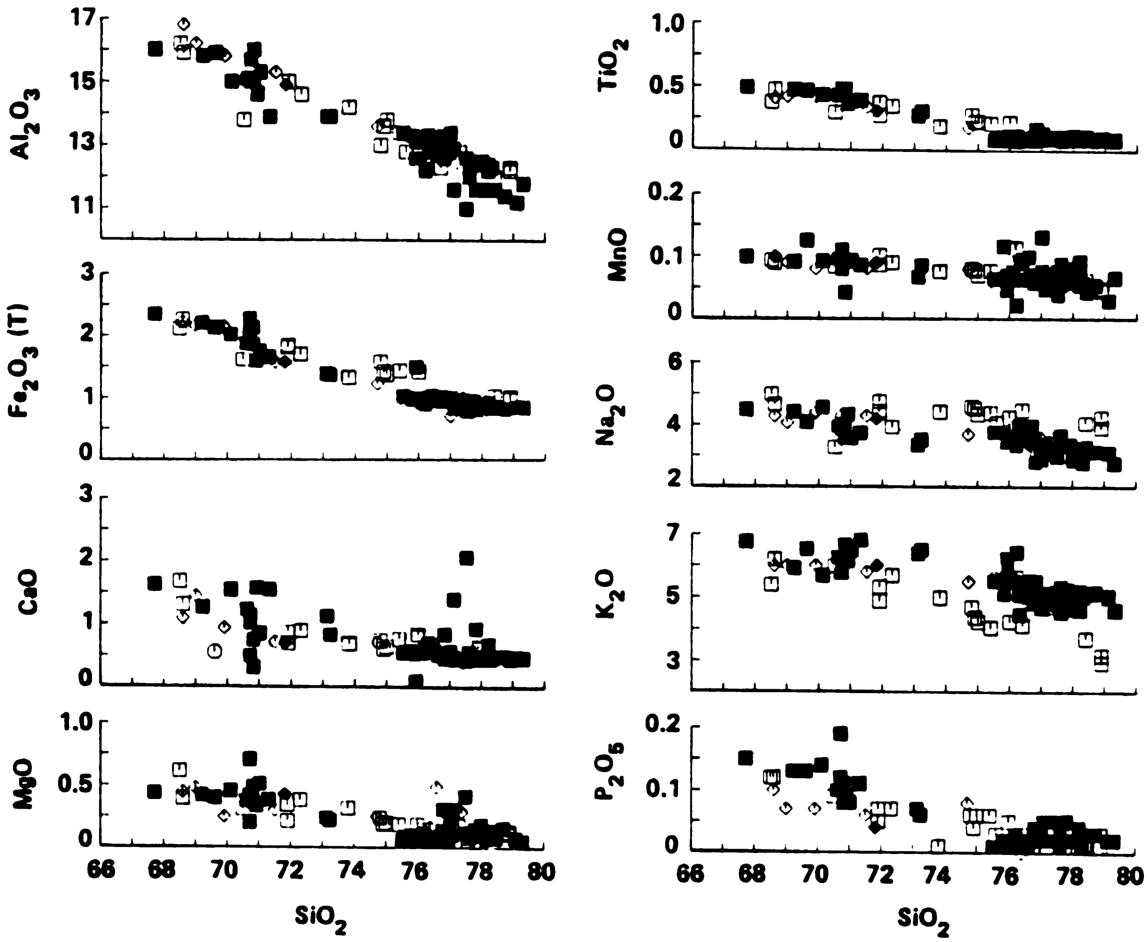

Figure 4. Variation of major element oxides vs. silica. Units in weight percent. Solid symbols = whole pumice; open symbols = whole-rock tuff. Source of analytical data: squares from table 2; diamonds from Lipman et al., (1966).

of the six samples that occur in this interval are from the interior of the sequence. Alternatively, it may be that the occurrence of compositions in this interval is the result of limited mixing between compositionally contrasting magmas.

This latter view is supported by several lines of evidence. Four of the six samples in this interval are whole-rock tuff samples that contain more than one pumice type, and therefore do not represent the composition of a single parcel of magmatic liquid. The two pumice samples in this compositional interval were collected from the very top of the distal portion of the ash-flow sheet and occur alongside both more silicic and more mafic pumice samples, and thus their relative position in the magma chamber is uncertain; they may represent either mixed liquids or fractionates resulting from differentiation processes occurring near a compositional interface. In spite of the absence of a distinct compositional gap, the hypothesis of the existence of a sharp magmatic interface or a narrow transition zone is consistent with the interelement variation trends. From Figure 4, it is apparent that some of the major oxide trends are not strictly linear, but display a dichotomous distribution with a change in abundance occurring within the interval of the previously noted gap at approximately 74% SiO_2. This is best illustrated by the oxides Fe_2O_3(T), and TiO_2. The more abundant high-silica rhyolites (>75% SiO_2) do appear to define linear trends, generally having little scatter and showing very slight variation of the corresponding major elements with increasing SiO_2; this latter feature may be an artifact of the constant sum effect. Notable exceptions are the alkalies which may be mobilized during secondary hydration (Aramaki and Lipman, 1965; Lipman, 1965; Noble, 1965; 1967). Although there is a greater density of data points in the high-silica group, these analyses represent an equal number of samples from the upper and lower horizons of the ash-flow sheet.

These trends can be interpreted to indicate that high-silica rhyolitic magma was separated from underlying low-silica rhyolitic magma by a distinct compositional interface within a single magma body, and that two compositionally distinct magmas evolved concomitantly.

Trace Element Chemistry

Highly charged trace elements, particularly the rare earth elements (REE), are especially useful in evaluating petrogenetic models because they often display relatively large variations in abundance within coeval rocks that have only a modest range in major element composition. In the Topopah Spring Member, there is a strong correlation between the abundance of certain trace elements and major element concentrations. The chemical heterogeneity among pumice samples that is observed with the major elements is also observed with the trace elements. These data further support the hypothesis that a sharp compositional interface or narrow transition zone existed between chemically distinct magmas within a single source chamber. Trace element abundances of samples analyzed in this study are presented in Table 2.

Figure 5a illustrates the variation in the abundance of seven REE for all samples of the Topopah Spring Member. The ordinate value is the ratio of the concentration of an element in the sample to the average concentration of that element in chondrites reported by Haskin et al. (1968). With the exception of one whole-rock tuff sample

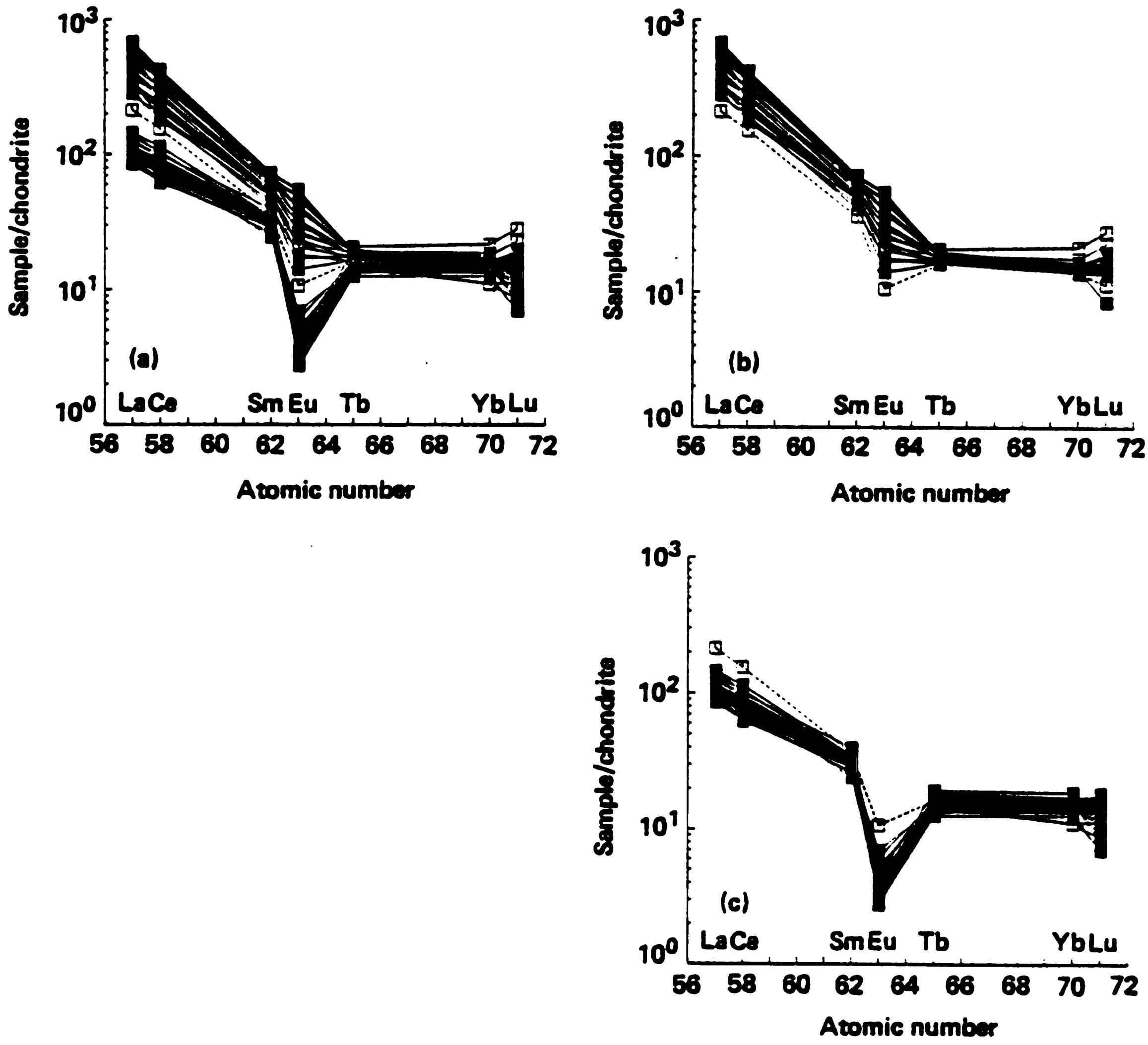

Figure 5. Chondrite-normalized REE abundances (log scale) vs. atomic number. Solid symbols = whole pumice; open symbols = whole-rock tuff. (A) All samples; (B) quartz latite (low-silica rhyolite); (C) high-silica rhyolite.

(CP4-60WR), indicated by the dashed line, there is a lack of samples with intermediate concentrations for the elements La, Ce, and Eu, which allows two major groups of REE patterns to be distinguished. Within each of the two groups, the individual patterns illustrate continuous variation, and most patterns within each group are subparallel, indicating an overall coherence in REE distribution. Several samples, however, have patterns that display a cross-over near Sm, with slight LREE depletion and corresponding HREEenrichment, similar to that observed in the Bishop Tuff (Hildreth, 1977).

The REE patterns that lie above the trend of CP4-60WR (Figure 5b), generally correspond to samples of low-silica rhyolite (quartz latite) and all of these samples occur in stratigraphic units that lie above CP4-60WR in the ash-flow sheet. Within this group, the negative Eu anomaly progressively diminishes to predicted values,* as the LREE concentration increases, with up to 7 times the La concentration of the high-silica pumice samples. The REE patterns that lie below the trend of CP4-60WR (Figure 5c) correspond to samples of high-silica rhyolite. These exhibit relatively little variation and are characterized by large negative Eu anomalies and maximum LREE enrichment of approximately 140 times chondritic abundances. In contrast to the LREE enriched samples, pumice samples that exhibit these trends occur throughout the ash-flow sheet. The REE patterns of individual samples in relation to their stratigraphic positions in the ash-flow sheet are illustrated in Figure 6.

---

* The predicted Eu concentration, Eu*, is that calculated by linear extrapolation between the chondrite normalized concentrations of Sm and Tb on a plot of REE concentration versus atomic number.

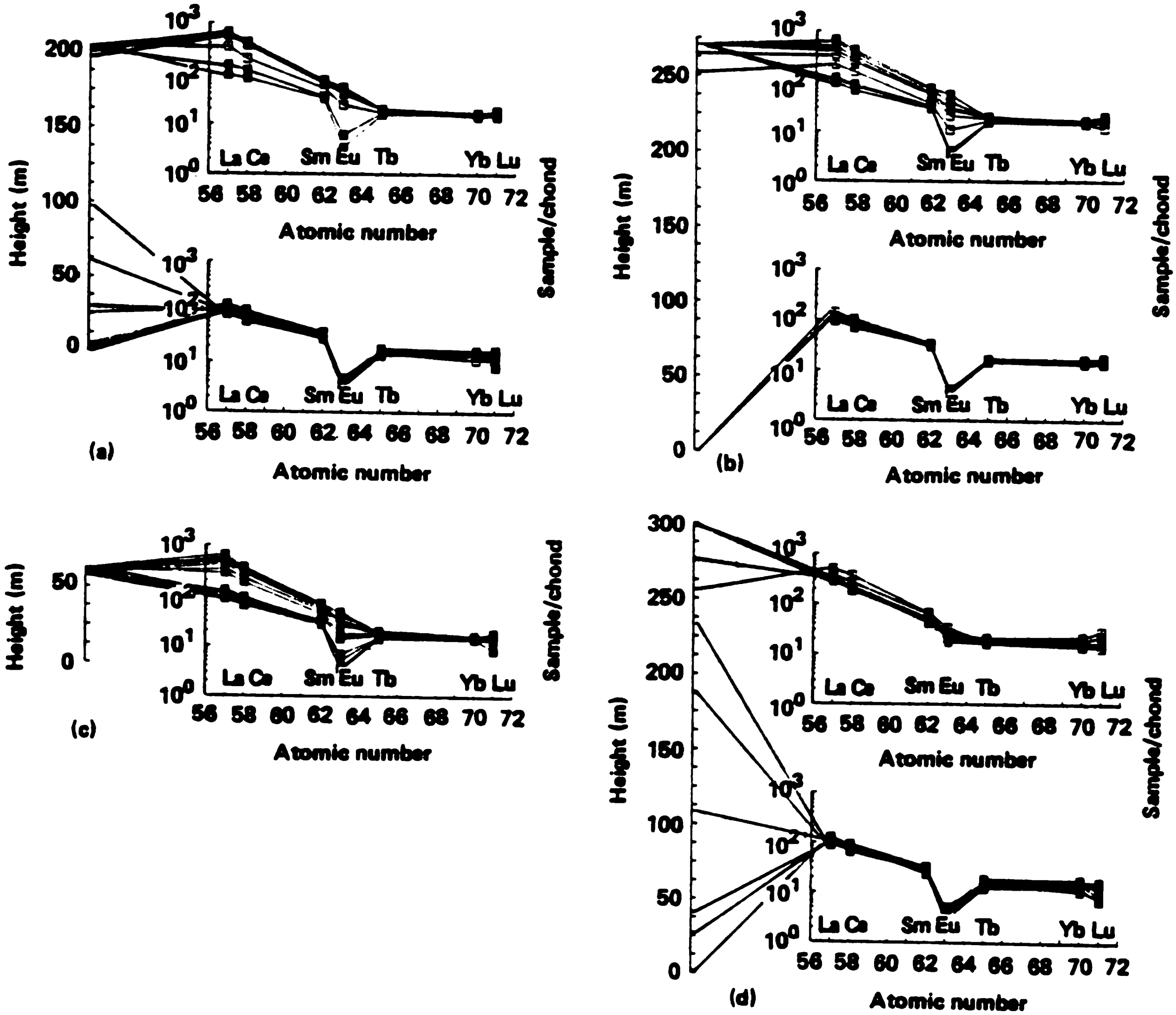

Figure 6. Chondrite-normalized REE patterns in relation to stratigraphic position. Solid symbols = whole pumice; open symbols = whole-rock tuff. (A) Busted Butte; (B) 311 Wash; (C) Lathrop Wells; (D) USW-GU3.

This systematic chemical heterogeneity among pumice samples, which is most pronounced at the top of the ash-flow sheet, is demonstrable for nearly all elements that have a significant range in concentration (see Table 2). Rather than plotting all the trace elements versus stratigraphic position, it is useful to consider the covariation of selected trace elements for which a large variation has been established.

In Figure 7, various trace elements are plotted against SiO_2 to illustrate their behavior with increasing differentiation. The elements Ba, Sr, Eu, Zr, and La, all decrease with increasing SiO_2. These trends are consistent with control by fractionation of alkali feldspar, plagioclase, zircon, and chevkinite/perrierite, phases that are petrographically observed in the low-silica samples. In contrast, the elements Ta, Rb, Cs, Th, and Sb display incompatible behavior, all increasing with SiO_2. A significant feature common to all elements shown in Figure 7 is a marked change in concentration at approximately 74% SiO_2, similar to that observed for the major element oxides. To illustrate that this rather abrupt change in elemental concentrations is not solely an artifact of the non-linear behavior of SiO_2, several of these elements are plotted against each other in Figure 8. The trends of Ta, Rb, Ba, and Hf vs. Th all display apparent inflections for the same abundance of Th, although the changes in abundance are less drastic for the incompatible elements Ta and Rb. Trends of compatible vs. incompatible elements (i.e., Ba vs. Rb) or of two elements that are compatible with different phases (i.e., Ba vs. Zr) generally show greater changes in abundance.

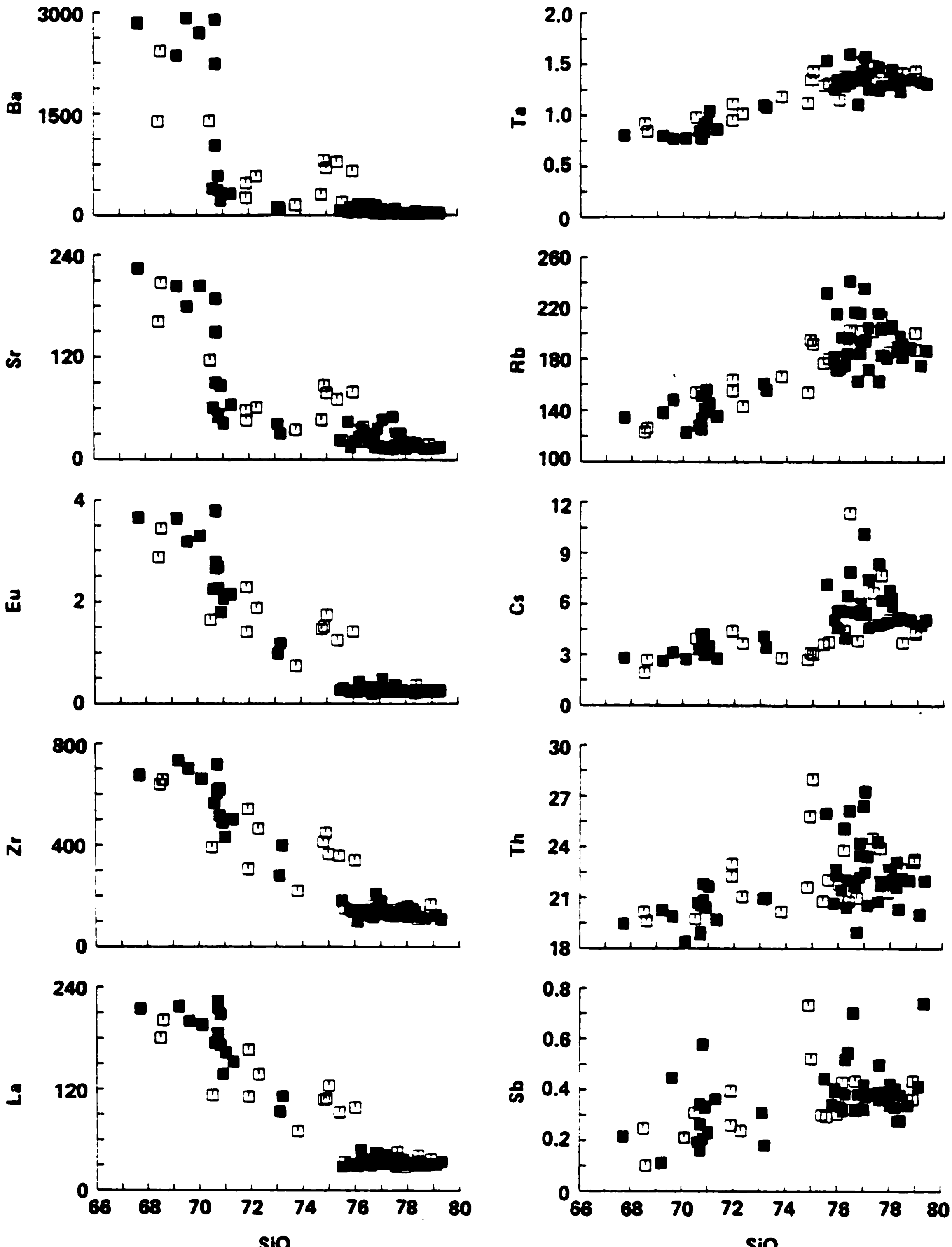

Figure 7. Trace element abundances (ppm) vs. silica (wt. %). Solid symbols = whole pumice; open symbols = whole-rock tuff.

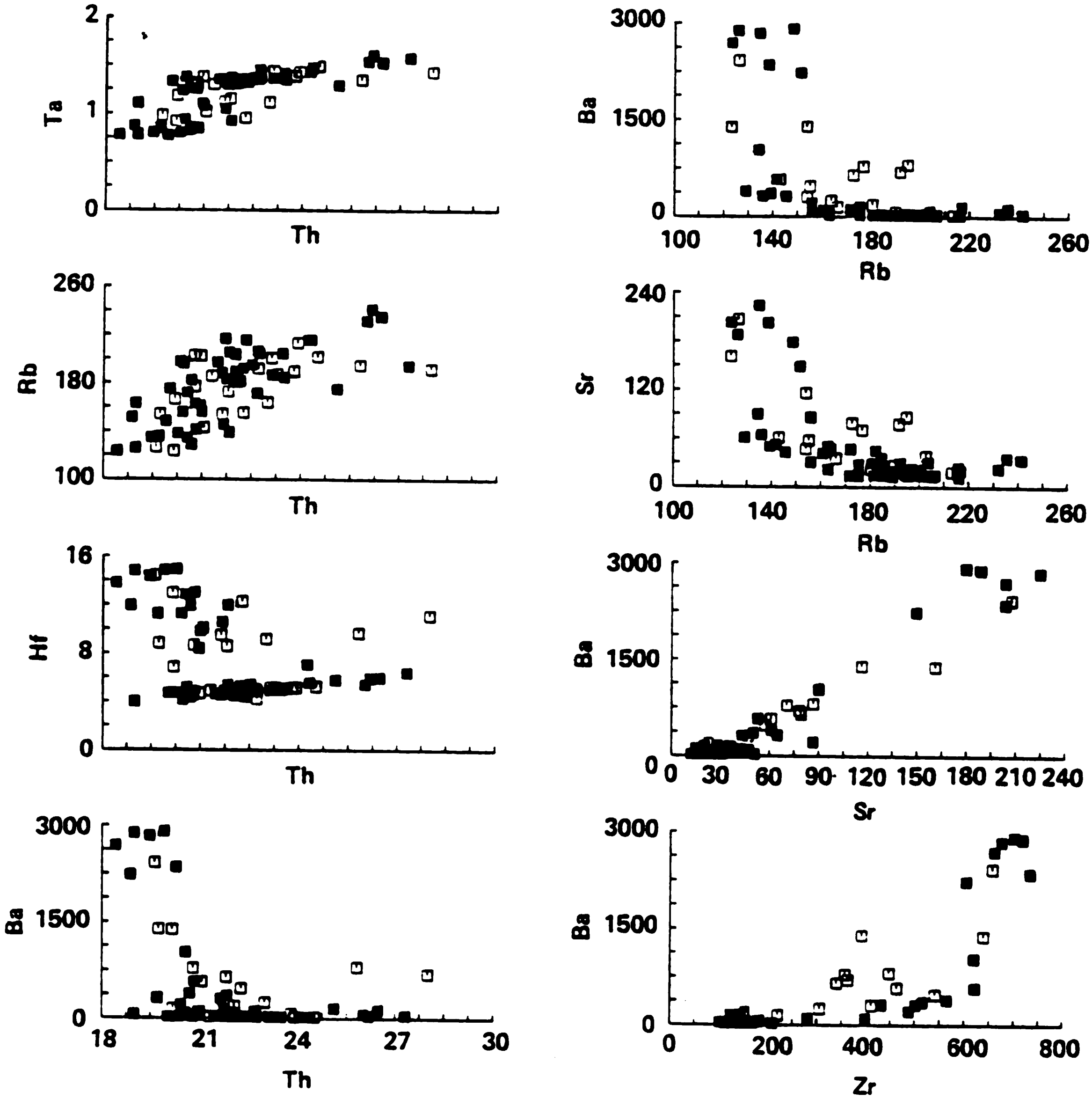

Figure 8. Inter-element variation of selected trace elements (ppm). Solid symbols = whole pumice; open symbols = whole-rock tuff.

Coexisting Iron-Titanium Oxides and Estimated Temperatures

In conceptual models of magma chambers, probably the least equivocal assumption is that the temperature of magma increases with depth in the chamber. In contrast, the assumption that the composition of magma becomes more mafic with depth in the chamber is largely based on inference from the overall whole-rock compositional variation with stratigraphic height within ash-flow sheets. Although this last assumption is considered quite reasonable, previous sections of this paper present clear evidence that pumice samples that most closely represent quenched parcels of magmatic liquid, do not strictly become more mafic with increasing stratigraphic height in the Topopah Spring Member. Therefore, it is desired to isolate some other position dependent parameter that can be used to constrain chemical gradients within the magma chamber. For reasons discussed above, the quenched equilibrium temperature of liquidus phases would appear to be a logical choice.

In order to employ the iron-titanium oxide geothermometer and oxybarometer of Spencer and Lindsley (1981), heavy mineral separates from 52 samples were prepared for microprobe analyses and 50 samples contained both magnetite and ilmenite phenocrysts. In many of these samples, either the magnetite or ilmenite or both display visible exsolution lamellae. The term "exsolution" used herein refers to the occurrence of $Ilm\text{-}Hem_{ss}$ along {111} cubic spinel planes due to oxidation of $Usp\text{-}Mt_{ss}$, and the occurrence of $Usp\text{-}Mt_{ss}$ along {0001} rhombohedral planes due to reduction of $Ilm\text{-}Hem_{ss}$. These processes of oxidation (and reduction) generally take place at temperatures above 600°C (Haggerty, 1976, p. 18). As pointed out by Buddington and

Lindsley (1964), this is not true exsolution in the classic sense but has been adopted for lack of a better term. Some grains also display oxidation to maghemite and hematite along grain margins and fractures, possibly due to ground water movement through the ash-flow sheet (Lipman, 1971). These grains were not considered for analyses.

Previous workers tried to minimize problems of subsolidus oxidation and unmixing during devitrification by studying Fe-Ti oxide phenocrysts only from glassy rocks (Carmichael, 1967; Lipman, 1971; Hildreth, 1977). Hildreth (1977) suggested that the exsolved oxide phenocrysts in the Bishop Tuff possibly resulted from protracted cooling in fully crystalline welded zones or were due to emplacement over wet ground of the nonwelded basal portions. However, even when only glassy rocks were considered (i. e., when nonwelded basal pumice samples were compared with densely welded vitrophyre), Lipman (1971) noted that there seemed to be little correlation between degree of oxidation of magnetite phenocrysts and cooling history.

Although post-emplacement processes were no doubt operative to some extent in the Topopah Spring Member (Lipman, 1971), the following evidence is used to suggest that exsolution may have resulted from dynamic processes occurring within the magma chamber prior to or concomitant with eruption: (1) several individual pumice fragments contain both unexsolved and exsolved oxide phenocrysts; (2) entirely vitric pumice fragments from the nonwelded top and base of the ash-flow, which may have been emplaced over wet ground but were certainly not subjected to slow cooling, contain both unexsolved and exsolved oxide phenocrysts; (3) samples from the central fully crystalline (devitrified) welded zone, where protracted cooling is unequivocal, contain both unexsolved and exsolved oxide phenocrysts. Any secondary alteration process, occurring outside the magma chamber and operating on a local scale (pumice fragment or handsample), should effect all oxide phenocrysts of the same composition more or less equally. If any such process is argued to be compositionally selective, then the presence of variably effected phenocrysts is strong evidence for primary compositional differences. Although the possibility of xenocrystic contamination during emplacement must be considered for whole-rock tuff samples, this problem is avoided for individual pumice samples (Lipman, 1971).

Therefore, the exsolved Fe-Ti oxide phenocrysts in the Topopah Spring Member are interpreted to reflect disequilibrium within the magma chamber. Because the compositions of Fe-Ti oxides are extremely sensitive to changes in temperature and oxygen fugacity of the surrounding silicate liquid, if the thermal regime is perturbed, the composition of the phenocrysts will change toward equilibrium with the ambient conditions. For example, during mechanical mixing or convection, magma parcels of greatly contrasting composition and temperature are juxtaposed and may commingle. If mixing is sluggish and the thermal regime changes gradually, zoned phenocrysts may result. However, if disruption of equilibrium occurs suddenly during vigorous mixing of relatively short duration, these oxide phenocrysts may respond by internal exsolution. Carmichael (1967) cites evidence that suggests the Fe-Ti oxides do not rapidly re-equilibrate to a change in environment, and interaction between these phenocrysts and the silicate liquid may be assumed to cease at the time the liquid is quenched. Therefore, with the assumption that exsolution only effects an internal rearrangement of these oxide phenocrysts, rather than a change in bulk mineral composition, it should be possible to assess the bulk composition of a single grain.

Several previous studies have attempted to obtain bulk analyses of exsolved Fe-Ti oxide phenocrysts. In a study of Fe-Ti oxides from compositionally zoned ash-flow sheets in southwestern Nevada (Lipman, 1971), which included four reported temperatures for the Topopah Spring Member, bulk compositions of exsolved phenocrysts were obtained by separate microprobe analyses of both the exsolved lamellae and the surrounding matrix. These analyses were then combined based on estimation of the relative contribution of each to the total area of the phenocryst. Rutherford and Hemming (1978) rejected wet chemical analysis because it was apparent that more than one composition of titanomagnetite occurred in the rocks under investigation and that these phenocrysts contained abundant inclusions. Their solution was to use the scanning capability of the microprobe to analyze several sufficiently large areas across individual grains.

This study used similar method to that used by Rutherford and Hemming (1978). Multiple analyses were collected along a trace across each grain, where each analysis was performed by rastering the microprobe beam over an area of $100\mu^2$. This posed a problem in some cases because the Bence-Albee correction program used in the data reduction (Bence and Albee, 1968) assumes homogeneity of the area being analyzed. This resulted in poor totals for chemical analyses of inhomogeneous regions. Because the microprobe can only determine total iron, which is reported as FeO, it is necessary to compute a value for Fe_2O_3 in order to recast the analyses into stoichiometric oxide minerals and to assess the quality of the analyses (Carmichael, 1967). Because analyses on unexsolved oxide phenocrysts invariably yielded excellent totals, and determinations on the standard both before and after each analytical session were reproducible, the recalculated totals provide some indication of the degree of exsolution within the analyzed area.

On the average, five grains each of magnetite and ilmenite were analyzed for each sample, with an average of three analyses per phenocryst. In some highly exsolved phenocrysts, as many as 10 analyses were performed. All multiple analyses of single grains were averaged. With few exceptions, unexsolved phenocrysts were internally homogeneous and unzoned, so that averaging of multiple analyses merely increases the precision with which the bulk composition can be reported. For the exsolved phenocrysts, it was assumed that averaging of multiple analyses yields the closest approximation to the bulk composition of the grain prior to exsolution. Those analyses that could not be recast into a stoichiometric oxide phase or that yielded recalculated totals less than 95 wt% were rejected from further consideration. The remaining data set consists of ilmenite and magnetite analyses from 46 samples, of which 25 are from individual pumice samples (Table 3).

In order to strictly employ the ilmenite-magnetite geothermometer to obtain an estimated quench temperature for an individual pumice sample, it is necessary to demonstrate that a single pair of ilmenite and magnetite phenocrysts and their surrounding glass coexisted in mutual equilibrium at the time of eruption. This requirement would generally be satisfied if a single composition of magnetite and ilmenite were present within a sample. The range of 2σ uncertainties in temperature and oxygen fugacity of the solution model of Spencer and Lindsley (1981) is reported assuming $\pm$1% uncertainties in Usp_{ss} and Ilm_{ss} compositions. This is interpreted to mean that if the compositional uncertainties in Usp_{ss} and Ilm_{ss} are $\leq$1% within a single sample, then a single population of magnetite and ilmenite may be assumed. However, in the Topopah Spring Member, the average uncertainties in the mole fractions of Usp_{ss} and Ilm_{ss} within a sample are approximately 3%. It is not clear whether this variation is due to the presence of multiple magnetite and/or ilmenite populations within a sample, or whether this variation is an artifact of averaging analyses from exsolved phenocrysts. Because it is not possible to resolve this dilemma with the available data, the estimated temperatures and oxygen fugacities presented herein are intended as approximations only. All respective ilmenite and magnetite analyses within a sample have been averaged to yield an ilmenite-magnetite pair for each sample. This approach is not totally without precedent. In a discussion of coexisting iron-titanium oxides of salic volcanic rocks, Carmichael (1967) states that "As there is little to no zoning in all the oxide minerals, the bulk analysis derived from the probe data of between 15 and 20 grains should very closely approximate to their bulk composition." (Carmichael, 1967, p. 43). Although Carmichael was not referring to exsolved phenocrysts, the intra-sample variation in this study is of the same or smaller order of magnitude.

Figure 9 illustrates the range in estimated quench temperature and oxygen fugacity for the samples of the Topopah Spring Member based on the mean composition of ilmenite and magnetite phenocrysts within a

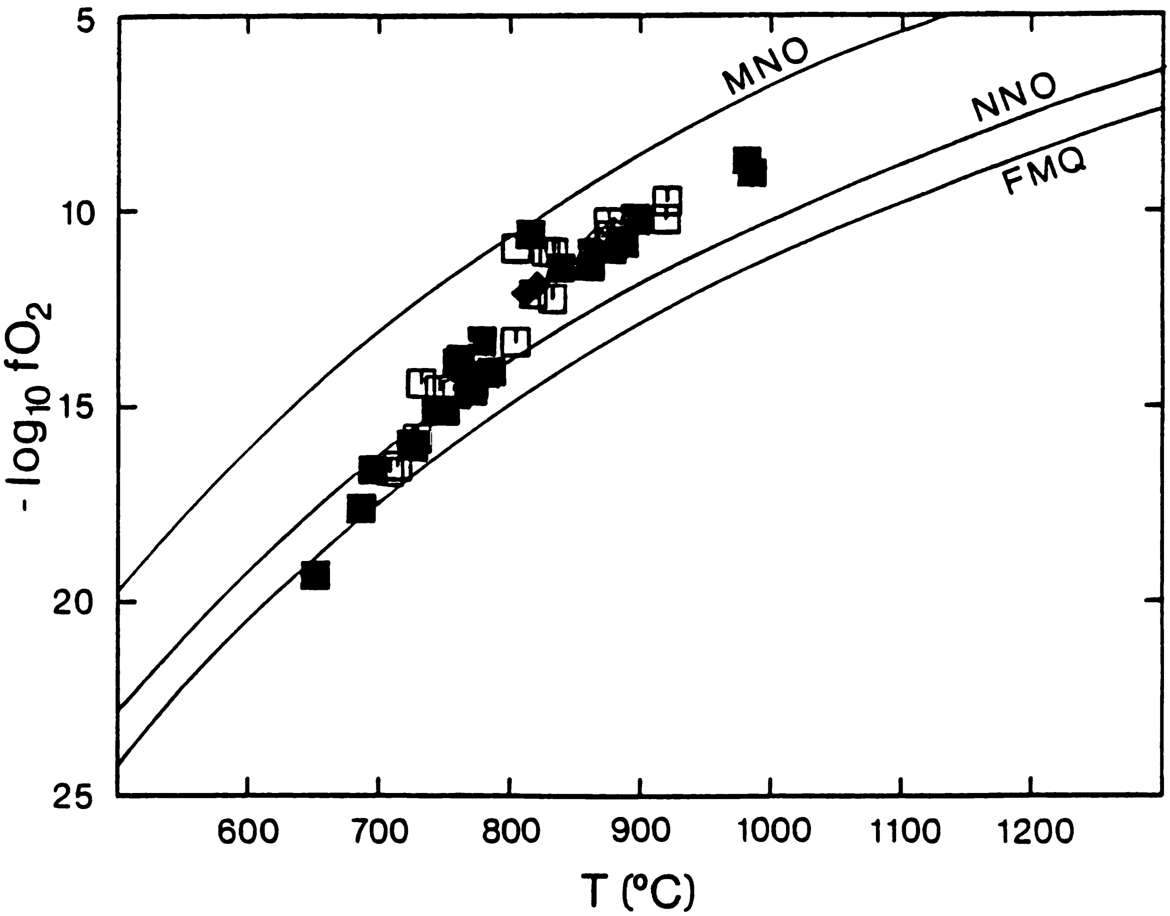

Figure 9. Estimated quench temperature and oxygen fugacity determined from coexisting ilmenite and magnetite phenocrysts. MNO, NNO, and FMQ indicate the experimental buffer curves for $MnO-Mn_3O_4$, nickel-nickel oxide, and fayalite-magnetite-quartz, respectively, at 1 bar total pressure (Haggerty, 1976).

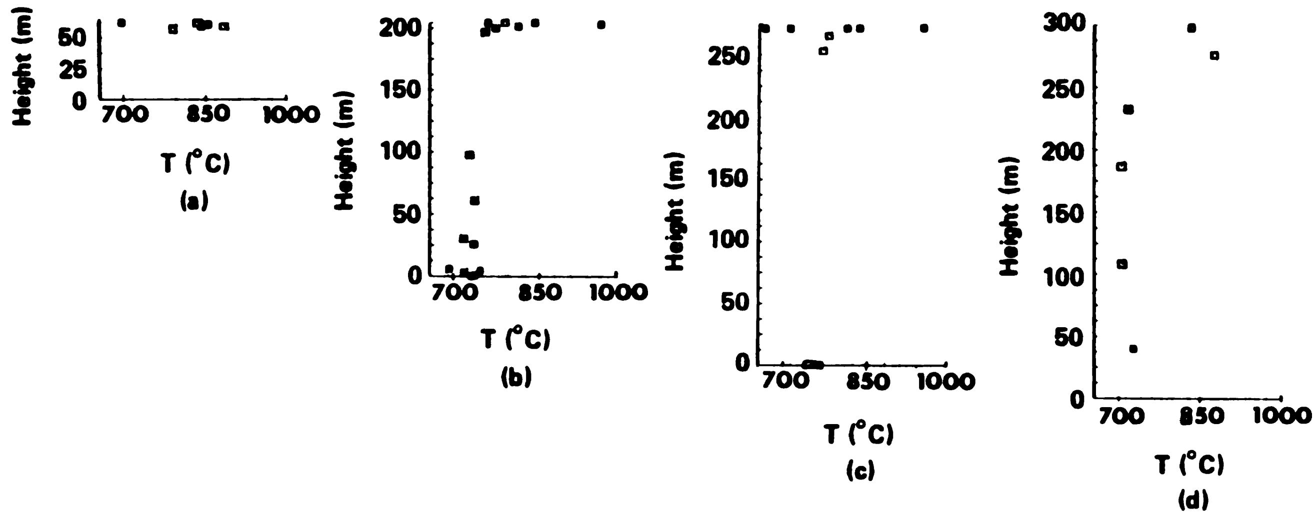

Figure 10. Estimated quench temperature of samples in relation to stratigraphic position in the ash-flow sheet. Solid symbols = whole pumice; open symbols = whole-rock tuff. (A) Lathrop Wells; (B) Busted Butte; (C) 311 Wash; (D) USW-GU3.

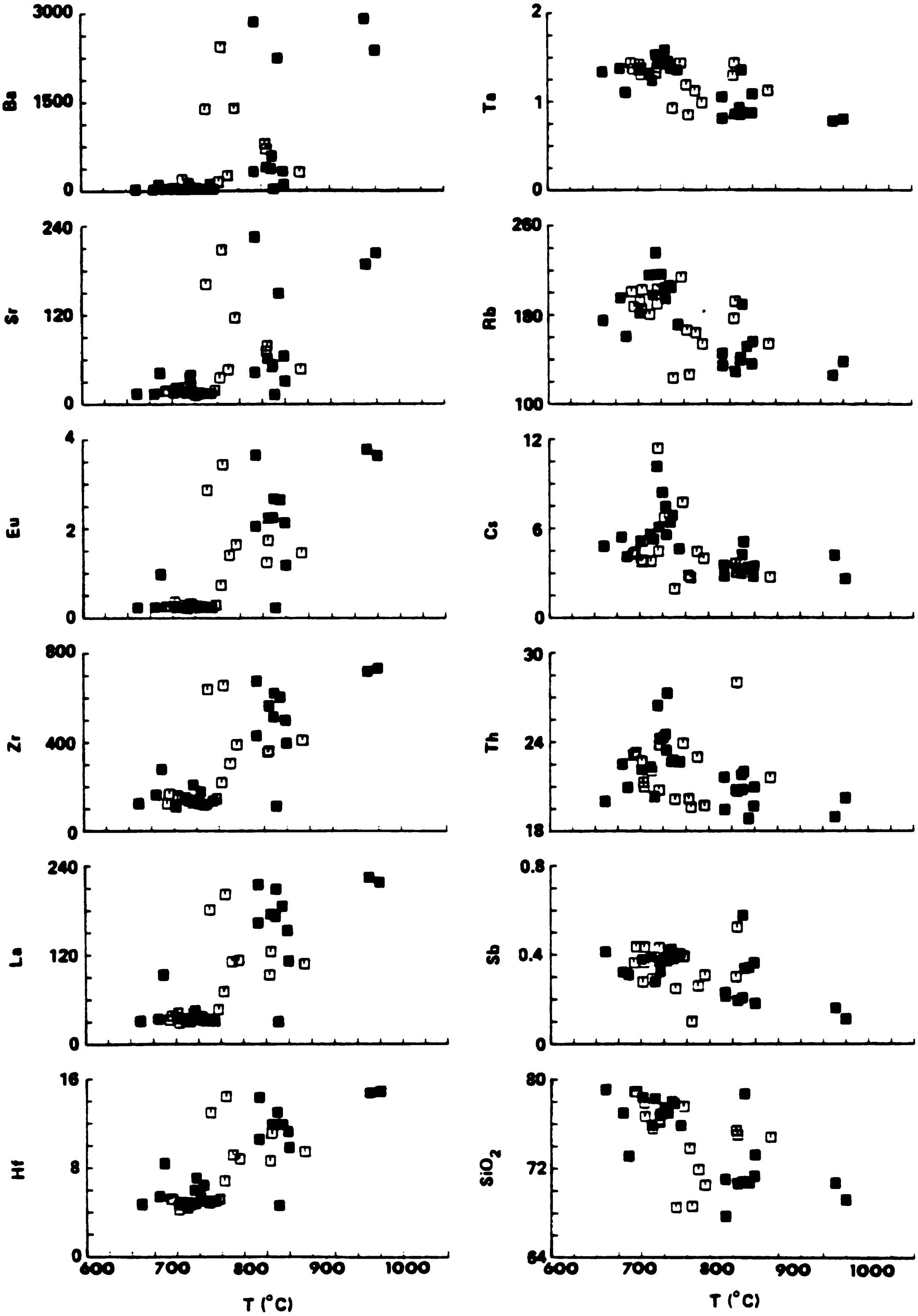

Figure 11. Chemical variation with estimated quench temperature. SiO_2 in weight %, all other elements in ppm. Solid symbols = whole pumice; open symbols = whole-rock tuff.

sample. Also included are four data points recalculated from analyses previously published by Lipman (1971). These temperatures and oxygen fugacities were calculated according to the method of Spencer and Lindsley (1981) using a modified Fortran version of their computer program TFO2. The mole fractions of ilmenite and ulvospinel were calculated according to the method prescribed by Stormer (1983), using a modified Fortran version of his computer program OXYCALC2. This latter program also calculates mole fraction values according to the schemes suggested by Carmichael (1967), Anderson (1968), and Spencer and Lindsley (1981). The deviation among these various methods has been thoroughly discussed by Stormer (1983). For the samples considered in this study, the difference in the calculated temperature and oxygen fugacity using the various methods is invariably less than the estimated model errors including the 2σ compositional uncertainty.

The temperature data in Figure 9 range from 650 to 985°C and show nearly continuous variation from approximately 700 to 900°C. Within this range, however, there appears to be a dichotomous distribution of the glassy pumice samples (solid symbols), evident by the absence of data in the interval from 786 to 812°C and the steeper slope of the oxygen fugacity trend for the lower temperature group.

As one might predict from the extreme chemical heterogeneity among pumice samples within the uppermost horizon of the ash-flow sheet, the estimated quench temperatures of individual pumice samples at this level span the entire temperature range of the eruptive sequence. Figure 10 illustrates this variation in estimated quench temperature with stratigraphic height at each of the sample locations. The open symbols, which represent samples of whole-rock tuff, show relatively little variation in quench temperature throughout the crystal-poor rhyolite, with a notable increase within the crystal rich caprock. Thus, the degree of heterogeneity in the compositions of the iron-titanium oxides and their respective temperatures, within and among pumice samples at a given stratigraphic horizon, correlate fairly well with the chemical heterogeneity at the same level.

Figure 11 illustrates the variation of several trace elements and SiO_2 with estimated quench temperature. All the trace elements show similar trends when plotted against SiO_2 (cf. Figure 8), but opposite in direction. There is considerably greater scatter in the distribution of these elements for estimated quench temperatures above 800 C, which distinguishes the two populations that correspond to the high-silica rhyolite and lower silica quartz latite samples. This is most clearly illustrated by the solid symbols which represent the glassy pumice samples. As noted previously, these two populations are more pronounced for the compatible elements and these elements are more abundant in the quartz latite. It is also apparent that the two somewhat higher estimated temperatures of 981 and 985°C correspond to pumice samples that are among the most mafic in composition.

Silicate Phenocryst and Glass Compositions

A common feature of compositionally zoned ash-flow sheets is the progressive increase in the abundance and variety of phenocrysts with stratigraphic height, which is interpreted to reflect a corresponding increase with depth in the magma body. As noted in the description of the Busted Butte section (p. 10), the variation in phenocryst content increases uniformly upward from 1 to 6% in the high-silica rhyolite, and increases to approximately 21% at the transition to quartz latitic caprock. Although the rate of increase in phenocrysts changes abruptly, Lipman et al. (1966) reported that no discontinuity in phenocryst content or in other physical aspects of the tuffs is evident at this transition, and that the changes appear to be entirely gradational. However, their description of this gradational change in phenocryst abundance is based on observations of whole-rock tuff, and therefore the exact nature of the gradient in phenocryst abundance within the magma body is not clear. In lieu of the discontinuities in chemical composition among the pumice samples, similar discontinuities in phenocryst abundance, composition, and variety may be expected to occur at the interface between magmas of contrasting composition, temperature, and water content. Whether such discontinuities are preserved or obscured would depend on the degree of interaction between the contrasting magmas. Because of the large uncertainties in modal determinations in thin sections of pumice samples with relatively few phenocrysts, the following discussion will emphasize compositional data. Descriptions of the chemical compositions of the phenocrysts will focus on those aspects that are sufficient to evaluate the hypothesis of a magmatic interface and to determine the degree of interaction (commingling) of the contrasting magmas.

Biotite

Biotite is the only ferromagnesian silicate that occurs throughout the eruptive sequence. Phenocrysts vary in abundance from approximately 0.05% in the high-silica rhyolite to 0.9% in the quartz latite, and typically occur as euhedral grains, 0.5 mm in length. Twenty four pumice samples that are representative of the total variation in pumice composition were selected for analyses. Microprobe analyses of biotite from these samples are presented in Table 4.

Individual biotite phenocrysts are relatively homogenous and unzoned, although a few grains were observed with overgrowths of a different biotite composition. This is in contrast to biotites from the Bishop Tuff, which are reported to be the most inhomogeneous phenocryst in the tuffs (Hildreth, 1977). Warren et al. (1984) report an unusual (herringbone) type of alteration for biotite in lithic fragments of the high-silica rhyolite portion of the Topopah Spring Member, and note that biotite with identical alteration is found in the groundmass of samples from this horizon. Analyses of these altered biotites (Warren et al., 1984) are 4 to 5 wt.% higher in SiO_2 than those from fresh samples, and have molecular Mg/(Mg+Fe) greater than 0.80. No such alteration textures or compositions were observed in any of the biotites from this study, which are all phenocryst separates from pumices samples. It therefore seems safe to conclude that the altered biotites were derived solely from lithic fragments and were not xenocrysts in the magma. Because individual phenocrysts are generally homogeneous, it was decided that a single analysis near the edge of the grain was the most efficient way to evaluate compositional variations among grains.

A single compositional parameter, the molecular Mg/(Mg+Fe) or Mg#, is used to facilitate comparison of the biotite analyses, as iron and magnesium display the largest variation (Barium also shows considerable variation, ranging from below detection in biotites from the high-silica rhyolite (<0.09 wt.% BaO) to a maximum of 4.68 wt.% BaO in biotites from the quartz latite). The compositional variation of all

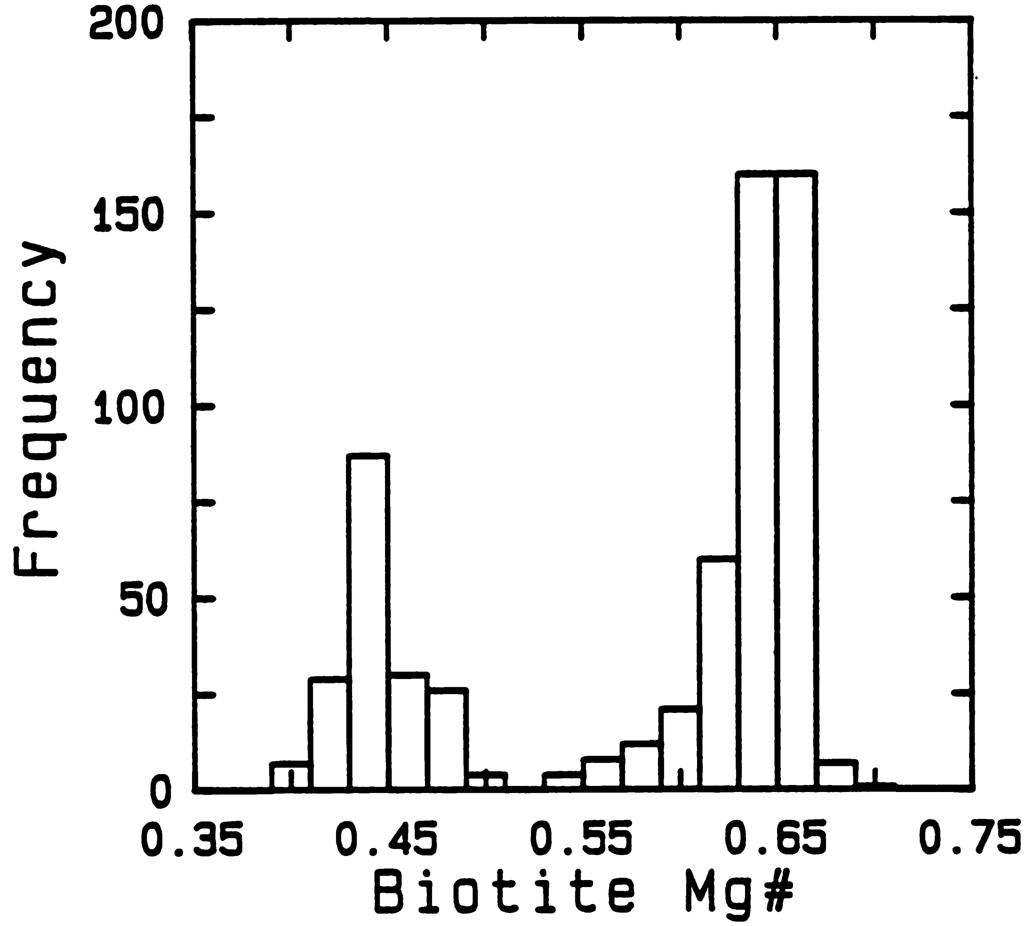

Figure 12. Histogram of Mg# for 617 biotite phenocrysts from 24 pumice samples, calculated from microprobe analyses in Table 4.

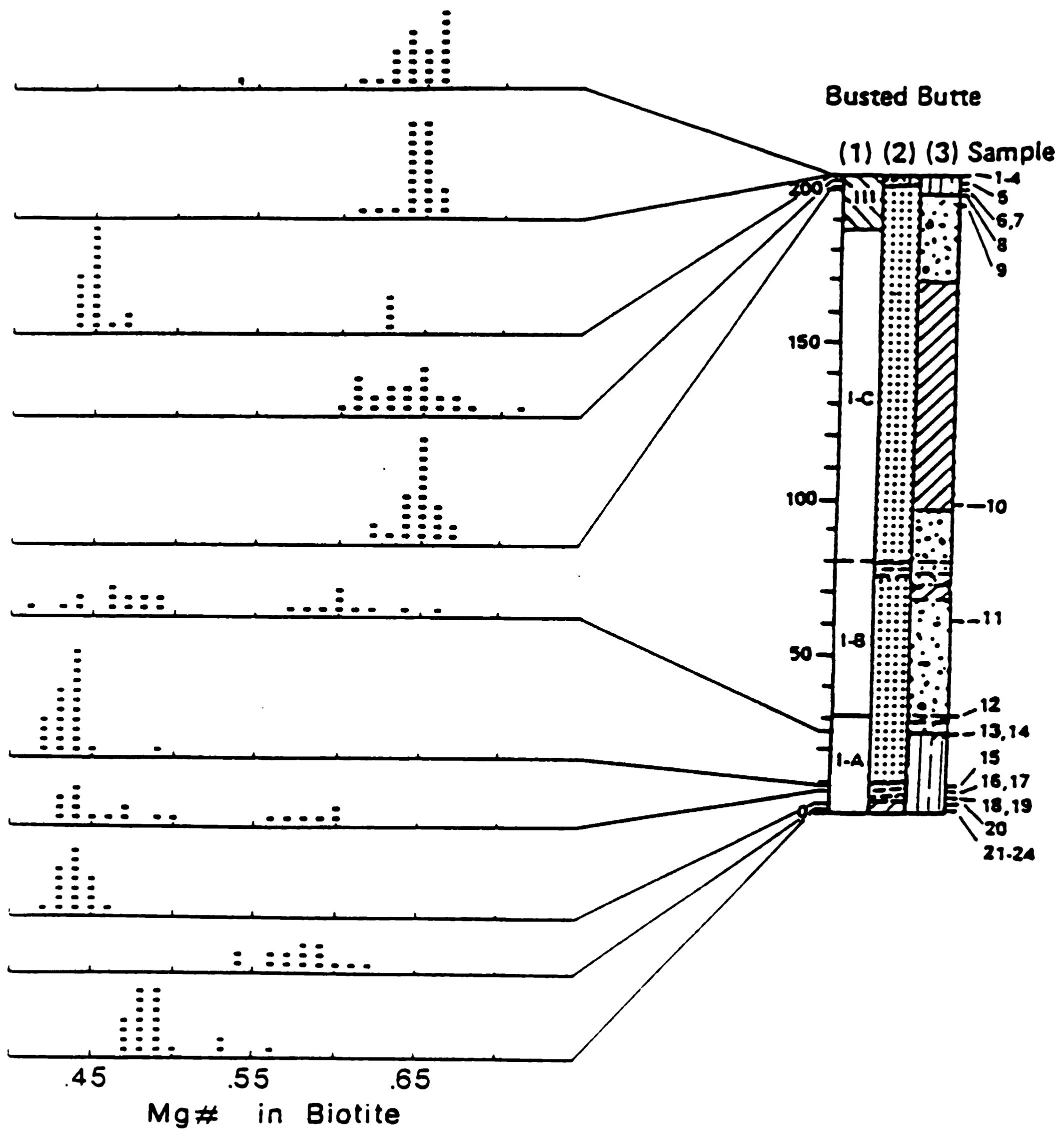

Figure 13. Mg# of biotite phenocrysts within pumice samples in relation to stratigraphic position in the Busted Butte section.

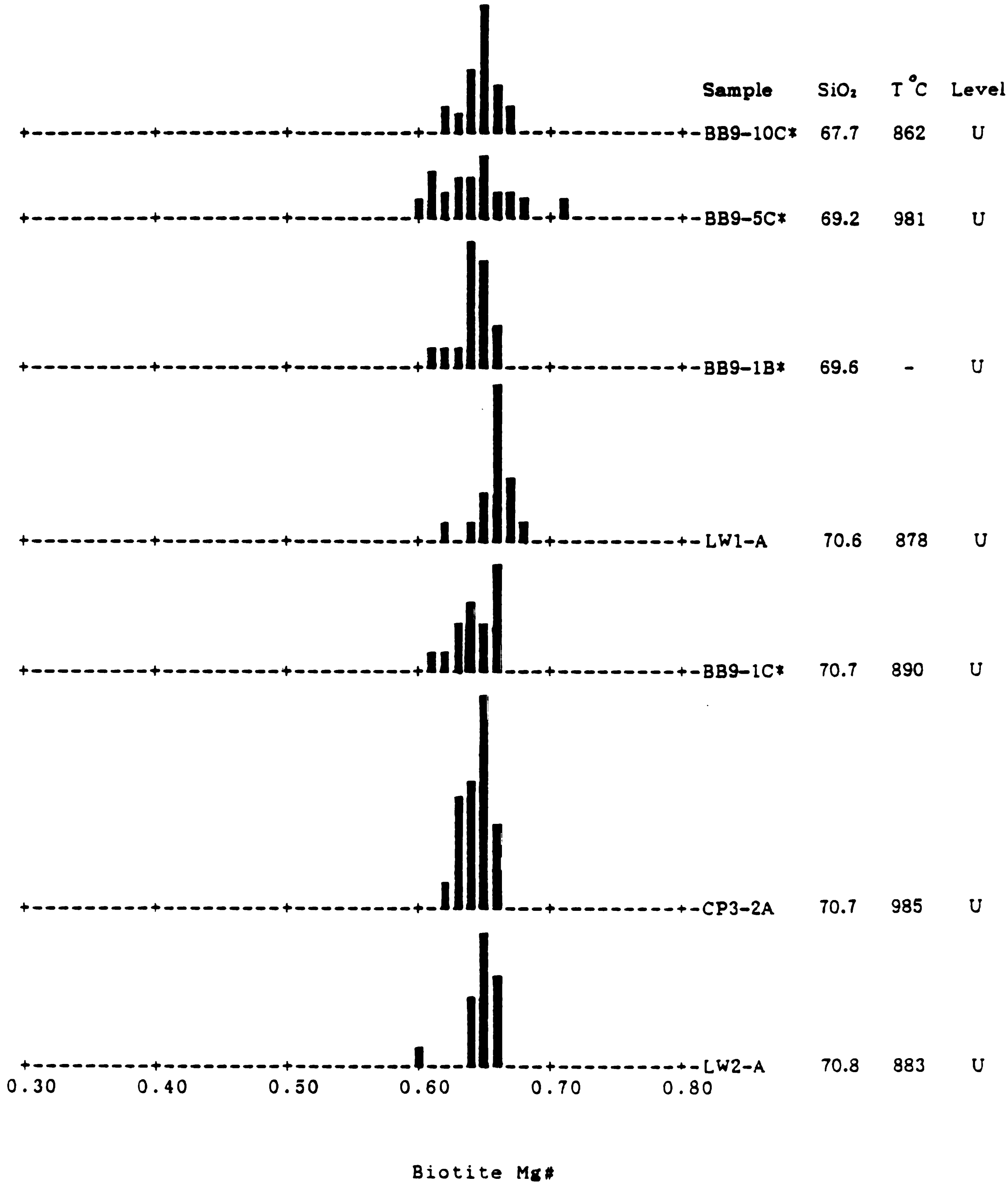

Figure 14. Mg# of biotite phenocrysts within pumice samples in relation to whole-pumice SiO_2 content, estimated quench temperature, and stratigraphic horizon (U = upper level; L = lower level). An asterisk following a sample name indicates a combined sample of texturally identical pumices (see text).

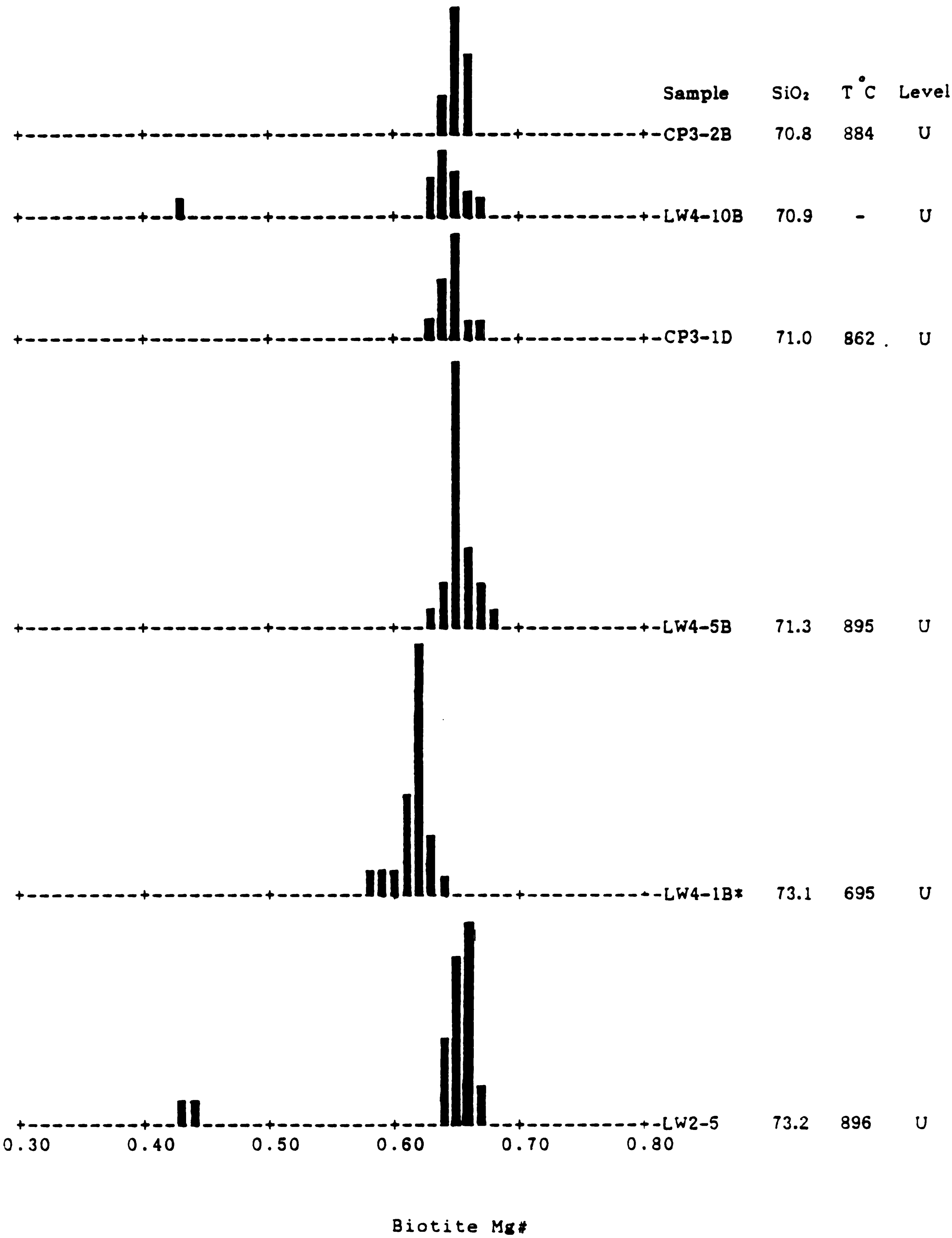
Sample
SiO2
T °C
Level
CP3-2B
70.8
884
U
LW4-10B
70.9
-
U
CP3-1D
71.0
862
U
LW4-5B
71.3
895
U
LW4-1B*
73.1
695
U
LW2-5
73.2
896
U
0.30
0.40
0.50
0.60
0.70
0.80
Biotite Mg#

Figure 14b.

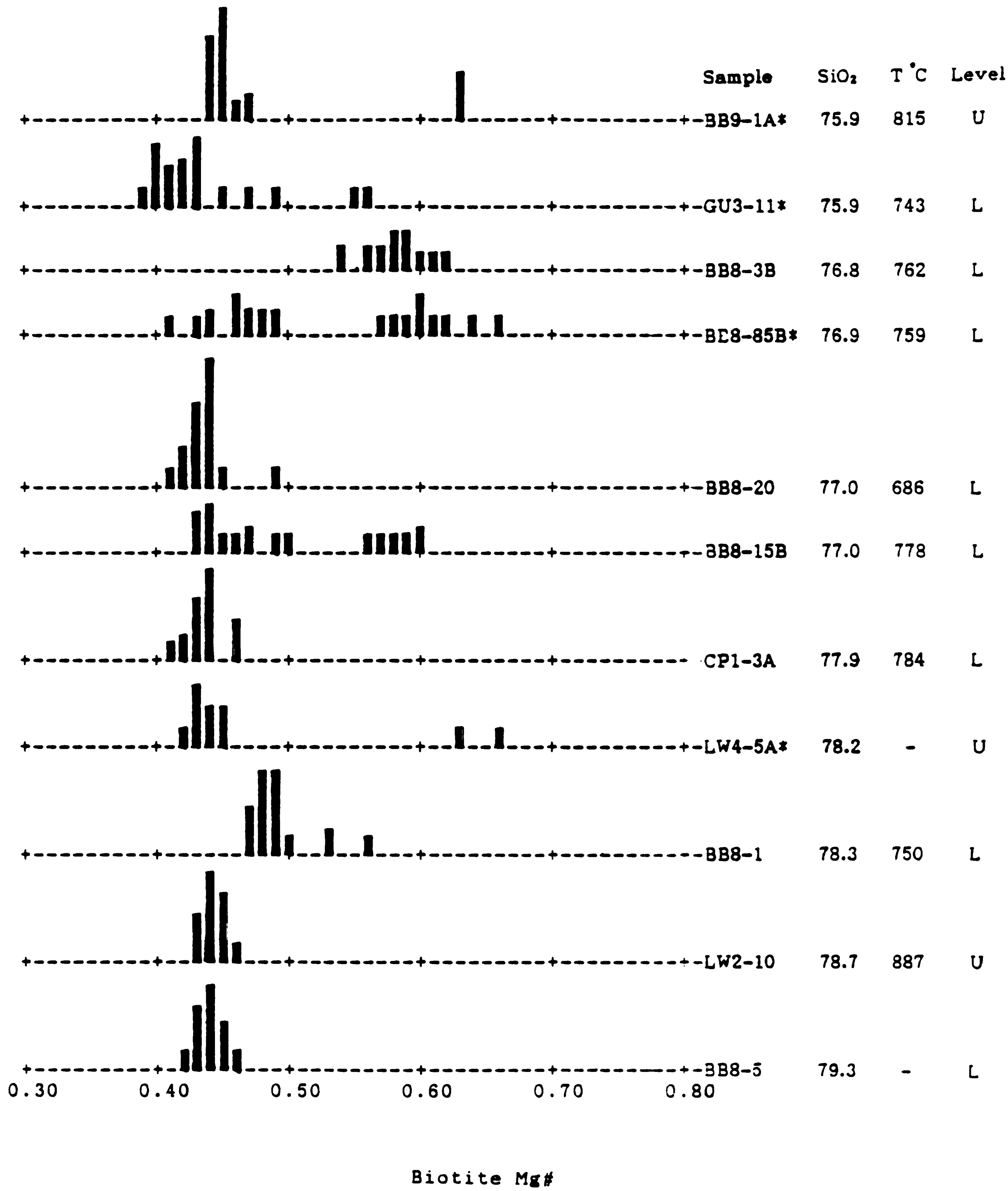
Sample SiO₂ T °C Level
BB9-1A* 75.9 815 U
GU3-11* 75.9 743 L
BB8-3B 76.8 762 L
BB8-85B* 76.9 759 L
BB8-20 77.0 686 L
BB8-15B 77.0 778 L
CP1-3A 77.9 784 L
LW4-5A* 78.2 - U
BB8-1 78.3 750 L
LW2-10 78.7 887 U
BB8-5 79.3 - L
0.30 0.40 0.50 0.60 0.70 0.80
Biotite Mg#

Figure 14c.

617 biotite analyses is presented in Figure 12. There is a total range in Mg# from 0.39 to 0.71, and a clearly bimodal distribution with modes at 0.44 and 0.65 corresponding to the high-silica rhyolite and quartz latite pumice samples, respectively. Biotites with an Mg# in the range of 0.50 to 0.60 are relatively scarce, and within this range, there is a small compositional gap between 0.50 and 0.53. This distribution of biotite compositions is interpreted to reflect the variation of liquidus conditions in the magma, and is consistent with the idea of a layered magma body. Biotites with Mg#≤0.50 were derived from the high-silica rhyolitic layer; those with Mg#≥0.60 were derived from the quartz latitic layer, and biotites within the range 0.53≤Mg#≤0.60 were derived from the interfacial region between the two magma layers.

The compositional variation of biotites within individual pumice samples is depicted in Figures 13 and 14. Figure 13 illustrates the variation of biotite Mg# in pumice samples according to their stratigraphic position in the Busted Butte section. Figure 14 displays the variation of biotite Mg# for all 24 pumice samples (11 quartz latites, 11 high-silica rhyolites, and 2 intermediate rhyolites), which are arranged in order of decreasing whole-pumice silica content. All of the quartz latite pumice samples (67.7-71.3 wt.% SiO_2) contain biotites with Mg# ≥ 0.60, with the exception of LW4-10B which also has a single biotite with an Mg# of 0.43. In contrast, all of the high-silica rhyolite pumice samples (≥75 wt.% SiO_2) contain biotites that generally have Mg# ≤ 0.60.

Several of the pumice samples contain a few biotites that have compositions distinctly different from the dominant population or display a bimodal distribution. Although the implication of a disequilibrium phenocryst assemblage is clear, extreme caution must be exercised in this interpretation here. It was noted in an earlier section that several of the pumice samples are combinations of texturally identical pumices fragments, necessitated because of their small size. It is emphasized that the colors of the glass of the different pumice types are sufficiently distinct that the choice of which pumice fragments to combine is straightforward, and it is highly unlikely that pumice fragments from the extremes of the compositional range were combined. While the author has a high degree of confidence that the pumice fragments that were combined were in fact identical, the subjective nature of this choice, and the simple fact that they are not single parcels of quenched magma, makes suspect any attempt to interpret variations within these samples. Therefore, although the heterogeneities are not considered to be artificially induced, the combined samples are indicated by an asterisk to allow the reader to ignore them if desired. In this paper, any of the conclusions based on heterogeneities within samples, will rest firmly on evidence from single, uncombined pumice samples.

In Figure 14, five of the nine combined pumice samples display unimodal biotite compositions, so that no artificial heterogeneity appears to have been induced in these samples. Four of these are quartz latites (BB9-10C, BB9-5C, BB9-1B, and BB9-1C), and the fifth sample (LW4-1B) falls between the quartz latite and high-silica groups at 73.1 wt.% SiO_2. Ten of the samples in Figure 14 display either a bimodal distribution or a sufficient range in biotite composition to be considered as evidence for magma mixing or commingling. All four of the combined pumice samples that display phenocryst heterogeneity are high-silica rhyolites, and in two of these samples (BB9-1A, LW4-5A), the expected low Mg# biotites predominate, with only a few biotites in the range of Mg# 0.63 to 0.66. Both of these samples occur within the upper few meters of the ash-flow sheet and are interpreted to reflect limited commingling of the high-silica rhyolitic and quartz latitic magmas during the final stages of the eruption. The other two combined samples that display heterogeneity (BB8-85B and GU3-11) are fiamme from the lower portions of the ash-flow sheet (cf. samples 14 and 64 in Figure 2). The majority of biotites in sample GU3-11 occur within the Mg# range expected for the high-silica rhyolites, and the small amount of heterogeneity is interpreted to indicate commingling of high-silica rhyolitic magma with magma from the interfacial region. Sample BB8-85B clearly displays a bimodal distribution of biotite compositions, with nearly half of the biotite analyses having an Mg# that indicates derivation from the quartz latitic magma and the region near the magmatic interface. Even if one denies the possibility that this sample represents commingled magma because it is a combined sample, the fact that biotites with Mg# $\geq$ 0.60 occur at this level suggests that some of the quartz latitic magma was deposited relatively early during the eruption.

There are six uncombined, single pumice samples shown in Figure 14 that contain a heterogeneous distribution of biotite phenocrysts, and are considered to be unequivocal evidence of magma commingling on the scale of a single pumice fragment (LW4-10B, LW2-5, BB8-3B, BB8-20, BB8-15B, and BB8-1). Sample LW4-10B is a quartz latite pumice fragment with all but one of the biotites having Mg# > 0.6; the single biotite with an Mg# of 0.43 is characteristic of biotites from the high-silica rhyolite. Similarly, sample LW2-5 is dominated by biotites in the range of Mg# 0.64 to 0.67, with only four biotites in the range of Mg# 0.43 to 0.44. The phenocryst heterogeneity in this sample (LW2-5, 73.2 wt.% SiO_2) is particularly noteworthy in that it supports the hypothesis that the few pumice samples that occur in the interval of the previously noted compositional gap between the quartz latite and the high-silica rhyolite (71.8 to 74.7 wt.% SiO_2) formed from limited mixing of the two contrasting magma types. The other pumice sample that occurs in this interval (LW4-1B, 73.1 wt.% SiO_2), appears to have a unimodal distribution of biotite compositions, although the mean Mg# is slightly lower than that of the quartz latites, and several biotites have Mg# < 0.60. The difference in biotite compositions between these two intermediate samples may reflect a difference in the relative positions of the end member magmas in the chamber (i.e., distant from or close to the interfacial region), and hence, in the timing and the degree of equilibrium attained after the mixing event ("commingled" versus "mixed"). Samples BB8-20, BB8-1, BB8-3B, and BB8-15B are all high-silica rhyolites, and the heterogeneous distribution of biotites within these samples is indicative of commingling of magma from various positions within the rhyolitic layer, and of commingling of high-silica rhyolitic magma with magma from the interfacial region and the quartz latitic magma.

In summary, the following conclusions may be drawn from the compositions of biotite phenocrysts and their distribution within and among single pumice samples: (1) the bimodal distribution of biotite compositions from the high-silica rhyolite (Mg#=0.44) and the quartz latite (Mg#=0.65) pumice samples, and the relative scarcity of compositions in the interval from 0.5 to 0.6, supports the hypothesis that the transition from high-silica rhyolitic to quartz latitic magma within the chamber was abrupt, with a liquid-liquid interface separating the two contrasting magma types; (2) biotites within the high-silica rhyolite pumice samples range from Mg# 0.39 to 0.50, suggesting that the high-silica rhyolitic magma was zoned, and that biotites in the range of Mg# 0.53 to 0.6 crystallized near the interface; (3) the occurrence of biotites with Mg# $\geq$ 0.6 in the lower horizon of the ash-flow sheet, indicates that plumes of quartz latitic magma may have risen into the high-silica rhyolitic magma during early stages of the eruption; (4) the presence of biotite phenocrysts from the extremes of the compositional range, within single pumice fragments, provides evidence that limited magma mixing or commingling between the high-silica rhyolitic and quartz latitic magma occurred during the eruption.

Pyroxene

Consistent with the hypothesis of a magmatic interface is the ubiquitous occurrence of pyroxene phenocrysts in all of the quartz latitic pumice samples, and the notable lack of pyroxene in the high-silica rhyolitic pumice samples. Of the 24 pumice samples in which biotites were analyzed, 14 contain pyroxene and only one of these is a high-silica rhyolite (LW4-5A). Not surprisingly, only one pyroxene grain was found in this high-silica rhyolitic pumice sample, which also contains a bimodal distribution in biotite composition.

In the quartz latite, euhedral pyroxene phenocrysts average 0.5 mm in length and reach an abundance of approximately 0.4%. Microprobe analyses of the edges of pyroxene phenocrysts are presented in Table 5.

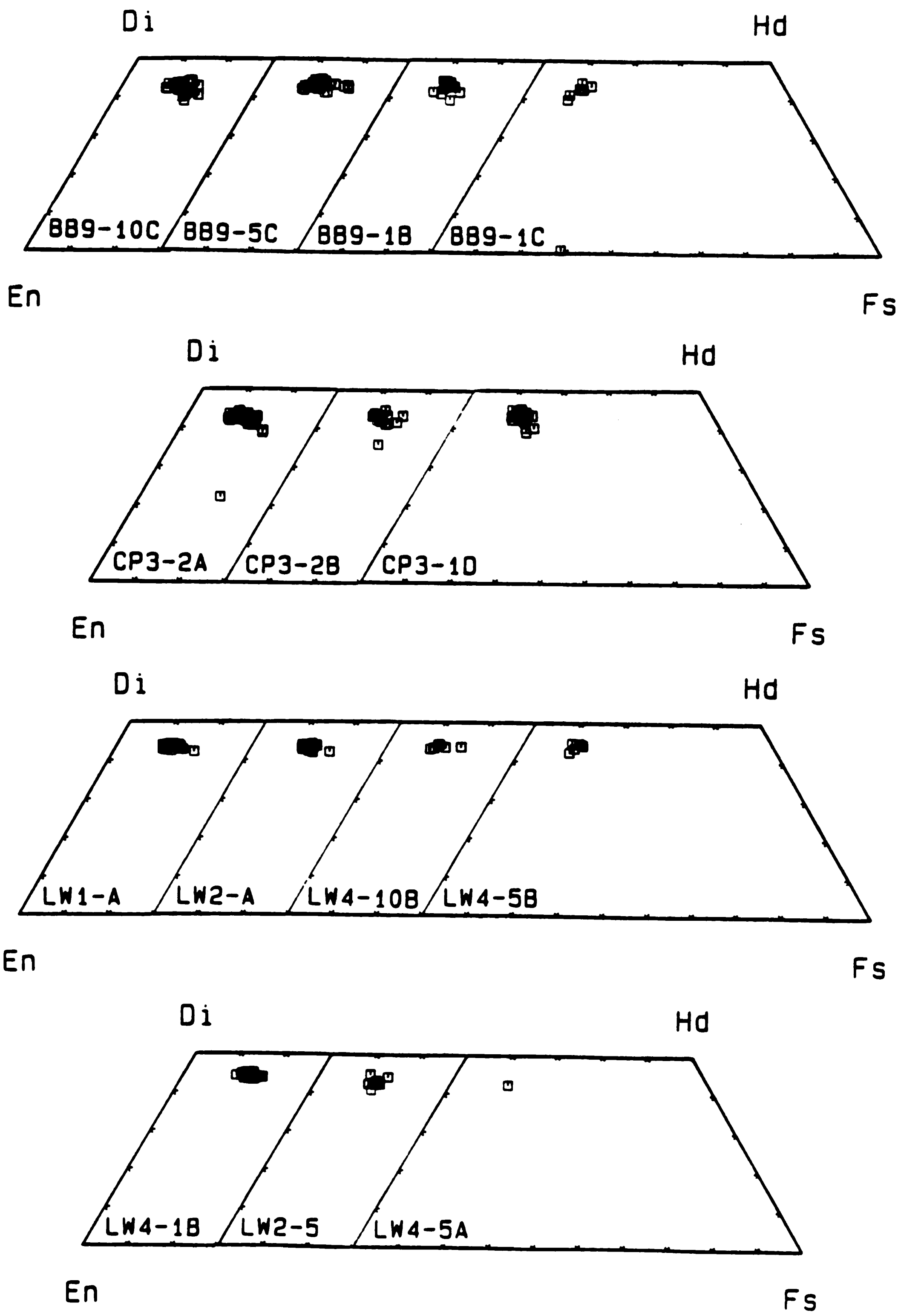

Figure 15. Compositional variations of pyroxene phenocrysts within pumice samples; data from microprobe analyses in Table 5.

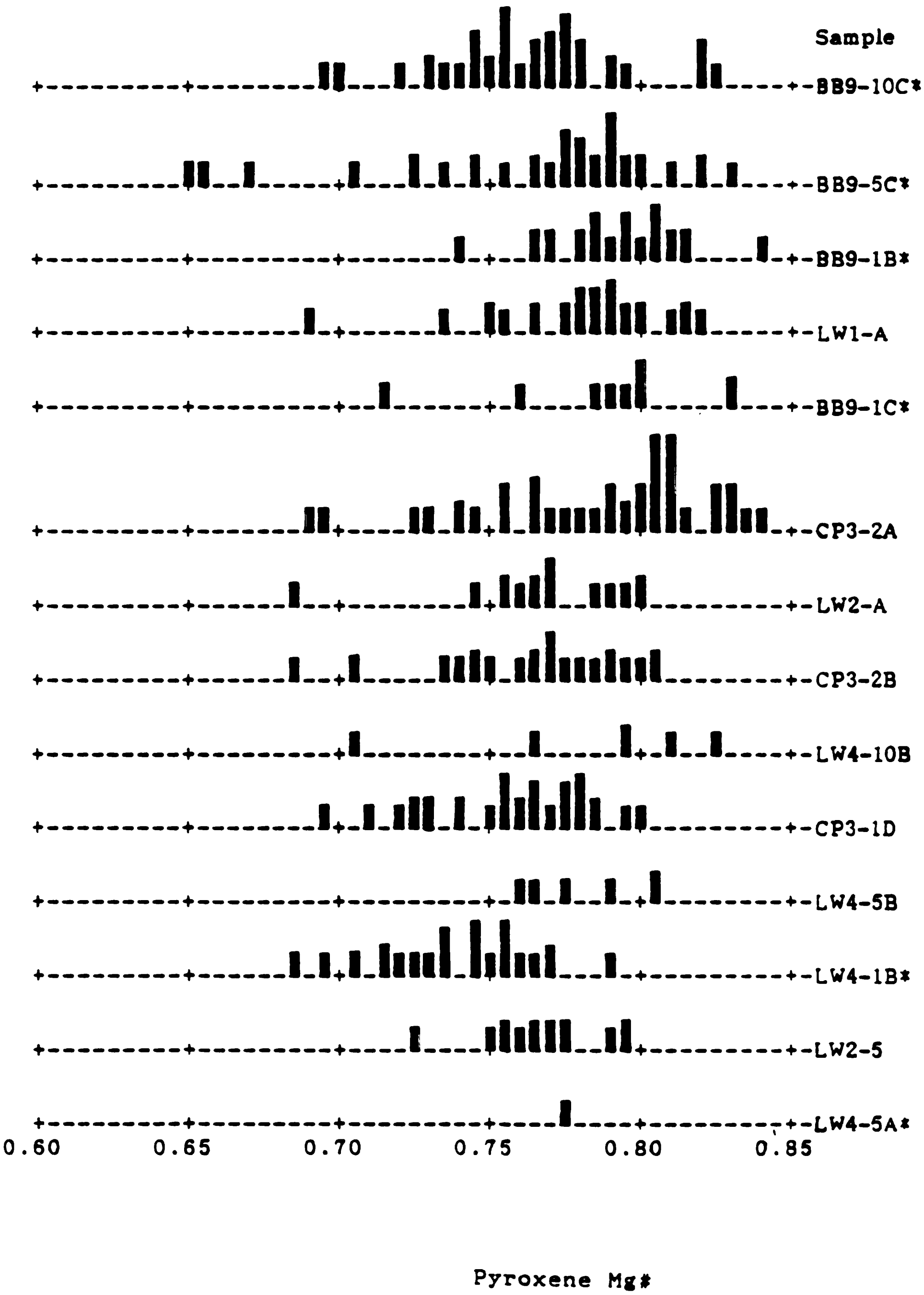

Sample	SiO_2	T°C	Level
BB9-10C*	67.7	862	U
BB9-5C*	69.2	981	U
BB9-1B*	69.6	-	U
LW1-A	70.6	878	U
BB9-1C*	70.7	890	U
CP3-2A	70.7	985	U
LW2-A	70.8	883	U
CP3-2B	70.8	884	U
LW4-10B	70.9	-	U
CP3-1D	71.0	862	U
LW4-5B	71.3	895	U
LW4-1B*	73.1	695	U
LW2-5	73.2	896	U
LW4-5A*	78.2	-	U

Figure 16. Mg# of pyroxene phenocrysts within pumice samples in relation to whole-pumice SiO_2 content, estimated quench temperature, and stratigraphic horizon (U = upper level; L = lower level). An asterisk following a sample name indicates a combined sample of texturally identical pumices (see text).

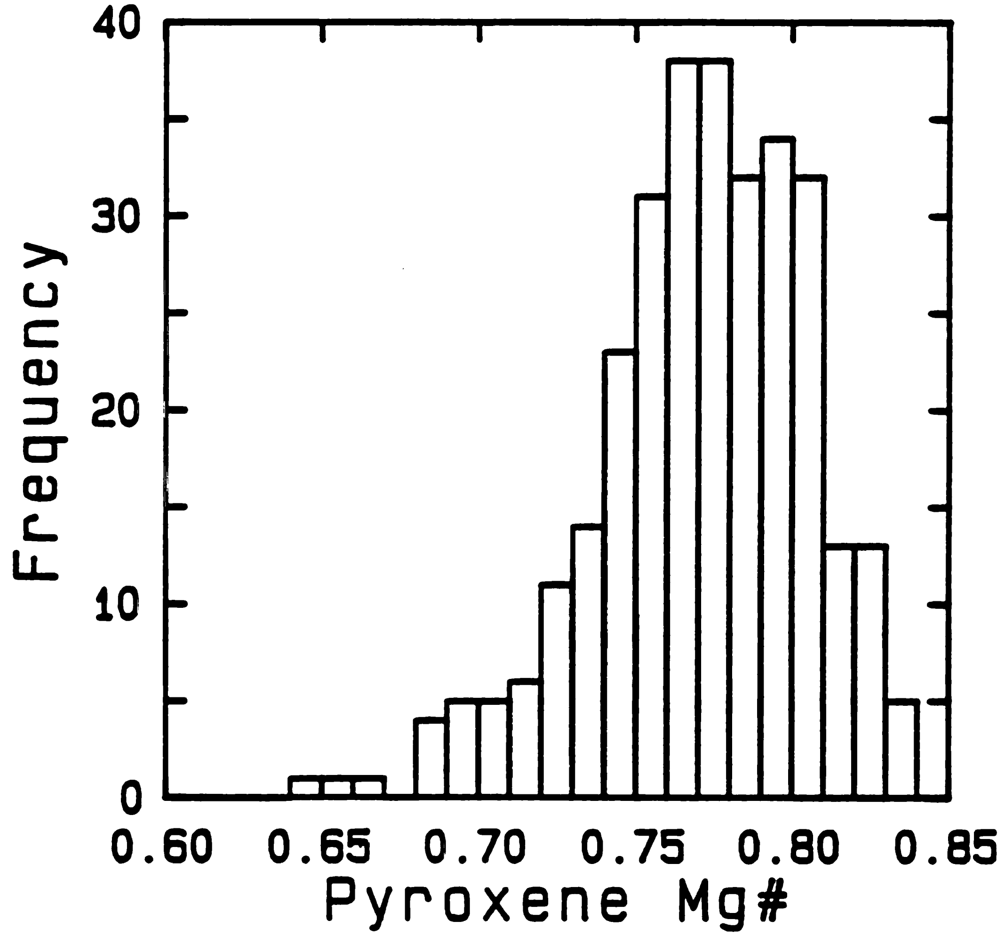

Figure 17. Histogram of Mg# for 307 pyroxene phenocrysts from 14 pumice samples, calculated from microprobe analyses in Table 5.

The compositional ranges of pyroxenes within pumice samples are illustrated in Figures 15 and 16. All but two of the pyroxene analyses plot in the augite field (Figure 15), the exceptions being a subcalcic augite (CP3-2A) and a clinohypersthene (BB9-1C). Although there is considerable scatter in the iron-magnesium ratios of the pyroxenes (Figure 16), the mean Mg# of the pyroxenes within each pumice sample falls within a relatively narrow range between 0.74 and 0.79 and lies within one standard deviation of the mean for all pyroxene analyses (Figure 17).

Hornblende

Of the 24 pumice samples in which ferromagnesian silicates were analyzed, only four were observed to contain hornblende. Previous studies of the Topopah Spring Member (Lipman et al., 1966; Byers et al., 1976) reported the presence of trace amounts of hornblende in the quartz latitic caprock only. However, three of the four pumice samples that contain hornblende are high-silica rhyolites, and two of these are from the base of the ash-flow sheet. Microprobe analyses of the hornblende phenocrysts are presented in Table 6, and their compositional variation in terms of Mg# is plotted in Figure 18. Because of the paucity and erratic distribution of hornblende in the pumice samples, they are of little use in evaluating the hypothesis of a magmatic interface.

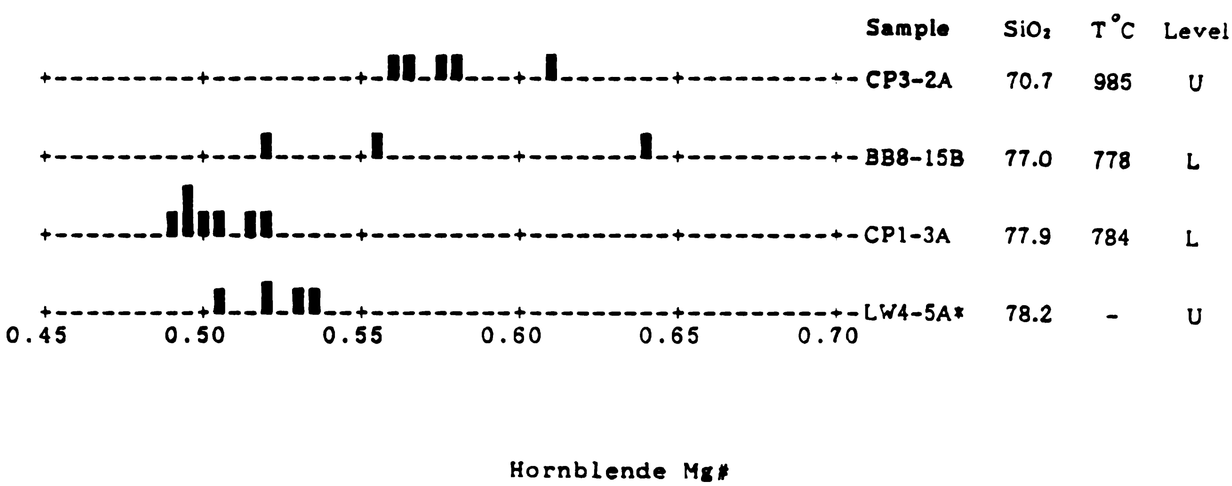

Figure 18. Histogram of Mg# for 22 hornblende phenocrysts from 4 pumice samples, calculated from microprobe analyses in Table 6.

Feldspar

Plagioclase and sanidine together make up approximately 90% of the total phenocryst assemblage in both the high-silica rhyolite and the quartz latite. Plagioclase abundances vary from 0.5% in the high-silica rhyolite to 7.3% in the quartz latite and sanidine abundances vary from 0.4% in the high-silica rhyolite to 11.6% in the quartz latite. Both feldspars occur as well formed crystals averaging 1 mm in length, however, sieve textures and embayed crystal faces are common, particularly in phenocrysts from quartz latitic pumice samples. Microprobe analyses of plagioclase and sanidine phenocrysts are presented in Tables 7 and 8, respectively.

The compositional variations of the feldspars are complex, due in part to the strong zoning profiles in some of the phenocrysts. The zoning profiles of plagioclase and sanidine phenocrysts from four pumice samples are shown in Figures 19 and 20. The data points in each ternary diagram are from a single phenocryst, with the smaller symbols representing analyses of phenocryst centers and the larger symbols representing analyses of phenocryst edges. In Figure 21, each ternary diagram illustrates the variation of only the edge compositions of feldspar phenocrysts within a single pumice sample. The samples depicted in Figure 21 span the entire range in whole-pumice chemical compositions. Although the variation of feldspar edge compositions within pumice samples is relatively large, and there is overlap between samples, it is possible to distinguish a dominant edge composition that is presumed to be the equilibrium composition for a given pumice sample. In general, the plagioclase in the quartz latitic pumice samples is more calcic, less sodic, more potassic, and contains more

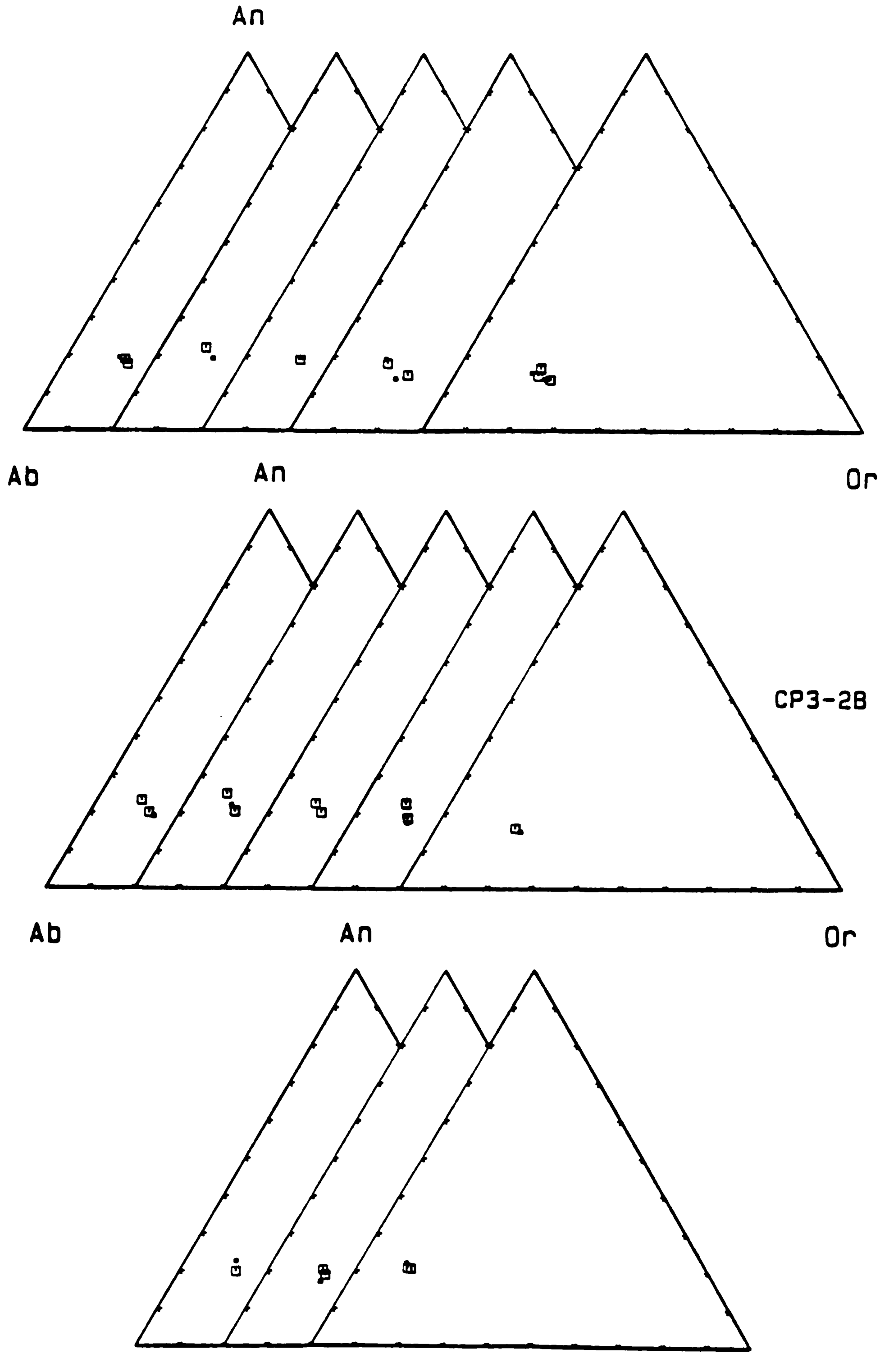

Figure 19. Zoning profiles in plagioclase phenocrysts from pumice samples. Each ternary diagram represents a single phenocryst. Large open squares = edge analyses; small asterisks = center analyses.

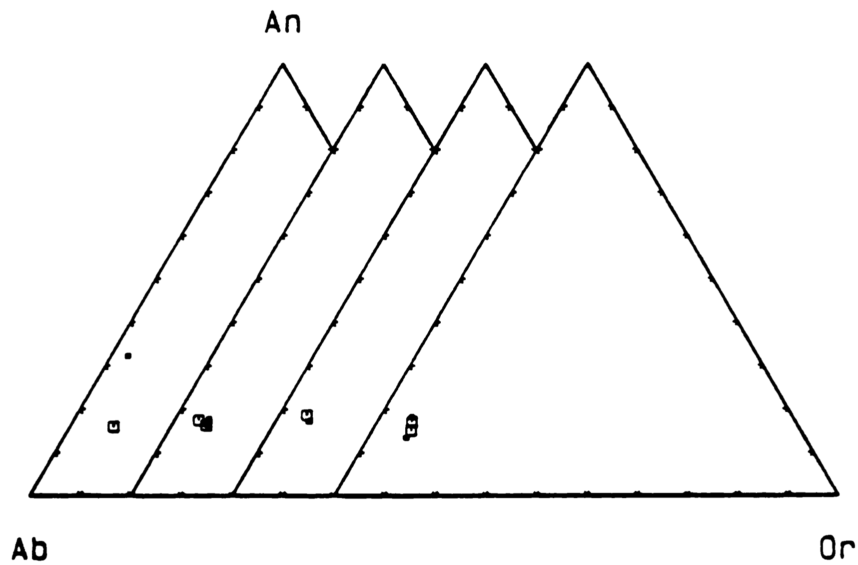

888-158

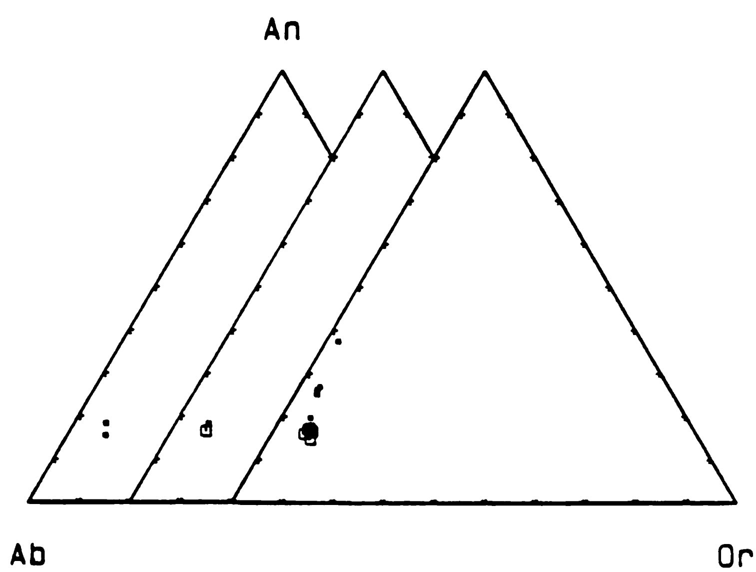

Figure 19 (cont'd.).

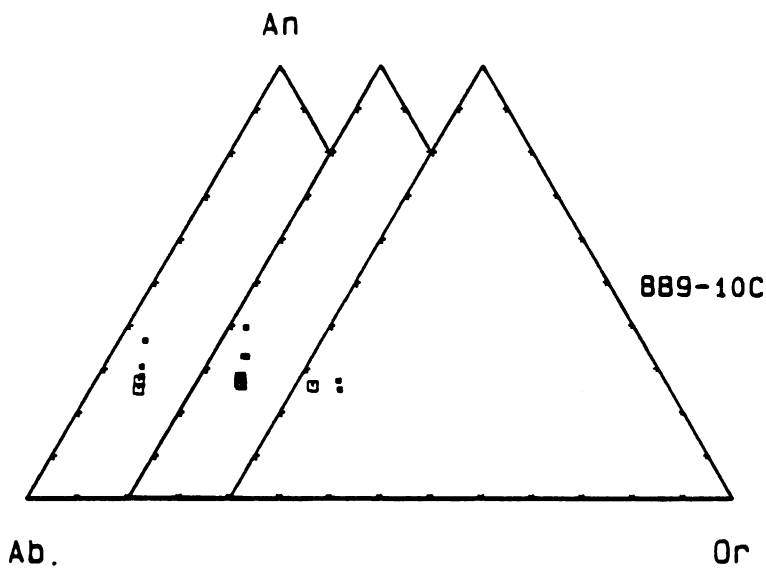

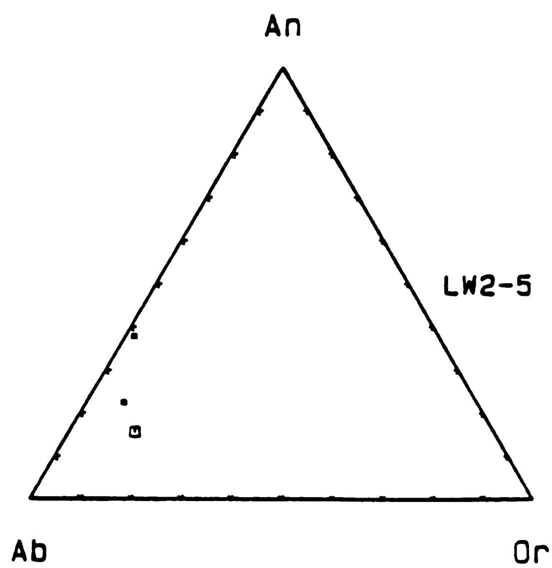

Figure 19 (cont'd.).

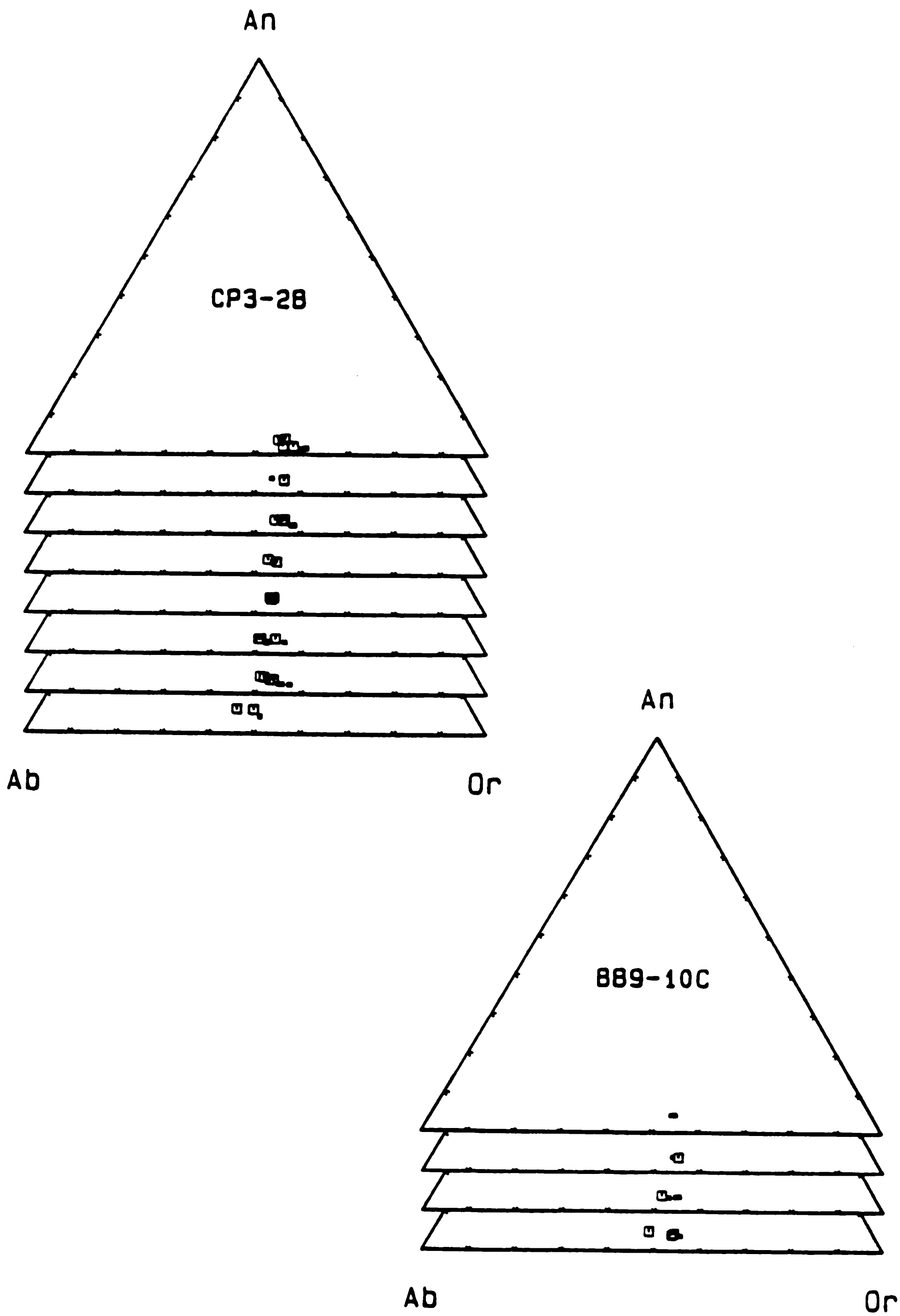

Figure 20. Zoning profiles in sanidine phenocrysts from pumice samples. Each ternary diagram represents a single phenocryst. Large open squares = edge analyses; small asterisks = center analyses.

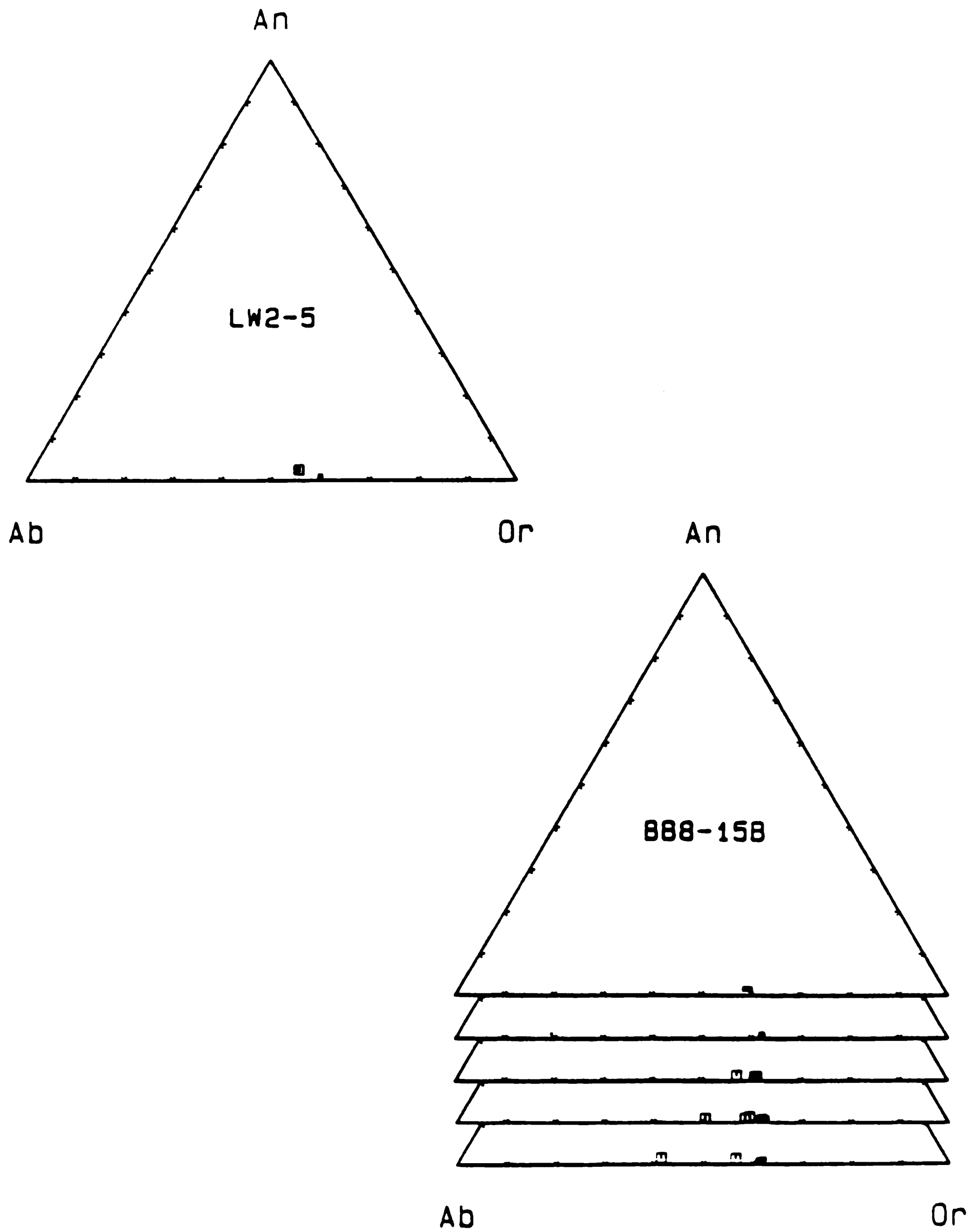

Figure 20 (cont'd.).

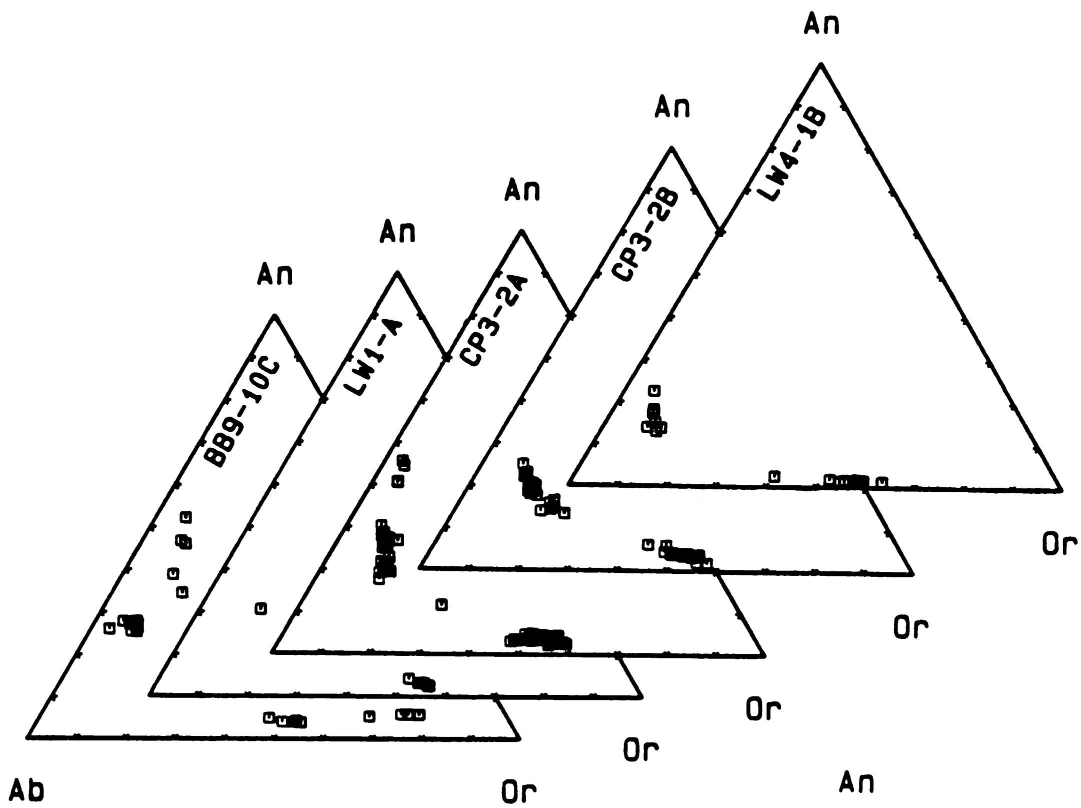

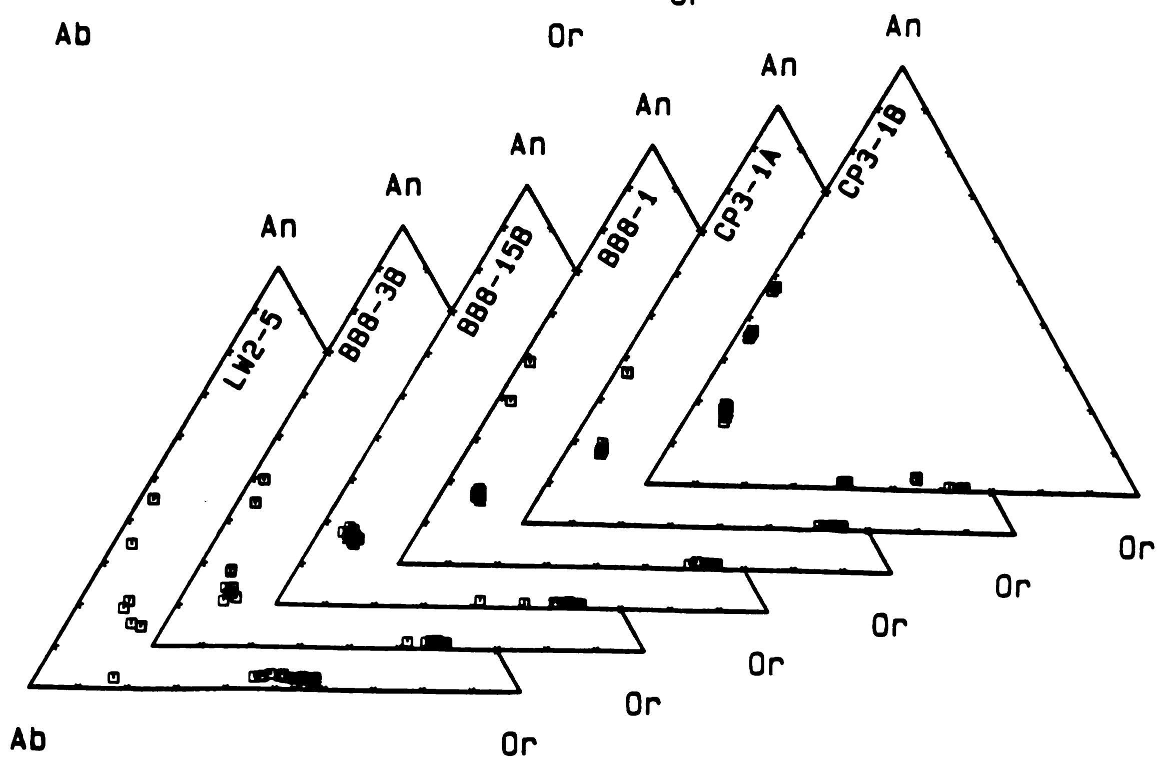

Figure 21. Compositional variations of microprobe edge analyses of feldspar phenocrysts within pumice samples. Data from Tables 7 and 8.

barium than the plagioclase in the high-silica rhyolitic pumice samples. Sanidine in the quartz latitic pumice samples is more calcic, more sodic, less potassic, and contains more barium than the sanidine in the high-silica rhyolitic pumice samples. For example, the dominant plagioclase composition in quartz latitic pumice CP3-2A is $An_{26}Ab_{64}Or_{10}$ compared with $An_{17}Ab_{76}Or_{7}$ for high-silica rhyolitic pumice BB8-1. Similarly, the dominant sanidine composition in CP3-2A is $An_{4}Ab_{42}Or_{54}$ compared with $An_{1}Ab_{37}Or_{62}$ for BB8-1. These compositional differences between feldspars from the quartz latitic and high-silica rhyolitic pumice samples are consistent with the interpretation that the magmatic liquid was compositionally stratified before the onset of crystallization. Furthermore, the compositional differences among feldspars within single pumice samples provide additional evidence of magma commingling during eruption.

Glass Compositions

A knowledge of the liquid composition of the Topopah Spring magma is crucial in evaluating the hypothesis that the magma body was layered. Bubble walls of glassy pumice fragments provide the closest approximation to quenched samples of the liquid portion of the magma, and can be easily analyzed using the microprobe, thereby avoiding problems of obtaining clean glass separates and allowing determination of the degree of homogeneity of the glass within a pumice fragment. Microprobe analyses of bubble walls from 10 representative pumice samples are presented in Table 9.

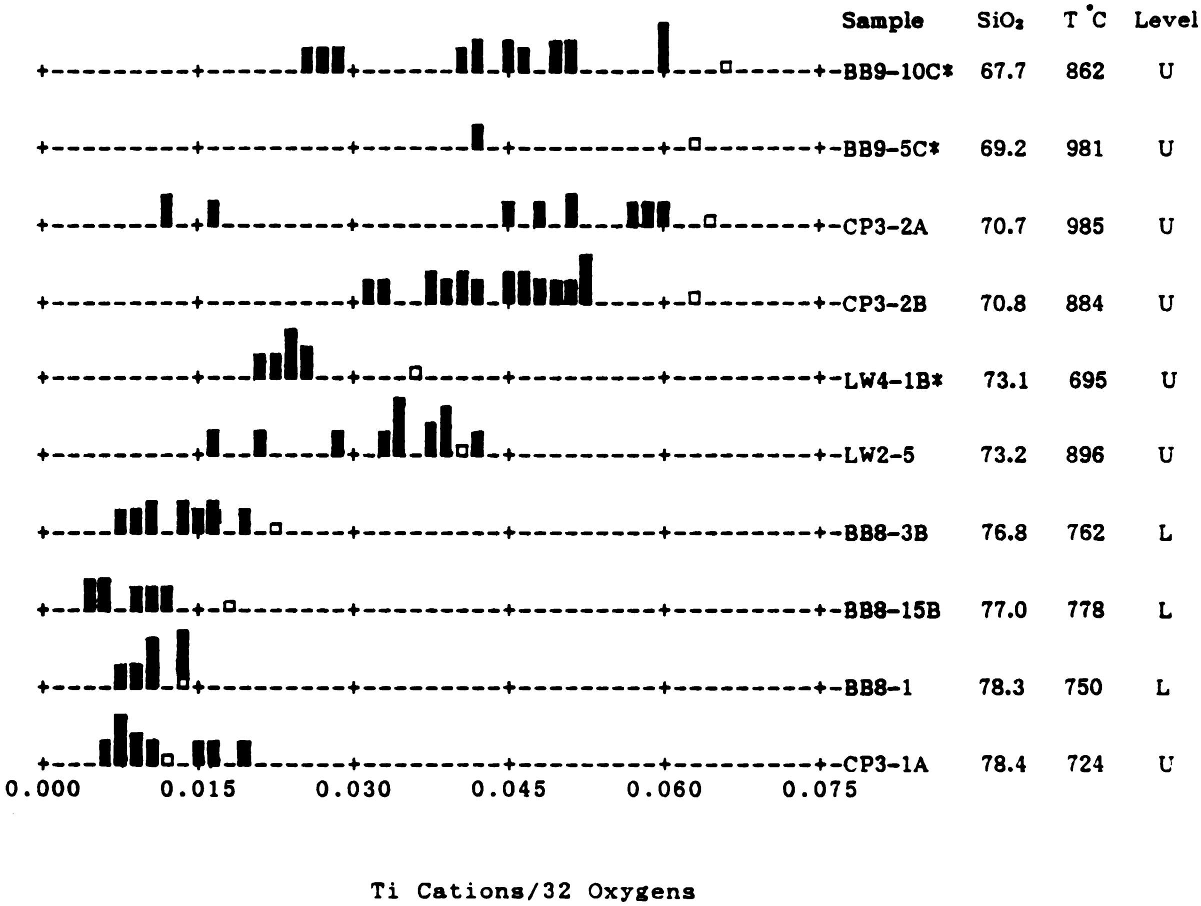

Figure 22. Histograms showing compositional variations in titanium in the bubble walls of pumice samples. Ti cations calculated on the basis of 32 oxygens from microprobe data in Table 9. Light colored square on baseline shows the composition of the whole-pumice calculated on the same basis from the data in Table 2.

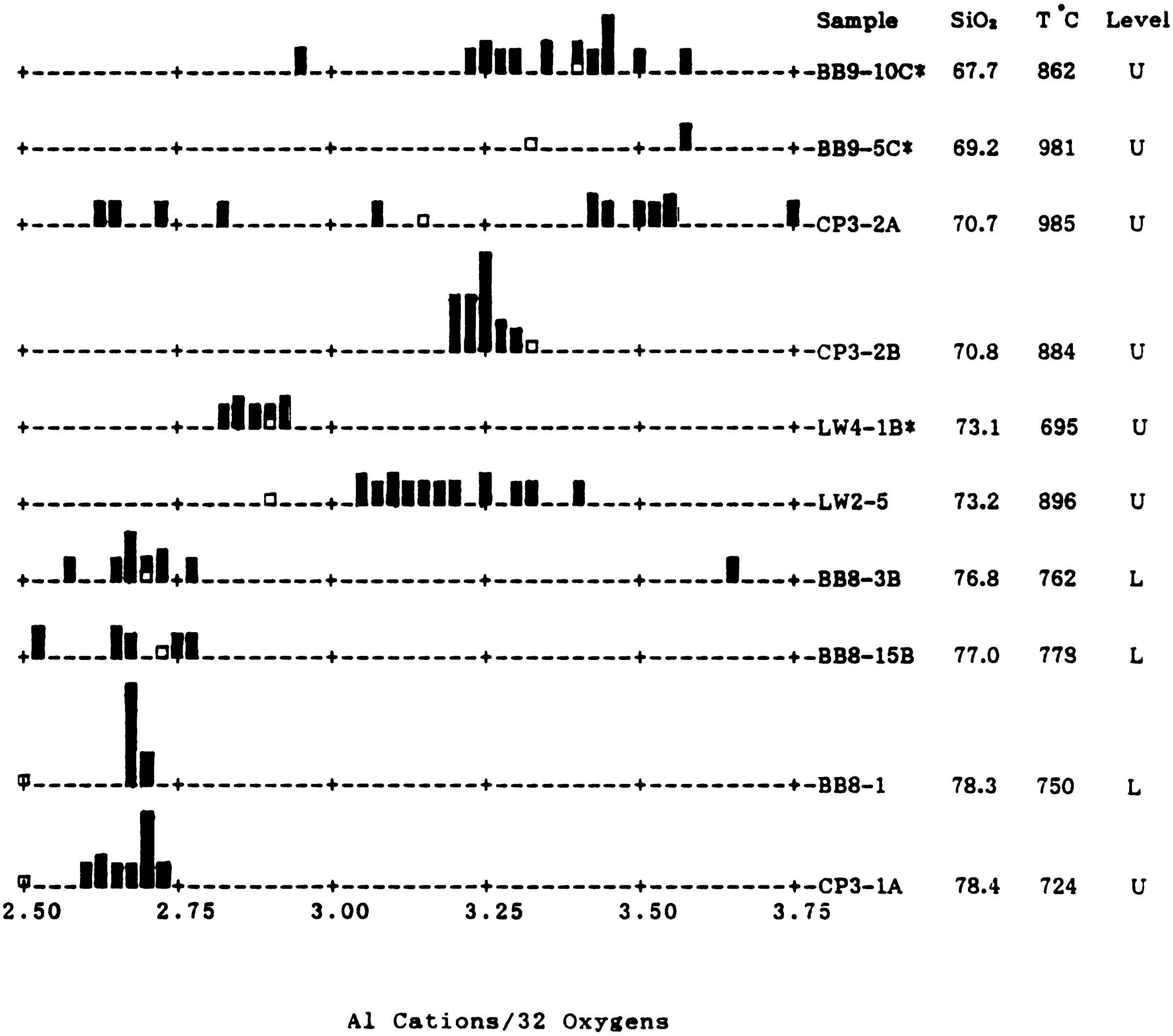

Figure 23. Histograms showing compositional variations in aluminum in the bubble walls of pumice samples. Al cations calculated on the basis of 32 oxygens from microprobe data in Table 9. Light colored square on baseline shows the composition of the whole-pumice calculated on the same basis from the data in Table 2.

It was noted earlier that the composition of the glass may differ from that of the magmatic liquid because of volatile loss and secondary hydration. An additional complexity is the possible volatization of sodium by themicroprobe beam (Nielsen and Sigurdsson, 1981). In lieu of these difficulties, discussion of the glass compositions will be limited to consideration of the elements titanium and aluminum, as they are considered to be relatively stable (Lipman, 1965). The glass analyses were recalculated to cation proportions on a 32 oxygen basis, and histograms of the Ti and Al data are presented in Figures 22 and 23. The Ti and Al concentrations in the glass show a general increase in concentration with decreasing whole-pumice SiO_2 content that is parallel to the whole-pumice Ti and Al concentrations. The glass analyses of the high-silica rhyolitic pumice samples show relatively little scatter, and their nearness in concentration to that of their respective whole-pumice is consistent with the low abundance of phenocrysts in these pumice samples. In contrast, glass analyses of the quartz latitic pumice samples show greater variability, and the higher concentration of Ti in the corresponding whole-pumice reflects the influence of the greater abundance of mafic phenocrysts. Glass analyses of the pumice samples with intermediate whole-pumice SiO_2 content have Ti and Al concentrations that are intermediate between those of the high-silica rhyolitic and quartz latitic pumice samples, consistent with the earlier contention that they are mixed rocks. In particular, sample LW2-5 shows the greatest degree of glass heterogeneity of the intermediate pumice samples, and also shows the greatest degree of heterogeneity with respect to biotite and feldspar compositions (cf. Figures 14b and 21).

It is apparent that there is a greater degree of heterogeneity within pumice samples from stratigraphic levels where there is a greater degree of heterogeneity among pumice samples. This is not surprising considering that the pumice samples from the upper level of the ash-flow sheet were ejected later in the eruption, and thus had a greater opportunity to commingle with overlying magma of contrasting compositions.

Other Mineral Variations

Several previous studies that include phenocryst data from the Topopah Spring Member have also suggested that the compositional variations of liquidus phases resulted from growth in a magma that was compositionally zoned prior to the onset of crystallization, although these studies used samples of whole-rock tuff (Lipman et al., 1966; Byers et al., 1976; Warren et al., 1984; Broxton et al., 1982). More recent work has suggested that there are also differences in the REE phases between the lower and upper units. Scott et al. (1984) have shown that the REE phase in the rhyolitic units is allanite, whereas in the quartz latitic units the REE phase is perrierite/chevkinite.

DISCUSSION

Origin of the Pumice Heterogeneity

The chemical, mineralogical, and textural heterogeneity within and among pumice samples in the Topopah Spring Member clearly emphasizes the importance of the scale of observation when evaluating petrogenetic processes. On the scale of a handsample of whole-rock tuff, the progressive variation from crystal-poor high-silica rhyolite to crystal-rich quartz latite with increasing stratigraphic height was inferred to reflect the trend toward increasingly more mafic, crystal-rich, high temperature magma with depth in the chamber (Lipman et al., 1966). On the scale of individual pumice samples, however, the relationship between stratigraphic position in the ash-flow sheet and depth in the magma chamber needs to be reevaluated because there is a variation in the compositions and estimated quench temperatures among pumice samples at any given stratigraphic level. Rather than assuming a chaotic state in the magma body, this compositional and textural heterogeneity is inferred to result from simultaneous eruption of compositionally contrasting magma from different parts of a magma chamber that was systematically zoned with respect to composition and temperature. Not only is there a host of evidence from other ash-flow sheets that indicates depth-dependent compositional and thermal gradients within magma chambers, but the theoretical fluid dynamic regime of magma withdrawal from a zoned magma chamber predicts that in most cases, the chamber will not be simply emptied in a layer cake fashion. For example, Blake (1981) comments that this view that ash-flow sheets simply represent inverted magma bodies is too simplistic because this would require an unrealistic flow pattern of magma removal. Blake (1981) approached the problem by a mathematical analysis of the removal of magma from a chamber by applying the solution of Weissberg (1962) for the velocity field within a large flat-topped reservoir as a fluid flows upward into a cylindrical conduit. If the diameter of the conduit is considerably smaller than the diameter of the reservoir, fluid will approach the conduit from all directions in a radial fashion, not just from directly below it. At large horizontal distances from the conduit, the radial component of fluid velocity is small in comparison to that directly below the conduit. Hence, the net, or angular velocity field developed near the entrance region to the conduit results in a parabolic velocity profile composed of hyperbolic streamlines along which fluid accelerates towards the conduit (Blake, 1981). By considering this velocity profile, one can determine the sub-circular locus of points within the fluid reservoir that will reach the conduit entrance at the same time. This hyperbolic profile, or "eruption isochron", as defined by Blake (1981), relates position within the reservoir to time of entrance in the conduit for a given eruptive volume. General theoretical solutions describing the dynamics of magma withdrawal and the geometries of evacuation isochrons for assumed boundary conditions have been presented by Blake (1981), Blake and Ivey (1986a, b), Spera (1983, 1984), and Spera et al., (1986).

Figure 24 is a highly schematic cross-sectional cartoon that illustrates the general model of a zoned magma body as proposed by Smith (1979), on which several hypothetical eruption isochrons have been superposed. Admittedly, this depiction is a gross

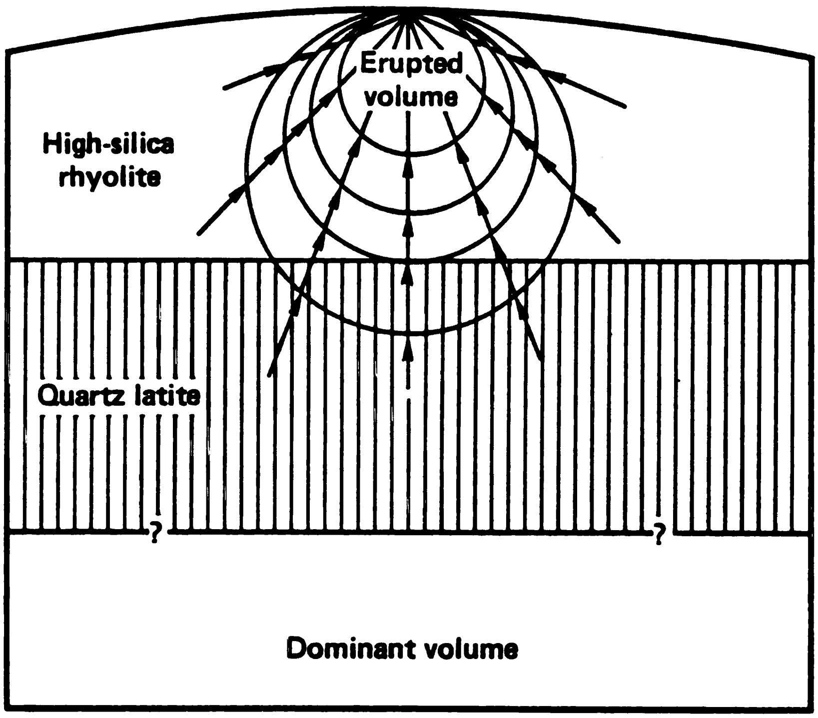

Figure 24. Cross-sectional cartoon of a layered magma body. Circles represent cross-sections through hyperbolic eruption isochrons (Blake, 1981), indicating the locus of points within the magma chamber of magma that will reach the vent simultaneously.

oversimplification, as the actual shapes of the 3-dimensional hyperbolic surfaces will be governed by the geometries of the conduit and reservoir and the physical properties of the magma. For example, eruption through a ring fracture system, which is more appropriate for the Topopah Spring Member, would be better approximated by a toroidal evacuation isochron with a large width to depth ratio. It is also apparent from geologic field evidence that the conduit plumbing systems of large caldera forming ash flows do not remain constant during the course of eruption. Precise mathematical modeling of the evacuation isochrons for these complex and transient geometries can quickly become intractable. The more immediate goal of this study is to show that the chemical heterogeneity of pumice samples in the Topopah Spring Member is consistent with the qualitative predictions of the general fluid dynamic models.

Figure 24 shows several of an infinite number of evacuation isochrons that could be considered from the onset to the final phase of eruption, with that representing the final phase having a volume equal to the total volume of the eruption. Each successive evacuation isochron will draw magma from progressively deeper levels at the expense of magma near the roof of the chamber. However, as illustrated by the largest isochron in Figure 24, magma near the roof of the chamber is not completely exhausted but is continually erupted along with magma from all levels down to the deepest level tapped. Assuming that the magmatic gradients change monotonically with depth in the chamber, each successive isochron will sample magma of progressively greater differences in chemical and physical properties. Thus, the fluid dynamic model for eruption from a zoned magma chamber predicts

that successive volumes of magma leaving the vent will be composite mixtures of magma with increasingly heterogeneous bulk properties.

The geochemical data from both the whole-rock tuff and whole pumice samples are consistent with this model for subterranean eruption dynamics. The whole-rock tuff samples, which become more mafic with increasing stratigraphic height in the ash-flow sheet, represent the bulk composition of a given eruption isochron and are composite mixtures of quenched magma from various positions within the magma chamber. The whole pumice samples, which span a progressively greater compositional range with increasing stratigraphic height in the ash-flow sheet, represent the composition of quenched parcels of magma from various positions along the periphery of an evacuation isochron.

There are several alternative mechanisms that might give rise to compositional heterogeneity within a "depositional isochron". For example, several ash flows that erupt from laterally separated vents that extend to different depths in the magma chamber could coalesce during emplacement to produce a composite mixture of compositionally contrasting pumice fragments. The possibility of subaerial coalescence during eruption from separate vents along the ring fracture system of the Claim Canyon caldera must be considered and obviates the need for development of criteria to distinguish between the effects of subaerial mixing and subterranean mixing in the magma chamber/vent system. However, it is emphasized that the fluid dynamic considerations discussed above would be applicable to each of the laterally separate vents or semi-continuous segments along a ring fracture system. It might also be considered that successive portions of a turbulent ash flow could entrain and suspend pumice fragments of different compositions as the ash flow passed over earlier erupted material. Subaerial mixing undoubtedly occurs to some extent, however, it is difficult to conceive of how pumice fragments from the top of the ash-flow sheet, that are identical in composition and estimated quench temperature to pumice fragments from the base of the sheet, could be continually rafted upward for the duration of the eruptive episode. Spera (1984) has noted that the time interval that a parcel of magma spends in the subaerial realm before coming to rest is on the order of 10^2 s in comparison to 10^4-10^5 s for the duration of an eruptive episode. Moreover, the heterogeneities in phenocryst and glass compositions within single pumice samples provide clear evidence of subterranean mixing. The occurrence of macroscopically banded pumice fragments, such as those observed in the Valley of Ten Thousand Smokes and Crater Lake eruptives (Smith, 1979; Bacon, 1983, Hildreth, 1984) would provide further evidence for subterranean mixing, however, its apparent absence is not a limitation. In a study of the Black Mountain volcanics, Vogel et al. (in press) have documented the occurrence of unzoned, disequilibrium phenocryst assemblages within individual pumice samples that have homogeneous glass compositions. They conclude that the mixing event was vigorous enough to homogenize the liquid, yet short enough to inhibit zoning of the phenocrysts. Whether diverse compositions of a stratified magma body will be simultaneously withdrawn, and the degree to which the diverse compositions may mix will be largely governed by the driving force of the eruption and the viscosities of the magmas (Blake and Ivey, 1986a, b; Campbell and Turner, 1986; Blake and Campbell 1986).

Evidence for a Liquid-liquid Interface

The geochemical data from glassy pumice samples further constrains the inferred chemical and thermal gradients within the pre-eruptive magma chamber. In contrast to the whole-rock tuff samples, which are composite mixtures of compositionally heterogeneous pumices fragments, the pumice samples define trends that display abrupt changes in abundance on interelement variation diagrams and apparent compositional gaps for certain elements. Because the pumice samples from the uppermost horizon of the ash-flow sheet span the entire range in major and trace element composition and estimated quench temperature, these gaps do not appear to be an artifact of inadequate sampling of pumice fragments from the central portion of the eruptive sequence. Rather, these gaps and abrupt changes in elemental concentrations are inferred to reflect the changes in composition and temperature across a liquid-liquid interface between chemically and thermally contrasting magmas within a single chamber (Schuraytz et al., 1985). Similar conclusions have been drawn from other pyroclastic deposits in which heterogeneous pumice samples preserve evidence of compositional gaps (Fridrich and Mahood, 1987).

This hypothesis of a liquid-liquid interface within the magma body is further supported by the abrupt change in phenocryst compositions and increase in phenocryst content at the transition from rhyolite to quartz latite in the ash-flow sheet. Previous interpretation of this lithologic feature (Lipman et al., 1966) concluded that the abrupt change in crystal content did not result from downward settling of phenocrysts from the rhyolitic magma and simple accumulation in the erupted part of the quartz latitic magma. Because most of the chemical variation is due to differences in groundmass composition, they inferred that crystallization occurred in place within a magma body that was chemically zoned in the liquid state. The more advanced stage of crystallization in the lower, quartz latitic part of the magma chamber, in spite of its higher temperature, could be explained by an increased water content in the upper part of the magma chamber resulting in a lowering of the liquidus temperature. However, as this change in crystal content is more abrupt than gradational, this feature is reinterpreted in light of recent theoretical and experimental fluid dynamic studies.

Theoretical interpretation of the occurrence of mafic inclusions in silicic lavas (Eichelberger, 1980) and laboratory models of replenished magma chambers have illuminated a host of fluid dynamic phenomena that can result when a relatively hot, compositionally dense liquid is injected below a cooler, less dense liquid (Huppert and Sparks, 1980; Huppert and Turner, 1981; Huppert et al., 1982b, 1984; McBirney et al., 1985; Baker and McBirney, 1985).

Of particular interest is a recent experiment (Huppert et al., 1984) in which the viscosity of the cooler and compositionally less dense upper layer was considerably greater than that of the hotter and denser layer below. An immediate effect of this thermally unstable situation is the growth of crystals in the lower layer at the interface due to heat transfer to the upper layer. Crystallization in the lower layer causes the surrounding fluid to become less dense and this less dense fluid was released immediately and continuously from the interface into the overlying layer with no significant mixing. Subsequent crystallization also occurred within the plumes that had risen from the interface. By varying the initial conditions of temperature, composition, viscosity, and configuration of the various fluid layers, Huppert et al. (1984) have observed numerous double-diffusive effects of relevance to magmatic processes.

It has been pointed out that the existence of compositional gaps within pyroclastic deposits does not necessarily mean that one existed in the parental magma chamber (Spera et al., 1986). A short eruption hiatus or an abrupt increase or decrease in magma discharge could produce a compositional gap in the eruptive products of a continuously zoned magma chamber. Spera et al. (1986) maintain that it is impossible to invert stratigraphically controlled geochemical data to obtain in situ magmatic gradients unless one has knowledge of the location of vents and the variation of magma discharge with time. While it is not possible to directly ascertain the discharge rate of the Topopah Spring magma, the occurrence of bimodal phenocryst compositions within pumice samples from both early and later stages of the eruption, the overall continuity in estimates of magmatic temperatures, and the absence of even a partial cooling break at the transition from high-silica rhyolite to quartz latite support the hypothesis of compositional gap within the magma body.

The discontinuous chemical gradients and abrupt change in phenocryst content and composition in the Topopah Spring Member are consistent with a model in which a distinct liquid-liquid interface separated relatively high temperature, phenocryst-rich quartz latite from overlying lower temperature, phenocryst-poor high-silica rhyolite in a single magma chamber. The geochemical data from this ash-flow sheet should provide useful boundary conditions for the evaluation of double-diffusive phenomena in a particular geologic system.

CONCLUSIONS

The magmatic gradients inferred from chemical analyses and estimated quench temperatures of glassy pumice samples and phenocrysts from the Topopah Spring Member indicate that the transition from high-silica rhyolitic to quartz latitic magma within the chamber was abrupt, rather than gradational, with a distinct liquid-liquid interface separating the two contrasting magmas. Concomitant with eruption, this interface was disrupted, causing magma of contrasting composition and temperature to erupt simultaneously. Although limited mixing occurred as a result of a convergent flow regime, the duration of the eruption interval was not sufficient to exhaust the high-silica rhyolitic magma nor to produce a completely homogeneous magma. This is supported by the chemical and textural heterogeneities observed both within and among pumice samples throughout the ash-flow sheet, and implies that the Topopah Spring Member does not reflect a "simple" inverse stratigraphy of the chemical zonation of magma in the source chamber. Similar heterogeneities observed within other ash-flow sheets emphasize the importance of the appropriate choice of scale for sampling, when evaluating dynamic petrologic processes.

APPENDIX

Table 3. Microprobe Analyses of Ilmenite and Magnetite.

Field No.	TiO_2	Cr_2O_3	Al_2O_3	Fe_2O_3	FeO	MgO	MnO	Total	USP	ILM
BB9-1WR										
	0.87	0.00	0.46	64.50	27.91	0.11	2.76	96.61	0.024	
	7.13	0.02	1.15	51.53	33.56	0.81	1.80	95.99	0.207	
	9.53	0.01	2.35	46.19	34.57	2.11	1.23	95.99	0.280	
	8.43	0.00	2.63	47.98	33.56	2.19	1.12	95.92	0.249	
*	7.23	0.01	1.94	50.91	32.85	1.60	1.56	96.09	0.210	
	44.81	0.00	0.56	13.26	34.53	2.14	1.93	97.23		0.862
	41.17	0.00	0.50	21.07	29.91	2.75	2.18	97.58		0.778
	42.68	0.00	0.53	15.04	33.87	1.01	2.68	95.81		0.842
	37.50	0.00	0.35	27.75	27.58	2.30	2.02	97.50		0.709
*	42.33	0.00	0.50	17.91	32.11	2.13	2.13	97.11		0.813
BB9-1A										
	1.19	0.03	0.51	63.11	27.98	0.12	2.68	95.62	0.033	
	0.11	0.05	0.24	65.37	25.57	0.06	4.07	95.47	0.003	
	10.15	0.04	1.46	44.83	37.27	0.37	1.52	95.64	0.310	
*	3.16	0.04	0.68	59.11	29.70	0.17	2.74	95.59	0.090	
*	35.53	0.01	1.06	29.79	26.44	1.59	2.64	97.07		0.684
BB9-1C										
	7.42	0.07	1.79	50.91	33.76	1.54	1.02	96.51	0.217	
	10.36	0.04	2.35	44.91	35.84	1.97	1.14	96.61	0.306	
	8.36	0.02	1.50	49.16	34.16	1.26	1.79	96.26	0.242	
	8.56	0.00	2.00	48.13	34.43	1.72	0.95	95.79	0.253	
	9.43	0.03	1.79	46.87	34.85	1.64	1.53	96.14	0.274	
	9.46	0.01	2.40	45.66	34.57	2.05	1.02	95.17	0.283	
*	8.79	0.03	1.88	48.02	34.56	1.62	1.29	96.19	0.257	
	41.33	0.02	0.28	19.72	30.96	2.38	1.94	96.63		0.793
	34.20	0.03	0.61	32.20	25.49	1.38	2.77	96.68		0.659
	41.98	0.02	0.34	18.98	31.46	2.41	1.97	97.16		0.801
	37.84	0.02	0.41	26.70	27.29	2.56	2.15	96.97		0.717
*	39.47	0.02	0.39	23.32	29.33	2.23	2.16	96.92		0.755
BB9-5C										
	12.09	0.04	1.52	42.17	37.21	1.78	1.41	96.22	0.350	
	9.49	0.03	1.96	47.13	34.22	2.25	1.42	96.49	0.270	
	6.58	0.03	1.71	52.05	31.31	2.14	1.33	95.16	0.186	
	8.57	0.04	1.37	49.53	32.98	2.41	1.39	96.29	0.235	
*	9.66	0.03	1.68	46.90	34.41	2.16	1.40	96.24	0.274	
	32.72	0.02	0.35	37.53	23.45	2.43	1.62	98.12		0.609
	32.10	0.00	0.33	37.50	23.63	1.99	1.67	97.22		0.608
	32.41	0.01	0.34	37.51	23.54	2.21	1.64	97.67		0.608
	29.07	0.01	0.37	44.79	18.70	3.06	1.96	97.96		0.523
*	30.74	0.01	0.35	41.16	21.11	2.64	1.80	97.81		0.566
BB9-1C										
	6.81	0.02	1.81	52.48	31.98	2.07	1.45	96.62	0.191	
	9.26	0.02	1.75	47.69	34.28	2.07	1.37	96.44	0.263	
	9.53	0.02	1.40	47.63	35.13	1.90	1.03	96.64	0.271	
	8.56	0.04	1.12	49.48	34.81	1.53	0.92	96.46	0.245	
*	8.48	0.02	1.48	49.43	34.05	1.85	1.18	96.49	0.241	

*Mole fraction of ilmenite (ILM) and ulvospinel (USP) calculated according to the method of Stormer (1983). Asterisks indicate the mean values used for estimated temperature and oxygen fugacity determinations.

Table 3 (cont'd.).

Field No.	TiO_2	Cr_2O_3	Al_2O_3	Fe_2O_3	FeO	MgO	MnO	Total	USP	ILM
BB9-1C (cont'd.)										
	40.33	0.04	0.30	20.87	31.42	1.72	1.76	96.44		0.782
	41.39	0.05	0.28	20.39	31.73	1.89	2.09	97.82		0.789
	47.18	0.02	0.28	9.19	36.67	2.41	1.44	97.19		0.905
	36.49	0.04	0.45	29.38	26.32	2.67	1.71	97.06		0.690
	43.46	0.05	0.30	13.77	34.46	1.77	1.45	95.26		0.856
*	41.50	0.04	0.33	19.61	31.68	2.18	1.73	97.08		0.796
BB9-15WR										
	6.17	0.05	1.68	55.94	32.95	1.60	1.65	100.05	0.169	
	5.27	0.05	2.10	58.19	32.20	2.04	1.31	101.16	0.142	
	5.33	0.05	1.99	57.94	33.08	1.52	1.27	101.19	0.148	
	4.40	0.03	1.93	59.32	32.02	1.35	1.53	100.58	0.122	
	5.52	0.03	1.97	57.66	32.83	1.66	1.46	101.13	0.151	
	5.17	0.05	2.16	57.89	32.32	1.70	1.52	100.81	0.142	
	4.92	0.06	1.99	59.23	32.82	1.40	1.59	102.00	0.135	
	4.95	0.02	2.13	58.06	32.28	1.46	1.63	100.54	0.137	
*	5.23	0.04	1.99	58.03	32.57	1.60	1.49	100.95	0.143	
	50.44	0.02	0.11	9.52	31.23	5.13	4.92	101.37		0.898
	41.89	0.00	0.22	23.14	30.64	2.58	2.40	100.87		0.765
	42.78	0.00	0.16	22.26	29.86	2.94	3.33	101.33		0.772
	40.19	0.00	0.28	27.44	28.12	3.50	1.76	101.29		0.721
	41.50	0.00	0.32	22.94	31.22	2.24	2.08	100.30		0.768
	43.22	0.00	0.11	22.06	30.51	2.71	3.48	102.09		0.776
	41.39	0.00	0.21	23.62	29.72	2.77	2.53	100.24		0.758
	40.39	0.00	0.25	26.04	29.52	2.96	1.51	100.67		0.736
	41.84	0.00	0.12	22.64	30.34	2.61	2.60	100.15		0.768
	42.26	0.00	0.18	22.83	30.80	2.56	2.61	101.24		0.769
*	41.84	0.00	0.20	23.35	30.25	2.70	2.53	100.87		0.763
BB9-25WR										
	1.68	0.02	0.69	62.36	31.12	0.08	0.31	96.26	0.051	
	1.71	0.01	1.00	62.86	30.21	0.63	0.72	97.14	0.050	
	3.46	0.02	1.40	59.59	29.17	1.47	2.21	97.32	0.094	
	2.84	0.01	1.28	59.98	32.01	0.06	0.87	97.05	0.087	
	2.85	0.02	1.00	59.50	28.49	0.87	2.54	95.27	0.079	
	6.36	0.02	1.60	54.95	32.40	1.68	1.88	98.89	0.174	
	3.14	0.00	1.11	59.01	32.65	0.10	0.15	96.15	0.098	
	1.96	0.00	1.37	61.60	29.90	0.42	1.53	96.78	0.058	
*	3.15	0.01	1.21	59.78	30.91	0.70	1.25	97.01	0.091	
	42.82	0.01	0.14	17.80	32.49	1.53	3.25	98.03		0.815
	38.59	0.02	0.25	29.84	22.43	4.25	4.64	100.02		0.675
	38.53	0.01	0.15	26.38	27.19	2.18	3.53	97.96		0.721
	33.51	0.01	0.70	33.93	23.44	1.42	4.11	97.12		0.635
	37.77	0.00	0.23	27.52	28.27	1.63	2.75	98.18		0.714
	41.21	0.01	0.26	21.02	29.12	0.99	6.10	98.71		0.776
	40.88	0.01	0.22	20.93	29.80	2.15	3.09	97.08		0.779
*	38.97	0.01	0.27	25.56	27.56	1.98	3.90	98.25		0.730
BB8-320WR										
	7.72	0.01	1.64	52.42	36.48	0.25	1.68	100.20	0.226	
	5.98	0.00	1.31	55.77	33.85	0.34	2.28	99.53	0.170	

Table 3 (cont'd.).

Field No.	TiO_2	Cr_2O_3	Al_2O_3	Fe_2O_3	FeO	MgO	MnO	Total	USP	ILM
BB8-320WR (cont'd.)										
	7.94	0.01	1.71	51.14	36.19	0.24	1.86	99.08	0.235	
*	7.21	0.01	1.55	53.10	35.51	0.27	1.94	99.59	0.210	
*	48.11	0.00	0.10	8.87	38.67	0.78	3.16	99.69		0.911
BB8-200WR										
	10.20	0.01	1.68	48.36	38.92	0.26	1.88	101.32	0.295	
	9.56	0.03	1.40	49.80	38.36	0.18	1.90	101.23	0.275	
	8.89	0.02	1.24	49.80	37.17	0.01	2.06	99.19	0.260	
	9.94	0.02	1.51	48.50	38.09	0.27	2.17	100.50	0.287	
	9.93	0.04	1.51	47.86	38.15	0.03	2.24	99.76	0.291	
	9.94	0.04	1.45	48.67	38.58	0.03	2.15	100.87	0.288	
	9.39	0.03	1.37	49.34	38.07	0.03	1.92	100.14	0.274	
	10.05	0.03	1.68	48.44	38.78	0.08	2.12	101.17	0.292	
	7.98	0.01	1.71	50.21	35.04	0.10	2.89	97.94	0.235	
*	9.69	0.03	1.50	48.88	38.17	0.12	2.08	100.47	0.281	
	48.53	0.02	0.08	6.00	37.03	0.11	6.33	98.10		0.937
	47.76	0.01	0.08	8.07	34.49	0.11	8.16	98.68		0.914
	45.81	0.01	0.28	11.26	37.54	0.19	3.27	98.37		0.886
	47.97	0.01	0.07	7.38	38.41	0.19	4.33	98.36		0.925
	48.18	0.01	0.09	7.62	37.79	0.13	5.24	99.05		0.922
	48.30	0.03	0.09	7.05	36.96	0.13	6.16	98.73		0.927
	47.94	0.03	0.07	7.18	34.78	0.13	8.00	98.13		0.923
*	47.75	0.02	0.12	7.86	36.76	0.14	5.85	98.51		0.918
BB8-100WR										
	3.82	0.02	0.65	59.07	32.22	0.54	0.72	97.04	0.111	
	5.56	0.00	0.87	54.78	33.83	0.01	1.39	96.44	0.166	
	2.13	0.00	0.87	62.42	31.36	0.00	1.15	97.93	0.063	
	5.22	0.00	1.02	55.67	33.46	0.17	1.37	96.92	0.155	
*	4.79	0.00	0.90	56.61	33.18	0.14	1.27	96.89	0.142	
	46.83	0.00	0.11	10.91	36.70	0.42	4.60	99.57		0.889
	48.44	0.00	0.18	7.56	39.45	0.50	3.18	99.31		0.924
	48.25	0.00	0.06	8.53	38.75	0.42	3.84	99.86		0.914
	46.97	0.00	0.06	11.17	35.58	0.66	5.41	99.85		0.885
*	47.57	0.00	0.10	9.67	37.46	0.51	4.35	99.66		0.902
BB8-85BWR										
	6.63	0.02	1.04	54.05	33.93	0.52	2.10	98.29	0.188	
	6.99	0.00	1.05	52.98	33.58	0.68	2.33	97.61	0.197	
	6.85	0.02	0.98	54.27	33.83	0.65	2.42	99.02	0.190	
	6.81	0.01	0.99	53.93	33.93	0.57	2.24	98.48	0.191	
*	6.84	0.01	1.01	53.78	33.81	0.61	2.29	98.35	0.192	
	48.42	0.00	0.19	8.14	37.59	1.04	4.05	99.43		0.917
	46.54	0.00	0.06	11.89	34.93	1.31	4.53	99.26		0.877
	46.18	0.00	0.03	12.66	34.40	1.33	4.70	99.30		0.869
	47.97	0.00	0.11	9.19	37.66	1.07	3.52	99.52		0.907
*	47.33	0.00	0.10	10.37	36.25	1.18	4.15	99.39		0.894
BB8-85B										
	6.39	0.05	1.27	53.51	33.17	0.50	2.39	97.28	0.184	
	6.66	0.02	1.02	53.56	33.21	0.57	2.55	97.59	0.188	
	6.84	0.06	1.00	53.82	33.63	0.64	2.45	98.44	0.191	
	6.71	0.02	1.12	52.61	33.26	0.52	2.32	96.56	0.193	
*	6.64	0.04	1.10	53.48	33.33	0.56	2.44	97.59	0.188	

Table 3 (cont'd.).

Field No.	TiO_2	Cr_2O_3	Al_2O_3	Fe_2O_3	FeO	MgO	MnO	Total	USP	ILM
BB8-85B (cont'd.)										
	49.02	0.00	0.10	8.83	38.00	1.18	3.93	101.05		0.912
	45.19	0.00	0.13	14.72	33.90	1.37	4.24	99.56		0.849
	49.54	0.05	0.11	6.15	39.15	0.91	3.73	99.64		0.938
	47.24	0.02	0.06	11.49	35.73	1.21	4.54	100.28		0.883
	46.01	0.01	0.21	12.23	34.06	1.33	4.88	98.74		0.872
*	47.58	0.02	0.12	10.31	36.37	1.19	4.24	99.83		0.895
BB8-20										
	7.67	0.01	1.14	50.79	34.53	0.54	1.94	96.62	0.224	
	9.62	0.02	1.10	48.19	36.85	0.43	2.12	98.33	0.277	
	11.20	0.00	1.00	42.86	38.57	0.00	1.54	95.16	0.342	
	11.28	0.02	1.18	43.16	38.45	0.00	2.07	96.15	0.341	
*	9.76	0.01	1.12	46.73	36.88	0.28	1.97	96.75	0.289	
	47.46	0.06	0.03	9.45	35.77	0.62	5.73	99.12		0.902
	49.66	0.05	0.09	1.38	39.13	0.76	4.12	95.19		0.985
	48.60	0.05	0.07	7.30	35.58	1.05	6.17	98.82		0.923
	49.66	0.04	0.14	3.72	38.39	1.03	4.37	97.35		0.961
	49.79	0.04	0.08	3.93	39.26	0.88	3.90	97.87		0.960
*	49.27	0.05	0.09	4.83	37.91	0.92	4.70	97.76		0.950
BB8-15B										
	7.59	0.01	1.02	52.61	34.31	0.71	2.44	98.69	0.211	
	6.85	0.00	0.85	53.92	32.67	0.83	2.99	98.11	0.186	
	7.01	0.02	0.84	52.78	32.46	0.71	3.19	97.01	0.193	
	7.31	0.01	0.94	53.38	33.33	0.72	3.18	98.87	0.199	
	7.32	0.02	0.98	52.75	33.06	0.72	3.21	98.07	0.201	
	7.12	0.02	1.01	52.93	33.58	0.73	2.43	97.81	0.199	
	7.77	0.00	0.97	52.26	34.32	0.71	2.55	98.59	0.216	
	7.43	0.04	0.93	52.77	33.83	0.71	2.65	98.36	0.206	
*	7.33	0.01	0.96	52.91	33.59	0.73	2.74	98.27	0.203	
	48.38	0.01	0.05	5.51	37.97	0.95	3.79	96.66		0.943
	47.47	0.01	0.05	7.43	34.50	1.33	5.74	96.53		0.920
	46.80	0.00	0.05	11.52	34.84	1.35	4.78	99.33		0.881
	47.91	0.00	0.03	7.13	35.31	0.63	6.57	97.57		0.924
	49.61	0.00	0.00	1.23	43.06	0.00	1.53	95.43		0.988
	46.43	0.00	0.07	13.44	33.29	1.26	6.14	100.63		0.860
	46.27	0.00	0.07	13.42	32.75	1.52	6.07	100.11		0.859
	45.10	0.02	0.05	15.58	28.68	1.82	8.52	99.77		0.830
	45.10	0.04	0.09	14.46	30.56	1.24	7.69	99.18		0.844
	44.61	0.03	0.04	14.51	31.52	1.38	6.06	98.14		0.845
*	46.64	0.01	0.05	10.99	33.96	1.25	5.68	98.58		0.884
BB8-10WR										
	10.75	0.02	1.32	43.91	37.32	0.37	2.03	95.72	0.323	
	9.06	0.03	1.10	48.43	35.49	0.42	2.60	97.13	0.261	
	8.83	0.02	1.05	48.60	35.54	0.48	2.07	96.59	0.258	
*	9.63	0.02	1.17	46.80	36.17	0.42	2.26	96.47	0.283	
	51.17	0.03	0.02	0.62	39.50	1.15	4.41	96.90		0.993
	45.57	0.05	0.06	11.83	33.04	1.39	5.39	97.34		0.874
	49.82	0.01	0.06	1.81	38.27	0.94	4.79	95.70		0.981
	48.02	0.04	0.06	6.50	37.55	0.59	4.52	97.28		0.932
	47.81	0.02	0.07	7.52	36.14	1.11	4.81	97.48		0.921
*	48.15	0.03	0.06	6.32	36.46	1.08	4.85	96.95		0.933

Table 3 (cont'd.).

Field No.	TiO_2	Cr_2O_3	Al_2O_3	Fe_2O_3	FeO	MgO	MnO	Total	USP	ILM
BB8-3B										
	7.52	0.02	0.89	51.34	34.11	0.51	2.21	96.60	0.216	
	7.50	0.00	0.88	51.03	33.54	0.60	2.43	95.98	0.214	
*	7.51	0.01	0.88	51.18	33.83	0.55	2.32	96.28	0.215	
	47.61	0.04	0.02	6.84	36.18	0.51	5.65	96.86		0.927
	47.60	0.02	0.10	8.51	36.23	1.33	4.15	97.94		0.911
	45.95	0.01	0.06	12.20	33.29	0.98	6.20	98.69		0.871
	47.14	0.00	0.07	7.93	35.63	1.16	4.63	96.56		0.916
	44.44	0.00	0.06	11.68	34.11	0.94	4.12	95.35		0.875
	47.49	0.00	0.03	7.10	35.95	1.22	4.52	96.31		0.925
	46.59	0.00	0.07	9.88	34.99	1.12	4.85	97.50		0.896
	46.57	0.00	0.08	11.29	33.23	1.55	5.81	98.53		0.880
	45.98	0.00	0.05	11.48	33.59	1.20	5.55	97.85		0.878
	47.48	0.00	0.12	7.92	36.39	0.63	5.12	97.65		0.917
	46.21	0.04	0.08	12.45	32.85	1.78	5.46	98.87		0.868
	48.63	0.02	0.09	5.54	37.12	1.19	4.43	97.03		0.942
*	46.95	0.01	0.07	9.38	35.13	1.17	4.94	97.65		0.901
BB8-1										
	10.21	0.02	1.09	46.52	36.99	0.57	2.04	97.44	0.296	
	9.79	0.03	1.04	46.81	36.17	0.69	1.99	96.52	0.284	
	10.52	0.06	0.89	45.27	37.30	0.43	1.85	96.33	0.309	
*	10.11	0.04	1.00	46.23	36.70	0.58	1.95	96.61	0.295	
	48.52	0.02	0.07	7.91	35.87	1.18	5.59	99.15		0.918
	48.35	0.01	0.07	6.61	37.32	0.66	4.92	97.94		0.931
	48.12	0.01	0.08	8.25	38.00	0.93	3.57	98.96		0.916
	49.43	0.01	0.12	4.72	38.98	1.04	3.57	97.87		0.951
	47.88	0.01	0.05	8.91	35.40	1.18	5.48	98.91		0.907
*	48.45	0.01	0.08	7.31	37.32	0.98	4.44	98.59		0.925
CP3-2A										
	12.37	0.03	1.01	41.01	39.28	0.36	1.49	95.55	0.373	
	13.77	0.06	0.65	39.43	40.60	0.75	1.04	96.30	0.404	
	12.33	0.04	0.75	42.96	38.93	0.83	1.62	97.46	0.353	
	8.85	0.02	1.38	48.08	35.19	0.51	2.40	96.43	0.260	
	9.42	0.02	1.64	46.47	33.18	1.30	3.47	95.50	0.267	
*	11.29	0.03	1.10	43.51	37.61	0.62	1.93	96.09	0.333	
*	33.74	0.05	0.17	33.49	24.15	1.36	3.72	96.68		0.642
CP3-2B										
	8.95	0.00	2.16	47.97	34.06	1.88	1.77	96.79	0.258	
	10.07	0.00	2.10	45.46	34.89	1.88	1.78	96.17	0.293	
	9.67	0.00	1.85	46.77	35.11	1.64	1.68	96.72	0.279	
	9.05	0.00	1.95	47.46	34.63	1.68	1.36	96.13	0.265	
	9.10	0.01	2.24	47.89	33.76	2.18	1.83	97.01	0.258	
	11.04	0.00	2.00	43.84	36.66	1.55	1.54	96.63	0.325	
	8.75	0.00	2.42	48.08	33.69	1.97	1.85	96.76	0.253	
*	9.49	0.00	2.10	46.84	34.65	1.83	1.69	96.59	0.275	
	41.82	0.00	0.33	18.30	30.82	2.86	1.67	95.79		0.805
	41.92	0.00	0.32	19.22	30.08	3.36	1.61	96.51		0.796
	41.38	0.04	0.38	20.36	30.45	2.96	1.47	97.04		0.786
	38.37	0.00	0.35	24.99	27.85	2.88	1.50	95.94		0.734
	42.51	0.00	0.31	17.28	31.19	3.01	1.65	95.95		0.816
	37.82	0.02	0.31	27.53	26.55	3.32	1.52	97.07		0.708
*	41.17	0.00	0.33	20.03	30.00	3.03	1.60	96.16		0.787

Table 3 (cont'd.).

Field No.	TiO_2	Cr_2O_3	Al_2O_3	Fe_2O_3	FeO	MgO	MnO	Total	USP	ILM
CP3-1A										
	10.62	0.00	1.17	44.36	37.81	0.27	1.57	95.81	0.321	
	10.88	0.00	1.03	43.88	37.75	0.31	1.71	95.57	0.326	
	8.11	0.00	0.80	50.10	35.61	0.20	1.70	96.52	0.239	
	12.02	0.00	0.98	42.18	38.61	0.33	2.06	96.19	0.356	
	10.88	0.01	0.98	44.03	37.87	0.31	1.63	95.71	0.326	
	7.49	0.00	1.00	50.83	34.80	0.35	1.60	96.06	0.222	
	9.89	0.00	0.94	46.44	36.53	0.49	1.91	96.20	0.290	
	6.49	0.00	0.77	53.35	34.49	0.28	1.21	96.60	0.191	
*	9.26	0.00	0.96	47.43	36.47	0.32	1.61	96.04	0.275	
	50.79	0.00	0.14	2.17	39.24	1.53	3.66	97.53		0.977
	47.63	0.00	0.07	9.06	37.89	1.03	3.07	98.75		0.908
	47.61	0.00	0.30	5.52	38.82	0.78	2.57	95.60		0.943
	49.65	0.01	0.08	2.32	41.24	0.78	1.99	96.07		0.976
	39.63	0.00	0.15	23.35	29.92	1.11	3.69	97.85		0.757
	50.28	0.00	0.15	0.83	38.65	1.01	4.70	95.62		0.991
*	47.85	0.00	0.16	6.39	38.23	0.97	3.03	96.63		0.934
CP3-1B										
	9.92	0.01	1.08	46.69	37.28	0.37	1.65	97.00	0.293	
	11.53	0.01	1.19	43.70	38.10	0.70	1.87	97.10	0.337	
	8.80	0.01	1.26	47.94	35.74	0.45	1.72	95.92	0.263	
	10.70	0.01	1.17	45.87	38.34	0.40	1.64	98.13	0.314	
	10.15	0.01	1.14	45.33	37.06	0.40	1.66	95.75	0.304	
	11.28	0.00	1.29	44.07	38.63	0.38	1.69	97.35	0.335	
	12.44	0.00	1.29	40.68	39.27	0.36	1.65	95.70	0.377	
	10.94	0.13	1.33	43.99	38.08	0.41	1.63	96.51	0.330	
	10.97	0.00	1.53	44.62	38.69	0.33	1.58	97.72	0.329	
*	10.72	0.02	1.25	44.90	37.90	0.43	1.68	96.90	0.319	
	48.65	0.01	0.18	5.21	39.21	0.96	2.79	97.01		0.946
	50.05	0.01	0.23	3.05	40.87	0.80	2.68	97.69		0.969
	50.01	0.00	0.16	1.84	40.87	0.89	2.48	96.25		0.981
	49.71	0.02	0.19	3.34	41.75	0.46	2.10	97.57		0.966
*	49.39	0.01	0.18	3.68	40.28	0.85	2.59	96.98		0.962
CP3-1D										
	9.86	0.04	1.75	46.80	35.42	1.55	1.83	97.25	0.283	
	9.74	0.02	1.76	46.51	34.84	1.72	1.76	96.35	0.280	
	9.87	0.01	1.84	46.85	35.45	1.62	1.77	97.40	0.283	
	10.15	0.02	1.77	47.23	35.87	1.75	1.75	98.53	0.286	
	9.76	0.02	1.76	46.97	34.81	1.79	1.91	97.02	0.277	
	9.94	0.01	1.72	46.64	35.57	1.53	1.76	97.16	0.286	
	9.56	0.02	1.74	46.95	34.82	1.65	1.77	96.50	0.275	
	10.00	0.04	1.78	46.20	35.41	1.63	1.71	96.77	0.289	
*	9.85	0.02	1.76	46.77	35.26	1.65	1.78	97.09	0.282	
	41.59	0.02	0.21	19.30	31.35	2.30	1.93	96.69		0.798
	45.07	0.01	0.19	13.73	32.42	3.18	2.41	97.01		0.854
	43.04	0.04	0.16	16.14	32.38	2.48	1.88	96.12		0.830
	44.48	0.00	0.19	13.22	33.16	2.62	2.14	95.82		0.860
	42.51	0.03	0.18	17.22	31.37	2.58	2.23	96.11		0.817
	43.27	0.02	0.18	16.26	32.00	2.69	2.09	96.51		0.828
	43.13	0.02	0.25	15.52	32.17	2.56	2.03	95.68		0.835
	41.53	0.03	0.23	19.10	30.48	2.64	2.13	96.14		0.797
*	43.14	0.02	0.20	16.15	31.96	2.64	2.10	96.21		0.829

Table 3 (cont'd.).

Field No.	TiO_2	Cr_2O_3	Al_2O_3	Fe_2O_3	FeO	MgO	MnO	Total	USP	ILM
CP4-20BWR										
	5.61	0.05	1.82	57.47	32.59	1.18	2.53	101.25	0.152	
	6.12	0.06	1.79	55.91	32.95	1.47	1.86	100.16	0.168	
	5.87	0.04	1.24	56.76	32.81	1.03	2.31	100.07	0.159	
*	5.87	0.05	1.62	56.72	32.79	1.23	2.23	100.50	0.160	
	40.53	0.04	0.15	24.88	28.30	2.61	3.45	99.96		0.742
	40.18	0.04	0.15	24.06	28.50	2.55	3.05	98.53		0.748
	44.67	0.03	0.09	15.06	33.08	1.50	4.36	98.79		0.843
	42.04	0.04	0.13	20.93	30.49	2.15	3.44	99.22		0.783
	40.89	0.04	0.18	24.08	29.15	2.74	2.70	99.78		0.751
*	41.57	0.04	0.14	21.93	29.82	2.32	3.38	99.21		0.772
CP4-60WR										
	8.17	0.08	1.37	50.35	36.35	0.23	1.57	98.11	0.243	
	6.39	0.06	1.14	54.07	34.56	0.12	1.85	98.20	0.187	
	6.68	0.08	0.93	53.16	34.25	0.11	2.15	97.36	0.195	
	7.80	0.07	1.18	51.67	35.82	0.19	1.96	98.69	0.227	
*	7.26	0.07	1.16	52.30	35.25	0.16	1.88	98.08	0.213	
	43.74	0.05	0.03	17.02	36.02	0.35	2.66	99.87		0.831
	42.33	0.02	0.03	19.17	33.53	0.73	3.19	99.00		0.806
	45.79	0.00	0.01	11.95	37.46	0.40	2.97	98.58		0.880
	44.96	0.03	0.02	13.59	36.54	0.64	2.71	98.49		0.863
*	44.26	0.02	0.02	15.30	35.93	0.54	2.87	98.94		0.846
CP1-3WR										
	10.05	0.00	1.17	48.01	37.70	0.45	1.97	99.35	0.288	
	11.35	0.00	1.30	44.27	38.00	0.79	1.82	97.53	0.331	
	11.45	0.00	1.26	44.16	37.76	0.79	2.15	97.57	0.331	
	11.20	0.00	1.30	44.56	38.65	0.41	1.70	97.82	0.331	
	10.70	0.00	1.32	44.86	37.84	0.40	1.78	96.91	0.319	
	11.10	0.00	1.22	43.72	38.01	0.42	1.71	96.18	0.332	
	12.56	0.00	1.32	43.14	38.62	0.32	3.69	99.65	0.354	
	10.53	0.01	1.22	47.08	38.26	0.35	2.07	99.52	0.303	
*	11.17	0.00	1.26	44.81	38.09	0.51	2.11	97.95	0.325	
	48.96	0.01	0.08	6.93	35.47	0.70	7.22	99.36		0.927
	49.13	0.02	0.04	8.48	37.95	1.23	3.99	100.84		0.915
	49.29	0.02	0.07	7.49	38.58	0.80	4.26	100.51		0.925
	48.79	0.03	0.08	8.10	38.59	0.89	3.65	100.13		0.919
	49.71	0.02	0.07	8.18	38.92	1.17	3.65	101.72		0.919
	49.17	0.00	0.16	8.66	39.04	0.86	3.60	101.49		0.914
	49.91	0.00	0.08	7.37	40.22	0.78	3.23	101.59		0.928
	49.04	0.00	0.05	8.53	38.42	0.82	4.16	101.02		0.915
	49.03	0.00	0.10	8.45	38.56	1.36	3.07	100.57		0.916
*	49.24	0.01	0.08	7.99	38.40	0.95	4.13	100.80		0.920
CP1-3A										
	10.51	0.02	1.03	44.61	37.84	0.35	1.23	95.59	0.317	
	10.84	0.01	1.11	44.86	37.77	0.40	1.96	96.94	0.319	
	10.80	0.01	1.08	44.61	37.67	0.32	1.99	96.48	0.320	
	10.68	0.04	1.02	44.10	37.40	0.37	1.70	95.31	0.321	
	11.17	0.00	1.15	43.73	37.71	0.56	1.84	96.16	0.331	
*	10.83	0.01	1.08	44.35	37.67	0.41	1.77	96.12	0.322	
	48.01	0.00	0.10	7.78	38.79	0.76	2.99	98.43		0.921
	47.72	0.00	0.09	8.51	38.33	0.80	3.12	98.56		0.914

Table 3 (cont'd.).

Field No.	TiO_2	Cr_2O_3	Al_2O_3	Fe_2O_3	FeO	MgO	MnO	Total	USP	ILM
CP1-3A (cont'd.)										
	48.46	0.00	0.10	8.25	38.84	0.83	3.22	99.70		0.917
	47.64	0.00	0.30	8.71	38.35	0.75	3.11	98.86		0.912
	47.55	0.01	0.10	9.45	37.61	0.88	3.54	99.14		0.904
	47.50	0.00	0.08	8.26	38.10	0.78	3.18	97.91		0.916
	46.86	0.00	0.08	9.84	36.26	1.25	3.60	97.90		0.898
	47.19	0.00	0.09	8.43	37.90	0.81	3.05	97.47		0.914
	47.07	0.00	0.09	8.79	37.87	0.75	3.08	97.65		0.910
*	47.59	0.00	0.12	8.67	38.02	0.85	3.22	98.47		0.912
CP1-2E										
	12.03	0.00	0.92	42.40	38.84	0.43	1.73	96.35	0.355	
	9.93	0.01	0.83	46.19	36.84	0.33	1.78	95.91	0.293	
	11.24	0.00	1.01	43.45	38.00	0.38	1.77	95.85	0.335	
	10.89	0.02	0.97	44.34	37.87	0.38	1.66	96.13	0.323	
	11.59	0.00	1.01	44.17	36.75	1.67	1.68	96.87	0.325	
	10.14	0.01	1.04	46.11	36.98	0.60	1.65	96.53	0.298	
	10.54	0.00	0.90	44.72	36.81	0.41	2.14	95.52	0.311	
*	10.63	0.01	0.96	45.04	37.32	0.55	1.74	96.25	0.312	
	47.51	0.01	0.05	9.66	37.95	0.91	3.11	99.20		0.903
	47.77	0.01	0.02	8.94	37.99	0.93	3.27	98.93		0.909
	47.89	0.01	0.04	7.80	38.38	0.87	3.09	98.08		0.921
	48.40	0.00	0.31	8.73	37.99	1.25	3.26	99.94		0.912
	47.51	0.02	0.02	9.21	37.67	1.01	3.21	98.65		0.906
	47.60	0.01	0.18	8.41	37.04	0.93	4.05	98.22		0.913
	48.70	0.02	0.04	8.28	38.50	1.12	3.26	99.92		0.917
	47.57	0.02	0.01	8.66	37.90	0.90	3.23	98.29		0.912
*	47.90	0.01	0.08	8.68	37.96	0.99	3.31	98.93		0.912
CP1-1G										
	10.47	0.01	1.13	44.57	37.43	0.39	1.54	95.54	0.315	
	10.77	0.00	1.11	44.36	37.82	0.32	1.70	96.07	0.322	
	10.90	0.01	1.10	44.12	37.95	0.37	1.60	96.05	0.326	
	10.63	0.01	1.11	44.52	37.42	0.50	1.60	95.79	0.317	
	10.88	0.03	1.30	43.31	37.58	0.45	1.58	95.13	0.331	
	11.46	0.02	1.08	42.54	38.20	0.32	1.73	95.35	0.346	
	12.18	0.01	1.21	41.70	39.10	0.42	1.66	96.28	0.365	
	11.05	0.00	1.14	43.19	37.85	0.42	1.49	95.14	0.334	
*	10.99	0.01	1.13	43.74	37.89	0.40	1.62	95.78	0.330	
	48.54	0.01	0.02	8.38	39.02	0.88	3.02	99.87		0.916
	49.56	0.00	0.06	6.52	39.60	0.93	3.27	99.93		0.935
	48.75	0.00	0.07	7.68	39.18	0.86	3.09	99.63		0.923
	49.31	0.00	0.06	7.44	39.56	0.88	3.17	100.43		0.926
	48.38	0.01	0.07	9.47	38.19	1.28	3.00	100.40		0.905
	48.03	0.01	0.09	8.63	38.43	0.89	3.13	99.21		0.913
	49.55	0.01	0.11	7.82	39.88	0.90	3.03	101.30		0.923
	48.02	0.03	0.11	8.43	38.51	0.87	3.08	99.06		0.915
	48.86	0.02	0.10	7.55	39.32	0.87	3.03	99.75		0.924
*	48.81	0.01	0.07	8.00	39.12	0.93	3.08	100.01		0.920
CP1-AFB										
	10.51	0.01	1.14	44.51	37.10	0.38	1.93	95.58	0.314	
	9.54	0.00	1.12	46.08	35.67	0.51	2.07	95.00	0.284	
*	10.03	0.01	1.13	45.30	36.39	0.45	2.00	95.31	0.299	

Table 3 (cont'd.).

Field No.	TiO_2	Cr_2O_3	Al_2O_3	Fe_2O_3	FeO	MgO	MnO	Total	USP	ILM
CP1-AFB (cont'd.)										
	47.61	0.02	0.07	8.07	37.46	0.98	3.56	97.77		0.917
	47.69	0.03	0.06	8.71	37.55	0.99	3.53	98.55		0.911
	47.35	0.01	0.06	8.62	37.15	1.01	3.58	97.78		0.911
	47.44	0.03	0.06	7.82	37.55	0.96	3.36	97.21		0.919
	46.62	0.00	0.07	8.86	36.84	0.91	3.42	96.72		0.908
	47.62	0.00	0.09	8.78	37.56	0.99	3.45	98.49		0.910
	47.99	0.04	0.09	7.73	37.82	0.99	3.53	98.18		0.921
	47.71	0.01	0.08	8.16	37.65	1.02	3.39	98.02		0.916
	47.72	0.02	0.07	7.89	37.71	0.96	3.45	97.82		0.919
	48.50	0.00	0.06	6.45	38.95	0.81	3.18	97.95		0.934
*	47.65	0.02	0.07	8.11	37.62	0.97	3.46	97.89		0.917
CP1-AFWR										
	9.55	0.03	1.31	47.81	36.48	0.30	2.57	98.05	0.277	
	10.67	0.02	1.31	45.84	35.90	0.59	3.75	98.07	0.300	
	11.14	0.03	1.23	43.36	36.52	0.24	3.43	95.95	0.327	
	10.58	0.02	1.29	44.53	36.36	0.30	3.05	96.13	0.311	
	10.69	0.03	1.35	43.98	37.49	0.39	1.77	95.70	0.323	
	10.92	0.02	0.44	44.37	36.19	0.06	3.58	95.58	0.312	
	10.65	0.02	1.27	45.48	37.62	0.36	2.23	97.63	0.312	
*	10.48	0.02	1.21	45.45	36.76	0.34	2.76	97.01	0.305	
	48.17	0.03	0.09	8.64	34.65	0.99	6.81	99.39		0.909
	47.58	0.02	0.09	11.04	36.57	1.00	4.38	100.68		0.888
	44.66	0.01	0.13	16.21	32.73	1.59	4.54	99.86		0.833
	48.64	0.01	0.09	8.85	38.73	0.91	3.34	100.58		0.912
	47.04	0.02	0.09	10.15	36.76	0.98	3.75	98.79		0.896
	47.81	0.03	0.16	9.98	37.17	1.03	3.94	100.12		0.899
	48.59	0.03	0.13	8.87	35.43	1.02	6.36	100.44		0.908
	48.46	0.01	0.08	8.17	38.77	0.87	3.22	99.58		0.918
*	47.66	0.02	0.11	10.17	36.33	1.04	4.62	99.95		0.896
LW1-A										
	9.72	0.03	1.90	46.74	35.32	1.57	1.72	97.00	0.282	
	10.06	0.05	1.78	45.41	35.97	1.37	1.37	96.01	0.298	
	9.41	0.05	1.97	47.35	35.75	1.38	1.41	97.31	0.276	
	9.56	0.01	1.92	47.23	34.47	1.91	1.90	97.00	0.272	
	7.77	0.02	1.14	49.87	33.70	0.91	1.88	95.29	0.226	
	8.52	0.04	1.99	48.46	34.06	1.52	1.76	96.35	0.249	
	9.14	0.03	1.69	47.20	35.49	1.10	1.41	96.06	0.272	
*	9.32	0.03	1.85	47.25	35.08	1.46	1.63	96.62	0.272	
	39.48	0.00	0.22	22.18	29.16	2.55	1.77	95.36		0.763
	44.35	0.00	0.16	13.33	34.50	2.04	1.72	96.11		0.861
	41.95	0.00	0.24	18.63	30.87	2.54	2.30	96.53		0.803
	36.79	0.00	0.22	29.25	26.29	2.67	2.01	97.23		0.691
	36.65	0.00	0.15	28.65	26.00	2.46	2.54	96.45		0.694
	41.74	0.00	0.19	19.59	30.19	3.03	1.92	96.66		0.792
	45.44	0.00	0.19	12.43	34.20	2.59	2.02	96.87		0.870
	42.90	0.02	0.56	16.21	31.18	3.10	1.85	95.81		0.826
	41.61	0.00	0.21	19.14	29.55	3.21	2.12	95.84		0.794
	43.03	0.01	0.24	17.94	27.93	3.99	3.61	96.75		0.803
*	41.72	0.00	0.24	19.16	30.10	2.89	2.24	96.35		0.796

Table 3 (cont'd.).

Field No.		TiO_2	Cr_2O_3	Al_2O_3	Fe_2O_3	FeO	MgO	MnO	Total	USP	ILM
LW2-A											
		8.49	0.00	1.25	48.84	34.54	1.14	1.53	95.79	0.247	
		8.89	0.01	1.71	48.83	34.32	1.63	1.92	97.30	0.252	
		8.89	0.00	1.55	49.77	34.98	1.48	1.83	98.50	0.249	
		10.28	0.00	1.47	45.78	35.95	1.60	1.30	96.39	0.297	
		9.09	0.00	1.63	48.89	34.64	1.63	1.92	97.81	0.255	
		8.91	0.00	1.62	48.67	34.24	1.55	2.03	97.03	0.252	
		9.95	0.01	1.67	46.31	35.33	1.51	1.86	96.64	0.287	
		10.88	0.02	1.36	45.69	36.90	1.39	1.69	97.93	0.309	
	*	9.44	0.00	1.55	47.84	35.11	1.51	1.77	97.22	0.269	
		41.22	0.00	0.16	19.88	30.61	2.58	1.83	96.28		0.790
		42.99	0.01	0.17	17.11	32.42	2.55	1.67	96.92		0.821
		39.30	0.02	0.22	24.02	29.07	2.41	1.95	96.99		0.748
		43.46	0.01	0.38	15.66	32.87	2.51	1.72	96.61		0.836
		36.35	0.01	0.17	30.38	25.15	2.96	2.23	97.25		0.677
		42.83	0.02	0.20	17.00	32.32	2.53	1.66	96.56		0.822
		42.37	0.01	0.19	18.11	31.57	2.69	1.71	96.65		0.810
		41.97	0.02	0.16	20.21	30.62	2.98	1.79	97.74		0.789
		39.33	0.03	0.58	24.62	29.14	2.42	1.89	98.01		0.744
	*	41.14	0.01	0.24	20.59	30.47	2.62	1.83	96.90		0.784
LW2-5											
		10.53	0.00	0.35	45.55	36.88	0.25	2.32	95.88	0.303	
		9.68	0.00	1.59	48.31	34.80	2.15	1.61	98.14	0.267	
		7.48	0.00	1.62	52.04	32.88	1.61	2.23	97.85	0.207	
		7.80	0.01	1.57	51.02	32.15	1.84	2.63	97.02	0.213	
		9.95	0.00	0.95	47.10	35.31	1.28	2.14	96.73	0.279	
		7.68	0.00	1.69	50.60	32.38	1.68	2.36	96.39	0.215	
		9.19	0.01	1.60	48.33	34.67	1.79	1.52	97.11	0.260	
	*	8.71	0.00	1.46	49.38	33.83	1.66	2.09	97.13	0.243	
		36.75	0.01	0.32	30.49	26.19	2.68	2.05	98.50		0.682
		40.30	0.02	0.20	22.24	29.89	2.01	2.73	97.39		0.767
		36.99	0.01	0.26	29.64	25.95	2.76	2.36	97.97		0.688
		50.40	0.01	0.14	1.93	40.47	1.29	2.52	96.76		0.980
		36.67	0.01	0.49	30.06	26.30	2.51	2.17	98.21		0.685
		36.59	0.00	0.22	30.72	25.92	2.62	2.28	98.36		0.679
		37.82	0.01	0.25	28.17	26.96	2.60	2.38	98.19		0.705
	*	38.54	0.01	0.28	26.45	27.94	2.44	2.34	98.00		0.723
LW2-10											
		10.96	0.06	1.97	44.80	36.23	2.10	1.30	97.42	0.315	
		10.04	0.05	2.20	46.59	34.43	2.45	1.77	97.53	0.282	
		10.34	0.05	2.08	46.50	36.00	2.04	1.35	98.37	0.295	
		10.44	0.02	2.32	44.92	35.98	1.96	1.14	96.78	0.308	
		9.31	0.04	1.97	48.16	35.56	1.76	1.11	97.91	0.269	
		9.33	0.04	1.93	48.23	33.89	2.48	1.53	97.42	0.259	
	*	10.19	0.05	2.07	46.38	35.47	2.13	1.39	97.69	0.291	
		42.74	0.02	0.17	17.19	32.16	2.82	1.23	96.33		0.820
		42.54	0.04	0.18	20.23	30.29	3.69	1.37	98.34		0.789
		42.60	0.02	0.18	17.55	31.89	2.78	1.44	96.47		0.816
		40.58	0.03	0.32	22.36	29.32	3.24	1.38	97.23		0.765
	*	42.12	0.03	0.21	19.33	30.92	3.13	1.36	97.10		0.797

Table 3 (cont'd.).

Field No.		TiO_2	Cr_2O_3	Al_2O_3	Fe_2O_3	FeO	MgO	MnO	Total	USP	ILM
LW4-1WR											
		9.84	0.00	1.78	47.18	35.56	1.57	1.80	97.73	0.281	
		10.91	0.02	3.34	44.86	36.11	2.42	1.72	99.39	0.317	
		10.92	0.00	2.68	44.66	36.64	1.95	1.49	98.33	0.320	
		7.31	0.01	1.76	51.91	31.73	2.19	2.08	96.99	0.200	
		8.84	0.03	2.07	48.90	34.45	1.77	1.75	97.81	0.252	
		9.65	0.02	0.91	48.16	36.75	0.44	2.11	98.05	0.276	
		10.13	0.00	1.84	45.46	36.97	0.98	1.24	96.62	0.305	
		9.32	0.03	2.38	48.28	35.10	1.97	1.54	98.62	0.267	
		8.04	0.03	1.81	50.21	34.25	1.11	2.08	97.53	0.232	
		11.02	0.06	2.51	43.56	35.51	2.12	1.90	96.67	0.322	
	*	9.72	0.02	2.16	47.08	35.43	1.68	1.75	97.84	0.281	
		42.60	0.00	0.23	22.81	22.94	6.12	4.40	99.11		0.743
		43.89	0.00	0.22	15.21	32.92	2.50	2.07	96.80		0.840
		42.79	0.00	0.23	20.56	24.72	5.36	4.15	97.81		0.769
		44.37	0.00	0.27	13.66	34.02	2.32	1.72	96.36		0.857
	*	43.41	0.00	0.24	18.08	28.63	4.08	3.09	97.53		0.804
LW4-1B											
		6.83	0.01	1.21	52.45	33.09	0.82	2.16	96.58	0.195	
		8.48	0.08	1.18	49.74	34.95	0.87	1.97	97.27	0.243	
		6.62	0.06	1.36	52.29	32.49	0.89	2.31	96.02	0.190	
		7.13	0.03	1.36	52.54	33.38	0.87	2.47	97.78	0.201	
		7.16	0.01	1.00	52.14	34.33	0.53	1.75	96.91	0.208	
	*	7.24	0.04	1.22	51.84	33.64	0.80	2.13	96.91	0.207	
		48.94	0.02	0.07	6.24	29.98	3.27	8.10	96.62		0.928
		48.55	0.00	0.09	4.22	38.19	1.39	2.95	95.39		0.956
	*	48.81	0.01	0.07	5.55	32.72	2.64	6.38	96.19		0.938
LW4-5B											
		9.39	0.00	1.52	49.08	34.26	1.93	2.31	98.49	0.255	
		7.76	0.00	0.95	50.44	32.88	1.13	2.39	95.55	0.218	
		8.36	0.00	0.90	49.31	32.78	1.40	2.55	95.30	0.232	
		8.97	0.00	0.74	47.81	35.08	0.38	2.37	95.35	0.261	
	*	8.90	0.00	1.28	49.32	33.88	1.59	2.35	97.32	0.245	
		36.20	0.00	0.18	28.61	27.21	1.68	2.32	96.20		0.698
		39.36	0.00	0.07	22.62	29.47	1.90	2.51	95.93		0.760
		38.92	0.00	0.04	22.64	28.94	1.81	2.80	95.15		0.758
	*	37.67	0.00	0.12	25.63	28.20	1.77	2.49	95.88		0.728
LW4-10WR											
		9.37	0.02	1.01	48.36	35.29	1.04	2.16	97.25	0.264	
		9.57	0.04	1.22	47.29	36.51	0.47	1.99	97.10	0.281	
		7.63	0.04	1.09	51.67	34.06	0.89	2.08	97.46	0.216	
	*	8.86	0.03	1.11	49.10	35.29	0.80	2.08	97.27	0.254	
	*	36.39	0.00	0.22	29.96	24.21	2.95	3.21	96.94		0.676
LW4-15WR											
		3.86	0.05	3.12	59.90	19.92	5.16	6.91	98.92	0.071	
		10.10	0.00	1.89	46.43	35.07	1.79	2.10	97.37	0.287	
		16.91	0.03	2.08	31.53	41.96	1.45	1.51	95.47	0.519	
	*	10.29	0.03	2.36	45.95	32.31	2.80	3.51	97.25	0.277	
		44.56	0.00	0.38	13.48	34.19	2.23	1.88	96.72		0.859
		44.64	0.00	0.17	12.80	33.64	2.19	2.57	96.00		0.865
	*	44.60	0.00	0.28	13.15	33.91	2.21	2.23	96.38		0.862

Table 3 (cont'd.).

Field No.	TiO_2	Cr_2O_3	Al_2O_3	Fe_2O_3	FeO	MgO	MnO	Total	USP	ILM
GU3-31AWR										
	10.70	0.00	1.15	44.60	33.47	1.46	4.00	95.38	0.294	
	8.85	0.00	1.62	47.71	33.13	1.48	2.72	95.51	0.251	
	3.53	0.00	2.11	57.50	29.59	1.50	1.42	95.65	0.102	
*	8.45	0.00	1.51	48.60	32.42	1.48	3.03	95.49	0.237	
*	39.71	0.00	0.64	22.08	28.32	2.98	2.05	95.78		0.762
GU3-28WR										
	6.18	0.03	3.54	52.75	33.44	0.48	3.02	99.45	0.188	
	8.12	0.02	1.77	51.14	33.12	1.64	2.79	98.60	0.222	
	6.49	0.03	2.25	53.86	30.36	1.99	3.55	98.54	0.172	
*	6.91	0.03	2.61	52.50	32.52	1.27	3.08	98.92	0.196	
	35.55	0.06	1.19	28.34	27.38	1.90	1.19	95.61		0.699
	37.69	0.00	0.35	26.10	25.73	2.30	4.01	96.19		0.715
*	36.97	0.02	0.63	26.86	26.27	2.17	3.07	95.99		0.710
GU3-23WR										
	11.04	0.02	2.34	43.27	35.53	2.03	1.81	96.04	0.324	
	9.66	0.01	1.99	46.47	34.78	1.72	1.82	96.45	0.280	
	12.53	0.02	1.11	40.85	37.91	0.63	2.64	95.68	0.368	
*	10.69	0.01	1.96	44.26	35.63	1.63	1.96	96.14	0.312	
	41.10	0.01	0.44	18.98	29.24	2.24	3.68	95.69		0.794
	38.76	0.01	0.65	24.72	26.39	2.81	3.41	96.76		0.732
	38.37	0.00	1.15	23.03	27.76	1.83	3.44	95.58		0.749
*	39.41	0.00	0.75	22.27	27.78	2.30	3.51	96.02		0.758
GU3-20WR										
	10.39	0.00	1.22	47.50	38.48	0.17	2.11	99.87	0.300	
	8.43	0.00	1.41	48.83	36.92	0.08	1.05	96.72	0.259	
	10.04	0.00	1.92	48.43	39.12	0.14	1.80	101.45	0.295	
	10.65	0.00	1.36	44.48	39.12	0.24	0.57	96.42	0.328	
*	9.92	0.00	1.39	47.20	38.33	0.16	1.42	98.42	0.296	
	48.38	0.00	0.05	7.18	37.98	0.27	4.98	98.84		0.926
	50.44	0.00	0.08	4.10	38.14	0.28	6.63	99.67		0.958
	49.24	0.00	0.04	7.14	37.48	0.39	6.03	100.32		0.927
	46.63	0.00	0.13	10.25	36.91	0.21	4.59	98.72		0.895
*	49.28	0.00	0.07	6.24	37.78	0.30	5.92	99.60		0.936
GU3-17WR										
	10.39	0.01	1.38	47.53	37.25	0.11	3.55	100.22	0.293	
	10.07	0.01	1.41	47.93	38.05	0.20	2.24	99.90	0.291	
	9.67	0.00	1.88	47.60	36.19	0.21	3.52	99.07	0.280	
*	10.04	0.01	1.55	47.68	37.16	0.17	3.10	99.72	0.288	
	49.81	0.00	0.07	4.62	36.89	0.09	7.64	99.12		0.951
	49.60	0.00	0.08	5.69	38.13	0.13	6.16	99.79		0.942
	49.09	0.00	0.16	6.13	36.56	0.21	7.12	99.26		0.936
*	49.43	0.00	0.11	5.57	37.01	0.16	7.06	99.35		0.942
GU3-14WR										
	9.85	0.04	1.25	45.64	37.42	0.10	1.53	95.83	0.301	
	9.83	0.06	1.31	46.94	37.60	0.23	1.72	97.68	0.293	
	10.03	0.02	1.62	45.79	36.85	0.11	2.71	97.13	0.300	
*	9.87	0.05	1.33	46.21	37.42	0.16	1.78	96.82	0.297	
	47.72	0.02	0.06	6.46	39.14	0.14	3.48	97.02		0.934
	49.48	0.02	0.05	4.42	38.66	0.29	5.25	98.17		0.954

Table 3 (cont'd.).

Field No.		TiO_2	Cr_2O_3	Al_2O_3	Fe_2O_3	FeO	MgO	MnO	Total	USP	ILM
GU3-14WR (cont'd.)											
		49.05	0.00	0.06	4.58	37.89	0.13	5.91	97.62		0.952
		47.74	0.06	0.08	7.39	39.44	0.15	3.18	98.04		0.925
	*	48.44	0.03	0.06	5.76	38.82	0.17	4.38	97.66		0.941
GU3-11											
		8.42	0.02	1.22	50.86	36.81	0.25	1.62	99.20	0.245	
		10.02	0.04	1.02	47.14	37.32	0.23	2.21	97.97	0.291	
		8.58	0.02	1.13	50.47	36.82	0.27	1.62	98.92	0.250	
	*	9.02	0.02	1.11	49.45	36.98	0.25	1.81	98.65	0.262	
		48.93	0.00	0.11	7.61	39.03	0.83	3.45	99.95		0.924
		48.44	0.02	0.20	7.60	38.23	0.80	3.85	99.14		0.923
		48.42	0.01	0.25	7.54	38.51	0.77	3.61	99.12		0.923
		47.99	0.01	0.16	7.89	38.45	0.85	3.15	98.50		0.920
	*	48.52	0.01	0.17	7.64	38.63	0.81	3.51	99.30		0.923

Table 4. Microprobe Analyses of Biotite.

Field No.	SiO_2	Al_2O_3	FeO	MgO	CaO	Na_2O	K_2O	TiO_2	MnO	BaO	Total
BB9-1A											
	36.27	13.51	21.22	9.88	-	0.60	8.71	4.34	0.56	-	95.09
	36.35	14.32	21.26	9.78	0.04	0.57	8.81	4.31	0.60	0.14	96.18
	35.24	14.16	21.28	9.47	-	0.59	8.20	4.82	0.91	1.29	95.96
	35.58	13.63	20.95	9.73	-	0.58	8.87	4.43	0.53	-	94.30
	35.82	13.41	21.34	9.83	-	0.52	8.70	4.36	1.15	-	95.13
	36.08	13.39	21.17	9.56	-	0.48	8.75	4.34	0.54	-	94.31
	36.69	13.45	21.99	9.79	-	0.57	8.72	4.55	0.60	-	96.36
	35.42	15.02	14.07	13.53	-	0.62	7.95	6.16	0.47	2.52	95.76
	34.75	14.44	14.00	13.51	-	0.64	7.92	5.97	0.41	2.25	93.89
	36.22	13.63	21.54	9.65	-	0.59	8.76	4.44	0.61	-	95.44
	36.78	13.25	21.94	9.79	-	0.59	8.84	4.60	0.60	-	96.39
	36.78	13.43	21.70	9.57	-	0.56	8.89	4.49	0.57	-	95.99
	36.14	13.28	19.74	9.93	-	0.60	8.82	4.29	1.78	-	94.58
	36.68	13.36	21.34	9.59	-	0.56	8.79	4.28	0.62	-	95.22
	36.00	13.18	20.29	9.91	-	0.60	8.44	4.38	1.81	0.15	94.76
	36.64	13.58	21.23	9.92	-	0.59	8.77	4.37	1.03	-	96.13
	35.21	14.29	14.52	13.84	-	0.63	7.77	6.09	0.48	2.42	95.25
	35.57	14.29	14.03	13.63	-	0.58	7.98	6.10	0.42	2.53	95.13
	35.73	12.95	21.19	9.65	-	0.51	8.47	4.13	0.62	-	93.25
	35.72	13.06	20.92	9.67	-	0.51	8.70	4.32	0.52	-	93.42
	36.16	12.99	21.41	9.63	-	0.53	8.68	4.41	0.61	-	94.42
	36.51	13.38	21.20	9.76	-	0.51	8.77	4.20	0.52	-	94.85
	36.89	13.07	20.90	9.83	-	0.59	8.63	4.37	0.55	0.09	94.92
	36.81	13.26	21.27	9.80	-	0.52	8.55	4.20	0.60	-	95.01
BB9-1B											
	36.47	14.42	14.03	14.30	-	0.73	8.67	8.52	0.28	1.30	98.72
	35.25	13.50	13.33	13.44	0.06	0.72	7.94	7.72	0.36	1.38	93.70
	36.31	14.11	13.33	14.38	-	0.76	8.37	7.85	0.35	1.49	96.95
	36.56	14.42	14.62	14.80	-	0.81	8.64	7.81	0.39	1.21	99.26
	35.81	14.76	13.56	14.02	-	0.82	8.23	6.99	0.30	2.35	96.84
	36.21	14.39	14.36	14.06	-	0.83	8.51	7.24	0.46	1.26	97.32
	36.94	14.25	13.84	14.51	-	0.77	8.80	7.06	0.29	0.59	97.05
	36.52	14.31	13.91	14.12	0.05	0.75	8.57	8.39	0.38	1.33	98.33
	36.76	14.17	13.61	14.44	-	0.81	8.72	7.18	0.30	0.75	96.74
	34.68	15.15	15.03	13.24	-	0.94	7.73	7.81	0.33	3.85	98.76
	36.83	14.64	13.97	14.53	-	0.79	8.64	7.00	0.30	1.33	98.03
	36.52	14.32	14.30	14.71	-	0.72	8.57	6.98	0.36	1.33	97.81
	36.61	14.68	13.78	14.56	-	0.76	8.44	6.79	0.32	1.48	97.42
	36.13	14.54	14.22	14.42	-	0.78	8.62	6.75	0.40	1.21	97.07
	36.55	14.22	13.20	13.95	-	0.71	8.31	6.40	0.35	1.38	95.07
	35.90	14.50	14.07	14.09	-	0.80	8.72	6.87	0.31	1.33	96.59
	36.62	14.56	14.40	14.09	-	0.80	8.56	6.73	0.35	1.48	97.59
	36.18	14.28	14.67	13.60	-	0.71	8.57	6.79	0.60	1.39	96.79
	35.78	14.37	13.39	14.03	-	0.78	8.42	6.58	0.33	1.56	95.24
	36.41	14.55	14.25	14.32	-	0.74	8.67	6.44	0.40	1.25	97.03
	36.63	14.33	13.48	14.22	-	0.72	8.45	6.61	0.42	1.43	96.29
	36.28	14.61	14.37	14.15	-	0.75	8.51	6.85	0.35	1.64	97.51
	36.25	14.74	14.47	13.91	-	0.80	8.66	6.73	0.49	1.35	97.40

Table 4 (cont'd.)

Field No.	SiO_2	Al_2O_3	FeO	MgO	CaO	Na_2O	K_2O	TiO_2	MnO	BaO	Total
BB9-1B (cont'd.)											
	36.42	14.27	14.34	14.26	-	0.68	8.73	6.81	0.39	1.24	97.14
	37.22	14.26	13.19	14.68	-	0.77	8.87	6.68	0.31	0.47	96.45
	37.04	13.90	13.72	14.75	0.07	0.77	8.60	7.09	0.30	0.77	97.01
BB9-1C											
	37.22	13.93	14.06	14.53	-	0.74	9.21	5.78	0.35	0.22	96.04
	35.37	15.18	14.21	14.66	0.04	0.81	8.20	6.44	0.32	2.61	97.84
	35.39	15.04	14.43	13.88	0.04	0.88	8.21	6.66	0.36	2.93	97.82
	36.17	14.80	14.00	14.47	0.05	0.73	8.57	6.53	0.25	1.72	97.29
	36.10	14.48	14.21	14.06	-	0.80	8.33	6.60	0.31	2.29	97.18
	36.29	15.00	14.28	14.30	-	0.72	8.79	6.46	0.30	1.34	97.48
	34.65	15.64	14.56	12.87	0.05	0.67	7.45	6.96	0.32	4.68	97.85
	36.37	14.61	14.21	14.27	-	0.76	8.83	6.30	0.30	1.29	96.94
	36.66	14.49	13.52	14.78	-	0.78	8.97	6.03	0.32	0.59	96.14
	33.32	15.32	14.51	13.36	-	0.73	7.69	6.95	0.29	4.05	96.22
	38.23	14.09	14.06	15.31	-	0.64	9.13	6.18	0.31	-	97.95
	37.17	14.13	13.87	14.99	-	0.73	8.99	5.62	0.44	0.09	96.03
	34.59	15.55	14.47	13.59	0.04	0.76	7.99	6.63	0.30	3.40	97.32
	37.28	14.07	13.57	14.97	-	0.82	8.79	6.07	0.25	0.18	96.00
	38.33	13.54	14.50	15.55	-	0.53	9.33	5.06	0.50	0.10	97.44
	37.56	14.06	14.22	15.28	0.07	0.72	9.08	6.26	0.30	0.11	97.66
	37.32	14.82	13.98	15.06	0.07	0.70	8.97	6.15	0.23	0.59	97.89
	34.22	15.00	14.43	13.60	0.08	0.71	8.05	6.66	0.35	2.79	95.89
	35.62	14.90	14.41	13.95	0.05	0.73	8.22	6.56	0.24	2.46	97.14
	35.62	14.78	14.10	14.26	0.04	0.69	8.20	6.51	0.31	2.04	96.55
	37.29	14.79	14.00	15.04	0.03	0.72	8.94	6.25	0.32	0.74	98.12
	35.10	14.72	14.36	14.23	0.03	0.70	8.25	6.46	0.35	1.86	96.06
	36.55	14.71	14.30	14.41	0.04	0.71	8.80	6.36	0.32	1.39	97.59
	36.50	14.28	13.69	15.01	-	0.71	9.04	5.99	0.23	0.13	95.58
	35.62	14.88	13.98	14.51	0.03	0.74	8.81	6.49	0.30	1.32	96.68
BB9-5C											
	36.47	14.96	15.17	13.27	0.07	0.84	8.54	7.54	0.36	1.48	98.70
	37.24	14.37	14.55	14.85	0.05	0.83	8.83	7.00	0.34	0.72	98.78
	36.84	14.65	12.65	14.85	0.03	0.71	8.38	7.06	0.27	1.40	96.84
	34.57	14.61	15.42	13.24	0.04	0.81	7.72	8.08	0.40	3.22	98.11
	35.95	14.50	13.53	13.85	0.05	0.72	8.38	7.30	0.32	2.05	96.65
	35.37	14.62	15.38	14.24	0.04	0.71	8.27	7.08	0.37	2.18	98.26
	35.13	14.45	13.57	13.80	0.05	0.78	8.09	6.12	0.37	1.69	94.05
	35.50	14.06	14.74	14.55	0.14	0.80	8.28	7.03	0.75	1.70	97.61
	35.66	14.04	14.12	14.42	0.06	0.83	8.49	6.88	0.64	1.15	96.29
	36.91	13.10	14.02	15.83	0.05	0.67	9.17	6.64	0.38	-	96.77
	37.12	14.49	13.76	14.55	0.05	0.87	8.51	6.45	0.38	1.37	97.63
	37.13	14.59	14.68	14.80	0.04	0.87	8.72	6.59	0.34	1.52	99.28
	36.40	14.06	13.77	14.74	0.05	0.65	8.71	7.16	0.34	0.97	96.85
	35.97	14.52	14.61	13.99	0.03	0.82	8.63	6.92	0.37	1.73	97.59
	35.76	13.99	13.45	14.24	0.07	0.76	8.26	6.88	0.91	1.72	96.04
	36.02	14.33	15.25	13.87	0.04	0.75	8.37	7.50	0.40	1.84	98.37
	35.80	14.02	15.07	13.31	0.05	0.79	8.36	5.93	0.42	1.19	94.94
	35.11	14.58	14.92	13.25	0.03	0.96	7.94	7.21	0.33	2.99	97.32
	35.72	13.84	16.01	13.91	0.11	0.59	8.70	6.45	0.41	0.82	96.56

Table 4 (cont'd.).

Field No.	SiO_2	Al_2O_3	FeO	MgO	CaO	Na_2O	K_2O	TiO_2	MnO	BaO	Total
BB9-5C (cont'd.)											
	35.80	13.91	11.46	15.51	0.03	0.86	8.27	6.41	0.62	1.21	94.08
	36.61	14.25	13.24	15.04	0.07	0.76	8.68	7.13	1.07	1.31	98.16
	36.08	14.61	15.02	14.29	0.05	0.80	8.58	6.64	0.33	1.64	98.04
	36.18	14.42	13.43	14.43	0.11	0.76	8.57	7.05	0.83	1.25	97.03
	36.12	14.31	14.86	14.05	0.06	0.83	7.91	7.26	0.37	3.03	98.80
BB9-10C											
	35.28	15.03	14.41	14.07	-	0.72	8.13	6.79	0.33	3.00	97.76
	35.98	15.02	14.89	14.27	0.06	0.66	8.52	6.45	0.39	1.63	97.87
	35.06	14.75	14.52	13.53	0.03	0.68	8.09	6.61	0.27	2.78	96.32
	35.41	14.59	14.12	14.82	-	0.82	8.24	6.47	0.32	1.99	96.78
	37.24	14.09	13.98	14.82	-	0.74	9.00	5.69	0.32	0.09	95.97
	34.83	14.00	13.35	14.80	-	0.73	8.23	6.19	0.27	1.67	94.07
	35.66	13.92	13.42	14.25	0.03	0.76	8.81	6.02	0.30	0.82	93.99
	33.95	13.84	13.99	14.56	0.03	0.73	8.56	5.92	0.45	1.42	93.45
	34.68	14.24	14.04	14.01	-	0.76	7.67	6.45	0.31	2.58	94.74
	36.53	14.05	13.61	14.57	-	0.79	8.59	6.36	0.35	1.26	96.11
	35.39	14.16	13.82	13.84	-	0.78	8.38	6.40	0.51	1.64	94.92
	34.89	14.94	13.77	14.19	0.03	0.82	8.14	6.15	0.24	2.44	95.61
	33.03	14.08	14.12	13.03	-	0.73	7.55	6.42	0.34	3.31	92.61
	35.66	14.33	13.88	14.45	-	0.77	8.60	6.39	0.52	1.38	95.98
	35.75	14.42	14.40	14.80	-	0.80	8.83	6.52	0.33	1.43	97.28
	34.60	15.15	13.21	13.61	-	0.81	7.67	6.58	0.20	3.53	95.36
	36.14	14.68	13.88	13.91	-	0.72	8.63	6.25	0.47	1.66	96.34
	34.65	15.00	13.41	14.11	-	0.77	7.92	6.61	0.26	3.05	95.78
	35.41	14.53	13.57	13.30	-	0.68	6.75	5.91	0.27	1.49	91.91
	34.69	14.27	13.70	14.02	0.05	0.81	8.57	6.06	0.86	1.54	94.57
	35.25	14.36	12.29	13.87	0.02	0.78	8.51	5.98	0.25	1.22	92.53
	36.95	14.16	13.26	14.61	-	0.74	9.07	5.84	0.27	0.11	95.01
	36.29	13.83	13.82	15.67	-	0.71	9.16	5.87	0.37	0.30	96.02
	35.93	14.61	13.36	14.46	-	0.74	8.54	6.30	0.46	1.43	95.83
	34.73	13.68	13.51	13.90	-	0.84	8.79	5.85	0.36	0.58	92.24
BB8-85B											
	36.54	13.75	20.06	10.62	-	0.54	8.61	4.21	0.65	0.09	95.07
	36.31	13.30	20.20	10.38	-	0.54	8.56	4.48	0.60	0.13	94.50
	36.29	13.47	20.71	10.24	-	0.58	8.77	4.33	0.49	0.10	94.98
	36.46	13.10	20.45	10.37	-	0.58	8.71	4.38	0.56	0.11	94.72
	37.39	12.64	16.18	13.35	-	0.60	8.67	3.89	0.79	-	93.51
	37.27	13.28	15.76	14.52	-	0.63	8.71	4.30	0.70	-	95.17
	35.97	14.19	13.39	14.30	-	0.69	8.40	6.22	0.26	1.20	94.63
	36.47	13.17	21.65	9.42	-	0.52	8.66	4.15	0.72	0.15	94.91
	35.82	12.74	23.08	9.18	-	0.62	8.23	4.11	0.62	0.11	94.51
	40.15	12.65	19.14	10.04	-	0.53	8.12	4.18	0.52	0.12	95.45
	36.68	13.11	16.79	13.04	-	0.62	8.69	4.38	0.69	0.11	94.11
	35.77	13.35	20.71	9.73	-	0.51	8.82	4.41	0.55	0.11	93.96
	36.53	13.46	19.59	10.40	-	0.56	8.75	4.53	0.62	0.12	94.56
	36.13	13.24	21.26	9.09	-	0.52	8.70	4.35	0.54	0.14	93.97
	37.05	13.61	15.64	13.23	-	0.56	8.87	4.55	0.71	-	94.22
	36.41	13.31	21.34	9.54	-	0.48	8.50	4.50	0.55	0.10	94.73
	36.99	13.08	15.92	13.67	-	0.54	9.06	4.44	0.70	0.09	94.49

Table 4 (cont'd.).

Field No.	SiO_2	Al_2O_3	FeO	MgO	CaO	Na_2O	K_2O	TiO_2	MnO	BaO	Total
BB8-85B (cont'd.)											
	36.21	12.81	20.43	9.86	-	0.64	8.86	4.36	0.67	0.12	93.96
	35.18	14.55	13.60	13.69	-	0.70	8.19	6.50	0.28	2.82	95.51
	36.75	13.20	15.80	13.02	-	0.57	9.00	4.56	0.63	0.12	93.65
	35.59	13.45	20.60	9.74	-	0.51	8.63	4.52	0.58	0.13	93.75
	36.50	13.16	16.26	12.33	-	0.58	8.77	4.11	0.76	-	92.47
	37.34	13.15	15.50	13.82	-	0.63	8.91	4.51	0.73	0.11	94.70
BB8-20											
	35.10	13.45	23.03	9.47	-	0.47	8.99	4.54	0.61	-	95.66
	35.69	13.26	22.51	9.93	0.16	0.51	8.67	4.32	0.60	-	95.65
	36.66	13.77	22.91	9.70	0.05	0.49	8.82	4.51	0.65	-	97.61
	35.84	13.77	22.83	10.24	-	0.35	9.21	4.62	0.53	-	97.39
	35.63	13.54	22.21	9.94	0.04	0.49	8.84	4.64	0.60	-	95.93
	35.69	13.41	22.08	9.60	0.07	0.55	8.71	4.39	0.49	-	94.99
	33.98	13.20	22.31	8.88	0.08	0.51	8.64	4.37	0.66	-	92.63
	35.92	13.56	22.99	9.91	-	0.55	9.06	4.58	0.56	-	97.16
	34.75	13.33	23.09	9.80	0.06	0.50	8.48	4.34	0.49	-	94.96
	35.58	13.76	22.44	9.63	0.07	0.52	8.63	4.55	0.56	-	95.74
	35.76	13.25	22.71	10.00	-	0.52	8.77	4.64	0.59	0.19	96.43
	36.76	13.86	22.72	10.04	-	0.54	8.87	4.39	0.55	-	97.73
	34.91	13.07	21.72	9.85	0.14	0.54	8.52	4.28	0.58	-	93.61
	34.87	13.42	21.94	9.76	0.10	0.54	8.76	4.35	0.53	-	94.27
	36.24	13.66	22.76	10.17	0.07	0.52	9.16	4.64	0.55	-	97.77
	36.16	13.84	20.80	11.06	0.06	0.21	9.33	4.73	0.61	-	96.80
	34.94	13.35	22.35	9.74	0.07	0.54	8.65	4.60	0.56	0.09	94.89
	35.35	13.55	22.49	9.88	-	0.51	8.92	4.40	0.53	-	95.63
	36.14	13.53	22.81	9.55	-	0.48	8.98	4.58	0.75	-	96.82
	36.23	13.79	23.51	9.46	-	0.53	9.09	4.77	0.76	-	98.14
	36.16	13.89	23.33	9.93	-	0.52	9.32	4.65	0.56	-	98.36
	36.49	13.79	22.34	9.93	-	0.52	9.22	4.50	0.54	-	97.33
	35.79	13.53	23.12	9.22	-	0.54	9.25	4.49	0.75	-	96.69
	35.50	13.17	22.70	9.52	-	0.52	8.97	4.54	0.53	-	95.45
BB8-15B											
	38.15	13.69	16.54	13.67	0.05	0.57	9.08	4.25	0.80	-	96.80
	36.70	14.35	21.94	9.79	0.05	0.49	8.74	4.54	0.60	0.24	97.44
	36.28	14.88	20.62	9.81	0.03	0.48	8.54	4.27	0.64	0.22	95.77
	34.43	12.70	20.13	10.16	0.10	0.30	8.64	4.35	0.65	-	91.46
	35.65	13.23	22.53	10.00	0.03	0.48	8.88	4.65	0.54	-	95.99
	35.94	13.62	23.09	9.79	0.05	0.52	8.99	4.75	0.68	-	97.43
	35.48	13.80	21.02	10.66	0.04	0.50	9.17	4.54	0.68	-	95.89
	38.63	15.67	15.01	12.55	0.10	0.49	8.16	3.67	0.72	-	95.00
	38.37	13.76	16.50	13.48	0.03	0.57	8.93	4.12	0.78	-	96.54
	38.55	18.85	13.98	10.06	0.14	0.34	7.11	3.80	0.49	-	93.32
	35.13	13.43	22.71	9.94	0.04	0.51	9.02	4.44	0.59	-	95.81
	35.59	13.36	22.54	9.98	0.03	0.55	9.04	4.44	0.58	-	96.11
	35.84	12.93	21.02	9.66	0.15	0.62	8.45	4.19	0.67	-	93.53
	39.66	23.45	10.42	7.94	0.19	0.30	5.58	2.66	0.43	-	90.63
	36.56	13.62	20.56	11.13	0.04	0.45	9.25	4.52	0.59	-	96.72
	35.39	13.10	22.05	9.31	0.07	0.50	8.64	4.40	0.56	-	94.02
	37.24	15.64	16.10	12.05	0.13	0.36	8.36	4.26	0.71	0.09	94.94
	36.30	13.42	22.94	9.84	-	0.47	9.04	4.83	0.58	-	97.42
	38.49	16.24	18.37	10.27	0.10	0.49	8.00	3.84	0.59	-	96.39

Table 4 (cont'd.).

Field No.	SiO_2	Al_2O_3	FeO	MgO	CaO	Na_2O	K_2O	TiO_2	MnO	BaO	Total
BB8-5											
	36.17	15.16	20.38	8.86	0.15	0.52	7.55	4.07	0.51	0.10	93.47
	38.24	14.63	21.58	9.03	0.05	0.56	8.83	4.52	0.47	0.13	98.04
	36.42	13.79	22.55	10.13	0.03	0.54	9.18	4.80	0.98	0.26	98.68
	34.59	13.01	20.98	9.77	0.08	0.68	8.91	4.38	0.57	0.17	93.14
	35.86	13.70	21.50	9.57	0.09	0.54	8.66	4.52	0.46	0.26	95.18
	36.30	14.06	21.25	9.42	0.04	0.50	8.45	4.26	0.57	0.26	95.11
	35.42	13.55	22.07	9.32	0.03	0.52	8.58	4.30	0.52	0.15	94.46
	35.31	13.74	20.53	8.68	0.11	0.58	7.84	4.18	0.55	0.09	91.61
	35.17	13.02	21.57	9.90	-	0.58	8.97	4.41	0.54	0.11	94.27
	36.44	15.75	19.96	8.26	0.11	0.54	7.77	3.82	0.49	0.12	93.26
	35.41	13.22	22.19	9.79	0.06	0.65	8.37	4.37	0.57	0.10	94.73
	35.38	13.31	21.45	9.58	-	0.52	9.05	4.42	0.59	0.10	94.40
	35.76	13.32	22.53	9.66	0.03	0.58	8.75	4.53	0.51	0.09	95.76
	33.30	12.51	20.21	9.19	0.18	0.55	8.27	4.28	0.52	0.12	89.13
	36.27	13.59	21.89	9.95	0.04	0.60	8.87	4.53	0.51	0.09	96.34
	35.19	12.69	21.06	9.89	0.06	0.49	8.92	4.30	0.54	0.10	93.24
	35.90	13.34	22.49	9.94	0.04	0.60	8.88	4.48	0.48	0.09	96.24
	35.22	13.97	21.47	9.08	0.11	0.64	8.19	4.04	0.58	0.13	93.43
BB8-3B											
	36.45	12.69	15.98	12.90	-	0.56	8.77	3.87	0.74	-	91.96
	35.76	13.50	16.99	12.26	0.05	0.53	8.67	4.64	0.72	-	93.12
	37.46	14.00	15.46	13.46	-	0.51	8.80	3.92	0.72	-	94.33
	37.47	12.83	17.02	13.77	0.06	0.54	8.87	4.17	0.72	-	95.45
	36.27	13.64	16.84	12.80	-	0.52	8.98	4.44	0.75	-	94.24
	36.63	12.68	16.38	13.73	-	0.64	9.19	4.15	0.70	-	94.10
	36.45	15.07	16.63	10.79	0.05	0.54	8.08	4.21	0.72	-	92.54
	37.20	14.10	16.10	12.78	0.04	0.56	8.66	3.95	0.76	-	94.15
	35.85	13.51	14.61	13.43	0.06	0.61	8.48	3.84	0.73	-	91.12
	35.79	13.17	17.38	12.81	-	0.55	9.01	4.33	0.74	0.29	94.07
	35.91	14.00	17.05	12.43	0.03	0.55	8.69	4.48	0.78	0.23	94.15
	35.02	13.06	17.53	11.59	0.06	0.52	9.11	4.42	0.72	-	92.03
	35.72	13.31	17.41	12.20	-	0.54	8.72	4.58	0.66	-	93.14
	36.67	14.44	15.60	12.27	0.04	0.63	8.41	3.83	0.71	-	92.60
	36.20	13.99	16.41	12.48	0.03	0.53	8.81	4.28	0.77	-	93.50
BB8-1											
	36.57	13.00	21.09	11.29	0.19	0.54	8.90	4.18	0.59	-	96.35
	36.84	14.64	19.42	9.92	0.14	0.42	8.19	4.24	0.55	-	94.36
	35.84	12.96	18.58	11.77	0.11	0.52	8.51	3.78	0.55	-	92.62
	36.82	12.93	18.05	12.69	0.26	0.51	8.82	4.00	0.69	-	94.77
	36.48	13.69	20.67	10.38	0.14	0.48	8.85	4.35	1.20	-	96.24
	36.04	13.54	20.67	10.73	0.16	0.53	9.16	4.46	0.70	-	95.99
	36.54	12.79	21.10	10.80	0.12	0.53	8.93	4.62	0.63	-	96.06
	35.86	12.94	20.76	10.15	0.14	0.52	9.07	4.74	0.64	0.16	94.98
	36.03	13.30	20.41	10.87	0.08	0.50	8.93	4.47	0.88	-	95.47
	36.70	12.82	21.21	11.25	0.04	0.56	9.25	4.47	0.70	-	97.00
	36.41	12.92	18.70	11.86	0.19	0.55	8.70	4.57	0.62	-	94.52
	36.09	13.46	20.97	11.05	0.13	0.56	9.06	4.61	0.62	-	96.55
	36.34	13.65	20.50	10.41	0.12	0.46	9.00	4.49	0.62	-	95.59
	36.35	13.52	20.31	11.41	0.14	0.53	9.10	4.34	0.58	0.09	96.37

Table 4 (cont'd.).

Field No.	SiO_2	Al_2O_3	FeO	MgO	CaO	Na_2O	K_2O	TiO_2	MnO	BaO	Total
BB8-1 (cont'd.)											
	36.00	13.06	21.55	10.71	0.05	0.53	9.16	4.71	0.69	-	96.46
	36.12	12.36	19.31	10.03	1.08	0.44	7.88	4.35	0.58	-	92.15
	35.55	12.74	21.27	10.78	0.05	0.47	9.29	4.39	0.62	-	95.16
	36.44	13.44	21.09	11.18	0.04	0.54	9.12	4.54	0.64	-	97.03
	35.94	13.13	20.22	10.76	0.03	0.52	9.05	4.59	0.58	-	94.82
	36.15	13.54	21.03	10.71	0.04	0.48	9.21	4.60	0.60	-	96.36
	36.75	13.38	21.07	11.29	0.06	0.47	9.46	4.52	0.63	-	97.63
	35.72	13.10	20.09	10.75	0.05	0.45	8.34	4.19	0.54	-	93.23
LW1-A											
	35.23	13.33	13.58	13.97	0.07	0.62	8.24	5.58	0.39	0.20	91.21
	37.42	13.72	13.63	14.91	-	0.69	9.05	5.75	0.41	0.20	95.78
	37.42	14.03	13.98	14.87	-	0.70	9.06	5.80	0.36	0.12	96.34
	37.64	14.11	13.37	15.29	0.06	0.73	9.01	5.60	0.60	0.21	96.62
	37.49	14.03	13.81	15.03	0.11	0.72	9.01	5.92	0.39	0.28	96.79
	37.09	13.56	13.73	14.86	-	0.67	8.80	5.75	0.42	0.12	95.00
	37.40	13.83	14.09	14.91	0.03	0.71	9.15	5.98	0.38	0.15	96.63
	37.70	13.84	13.24	14.91	-	0.71	8.96	5.73	0.42	0.10	95.61
	37.78	14.29	13.92	15.06	0.02	0.70	9.07	5.89	0.43	0.20	97.36
	37.87	14.12	13.79	15.39	-	0.72	8.89	5.77	0.40	0.10	97.05
	37.96	14.09	13.49	15.22	0.04	0.72	8.97	5.59	0.35	-	96.43
	35.00	14.17	14.21	14.96	0.04	0.83	8.60	6.01	0.33	0.22	94.37
	36.88	13.52	13.61	14.64	0.03	0.59	8.55	5.69	0.32	0.12	93.95
	38.85	14.38	13.45	15.92	0.04	0.71	8.80	5.95	0.38	-	98.48
	37.36	14.01	13.69	14.64	-	0.71	8.98	5.89	0.79	0.27	96.34
	35.82	14.27	13.87	13.93	0.05	0.74	8.51	6.27	0.43	1.38	95.27
	37.34	13.62	13.85	15.29	0.05	0.66	9.02	5.95	0.38	0.10	96.26
	36.84	14.32	13.43	14.80	0.03	0.69	8.81	5.82	0.43	0.77	95.94
	34.77	15.24	14.41	13.41	0.03	0.75	7.62	6.59	0.40	3.77	96.99
	37.22	13.90	13.72	14.83	-	0.70	8.96	5.84	0.39	0.22	95.78
	38.28	14.06	13.57	15.30	-	0.72	9.01	5.68	0.38	0.12	97.12
	37.95	14.11	13.57	15.04	0.06	0.67	9.07	5.74	0.40	0.10	96.71
	37.39	14.25	13.86	14.78	-	0.69	9.06	6.22	0.40	0.26	96.91
	37.53	13.64	13.97	15.22	-	0.71	8.92	5.98	0.36	-	96.33
	37.00	13.78	13.63	14.99	-	0.64	9.09	5.70	0.44	-	95.27
	36.86	14.17	13.71	14.89	-	0.69	8.97	5.76	0.36	-	95.41
LW2-A											
	37.22	14.18	14.06	14.32	0.05	0.68	9.01	5.84	0.41	0.31	96.08
	37.59	14.35	14.23	14.42	0.03	0.69	9.24	5.84	0.43	0.19	97.01
	37.69	13.90	14.01	14.72	0.03	0.69	9.24	5.71	0.35	0.15	96.49
	37.98	14.36	14.12	15.09	-	0.70	9.17	5.88	0.78	0.09	98.17
	37.79	14.08	13.93	15.21	0.03	0.67	9.21	5.76	0.38	0.09	97.15
	37.58	14.15	14.01	14.89	0.06	0.69	9.09	5.77	0.38	0.19	96.81
	37.62	14.39	14.58	14.72	-	0.66	8.80	6.11	0.39	0.32	97.59
	37.27	13.96	13.80	15.02	-	0.67	8.87	5.56	0.36	0.09	95.60
	36.48	14.18	13.90	13.94	-	0.69	8.19	6.00	0.42	1.11	94.91
	36.64	14.04	14.65	14.74	-	0.68	9.26	6.05	0.39	0.17	96.62
	36.69	14.29	14.10	14.92	0.05	0.71	8.70	5.79	0.63	0.21	96.09
	37.35	13.88	14.18	15.26	0.04	0.74	8.80	5.89	0.38	0.09	96.61
	37.22	13.95	13.92	15.14	-	0.66	9.07	5.70	0.41	0.20	96.27

Table 4 (cont'd.).

Field No.	SiO_2	Al_2O_3	FeO	MgO	CaO	Na_2O	K_2O	TiO_2	MnO	BaO	Total
LW2-A (cont'd.)											
	36.48	14.51	14.27	14.92	-	0.69	8.87	6.04	0.36	0.89	97.03
	36.89	14.25	14.43	15.06	0.07	0.71	8.73	5.78	0.46	0.28	96.66
	36.39	13.76	14.51	14.73	0.06	0.64	8.62	5.92	0.43	0.21	95.27
	38.04	13.82	13.70	15.22	0.04	0.73	9.06	5.75	0.41	0.13	96.90
	37.37	14.14	14.09	14.60	0.04	0.66	8.73	5.75	0.42	0.51	96.31
	37.19	13.74	13.38	14.61	0.10	0.77	8.56	5.64	1.63	0.36	95.98
	38.09	13.91	13.99	15.28	0.04	0.77	9.04	6.04	0.36	-	97.52
	37.39	13.77	14.04	14.66	-	0.67	9.05	5.91	0.46	0.21	96.16
	38.49	14.07	14.33	15.02	0.05	0.64	9.10	5.87	0.36	0.26	98.19
	34.95	14.99	15.42	13.05	0.04	0.70	7.68	6.91	0.41	4.21	98.36
	37.52	14.04	14.10	14.87	-	0.73	9.09	5.81	0.37	-	96.53
	36.61	13.68	13.99	14.43	0.07	0.72	8.48	5.58	0.46	0.12	94.14
	37.34	13.97	14.41	14.92	-	0.69	9.08	5.93	0.32	0.26	96.92
	36.96	14.31	14.24	14.95	-	0.73	9.04	5.88	0.37	0.17	96.65
	37.22	13.88	14.04	14.88	-	0.73	9.14	5.84	0.42	0.12	96.27
LW2-5											
	35.85	15.28	14.11	14.42	-	0.77	7.79	6.88	0.28	3.13	98.51
	38.35	13.87	14.28	15.42	-	0.75	9.01	5.79	0.45	-	97.92
	37.73	14.03	14.48	15.04	0.06	0.75	9.01	5.41	0.53	0.10	97.14
	34.88	14.39	14.17	14.06	0.04	0.82	7.96	6.25	0.74	1.77	95.08
	36.50	14.24	13.95	14.93	0.10	0.83	8.50	6.19	0.33	0.55	96.12
	35.96	13.36	22.21	9.55	-	0.58	9.01	4.61	0.63	0.13	96.04
	37.21	13.94	14.82	14.68	0.06	0.77	8.76	6.19	0.45	0.52	97.40
	36.85	13.87	14.38	14.79	-	0.71	8.95	5.80	0.44	0.21	96.00
	36.60	14.44	14.78	14.65	-	0.69	8.37	6.26	0.43	1.61	97.83
	37.20	14.15	13.93	14.91	0.03	0.75	8.83	6.07	0.43	0.36	96.66
	37.47	13.86	14.45	14.93	0.04	0.71	9.05	5.20	0.54	-	96.25
	37.33	13.61	14.65	14.63	-	0.76	9.15	4.99	0.57	0.11	95.80
	38.15	13.80	14.65	15.44	-	0.69	9.07	5.16	0.54	0.09	97.59
	37.17	14.24	13.82	15.04	-	0.77	8.88	6.26	0.66	0.44	97.28
	37.34	14.62	14.28	15.22	-	0.77	8.52	6.07	0.41	0.44	97.67
	37.86	14.82	14.66	15.21	-	0.76	8.65	5.96	0.49	0.80	99.21
	36.73	13.85	14.31	14.72	-	0.73	8.55	6.00	0.42	0.23	95.54
	38.49	14.26	14.52	14.89	-	0.79	8.95	5.78	0.38	0.12	98.18
	38.36	14.12	14.41	15.46	0.07	0.81	9.02	5.74	0.39	0.09	98.47
	36.54	14.64	13.77	15.01	-	0.76	8.45	6.40	1.56	1.24	98.37
	37.21	13.71	14.53	14.73	-	0.71	8.97	5.95	0.44	0.19	96.44
	37.56	14.28	14.38	14.70	-	0.67	8.99	5.94	0.40	0.21	97.13
	37.52	14.00	14.10	15.00	0.10	0.70	8.77	5.76	1.36	0.18	97.49
	37.10	14.05	14.57	14.80	-	0.72	9.06	5.78	0.45	0.09	96.62
	35.18	15.07	12.73	13.74	-	0.77	7.57	6.65	0.24	2.92	94.87
	35.47	15.30	12.99	13.94	-	0.73	7.58	6.74	0.19	3.39	96.33
	36.79	13.50	21.43	9.63	-	0.55	8.95	4.70	0.52	0.23	96.30
	36.81	13.65	21.82	9.62	-	0.53	9.03	4.65	0.57	0.23	96.91
	35.80	13.42	22.07	9.30	-	0.57	8.89	4.68	0.57	0.15	95.45
	37.65	13.86	12.92	14.81	-	0.66	8.82	6.04	0.38	0.24	95.38
	37.74	13.97	13.36	14.61	-	0.71	9.04	6.12	0.35	0.22	96.12
	36.78	14.58	13.51	14.27	-	0.62	8.77	6.18	0.47	1.07	96.25
	37.09	13.91	13.34	14.85	-	0.66	8.98	5.96	0.38	0.24	95.41

Table 4 (cont'd.).

Field No.	SiO_2	Al_2O_3	FeO	MgO	CaO	Na_2O	K_2O	TiO_2	MnO	BaO	Total
LW2-5 (cont'd.)											
	37.04	14.23	13.40	14.95	-	0.67	8.98	6.04	0.41	0.40	96.12
	37.58	14.12	13.69	14.93	-	0.74	8.91	5.99	0.44	0.33	96.73
	36.78	13.57	14.28	14.82	0.07	0.72	9.06	5.13	0.54	0.09	95.06
	38.04	13.79	13.90	14.97	-	0.79	9.15	5.11	0.50	-	96.25
	37.17	13.56	14.05	14.89	-	0.74	9.15	5.12	0.49	-	95.17
	36.74	13.59	14.02	15.15	-	0.73	8.98	5.51	0.54	0.09	95.35
	37.49	13.66	13.70	15.46	-	0.68	9.00	4.87	0.52	-	95.38
	37.78	14.15	14.14	15.40	-	0.71	9.29	5.10	0.55	-	97.12
	37.74	14.08	14.33	15.36	-	0.74	9.12	5.13	0.45	-	96.95
	37.12	14.56	14.44	14.36	0.11	0.62	9.00	5.18	0.59	0.44	96.42
	36.43	14.02	14.63	14.89	0.05	0.67	8.96	5.09	0.53	0.34	95.61
	37.00	14.22	14.68	15.06	0.03	0.70	8.89	5.18	0.55	0.36	96.67
	37.41	13.69	13.98	15.29	0.05	0.72	8.88	5.14	0.47	0.11	95.74
	36.89	13.38	13.81	14.59	0.03	0.72	8.87	5.10	0.49	-	93.88
	36.47	13.67	13.41	14.70	-	0.64	8.95	5.16	0.51	-	93.51
	36.26	13.82	13.69	14.88	0.03	0.68	9.12	5.13	0.54	0.10	94.25
LW2-10											
	36.53	13.83	21.89	9.87	0.05	0.56	8.94	4.49	0.68	0.22	97.23
	37.07	13.38	20.00	9.53	0.21	0.47	8.18	4.05	0.57	0.23	93.84
	37.05	13.79	22.10	10.19	0.04	0.57	8.94	4.45	0.65	0.24	98.18
	34.37	13.39	21.11	9.67	0.05	0.64	8.51	4.27	0.58	0.26	93.00
	35.52	14.01	22.44	9.51	0.07	0.59	8.77	4.77	0.70	0.75	97.30
	37.01	14.82	22.38	9.93	0.08	0.55	9.04	4.51	0.63	0.29	99.41
	36.30	13.99	22.21	9.81	0.06	0.61	9.10	4.57	0.63	0.25	97.69
	36.99	14.48	22.21	9.94	0.11	0.52	9.22	4.48	0.60	0.29	99.02
	36.79	14.18	22.89	10.02	0.11	0.62	9.01	4.55	0.62	0.25	99.19
	37.09	14.15	22.52	10.16	0.10	0.51	8.99	4.56	0.63	0.28	99.18
	36.16	13.65	22.37	9.78	0.11	0.54	9.00	4.66	0.73	0.27	97.41
	36.15	13.75	21.78	9.49	0.08	0.61	9.19	4.60	0.66	0.33	96.80
	37.08	13.65	22.18	10.34	0.06	0.56	9.32	4.46	0.71	0.32	98.87
	36.17	14.36	23.14	9.89	0.06	0.58	9.17	4.66	0.65	0.29	99.12
	36.69	13.66	22.48	10.42	0.06	0.62	8.87	4.61	0.66	0.30	98.53
	36.37	14.00	22.74	10.06	0.09	0.58	9.18	4.66	0.71	0.21	98.78
	36.92	13.86	22.47	9.58	0.04	0.43	9.24	4.61	0.64	0.27	98.23
	36.87	14.07	22.48	10.05	0.07	0.57	9.09	4.63	0.65	0.28	98.94
	35.69	14.07	23.35	9.90	0.09	0.53	9.09	4.68	0.68	0.32	98.56
LW4-1B											
	36.33	13.33	16.03	13.81	0.03	0.51	9.17	4.48	0.62	0.21	94.52
	37.06	13.22	16.36	14.35	-	0.53	9.37	4.31	0.71	-	95.91
	37.57	13.40	15.85	14.54	0.15	0.50	9.32	4.26	1.80	-	97.43
	36.91	14.15	16.29	13.53	0.09	0.59	9.12	4.72	0.65	-	96.05
	38.36	13.32	15.57	14.58	0.07	0.57	9.15	4.26	0.72	-	96.65
	36.58	13.55	16.00	13.72	0.75	0.56	8.98	4.37	0.67	0.10	95.28
	37.46	13.62	15.67	13.97	0.08	0.56	9.30	4.33	0.67	-	95.66
	36.68	13.49	15.53	14.15	0.06	0.40	9.15	4.39	0.60	0.10	94.55
	34.57	14.01	16.45	13.26	0.07	0.54	8.91	4.89	0.76	0.93	94.39
	35.98	13.37	15.58	13.95	-	0.49	9.08	4.56	0.73	0.09	93.83
	36.01	13.29	15.49	14.63	0.26	0.54	8.93	4.25	0.77	-	94.17
	37.39	13.27	15.70	14.70	0.06	0.52	9.28	4.51	0.66	-	96.13

Table 4 (cont'd.).

Field No.	SiO_2	Al_2O_3	FeO	MgO	CaO	Na_2O	K_2O	TiO_2	MnO	BaO	Total
LW4-1B (cont'd.)											
	37.61	13.84	15.86	14.35	0.08	0.51	9.25	4.49	0.67	0.24	96.90
	36.15	13.48	16.06	14.27	0.08	0.45	9.19	4.57	0.62	0.31	95.18
	36.20	13.24	15.53	14.26	0.11	0.49	9.08	4.43	0.67	0.20	94.21
	36.72	13.43	16.13	14.05	0.09	0.34	9.23	4.94	0.69	-	95.62
	36.68	13.34	15.41	14.02	0.05	0.42	8.96	4.49	0.68	-	94.05
	35.29	14.12	16.23	12.82	0.42	0.57	8.64	4.70	0.76	0.80	94.35
	36.43	13.16	15.82	14.58	0.03	0.50	9.07	4.44	0.62	0.09	94.74
	36.85	13.30	15.60	14.41	-	0.50	9.22	4.36	0.70	-	94.94
	36.53	12.90	15.64	14.18	-	0.51	9.28	4.62	0.66	-	94.32
	37.81	13.69	15.60	14.39	0.05	0.38	9.37	4.41	0.61	0.16	96.47
	36.52	13.44	15.52	13.57	0.03	0.48	9.31	4.31	0.63	-	93.81
	36.50	14.14	16.56	13.14	0.08	0.57	8.83	4.41	0.68	0.89	95.80
	37.39	13.61	15.38	13.94	0.05	0.43	9.10	4.52	0.59	0.23	95.24
	37.66	13.99	15.67	14.33	0.14	0.54	9.20	4.34	0.70	0.22	96.79
	37.79	13.19	15.74	14.01	0.11	0.44	9.07	4.33	0.62	-	95.30
	35.41	14.26	16.38	12.80	0.32	0.46	8.69	4.64	0.72	1.09	94.77
	36.57	13.83	14.97	13.43	0.90	0.43	8.69	4.07	1.26	0.09	94.24
	37.89	13.09	15.57	14.33	0.16	0.48	9.23	4.43	0.64	0.18	96.00
	37.59	13.20	15.02	14.25	0.05	0.42	9.02	4.15	0.67	0.14	94.51
	39.38	14.32	14.81	14.71	0.26	0.45	8.66	4.13	0.59	-	97.31
	37.09	13.05	15.30	14.27	0.59	0.51	8.93	4.46	0.65	0.14	94.99
	36.74	13.52	16.10	14.12	0.17	0.45	9.11	4.44	0.65	0.11	95.41
	37.43	14.14	15.48	14.43	0.15	0.47	8.94	4.40	0.60	0.17	96.21
	37.61	13.43	15.53	14.45	0.03	0.51	9.46	4.43	0.66	0.12	96.23
	37.73	14.08	16.02	14.41	0.04	0.58	9.21	4.42	0.64	0.17	97.30
	37.47	13.57	15.59	14.13	0.05	0.45	9.21	4.53	0.64	0.23	95.87
	36.90	13.88	15.36	14.16	0.07	0.43	9.22	4.37	0.62	0.19	95.20
	36.49	13.24	15.39	13.87	1.18	0.43	8.80	4.25	0.65	0.16	94.46
	36.92	13.07	15.77	14.14	0.10	0.51	8.96	4.33	0.63	0.08	94.51
	38.26	13.59	15.63	14.83	0.37	0.49	9.29	4.39	0.71	0.09	97.65
	36.57	13.39	15.83	14.45	0.14	0.46	9.03	4.41	0.63	0.13	95.04
	36.76	13.24	15.55	14.22	0.05	0.50	9.07	4.43	0.66	0.13	94.61
	37.20	13.31	15.88	14.25	0.05	0.49	9.27	4.50	0.67	-	95.62
LW4-5A											
	40.00	13.48	21.72	9.30	0.06	0.61	8.81	3.91	0.51	0.13	98.53
	37.82	13.02	21.19	9.81	0.11	0.50	8.89	4.24	0.51	0.09	96.18
	35.89	13.59	21.78	9.60	-	0.48	9.14	4.32	0.58	0.08	95.46
	35.43	13.61	21.83	9.35	0.03	0.42	8.91	4.50	0.55	-	94.63
	32.85	14.26	13.68	13.11	0.03	0.67	7.67	6.33	0.29	2.70	91.59
	34.68	13.56	21.45	9.24	0.05	0.54	8.35	4.41	0.51	0.12	92.91
	35.11	14.30	21.75	9.65	0.08	0.78	8.70	4.51	0.51	0.07	95.49
	42.11	14.21	17.61	7.32	0.19	1.13	7.59	3.36	0.48	0.09	94.09
	36.45	13.97	22.59	9.79	0.03	0.40	9.11	4.59	0.57	0.16	97.66
	35.26	13.70	19.90	9.10	0.07	0.53	8.27	3.93	0.44	0.09	91.29
	35.27	14.58	22.77	9.19	0.03	0.44	8.91	4.76	0.58	0.77	97.35
	36.45	13.34	20.45	9.44	0.22	0.54	8.29	4.13	1.22	0.16	94.24
	35.44	13.61	22.71	9.44	0.07	0.49	8.58	4.62	0.56	0.21	95.73
	37.22	14.07	13.80	14.95	0.04	0.78	8.64	5.76	0.35	0.22	95.83

Table 4 (cont'd.).

Field No.	SiO_2	Al_2O_3	FeO	MgO	CaO	Na_2O	K_2O	TiO_2	MnO	BaO	Total
LW4-5B											
	37.13	14.11	14.48	14.90	0.03	0.77	9.25	5.81	0.45	0.22	97.15
	35.84	15.12	13.79	14.32	-	0.75	8.39	6.35	0.32	1.43	96.31
	36.64	14.00	14.03	14.61	0.03	0.73	8.84	5.75	0.40	0.13	95.16
	35.76	13.54	13.63	14.28	0.07	0.71	8.54	5.83	0.36	0.14	92.86
	35.56	14.78	13.97	14.30	0.09	0.72	8.38	6.11	0.33	0.74	94.98
	36.22	14.50	13.64	14.21	0.03	0.72	8.41	6.35	0.34	1.52	95.94
	37.63	14.25	14.73	15.12	0.04	0.73	9.09	5.70	0.43	0.13	97.85
	36.61	14.30	14.10	14.95	-	0.72	8.84	6.11	0.31	0.14	96.08
	36.67	14.49	14.30	14.47	0.06	0.75	8.82	5.89	0.36	0.37	96.18
	35.69	14.65	13.83	14.26	0.03	0.76	8.62	6.29	0.25	0.83	95.24
	36.54	14.16	14.64	14.68	0.04	0.69	9.06	5.83	0.44	0.19	96.27
	34.50	14.36	13.41	14.03	0.07	0.78	8.62	6.11	0.26	0.59	92.73
	36.10	14.06	14.39	14.72	0.08	0.75	8.88	5.75	0.38	0.13	95.24
	35.98	14.21	13.79	14.99	0.07	0.71	9.00	5.92	0.43	0.13	95.23
	35.48	15.00	14.18	14.60	-	0.77	8.48	6.35	0.29	2.14	97.29
	37.02	14.41	14.23	15.23	-	0.77	9.20	5.93	0.44	0.18	97.41
	37.98	14.73	13.31	15.44	-	0.76	9.24	6.24	0.30	0.21	98.21
	36.17	15.18	13.87	14.70	0.09	0.81	8.11	6.52	0.31	1.67	97.43
	34.81	15.50	14.55	13.93	0.03	0.75	8.02	6.84	0.29	2.95	97.71
	36.13	14.95	13.71	15.22	0.56	0.76	8.95	6.33	0.33	1.36	98.30
	36.58	13.94	14.35	14.57	-	0.67	9.08	5.58	0.39	-	95.16
	37.94	13.82	13.85	14.92	0.41	0.80	9.07	5.64	0.36	-	96.81
	35.46	17.48	13.30	15.63	0.31	0.73	9.10	3.08	0.42	0.48	95.99
	36.96	14.13	14.29	14.84	0.08	0.75	8.86	6.38	0.32	0.47	97.08
	36.43	14.72	13.86	14.19	0.04	0.83	8.45	6.30	0.33	1.88	97.03
	37.56	14.20	14.26	14.83	0.08	0.73	9.09	5.99	0.39	0.20	97.33
	36.03	14.84	14.40	14.11	0.06	0.72	8.49	6.56	0.34	1.76	97.31
	37.38	14.50	14.34	14.91	0.08	0.69	9.15	6.08	0.29	0.32	97.74
	35.88	14.53	13.91	14.40	0.05	0.78	8.82	6.44	0.31	1.36	96.48
	37.31	14.41	14.10	14.94	0.04	0.70	9.09	5.89	0.39	0.19	97.06
	36.83	14.57	13.85	14.75	0.10	0.67	8.84	5.93	0.35	0.33	96.22
	36.12	14.73	13.73	14.70	0.08	0.72	8.60	6.23	0.32	1.78	97.01
	37.75	13.92	14.42	15.33	0.07	0.78	9.28	5.73	0.40	0.11	97.79
	36.08	14.79	14.01	14.53	0.91	0.80	8.10	6.47	0.27	1.86	97.82
	35.86	13.31	13.60	15.40	0.05	0.68	9.02	5.59	0.39	-	93.90
	37.36	13.92	14.40	15.00	0.07	0.74	9.05	6.00	0.42	0.14	97.10
	36.58	14.22	13.94	14.71	0.10	0.74	8.96	5.98	0.41	0.28	95.92
	37.74	14.49	13.82	14.81	0.07	0.70	9.33	6.05	0.44	0.15	97.61
	38.23	13.96	13.89	15.57	-	0.73	9.38	5.67	0.42	0.09	97.94
	36.29	13.91	13.95	14.93	0.07	0.72	9.16	5.67	0.40	0.26	95.36
	37.42	14.46	14.25	14.98	0.08	0.73	9.27	5.78	0.40	0.24	97.61
	36.86	13.88	13.31	15.17	0.05	0.70	9.13	5.92	0.34	-	95.41
LW4-10B											
	37.17	13.99	14.50	15.11	-	0.71	9.13	6.02	0.11	0.16	96.90
	36.75	13.22	14.28	14.89	-	0.74	8.88	5.49	0.20	0.14	94.59
	36.53	14.00	15.17	14.63	-	0.71	8.97	6.21	0.16	0.72	97.10
	36.81	13.79	15.55	14.66	-	0.70	9.08	5.97	0.23	0.21	97.00
	35.95	14.68	13.90	14.04	0.07	0.69	8.58	6.10	0.18	0.80	94.99
	37.37	14.14	14.89	14.72	0.14	0.71	9.12	5.87	0.19	0.33	97.52

Table 4 (cont'd.).

Field No.	SiO_2	Al_2O_3	FeO	MgO	CaO	Na_2O	K_2O	TiO_2	MnO	BaO	Total
LW4-10B (cont'd.)											
	35.06	14.30	14.03	14.21	0.07	0.83	8.08	6.48	0.09	1.39	94.58
	36.46	14.09	14.81	14.45	0.19	0.63	8.91	5.98	0.16	0.72	96.40
	35.93	14.16	14.34	14.47	0.11	0.74	8.56	5.83	0.09	0.33	94.56
	37.01	14.45	14.27	15.10	0.02	0.71	9.00	6.17	0.13	0.49	97.35
	36.62	14.00	13.19	14.89	-	0.68	8.97	5.04	0.10	0.08	93.57
	33.63	15.49	13.23	13.41	-	0.83	7.29	6.85	0.22	4.07	95.02
	37.24	14.21	13.76	14.80	-	0.82	9.11	5.82	0.14	0.24	96.14
	37.39	14.10	14.25	15.25	0.04	0.74	8.98	5.64	0.18	0.19	96.76
	36.98	13.88	14.00	14.82	-	0.69	8.57	5.51	0.14	-	94.59
	36.18	14.08	22.97	9.85	-	0.57	9.18	4.52	0.30	0.16	97.81
	35.95	14.04	13.69	13.63	0.14	0.78	8.13	5.41	0.15	0.31	92.23
CP3-2A											
	36.89	15.25	13.77	14.90	-	0.59	8.43	6.40	0.29	1.42	97.94
	35.69	15.54	14.74	13.96	-	0.56	8.06	7.00	0.32	3.33	99.20
	36.82	14.89	14.36	14.58	-	0.59	8.59	6.61	0.35	1.80	98.59
	36.92	15.07	13.81	14.84	0.04	0.64	8.49	6.40	0.35	1.45	98.01
	36.28	14.87	13.96	14.74	-	0.68	8.54	6.42	0.36	1.16	97.01
	37.00	15.00	13.83	14.70	0.06	0.56	8.65	6.35	0.30	1.23	97.68
	37.10	14.93	14.20	14.74	0.04	0.57	8.73	6.35	0.28	0.83	97.77
	35.31	15.83	14.46	13.98	0.07	0.54	7.77	6.93	0.34	3.34	98.57
	35.51	14.91	14.25	14.43	-	0.56	8.54	6.57	0.32	1.78	96.87
	35.41	15.22	13.86	14.46	-	0.61	8.46	6.42	0.33	1.53	96.30
	35.00	15.79	14.46	13.91	-	0.53	7.88	6.96	0.34	3.59	98.46
	34.77	15.43	14.56	13.83	-	0.58	7.83	7.09	0.32	3.83	98.24
	37.27	14.70	14.15	14.71	-	0.59	8.60	6.21	0.29	0.85	97.37
	36.86	14.72	13.94	14.93	-	0.39	8.60	6.22	0.28	0.71	96.65
	37.10	14.94	14.28	14.80	-	0.65	8.72	6.58	0.37	1.48	98.92
	36.66	14.60	13.83	14.75	-	0.61	8.56	6.51	0.28	1.42	97.22
	37.36	14.74	13.53	14.93	-	0.58	8.75	6.40	0.26	0.77	97.32
	36.49	14.50	13.97	14.76	0.08	0.63	8.75	6.47	0.30	1.28	97.23
	36.75	14.38	14.25	14.69	-	0.67	8.63	6.52	0.31	1.29	97.49
	36.01	14.98	14.23	14.35	-	0.69	8.19	6.48	0.35	2.06	97.34
	34.65	14.75	14.65	13.27	-	0.65	7.55	6.68	0.42	3.24	95.86
	35.65	14.81	14.10	13.75	0.04	0.81	8.21	6.35	0.33	1.72	95.77
	36.95	15.20	15.11	14.49	0.04	0.75	8.26	6.37	0.30	1.50	99.02
	36.17	14.57	14.39	13.67	-	0.78	8.60	6.32	0.32	1.25	96.07
	36.89	14.60	14.01	14.40	-	0.69	8.86	6.18	0.35	1.17	97.15
	36.46	13.63	13.52	14.24	-	0.75	8.54	6.10	0.31	0.15	93.70
	35.64	14.73	14.64	14.06	-	0.67	8.42	6.70	0.37	2.47	97.70
	36.08	14.46	14.31	14.17	-	0.65	8.72	6.36	0.35	1.44	96.54
	35.89	14.52	13.91	14.02	-	0.72	8.00	6.25	0.33	1.40	95.04
	36.61	15.26	14.06	14.06	0.06	1.46	8.43	6.45	0.37	2.09	98.85
	36.02	14.69	13.79	14.32	0.06	0.63	8.77	6.28	0.36	1.08	96.00
	35.81	14.53	14.61	14.20	-	0.73	8.53	6.30	0.34	1.39	96.44
	36.68	14.75	14.14	14.44	-	0.73	8.71	6.32	0.34	1.26	97.37
	36.10	14.44	14.15	14.22	-	0.66	8.48	6.59	0.34	1.59	96.57
	36.42	14.60	14.05	14.20	-	0.65	8.70	6.39	0.39	1.40	96.80
	34.33	15.00	14.45	13.63	-	0.72	7.63	6.55	0.33	3.51	96.15
	37.15	14.90	13.63	14.88	-	0.72	8.87	6.30	0.32	0.89	97.66

Table 4 (cont'd.).

Field No.	SiO_2	Al_2O_3	FeO	MgO	CaO	Na_2O	K_2O	TiO_2	MnO	BaO	Total
CP3-2A (cont'd).											
	36.35	14.55	14.12	14.49	-	0.74	8.56	6.48	0.31	1.78	97.38
	35.90	14.45	13.90	14.26	-	0.66	7.96	6.29	0.29	1.56	95.27
	35.83	14.54	13.99	14.62	0.05	0.71	8.48	6.40	0.29	1.60	96.51
	35.85	14.65	14.19	13.95	-	0.75	8.55	6.43	0.34	1.41	96.12
	35.71	14.37	13.60	14.26	-	0.69	8.76	6.50	0.32	1.35	95.56
	36.13	15.37	14.50	14.61	-	0.74	8.36	6.35	0.30	2.44	98.80
	36.00	14.86	14.09	14.49	-	0.73	8.59	6.29	0.32	1.40	96.77
	35.23	15.57	14.68	13.69	0.11	0.78	8.31	7.00	0.40	3.47	99.43
	36.68	14.94	14.52	14.81	0.06	0.81	8.71	6.56	0.51	1.91	99.70
	34.04	13.84	13.85	14.31	0.39	0.78	7.74	6.16	5.99	2.94	100.23
	35.71	14.96	14.63	14.54	0.07	0.78	8.24	6.69	0.43	2.29	98.52
	38.07	15.17	13.57	15.04	0.16	0.74	8.70	6.25	0.40	0.71	99.01
CP3-2B											
	37.03	14.02	13.91	14.76	0.06	0.59	8.33	6.16	0.34	0.36	95.56
	37.08	14.14	13.91	14.58	-	0.57	8.86	6.21	0.31	0.45	96.11
	35.13	13.48	13.86	13.99	0.04	0.56	8.28	5.91	0.30	0.39	91.94
	37.20	14.12	13.84	14.56	0.05	0.68	8.89	6.11	0.37	0.44	96.26
	36.62	14.15	13.95	14.49	0.04	0.64	8.80	6.15	0.33	0.47	95.64
	36.43	14.05	13.65	14.06	-	0.61	8.87	6.17	0.34	0.75	94.93
	37.81	14.02	13.99	14.91	-	0.58	8.89	6.08	0.30	0.11	96.69
	35.69	14.36	13.60	14.07	-	0.60	8.28	6.29	0.35	1.27	94.51
	37.11	14.08	13.67	14.61	0.04	0.60	8.56	6.09	0.26	0.45	95.47
	37.16	14.32	14.34	14.94	0.04	0.59	8.91	6.18	0.32	0.45	97.25
	36.79	14.19	14.21	14.57	-	0.57	8.51	6.26	0.32	0.64	96.06
	36.86	14.06	14.12	14.50	-	0.60	8.82	5.82	0.27	0.40	95.45
	37.93	14.36	13.81	14.76	0.04	0.60	8.49	6.16	0.32	0.53	97.00
	37.23	13.86	13.75	15.00	-	0.59	8.78	5.94	0.29	0.18	95.62
	35.30	13.66	13.44	13.70	0.04	0.64	8.30	5.85	0.29	0.58	91.80
	36.69	14.21	13.54	14.88	-	0.61	8.71	6.04	0.28	0.08	95.04
	37.05	14.39	14.31	14.64	0.12	0.66	8.70	6.34	0.32	0.56	97.09
	36.11	14.23	13.53	14.61	-	0.63	8.23	5.97	0.29	0.43	94.03
	37.22	13.70	13.54	14.87	0.03	0.58	8.94	5.71	0.28	-	94.87
	36.80	14.13	14.02	14.37	-	0.63	8.57	6.16	0.34	0.62	95.64
	37.05	14.04	13.65	14.39	0.06	0.62	8.59	6.18	0.31	0.69	95.58
	35.40	13.82	13.84	14.06	0.19	0.72	8.50	6.27	0.30	0.51	93.61
CP3-1D											
	37.36	14.12	14.65	15.23	-	0.68	9.17	5.51	0.43	0.15	97.30
	36.98	14.22	14.67	14.63	0.04	0.62	9.00	5.88	0.47	0.32	96.83
	37.68	13.77	14.36	14.94	0.03	0.56	8.99	5.86	0.37	-	96.56
	37.15	14.34	14.28	14.86	0.05	0.62	8.89	5.80	0.42	0.26	96.67
	37.61	14.01	14.47	15.32	-	0.65	9.32	5.40	0.45	0.16	97.39
	36.08	13.57	14.08	14.04	0.10	0.62	8.75	5.72	0.36	0.22	93.54
	37.89	14.40	14.52	14.99	-	0.43	9.26	5.86	0.44	0.20	97.99
	38.07	14.29	14.21	14.55	-	0.66	9.23	5.85	0.45	0.13	97.44
	37.82	14.48	14.37	14.71	-	0.65	9.23	5.80	0.47	0.29	97.82
	37.20	14.00	14.12	14.99	-	0.68	9.09	5.70	0.70	0.17	96.65
	37.17	13.47	14.34	14.58	0.06	0.58	9.01	5.79	0.41	-	95.41
	37.31	14.37	14.23	14.80	-	0.66	9.08	5.65	0.54	-	96.64
	36.65	14.26	14.63	14.61	0.04	0.66	9.00	5.66	0.44	0.22	96.17

Table 4 (cont'd.).

Field No.	SiO_2	Al_2O_3	FeO	MgO	CaO	Na_2O	K_2O	TiO_2	MnO	BaO	Total
CP3-1D (cont'd).											
	35.93	14.36	14.63	14.13	0.05	0.55	8.82	5.78	0.43	0.56	95.24
	35.95	14.81	14.30	14.10	-	0.63	8.27	6.04	0.46	2.29	96.85
	39.32	14.23	13.52	15.33	0.08	0.66	8.65	5.61	0.33	0.23	97.96
	36.88	14.19	14.30	14.95	-	0.64	8.88	5.87	0.42	0.25	96.38
	37.94	14.09	14.36	15.39	-	0.65	9.05	5.68	0.39	-	97.55
CP1-3A											
	36.34	13.88	22.22	9.55	-	0.52	8.81	4.39	0.54	0.15	96.40
	36.47	13.18	21.64	9.69	0.15	0.46	8.55	4.40	0.56	0.13	95.23
	36.19	12.91	21.36	10.16	0.03	0.54	8.21	4.32	0.49	0.10	94.31
	35.61	13.14	20.69	9.83	-	0.51	8.22	4.36	0.55	0.14	93.05
	36.14	13.58	22.64	9.63	0.07	0.52	8.52	4.53	0.54	0.10	96.27
	36.24	12.71	20.51	9.61	0.43	0.38	6.65	4.11	0.46	0.15	91.25
	34.81	13.68	23.33	9.23	0.03	0.51	8.79	4.66	0.61	0.67	96.32
	35.34	13.07	22.15	9.42	-	0.47	8.68	4.32	0.51	0.18	94.14
	37.25	13.90	22.97	9.94	-	0.36	9.05	4.39	0.46	-	98.32
	35.64	13.36	23.05	9.73	-	0.42	9.03	4.49	0.47	-	96.19
	37.12	13.67	22.15	9.91	-	0.41	8.95	4.36	0.41	-	96.98
	36.01	13.47	21.91	9.73	-	0.46	8.88	4.36	0.48	-	95.30
	36.26	14.10	21.89	9.71	-	0.40	9.05	4.46	0.51	-	96.38
	36.55	13.75	22.94	9.67	-	0.48	9.01	4.33	0.58	-	97.31
	37.53	14.00	21.67	9.38	0.09	0.39	8.40	4.33	0.42	-	96.21
	38.58	12.82	20.51	8.34	0.40	0.13	6.38	4.09	0.35	-	91.60
	37.14	12.81	20.86	8.64	0.35	0.25	6.78	4.09	0.39	-	91.31
	36.54	13.38	22.46	9.74	0.07	0.39	8.95	4.24	0.45	-	96.22
	36.04	13.84	22.80	9.97	-	0.46	9.08	4.53	0.48	-	97.20
GU3-11											
	36.18	13.33	23.21	9.24	-	0.57	8.94	4.35	0.64	-	96.46
	36.45	13.55	22.83	9.38	-	0.62	9.04	4.51	0.66	0.09	97.13
	36.45	13.72	22.76	9.81	-	0.52	9.13	4.59	0.50	-	97.48
	35.31	12.90	23.44	8.76	0.07	0.51	9.02	4.39	0.61	-	95.01
	36.37	13.74	20.05	11.02	-	0.59	9.01	4.32	0.71	-	95.81
	36.23	13.34	22.30	9.46	-	0.53	9.04	4.37	0.82	-	96.09
	35.69	13.51	23.77	8.86	-	0.53	8.97	4.47	0.56	-	96.36
	35.94	13.46	22.25	9.40	-	0.52	8.88	4.48	0.53	-	95.46
	41.17	14.55	14.52	10.03	0.06	0.39	10.58	5.00	0.43	-	96.73
	35.76	14.00	24.29	9.03	0.03	0.56	9.19	4.52	0.53	-	97.91
	37.07	13.97	23.10	9.89	-	0.56	9.33	4.50	0.77	-	99.19
	36.20	13.52	23.76	8.87	0.03	0.56	9.14	4.45	0.75	0.12	97.40
	36.48	13.26	22.62	9.44	0.07	0.71	9.10	4.44	0.74	0.07	96.93
	35.79	13.59	23.90	8.57	-	0.61	8.94	4.53	0.66	-	96.59
	36.04	13.28	22.92	9.29	-	0.58	8.91	4.43	0.56	-	96.01
	35.80	13.44	22.09	9.49	-	0.64	8.78	4.40	0.83	-	95.47
	36.59	13.86	23.21	8.90	-	0.56	9.09	4.50	0.59	-	97.30
	38.98	13.54	16.73	12.05	0.03	0.63	9.03	4.17	0.67	-	95.83
	36.09	13.90	22.98	9.53	0.04	0.61	9.02	4.52	0.62	0.16	97.47
	36.44	13.34	22.15	9.97	0.03	0.64	9.00	4.34	0.50	-	96.41
	36.35	13.63	24.02	9.24	-	0.63	9.19	4.62	0.67	-	98.35
	37.38	13.67	20.41	10.18	-	0.40	9.45	4.51	0.52	-	96.52
	36.48	13.84	23.85	9.11	-	0.55	9.30	4.59	0.58	-	98.30
	35.82	13.59	22.41	9.11	-	0.53	8.98	4.45	0.98	-	95.87

Table 5. Microprobe Analyses of Pyroxene.

Field No.	SiO_2	Al_2O_3	FeO	MgO	CaO	Na_2O	K_2O	TiO_2	MnO	BaO	Total
BB9-1B											
	52.02	1.58	8.98	14.27	21.06	0.64	-	0.82	1.08	-	100.45
	52.72	1.49	8.38	14.32	20.95	0.64	-	0.55	0.93	-	99.98
	51.06	1.81	8.65	13.62	21.59	0.66	-	0.57	0.97	-	98.93
	52.20	1.99	9.10	13.65	21.57	0.74	-	0.82	1.10	-	101.17
	52.55	1.35	8.50	14.22	21.31	0.61	-	0.61	0.96	-	100.11
	51.54	1.34	8.42	14.15	21.07	0.59	-	0.44	0.94	-	98.49
	50.41	1.46	9.02	14.25	21.38	0.59	-	0.48	0.90	-	98.49
	50.17	1.67	8.50	13.87	21.56	0.65	-	0.65	0.94	-	98.01
	50.47	1.54	8.16	14.07	21.48	0.65	-	0.62	0.80	-	97.79
	50.90	1.61	8.70	14.04	21.77	0.62	-	0.65	1.00	-	99.29
	52.24	1.60	9.16	13.93	21.54	0.64	-	0.55	1.10	-	100.76
	52.65	1.69	8.30	14.21	21.55	0.62	-	0.80	0.90	-	100.72
	52.27	1.75	8.98	14.23	21.38	0.67	-	0.48	0.96	-	100.72
	51.60	1.71	8.38	13.77	21.52	0.73	-	0.59	1.02	-	99.32
	51.92	1.23	8.81	14.14	21.33	0.65	-	0.52	1.22	-	99.82
	53.60	1.33	8.85	14.43	21.24	0.64	-	0.59	1.04	-	101.72
	52.40	1.24	9.11	14.38	21.06	0.64	-	1.80	1.21	-	101.84
	52.38	1.82	8.55	14.42	21.20	0.66	-	0.46	0.86	-	100.35
	52.97	1.63	9.09	13.79	21.07	0.71	-	0.44	1.26	-	100.96
	52.95	1.75	8.31	14.05	21.39	0.62	-	0.55	0.96	-	100.58
	51.93	3.43	8.37	13.10	19.61	1.03	0.41	0.56	0.97	-	99.41
	50.25	1.44	8.27	14.49	20.48	0.66	-	0.14	1.03	-	96.76
	52.78	1.50	8.59	14.27	21.20	0.63	-	0.38	0.84	-	100.19
	52.53	1.55	9.13	14.64	20.96	0.61	-	0.25	1.00	-	100.67
BB9-1C											
	49.66	2.10	8.26	14.60	19.68	0.56	-	0.51	0.65	-	96.02
	51.46	1.99	8.65	13.91	20.69	0.73	-	0.52	0.94	-	98.89
	50.67	2.05	8.49	14.46	20.85	0.56	-	0.52	0.71	-	98.31
	51.46	1.65	8.63	13.87	20.94	0.68	-	0.49	1.17	-	98.89
	52.43	1.74	8.44	14.32	21.25	0.57	-	0.42	0.91	-	100.08
	52.02	1.06	9.07	13.47	20.68	0.63	-	0.31	1.36	-	98.60
	51.62	1.46	8.89	13.77	21.22	0.57	-	0.33	1.42	-	99.28
	52.20	0.99	8.51	14.03	21.65	0.60	-	0.31	1.24	-	99.53
	53.59	2.07	17.47	24.40	1.30	-	-	0.37	0.58	-	99.78
	51.29	1.84	8.92	13.68	20.68	0.67	-	0.53	1.10	-	98.71
BB9-5C											
	52.21	1.02	10.95	12.28	20.61	0.69	-	0.44	2.10	-	100.30
	53.17	1.38	8.11	14.31	21.20	0.58	-	0.50	0.99	-	100.24
	50.25	2.10	8.27	13.65	20.45	0.62	-	0.71	0.84	-	96.89
	52.18	2.19	8.62	13.91	20.97	0.70	-	0.73	0.98	-	100.28
	51.77	2.50	8.01	14.61	21.27	0.57	-	0.89	0.95	-	100.57
	51.94	0.92	10.10	12.83	21.07	0.61	-	0.27	2.03	-	99.77
	52.96	1.12	8.91	13.80	21.61	0.62	-	0.37	1.41	-	100.80
	52.72	2.08	9.49	13.56	20.75	0.64	-	0.76	0.87	-	100.87

Table 5 (cont'd.).

Field No.	SiO_2	Al_2O_3	FeO	MgO	CaO	Na_2O	K_2O	TiO_2	MnO	BaO	Total
BB9-5C (cont'd.)											
	51.14	1.31	7.57	13.89	20.49	0.55	-	0.46	0.90	-	96.31
	51.39	1.51	8.16	14.15	21.17	0.65	-	0.34	0.94	-	98.31
	52.39	1.67	8.42	14.27	21.39	0.65	-	0.48	0.91	-	100.18
	51.83	1.87	8.27	14.16	21.29	0.61	-	0.63	0.93	-	99.59
	53.02	1.56	8.30	14.62	21.06	0.57	-	0.46	0.79	-	100.38
	52.38	1.57	7.82	13.98	21.86	0.57	-	0.49	0.87	-	99.54
	53.13	1.55	8.50	14.21	21.59	0.60	-	0.46	0.98	-	101.02
	52.83	1.65	8.08	14.38	21.75	0.54	-	0.67	0.80	-	100.70
	52.92	1.15	9.13	13.43	21.77	0.66	-	0.46	1.37	-	100.89
	53.48	1.55	7.85	14.60	21.69	0.60	-	0.43	0.83	-	101.03
	53.46	1.42	8.92	14.05	20.78	0.58	-	0.59	0.67	-	100.47
	51.38	0.77	12.05	11.46	19.93	0.51	-	0.27	2.25	-	98.62
	51.25	0.70	12.29	11.33	20.21	0.55	-	0.30	2.17	-	98.80
	53.24	0.86	11.43	12.00	20.83	0.64	-	0.33	2.29	-	101.62
	53.02	1.63	8.75	14.30	21.62	0.59	-	0.42	1.06	-	101.39
	52.59	1.68	8.38	14.17	21.59	0.66	-	0.54	0.89	-	100.50
	52.34	1.51	8.31	14.26	21.40	0.64	-	0.62	0.88	-	99.96
	52.12	1.05	9.87	12.68	21.42	0.65	-	0.29	1.81	-	99.89
	52.81	1.06	10.67	12.91	20.83	0.71	-	0.49	1.78	-	101.26
	52.76	1.06	9.15	13.46	21.29	0.62	-	0.34	1.51	-	100.19
	51.73	1.88	8.24	13.86	21.41	0.54	-	0.59	0.73	-	98.98
	52.01	1.71	8.41	14.62	21.47	0.61	-	0.44	0.82	-	100.09
	52.93	1.59	8.55	14.72	21.22	0.54	-	0.59	0.81	-	100.95
	52.87	1.53	8.29	14.59	21.48	0.66	-	0.48	0.93	-	100.83
	52.56	1.43	8.09	14.00	21.55	0.57	-	0.56	0.91	-	99.67
	52.63	1.93	8.80	14.17	20.90	0.60	-	0.57	0.96	-	100.56
	52.66	1.55	8.00	14.33	20.96	0.65	-	0.46	0.94	-	99.55
BB9-10C											
	53.21	2.71	7.90	12.77	19.65	0.74	0.33	0.57	0.90	-	98.78
	53.08	1.47	8.29	14.25	20.42	0.62	-	0.36	1.02	-	99.51
	51.80	1.63	8.57	14.06	20.60	0.56	-	0.29	0.89	-	98.40
	52.57	1.69	8.57	13.88	20.22	0.57	-	0.49	1.03	-	99.02
	52.41	1.58	8.41	14.12	20.55	0.64	-	0.26	0.95	-	98.92
	52.62	1.52	8.69	14.04	20.73	0.66	-	0.47	0.97	-	99.70
	51.48	1.43	8.06	14.34	21.03	0.57	-	0.10	0.93	-	97.94
	53.05	1.49	8.40	13.98	20.64	0.58	-	0.26	1.21	-	99.61
	52.64	1.37	8.44	13.78	20.02	0.63	-	0.31	1.15	-	98.34
	52.46	1.16	8.91	14.02	20.74	0.60	-	0.16	1.13	-	99.18
	52.81	1.58	8.32	14.25	20.77	0.65	-	0.21	0.94	-	99.53
	51.62	1.83	8.19	13.82	20.64	0.65	-	0.34	0.94	-	98.03
	52.13	1.42	8.43	13.82	20.66	0.61	-	0.55	0.92	-	98.54
	51.71	1.60	8.27	13.96	20.34	0.57	-	0.21	0.87	-	97.53
	52.87	1.59	8.15	14.06	20.76	0.59	-	0.83	0.94	-	99.79
	52.07	1.33	8.25	14.09	20.74	0.60	-	0.26	1.03	-	98.37
	52.80	0.97	10.13	12.89	20.03	0.58	-	0.39	1.92	-	99.71
	52.35	1.64	8.52	14.35	20.82	0.64	-	3.40	0.91	-	102.63
	51.94	1.32	9.00	13.23	20.11	0.69	-	0.18	1.12	-	97.59
	52.80	1.57	9.13	13.12	20.46	0.71	-	0.60	1.18	-	99.57
	52.44	1.60	8.49	14.32	21.14	0.56	-	0.49	0.80	-	99.84

Table 5 (cont'd.).

Field No.	SiO_2	Al_2O_3	FeO	MgO	CaO	Na_2O	K_2O	TiO_2	MnO	BaO	Total
BB9-10C (cont'd.)											
	52.41	1.55	7.97	13.91	20.37	0.63	-	0.29	0.86	-	97.99
	51.71	1.33	8.83	13.60	20.73	0.62	-	0.47	1.29	-	98.58
	52.57	0.90	8.69	13.73	20.63	0.63	-	0.23	1.48	-	98.86
	52.87	0.85	8.31	13.58	20.53	0.56	-	0.10	1.23	-	98.03
	50.83	3.02	8.71	14.08	20.17	0.40	-	1.11	0.79	-	99.11
	51.68	1.81	8.33	14.28	20.35	0.54	-	0.44	0.82	-	98.25
	52.62	1.58	8.30	14.51	20.51	0.60	-	0.41	0.91	-	99.44
	52.67	1.33	8.79	13.80	21.30	0.64	-	0.54	1.47	-	100.54
	51.32	0.78	9.67	12.66	21.21	0.54	-	0.23	1.73	-	98.14
	52.85	0.76	9.57	12.92	21.50	0.51	-	-	1.79	0.00	99.90
	52.31	1.22	8.84	13.65	21.06	0.63	-	0.44	1.21	-	99.36
	52.73	1.74	8.63	14.85	21.10	0.52	-	0.80	0.79	-	101.16
	52.60	1.77	8.41	14.78	21.73	0.59	-	0.36	0.77	-	101.01
	51.38	1.55	8.04	14.12	20.91	0.56	-	0.75	0.86	-	98.17
	53.21	0.97	10.11	13.17	21.39	0.49	-	0.49	0.94	-	100.77
	51.39	1.35	8.27	13.44	20.33	0.59	-	0.21	1.06	-	96.64
	52.38	1.33	7.97	14.44	21.24	0.53	-	0.18	0.80	-	98.87
	51.67	1.50	8.46	14.37	21.72	0.62	-	0.36	0.84	-	99.54
	51.13	1.82	8.49	14.29	20.98	0.62	-	0.46	0.74	-	98.53
	50.42	0.95	10.42	12.24	20.73	0.57	-	0.21	2.00	-	97.54
	51.89	1.26	8.59	13.63	21.02	0.59	-	0.39	1.18	-	98.55
LW1-A											
	52.63	1.24	9.27	13.49	21.29	0.75	-	0.33	1.75	-	100.75
	52.79	1.10	9.21	13.26	20.89	0.59	-	0.24	1.72	-	99.80
	51.83	1.52	8.54	13.74	20.84	0.72	-	0.45	1.13	-	98.77
	50.86	1.08	10.75	11.74	19.51	0.74	-	0.26	2.26	-	97.20
	51.78	1.51	9.14	13.04	20.77	0.88	-	0.44	1.81	-	99.37
	51.94	1.27	8.06	13.95	21.00	0.60	-	0.33	1.14	-	98.29
	52.35	1.34	8.60	13.67	21.31	0.74	-	0.33	1.26	-	99.60
	53.26	1.06	8.22	14.14	21.28	0.70	-	0.29	1.23	-	100.18
	51.49	1.65	8.79	13.87	21.19	0.70	-	0.44	1.13	-	99.26
	51.42	1.34	8.32	13.91	21.46	0.69	-	0.36	1.27	-	98.77
	52.21	1.12	8.27	14.37	21.29	0.66	-	0.33	1.32	-	99.57
	52.08	1.22	8.34	13.76	21.45	0.66	-	0.32	1.35	-	99.18
	51.92	1.31	8.02	14.07	21.25	0.66	-	0.36	1.28	-	98.87
	52.43	1.18	8.72	13.17	21.03	0.69	-	0.28	1.46	-	98.96
	52.56	1.02	8.47	13.27	21.20	0.66	-	0.25	1.56	-	98.99
	52.33	1.04	8.83	13.87	21.43	0.64	-	0.25	1.48	-	99.87
	52.83	1.30	8.63	13.79	20.98	0.70	-	0.36	1.22	-	99.81
	52.52	1.17	9.05	13.44	20.71	0.64	-	0.35	1.56	-	99.44
	52.68	1.20	8.81	13.74	21.21	0.79	-	0.33	1.38	-	100.14
	51.98	1.38	8.45	13.63	20.76	0.70	-	0.39	1.37	-	98.66
	51.86	1.50	8.40	14.28	20.75	0.64	-	0.45	1.03	-	98.91
	51.66	1.10	8.80	13.46	20.82	0.62	-	0.26	1.45	-	98.17
	51.50	1.40	8.68	13.23	21.09	0.72	-	0.40	1.32	-	98.34
	52.27	1.30	8.33	13.50	21.31	0.61	-	0.27	1.07	-	98.66
	51.83	1.26	7.96	13.82	20.93	0.64	-	0.21	1.10	-	97.75
	52.61	1.58	8.40	14.28	20.86	0.62	-	0.33	0.92	-	99.60
	52.35	1.21	8.23	13.97	21.56	0.59	-	0.26	1.05	-	99.22

Table 5 (cont'd.).

Field No.	SiO_2	Al_2O_3	FeO	MgO	CaO	Na_2O	K_2O	TiO_2	MnO	BaO	Total
LW2-A											
	52.59	1.21	8.26	13.69	20.89	0.67	-	0.24	1.24	-	98.79
	51.95	1.13	8.36	13.31	21.19	0.64	-	0.31	1.25	-	98.14
	52.63	1.00	8.43	13.63	21.24	0.63	-	0.32	1.18	-	99.06
	52.55	1.72	9.01	13.52	20.59	0.74	-	0.37	1.36	-	99.86
	51.66	1.11	8.07	13.90	21.12	0.62	-	0.32	1.21	-	98.01
	52.95	1.13	9.83	12.95	21.10	0.77	-	0.23	1.85	-	100.81
	52.50	1.05	8.36	14.24	21.05	0.66	-	0.26	1.28	-	99.40
	52.56	1.05	8.41	13.97	21.32	0.58	-	0.25	1.24	-	99.38
	52.92	1.30	9.19	13.91	20.93	0.69	-	0.30	1.35	-	100.59
	51.94	1.42	9.25	13.71	21.11	0.71	-	0.37	1.33	-	99.84
	53.10	1.07	9.30	13.60	21.06	0.65	-	0.25	1.60	-	100.63
	53.19	1.39	8.62	13.98	21.24	0.67	-	0.35	1.16	-	100.60
	53.01	1.34	8.71	14.29	21.15	0.66	-	0.32	1.17	-	100.65
	53.67	1.27	8.48	14.42	21.05	0.64	-	0.35	1.09	-	100.97
	52.50	0.69	11.03	12.15	20.09	0.62	-	0.10	2.70	-	99.88
LW2-5											
	53.16	1.98	7.59	14.58	20.78	0.63	-	0.42	0.69	-	99.83
	52.86	1.62	7.15	14.64	21.34	0.52	-	0.35	0.79	-	99.27
	53.07	1.54	7.72	14.96	21.12	0.51	-	0.45	0.82	-	100.19
	53.78	0.84	7.75	14.13	21.14	0.59	-	0.27	1.26	-	99.76
	53.21	0.68	8.02	13.66	21.02	0.57	-	0.19	1.72	-	99.07
	52.78	1.25	8.24	13.48	20.88	0.68	-	0.33	1.37	-	99.01
	52.57	1.54	8.13	13.48	21.10	0.68	-	0.46	1.30	-	99.26
	53.44	1.43	8.13	13.85	21.18	0.71	-	0.39	1.27	-	100.40
	52.36	1.48	7.51	14.05	21.08	0.58	-	0.42	0.90	-	98.38
	52.68	1.41	8.38	13.71	21.19	0.64	-	0.43	1.31	-	99.75
	53.29	1.48	7.48	13.90	21.19	0.68	-	0.45	1.08	-	99.55
	52.41	1.65	8.21	13.51	20.87	0.78	-	0.46	1.36	-	99.25
	51.45	1.13	7.87	13.55	21.37	0.61	-	0.30	1.27	-	97.55
	51.36	0.74	10.38	12.12	21.06	0.60	-	0.17	2.13	-	98.56
LW4-1B											
	49.41	0.77	9.93	12.34	20.75	0.59	-	0.24	1.02	-	95.05
	50.94	0.77	10.91	12.32	20.57	0.63	-	0.25	2.08	-	98.47
	51.54	0.89	10.57	12.79	21.40	0.65	-	0.26	1.82	-	99.92
	51.39	0.84	10.35	12.68	21.14	0.64	-	0.56	1.99	-	99.59
	52.43	1.01	10.20	12.72	20.80	0.66	-	0.29	1.97	-	100.08
	51.69	1.07	9.60	12.45	20.74	0.72	0.11	0.23	1.92	-	98.53
	52.19	0.82	9.17	13.30	21.79	0.59	-	0.23	1.53	-	99.62
	52.81	0.72	9.62	13.29	21.42	0.62	-	0.20	1.99	-	100.67
	50.74	1.09	10.17	12.12	20.90	0.72	-	0.27	2.05	-	98.06
	51.15	1.00	10.38	12.30	20.83	0.66	-	0.24	3.01	-	99.57
	50.74	1.28	8.89	13.83	21.27	0.62	-	0.53	1.14	-	98.30
	50.57	0.97	9.93	12.32	21.23	0.65	-	0.26	2.00	-	97.93
	50.38	1.28	9.94	12.79	21.12	0.57	-	0.30	1.64	-	98.02
	50.78	0.88	9.84	13.00	21.46	0.67	-	0.26	1.91	-	98.80
	49.78	0.79	11.19	11.09	20.30	0.56	-	0.21	2.13	-	96.05
	50.27	0.95	11.44	11.47	20.76	0.63	-	0.24	2.22	-	97.98
	50.71	0.88	11.17	11.88	20.68	0.64	-	0.25	2.13	-	98.34
	52.30	0.69	10.89	12.37	20.85	0.62	-	0.18	2.35	-	100.25

Table 5 (cont'd.).

Field No.	SiO_2	Al_2O_3	FeO	MgO	CaO	Na_2O	K_2O	TiO_2	MnO	BaO	Total
LW4-1B (cont'd.)											
	52.16	0.95	9.65	13.59	21.63	0.67	-	0.30	1.83	-	100.78
	51.78	1.02	10.07	12.76	21.05	0.72	-	0.25	1.99	-	99.64
	50.69	0.93	9.73	12.76	21.28	0.65	-	0.26	1.85	-	98.15
	51.75	0.79	9.43	12.83	21.26	0.69	-	0.20	1.81	-	98.76
	50.36	0.87	10.26	12.23	21.28	0.62	-	0.25	2.05	-	97.92
	51.77	0.83	9.90	13.05	21.54	0.63	-	0.29	1.94	-	99.95
	51.68	0.85	10.02	12.46	21.04	0.68	-	0.23	1.97	-	98.93
LW4-5A											
	52.80	1.28	9.01	14.74	21.44	0.35	-	0.18	0.36	-	100.16
LW4-5B											
	52.32	1.50	9.20	13.66	21.13	0.80	0.03	0.43	1.22	-	100.29
	52.17	1.32	8.43	14.62	20.65	0.63	-	0.39	0.92	-	99.13
	48.98	1.26	9.75	13.64	21.11	0.67	-	0.34	1.18	-	96.93
	51.71	1.05	9.21	13.02	21.11	0.62	-	0.28	1.60	-	98.60
	51.49	0.93	8.26	13.97	21.55	0.62	-	0.27	1.27	-	98.36
	51.86	1.18	9.06	13.27	21.27	0.63	-	0.31	1.15	-	98.73
LW4-10B											
	51.96	1.61	8.35	14.39	21.46	0.68	-	0.37	0.64	-	99.46
	51.79	0.97	9.38	13.42	20.98	0.60	-	0.20	1.19	-	98.53
	51.52	0.59	11.09	12.40	20.78	0.53	-	0.15	1.85	-	98.91
	52.17	1.17	8.40	14.32	21.27	0.64	-	0.29	0.92	-	99.18
	51.87	1.18	8.84	13.80	21.72	0.62	-	0.30	0.94	-	99.27
	51.49	1.28	8.91	13.43	21.59	0.65	-	0.35	1.07	-	98.77
CP3-2A											
	52.08	9.55	6.37	11.96	14.63	1.04	1.09	0.43	0.67	0.18	98.17
	53.39	1.51	8.35	15.32	21.51	0.70	-	0.43	1.06	0.22	102.68
	53.60	1.76	8.63	14.37	21.72	0.69	-	0.53	1.07	0.18	102.73
	51.82	1.69	8.40	14.25	21.29	0.72	-	0.51	1.03	0.19	100.07
	52.84	1.61	8.39	14.27	21.60	0.69	-	0.46	1.06	0.25	101.35
	52.75	1.64	8.36	14.13	21.55	0.69	0.07	0.51	1.13	0.26	101.28
	52.91	1.32	9.31	13.40	21.34	0.76	-	0.37	1.46	0.27	101.35
	52.80	1.37	8.76	14.45	21.50	0.71	-	0.42	1.29	0.24	101.73
	53.25	1.54	9.90	13.30	21.52	0.81	-	0.45	1.61	0.16	102.75
	53.24	1.73	8.31	14.64	21.73	0.63	-	0.53	1.01	0.26	102.29
	53.59	1.71	8.22	14.47	21.53	0.68	-	0.45	1.03	0.22	102.08
	53.07	1.20	9.58	13.61	20.79	0.68	-	0.34	1.74	0.20	101.39
	52.47	2.12	8.53	14.36	22.01	0.74	-	0.54	1.04	0.22	102.19
	52.67	1.77	8.37	14.70	21.50	0.68	-	0.46	0.99	0.23	101.56
	53.15	1.58	8.37	14.75	21.35	0.66	-	0.46	1.10	0.21	101.83
	52.87	1.63	8.43	14.93	21.35	0.67	-	0.43	1.02	0.19	101.70
	51.49	1.56	8.64	14.19	20.98	0.65	-	0.44	0.91	-	98.86
	51.56	1.75	8.49	14.38	20.72	0.64	-	0.50	0.81	-	98.85
	51.84	1.60	7.97	14.40	20.95	0.60	-	0.36	0.90	-	98.62
	50.28	1.59	8.25	14.02	21.38	0.58	-	0.40	0.90	-	97.40
	51.11	1.25	10.03	13.22	20.52	0.64	-	0.27	1.54	-	98.58
	50.79	1.56	7.95	14.75	21.71	0.57	-	0.38	0.79	-	98.50
	52.30	1.50	8.03	14.67	21.54	0.58	-	0.34	0.77	-	99.73
	52.70	1.53	7.90	14.96	21.05	0.55	-	0.34	0.81	-	99.84
	52.13	1.52	8.17	14.35	21.00	0.62	-	0.40	0.75	-	98.94

Table 5 (cont'd.).

Field No.	SiO_2	Al_2O_3	FeO	MgO	CaO	Na_2O	K_2O	TiO_2	MnO	BaO	Total
CP3-2A (cont'd.)											
	53.29	1.50	8.31	14.50	21.38	0.55	-	0.37	0.76	-	100.66
	52.46	1.55	8.18	14.77	21.00	0.60	-	0.35	0.73	-	99.64
	52.61	1.53	8.09	14.62	21.45	0.54	-	0.37	0.79	-	100.00
	52.76	1.50	7.92	14.53	20.89	0.56	-	0.35	0.76	-	99.27
	53.03	1.58	8.26	14.75	21.30	0.54	-	0.36	0.81	-	100.63
	52.49	1.58	8.11	14.69	21.25	0.59	-	0.40	0.84	-	99.95
	52.29	1.59	7.99	14.54	21.08	0.59	-	0.38	0.77	-	99.23
	52.37	1.60	7.90	14.58	20.71	0.54	-	0.40	0.81	-	98.91
	53.00	1.53	8.27	14.48	20.72	0.58	-	0.39	0.83	-	99.80
	52.90	1.60	8.01	14.69	21.42	0.58	-	0.37	0.74	-	100.31
	52.58	1.54	7.84	14.65	21.59	0.56	-	0.35	0.77	-	99.88
	52.17	1.52	7.98	14.60	20.99	0.57	-	0.41	0.80	-	99.04
	52.41	1.54	8.24	14.55	20.99	0.55	-	0.35	0.72	-	99.35
	50.86	1.46	10.81	13.27	19.53	0.63	-	0.61	1.47	-	98.64
	51.01	1.33	10.36	13.41	20.32	0.58	-	0.30	1.47	-	98.78
	51.08	1.27	10.78	13.64	20.50	0.56	-	0.80	1.45	-	100.08
	50.19	1.79	11.13	13.36	20.20	0.59	-	0.67	1.45	-	99.38
	51.72	1.31	10.89	13.58	20.62	0.51	-	0.62	0.72	-	99.97
	51.35	1.49	10.18	13.14	20.46	0.58	-	0.41	1.33	-	98.94
	51.73	1.02	10.48	14.31	19.99	0.50	-	0.26	0.72	-	99.01
	51.14	1.39	12.73	13.56	19.62	0.37	-	0.47	0.55	-	99.83
	51.46	1.35	12.80	13.60	19.48	0.37	-	0.39	0.54	-	99.99
	51.97	1.39	8.24	14.08	21.30	0.66	-	0.47	0.93	-	99.04
	50.74	1.44	8.57	13.80	21.58	0.63	-	0.45	0.92	-	98.13
CP3-2B											
	52.59	1.64	8.47	13.88	20.34	0.64	-	0.44	0.93	-	98.93
	52.17	1.24	8.03	14.19	20.38	0.59	-	0.31	1.06	-	97.97
	51.84	1.56	8.17	13.85	20.93	0.70	-	0.44	1.09	-	98.58
	51.78	1.59	8.63	13.66	20.87	0.65	-	0.40	1.07	-	98.65
	53.55	3.42	7.70	12.93	18.50	0.81	0.65	0.36	0.93	-	98.85
	51.52	1.63	8.36	13.58	21.42	0.67	-	0.41	1.16	-	98.75
	52.03	1.39	8.11	14.14	21.30	0.58	-	0.40	0.98	-	98.93
	51.83	1.04	10.51	11.81	20.59	0.68	-	0.24	1.92	-	98.62
	52.07	1.41	8.64	13.19	21.00	0.65	-	0.40	1.17	-	98.53
	52.01	1.27	8.55	13.75	20.10	0.60	-	0.35	0.49	-	97.12
	52.14	1.57	8.47	14.01	20.22	0.69	-	0.45	1.10	-	98.65
	53.20	1.32	7.99	14.55	20.73	0.69	-	0.39	1.09	-	99.96
	52.52	1.64	8.37	13.92	20.93	0.67	-	0.44	0.95	-	99.44
	52.38	1.54	8.06	14.16	20.56	0.61	-	0.50	0.83	-	98.64
	51.15	1.47	8.09	14.01	20.55	0.69	-	0.39	0.96	-	97.31
	52.45	0.95	9.46	12.54	20.38	0.64	-	0.26	1.84	-	98.52
	52.32	1.50	8.01	14.12	20.87	0.63	-	0.41	0.99	-	98.85
	52.54	1.09	8.54	13.45	20.36	0.64	-	0.28	1.42	-	98.32
	51.89	1.23	7.88	14.34	20.85	0.60	-	0.33	1.05	-	98.17
	52.11	1.36	8.25	13.84	20.44	0.70	-	0.35	1.18	-	98.23
	52.03	1.60	8.28	13.99	20.96	0.68	-	0.49	1.08	-	99.11
	52.56	1.09	8.93	13.58	21.51	0.66	-	0.33	0.69	-	99.35

Table 5 (cont'd.).

Field No.	SiO_2	Al_2O_3	FeO	MgO	CaO	Na_2O	K_2O	TiO_2	MnO	BaO	Total
CP3-1D											
	52.68	1.09	8.57	13.74	21.49	0.64	-	0.34	1.16	-	99.71
	52.65	2.49	8.25	11.82	19.28	0.71	0.56	0.27	1.08	-	97.11
	52.01	0.88	8.65	13.68	22.11	0.59	-	1.45	1.39	-	100.76
	52.92	1.23	8.30	13.96	20.95	0.56	-	0.20	1.16	-	99.28
	51.78	1.63	8.64	13.74	20.46	0.71	-	0.19	1.36	-	98.51
	52.96	0.71	8.95	13.40	20.44	0.53	-	-	1.85	0.00	98.84
	52.71	1.38	8.54	13.97	20.54	0.91	-	0.22	1.27	-	99.54
	52.29	1.06	9.36	12.97	21.58	0.68	-	0.56	1.84	-	100.34
	52.82	1.07	9.88	12.52	19.81	0.65	-	0.36	1.96	-	99.07
	52.62	1.49	8.82	13.45	20.71	0.62	-	0.18	1.28	-	99.17
	53.43	1.14	8.88	13.25	19.95	0.67	-	0.38	1.55	-	99.25
	52.60	1.38	6.95	13.80	21.53	0.61	-	0.30	1.34	-	98.51
	51.90	1.05	7.04	13.77	21.44	0.63	-	0.34	1.20	-	97.37
	52.88	0.94	7.58	13.46	22.23	0.63	-	0.22	0.62	-	98.56
	53.18	1.12	7.62	13.51	21.44	0.61	-	0.39	1.28	-	99.15
	52.61	0.98	7.28	13.47	21.55	0.60	-	0.26	1.29	-	98.04
	51.58	1.44	7.64	13.23	21.15	0.69	-	0.43	1.36	-	97.52
	51.93	1.51	8.14	12.17	21.26	0.79	-	0.41	1.38	-	97.59
	51.75	1.39	7.68	13.27	21.24	0.73	-	0.48	1.42	-	97.96
	52.80	1.52	7.65	13.11	21.38	0.75	-	0.41	1.17	-	98.79
	52.59	1.18	7.21	13.96	21.22	0.64	-	0.41	1.23	-	98.44
	52.34	1.34	7.25	12.69	21.23	0.67	-	0.34	1.30	-	97.16
	52.32	0.98	7.38	13.35	21.43	0.64	-	0.36	1.70	-	98.16
	52.49	1.00	8.39	11.52	21.09	0.65	-	0.24	2.07	-	97.45
	52.57	0.98	8.30	12.54	20.77	0.65	-	0.56	2.00	-	98.37
	52.02	1.32	7.53	13.16	21.38	0.64	-	0.33	1.13	-	97.51
	53.00	1.30	7.58	13.72	21.61	0.62	-	0.51	1.16	-	99.50
	52.77	1.03	7.08	13.17	21.30	0.56	-	0.33	1.26	-	97.50
	52.31	1.43	7.69	13.60	21.51	0.66	-	0.51	1.27	-	98.98
	52.04	1.43	7.76	12.86	21.56	0.69	-	0.39	1.20	-	97.93
	53.29	0.97	7.07	13.93	21.55	0.57	-	0.47	1.23	-	99.08

Table 6. Microprobe Analyses of Hornblende.

Field No.	SiO_2	Al_2O_3	FeO	MgO	CaO	Na_2O	K_2O	TiO_2	MnO	BaO	Total
BB8-15B											
	46.15	7.09	18.61	11.21	10.20	1.87	0.73	1.52	1.76	-	99.14
	46.87	6.27	17.24	11.99	10.51	1.87	0.64	1.46	1.41	-	98.26
	48.14	6.19	14.33	14.21	10.46	1.91	0.67	1.22	1.44	-	98.57
LW4-5A											
	46.85	6.74	18.64	11.26	10.40	1.98	0.73	1.43	1.41	-	99.44
	47.15	6.96	19.38	10.99	10.28	1.83	0.73	1.35	1.41	-	100.08
	46.24	6.56	18.32	11.11	10.40	1.72	0.68	1.68	1.44	-	98.15
	46.69	6.78	17.75	11.31	10.25	1.82	0.76	1.92	1.52	-	98.80
	46.84	6.80	18.00	11.57	10.49	1.91	0.71	3.10	1.54	-	100.96
CP3-2A											
	39.51	13.02	15.07	11.65	11.45	2.30	1.24	3.79	0.17	0.27	98.47
	39.72	13.10	14.94	11.37	11.41	2.16	1.32	4.32	0.56	0.30	99.20
	40.98	12.94	14.07	12.29	11.54	2.42	1.06	4.06	0.16	0.26	99.78
	39.84	13.21	15.35	11.27	11.58	2.26	1.21	4.21	0.24	0.23	99.40
	39.38	12.87	15.53	11.10	11.23	2.21	1.18	4.60	0.19	0.33	98.62
CP1-3A											
	45.03	6.74	18.28	10.93	10.11	1.77	0.78	1.31	1.35	0.12	96.42
	45.79	6.66	19.36	10.59	10.04	1.73	0.66	1.41	1.25	-	97.49
	46.31	6.86	19.51	10.85	9.99	1.81	0.68	1.44	1.24	0.11	98.80
	47.13	6.79	19.30	11.00	9.97	1.88	0.63	1.33	1.32	0.13	99.48
	46.65	6.88	19.24	10.51	10.17	1.80	0.77	1.42	1.37	0.09	98.90
	47.31	7.54	19.40	11.71	10.23	2.16	0.77	1.53	1.34	-	101.99
	45.12	6.48	19.51	10.44	10.00	1.75	0.65	1.31	1.42	0.10	96.78
	45.56	6.61	19.38	10.60	10.00	1.72	0.68	1.32	1.53	0.09	97.49

Table 7. Microprobe Analyses of Plagioclase.

Field No.	SiO_2	Al_2O_3	FeO	MgO	CaO	Na_2O	K_2O	TiO_2	MnO	BaO	Total
BB9-10C											
	56.88	25.53	0.32	-	7.31	3.93	1.02	-	0.39	0.10	95.48
	58.62	25.63	0.45	-	6.73	3.63	1.12	-	1.37	0.71	98.26
	60.33	23.54	0.44	-	5.37	4.42	1.85	-	-	0.43	96.38
	57.75	27.25	0.10	-	8.07	3.58	0.78	-	-	-	97.53
	59.11	24.79	0.33	-	5.94	4.32	1.30	-	-	0.33	96.12
	58.16	24.18	0.33	-	5.56	7.22	1.21	0.05	-	0.30	97.01
	58.22	24.12	0.36	-	5.32	7.18	1.20	0.05	-	0.25	96.70
	58.57	24.18	0.31	-	5.11	7.36	1.41	-	-	0.34	97.28
	59.95	23.56	0.31	-	5.74	7.06	1.47	-	-	0.52	98.61
	61.07	23.22	0.40	-	5.53	7.20	1.49	-	-	0.45	99.36
	58.46	24.35	0.36	-	6.12	6.87	1.27	-	-	0.67	98.10
	57.35	25.86	0.40	-	7.48	6.59	0.89	-	-	0.52	99.09
	60.52	23.50	0.43	-	5.20	7.38	1.63	-	-	0.34	99.00
	60.66	23.69	0.35	-	5.38	7.28	1.57	-	-	0.40	99.33
	59.34	25.13	0.45	-	6.70	6.85	1.08	0.08	-	0.80	100.43
	58.83	25.16	0.43	-	6.54	6.66	1.18	0.08	-	0.89	99.77
	60.16	23.64	0.39	-	5.67	7.20	1.41	0.06	-	0.47	99.00
	60.35	23.58	0.41	-	5.51	7.28	1.47	0.06	-	0.46	99.12
	57.32	25.69	0.40	-	7.96	6.36	0.59	-	-	0.57	98.89
	60.99	23.46	0.36	-	5.57	7.30	1.40	-	-	0.36	99.44
	61.32	23.31	0.44	-	5.16	7.40	1.63	-	-	0.40	99.66
	60.51	23.26	0.40	-	5.36	8.03	0.63	-	-	0.41	98.60
	60.04	22.95	0.41	-	5.64	7.48	0.96	-	-	0.31	97.79
BB8-15B											
	57.60	25.61	0.12	-	6.66	7.37	0.59	-	-	-	97.95
	61.44	22.38	0.14	-	3.33	8.75	1.54	-	-	-	97.58
	64.11	21.62	0.20	-	3.58	8.83	0.84	-	-	-	99.18
	64.43	22.26	0.17	-	3.72	8.77	1.17	-	-	-	100.52
	64.39	21.61	0.14	-	3.56	8.87	1.24	-	-	-	99.81
	64.52	22.26	0.16	-	3.54	8.89	1.21	-	-	-	100.58
	64.44	21.61	0.15	-	3.53	8.98	1.26	-	-	-	99.97
	63.82	21.89	0.20	-	3.46	9.05	1.24	-	-	-	99.66
	64.99	21.71	0.13	-	3.47	8.99	1.24	-	-	-	100.53
	64.16	21.95	0.16	-	3.93	8.86	0.99	-	-	-	100.05
	64.85	21.87	0.15	-	3.61	8.85	1.14	-	-	-	100.47
	63.59	21.96	0.24	-	3.61	8.80	1.18	-	-	-	99.38
	64.09	21.33	0.20	-	3.16	8.88	1.36	-	-	-	99.02
	63.33	21.88	0.19	-	3.89	8.89	1.12	-	-	-	99.30
	63.60	21.85	0.18	-	3.64	8.95	1.24	-	-	-	99.46
	64.98	21.26	0.16	-	2.90	9.41	1.37	-	-	-	100.08
	64.29	21.60	0.18	-	3.57	8.95	1.13	-	-	-	99.72
	63.13	22.55	0.20	-	3.87	8.81	1.12	-	-	-	99.68
	64.25	21.48	0.20	-	3.30	9.03	1.35	-	-	-	99.61
	63.35	22.40	0.20	-	3.54	9.07	1.25	-	-	-	99.81

Table 7 (cont'd.).

Field No.	SiO_2	Al_2O_3	FeO	MgO	CaO	Na_2O	K_2O	TiO_2	MnO	BaO	Total
BB8-15B (cont'd.)											
	63.72	22.46	0.18	-	3.84	8.73	1.15	-	-	-	100.08
	63.21	22.13	0.18	-	3.79	8.80	1.18	-	-	-	99.29
	63.97	22.05	0.24	-	3.59	8.94	1.26	-	-	-	100.05
	61.08	23.80	0.14	-	5.73	8.13	0.72	-	-	-	99.60
	64.25	21.85	0.20	-	3.50	8.77	1.31	-	-	-	99.88
	61.57	21.62	0.22	-	3.41	9.16	1.16	-	-	-	97.14
	61.65	23.63	0.20	-	5.31	8.22	0.77	-	-	-	99.78
	56.91	25.35	0.14	-	7.91	7.02	0.43	-	-	-	97.76
	61.15	23.27	0.18	-	5.63	8.28	0.69	-	-	-	99.20
	62.82	21.83	0.24	-	3.41	8.69	1.36	-	-	-	98.35
	61.21	21.29	0.22	-	3.58	8.91	1.16	-	-	-	96.37
	63.59	21.72	0.23	-	3.59	8.67	1.18	-	-	-	98.98
	64.19	20.89	0.21	-	3.06	8.87	1.46	-	-	-	98.68
	63.00	22.58	0.19	-	4.17	8.73	1.03	-	-	-	99.70
BB8-3B											
	62.97	22.58	0.13	-	3.68	8.68	1.21	-	-	-	99.25
	65.79	22.58	0.15	-	2.45	9.00	1.97	-	-	-	101.94
	63.98	21.74	0.25	-	2.68	8.97	1.66	-	-	-	99.28
	56.76	27.22	0.20	-	8.05	6.48	0.44	-	-	-	99.15
	64.02	21.75	0.20	-	2.90	8.79	1.61	-	-	-	99.27
	56.50	25.17	0.20	-	6.77	6.84	0.60	-	-	0.13	96.21
	64.73	21.93	0.20	-	2.58	10.55	1.78	-	-	-	101.77
	59.99	22.43	0.11	-	3.66	8.33	1.14	-	-	-	95.66
	62.97	21.81	0.25	-	2.81	8.72	1.32	-	-	-	97.88
	63.04	22.04	0.18	-	2.51	8.69	1.52	-	-	-	97.98
BB8-1											
	62.26	22.63	0.12	-	3.42	8.90	1.31	-	-	0.13	98.77
	62.57	21.58	0.12	-	3.42	8.63	1.29	-	-	-	97.61
	53.10	26.92	0.19	-	9.63	5.50	0.31	-	-	-	95.65
	62.30	22.54	0.15	-	3.43	8.69	1.30	-	-	-	98.41
	63.85	23.06	0.12	-	3.84	8.83	1.25	-	-	-	100.95
	61.87	21.89	0.15	-	3.53	8.33	1.26	-	-	0.08	97.11
	62.30	21.98	0.17	-	3.19	8.72	1.49	-	-	0.08	97.93
	55.31	25.93	0.10	-	7.95	6.57	0.46	-	-	0.11	96.43
	64.30	22.64	0.10	-	3.42	8.75	1.28	-	-	0.11	100.60
	62.74	22.94	0.94	-	3.53	8.62	1.19	-	-	0.10	100.06
LW1-A											
	61.91	23.50	0.12	-	4.10	7.40	2.07	-	-	-	99.10
LW2-5											
	61.03	23.03	0.08	-	3.22	8.15	2.27	-	-	-	97.78
	58.58	24.60	-	-	4.62	8.00	1.27	-	-	-	97.07
	55.77	26.94	-	-	7.67	6.79	0.29	-	-	-	97.46
	57.85	26.54	0.21	-	7.05	7.03	0.63	-	-	-	99.31
	60.87	23.23	0.64	-	3.03	7.89	2.64	-	-	-	98.30
	53.53	27.65	0.08	-	8.88	5.71	0.46	-	-	-	96.31
	59.77	22.67	0.21	-	4.21	7.74	1.69	-	-	-	96.29
	61.03	22.92	0.31	-	3.85	7.92	1.64	-	-	-	97.67

Table 7 (cont'd.).

Field No.	SiO_2	Al_2O_3	FeO	MgO	CaO	Na_2O	K_2O	TiO_2	MnO	BaO	Total
LW4-1B											
	64.22	21.61	0.23	-	2.81	8.39	2.02	-	-	-	99.28
	63.07	22.84	0.27	-	3.73	8.42	1.41	-	-	-	99.74
	61.77	24.18	0.20	-	4.64	8.17	1.03	-	-	0.11	100.10
	63.55	21.84	0.32	-	2.70	8.75	1.96	-	-	-	99.12
	62.87	22.37	0.24	-	3.61	8.64	1.48	-	-	-	99.21
	64.25	21.23	0.19	-	2.94	9.00	1.58	-	-	-	99.19
	63.40	21.53	0.24	-	3.08	8.47	1.71	-	-	-	98.43
CP3-2A											
	61.49	23.35	1.02	-	3.90	7.68	2.05	-	-	0.18	99.67
	60.35	23.28	0.88	-	3.94	7.16	2.01	-	-	-	97.62
	61.22	22.88	0.82	-	3.88	7.30	2.39	-	-	-	98.49
	62.65	23.87	0.79	-	3.71	8.07	2.27	-	-	-	101.36
	59.38	22.59	0.75	-	4.17	7.02	1.91	-	-	-	95.82
	61.34	23.76	0.82	-	4.34	7.49	1.91	-	-	-	99.66
	58.82	22.59	0.79	-	4.01	6.80	1.96	-	-	-	94.97
	59.57	22.65	0.72	-	3.94	7.20	2.08	-	-	0.18	96.34
	60.53	23.07	0.81	-	3.85	7.29	2.20	-	-	-	97.75
	59.44	22.95	0.83	-	4.23	7.16	1.81	-	-	-	96.42
	60.98	23.24	0.80	-	4.06	7.21	2.05	-	-	0.15	98.49
	59.31	24.48	0.90	-	5.41	6.88	1.34	-	-	0.30	98.62
	58.43	22.53	1.01	-	4.04	7.42	2.28	-	-	0.14	95.85
	61.37	21.70	0.51	-	2.36	6.63	4.82	-	-	0.43	97.82
	60.83	23.13	0.63	-	4.13	7.70	2.14	-	-	0.15	98.71
	58.73	22.72	0.65	-	4.17	7.33	2.10	-	-	-	95.70
	61.47	23.43	0.60	-	4.21	7.62	2.15	-	-	0.08	99.56
	58.80	24.06	0.39	-	5.53	7.10	1.55	-	-	0.34	97.77
	60.05	24.91	0.35	-	5.29	7.27	1.60	-	-	0.56	100.03
	59.25	23.39	0.39	-	5.09	7.29	1.76	-	-	0.36	97.53
	61.37	23.75	0.28	-	4.75	7.42	2.14	-	-	0.31	100.02
	58.81	24.58	0.40	-	5.83	7.07	1.42	-	-	0.36	98.47
	60.86	24.40	0.35	-	5.09	7.27	1.79	-	-	0.41	100.17
	60.58	25.02	0.44	-	5.15	7.24	1.67	-	-	0.24	100.34
	58.51	24.11	0.38	-	5.32	6.73	1.62	-	-	0.21	96.88
	61.71	24.97	0.36	-	5.26	7.58	1.73	-	-	0.35	101.96
	58.61	23.08	0.34	-	5.23	6.87	1.69	-	-	0.36	96.18
	59.62	22.38	0.36	-	5.17	6.48	1.94	-	-	0.30	96.25
	59.43	25.50	0.41	-	6.26	7.18	1.21	-	-	0.54	100.53
	53.66	26.86	0.43	0.07	8.82	5.44	0.57	0.09	-	0.40	96.34
	55.16	27.53	0.49	-	8.99	5.71	0.75	0.05	-	0.40	99.08
	55.43	26.39	0.49	-	8.05	5.96	0.84	0.08	-	0.52	97.76
	55.86	26.12	0.42	-	8.11	5.96	0.83	0.05	-	0.56	97.91
	58.42	23.54	0.38	-	5.26	6.99	1.54	0.09	-	0.34	96.56
	58.75	23.46	0.38	-	5.13	7.17	1.80	-	-	0.31	97.00
	60.39	24.28	0.39	-	5.15	7.20	1.82	-	-	0.50	99.73
	59.33	24.67	0.44	0.12	5.66	7.15	1.54	-	-	0.35	99.26

Table 7 (cont'd.).

Field No.	SiO_2	Al_2O_3	FeO	MgO	CaO	Na_2O	K_2O	TiO_2	MnO	BaO	Total
CP3-2B											
	62.88	21.38	0.28	-	3.66	7.75	2.59	-	-	0.18	98.72
	63.22	21.72	0.34	-	3.82	7.55	2.31	-	-	0.09	99.05
	62.09	21.53	0.35	-	3.84	7.54	2.32	-	-	0.13	97.80
	62.45	22.14	0.30	-	3.99	7.77	2.08	-	-	-	98.73
	63.22	21.98	0.31	-	3.78	7.77	2.31	-	-	0.11	99.48
	62.82	22.48	0.38	-	4.65	7.91	1.77	-	-	-	100.01
	63.14	21.98	0.29	-	4.00	7.74	2.25	-	-	0.08	99.48
	65.58	19.30	0.73	-	2.36	6.34	2.45	0.16	-	0.08	97.00
	62.20	22.19	0.38	-	4.10	8.11	2.35	-	-	-	99.33
	62.67	22.42	0.29	-	4.14	7.90	2.26	-	-	0.10	99.78
	63.86	21.34	0.17	-	3.20	7.74	3.49	-	-	-	99.80
	64.53	21.57	0.13	-	3.07	8.28	3.11	-	-	-	100.69
	64.17	22.11	0.15	-	3.91	7.71	2.10	-	-	-	100.15
	63.25	22.17	0.20	-	3.87	8.16	2.40	-	-	-	100.05
	62.38	21.72	0.30	-	4.29	7.97	2.07	-	-	0.13	98.86
	64.25	21.08	0.20	-	2.84	7.46	4.00	-	-	-	99.83
	63.51	21.45	0.15	-	3.40	7.46	3.34	-	-	-	99.31
	62.64	21.59	0.11	-	3.52	7.55	3.36	-	-	-	98.77
	63.42	20.99	0.08	-	2.86	7.52	3.80	-	-	-	98.67
	63.36	21.37	0.13	-	3.24	7.83	3.09	-	-	-	99.02
	63.78	21.55	0.17	-	3.15	7.96	3.53	-	-	-	100.14
	63.18	21.02	0.31	-	3.35	7.63	3.23	-	-	-	98.72
	62.76	21.02	0.30	-	3.14	7.49	3.48	-	-	-	98.19
	62.33	22.41	0.32	-	4.43	7.94	2.05	-	-	0.12	99.60
	62.42	21.74	0.34	-	3.75	7.64	2.09	-	-	0.20	98.18
	62.23	22.46	0.30	-	4.14	7.70	2.20	-	-	0.09	99.12
	61.76	22.05	0.36	-	4.18	7.78	2.14	-	-	0.11	98.38
	61.48	22.62	0.34	-	4.75	7.89	1.72	-	-	0.16	98.96
	61.47	22.62	0.34	-	4.76	7.76	1.77	-	-	0.07	98.79
	60.79	22.49	0.34	-	4.81	7.97	1.86	-	-	0.15	98.41
	62.65	22.16	0.23	-	4.08	7.98	2.01	-	-	-	99.11
	63.28	21.41	0.19	-	3.67	7.97	2.24	-	-	-	98.76
	62.79	21.86	0.21	-	4.03	8.16	2.27	-	-	-	99.32
	62.29	22.21	0.29	-	4.17	7.69	2.34	-	-	0.11	99.10
	61.45	22.37	0.36	-	4.83	7.69	1.76	-	-	0.11	98.57
	62.21	21.64	0.28	-	4.04	7.72	2.64	-	-	0.07	98.60
	62.42	22.36	0.37	-	4.28	7.77	2.20	-	-	0.11	99.51
	62.17	23.00	0.30	-	4.67	7.80	1.90	0.06	-	0.23	100.13
	61.01	23.27	0.32	-	5.34	7.85	1.48	0.06	-	0.19	99.52
	62.41	22.16	0.34	-	4.25	7.76	2.18	0.06	-	0.24	99.40
	62.36	22.49	0.33	-	4.35	8.01	2.08	-	-	0.14	99.76
	62.85	22.26	0.27	-	4.18	7.88	2.31	-	-	0.09	99.84
	60.86	22.56	0.37	-	4.67	7.54	2.03	-	-	0.11	98.14
	62.42	21.99	0.22	-	3.96	7.77	2.42	-	-	0.10	98.88
	62.44	21.93	0.36	-	4.28	7.81	2.23	-	-	0.14	99.19
	62.91	21.79	0.19	-	3.64	8.11	2.42	-	-	-	99.06
	61.97	22.52	0.35	-	4.25	7.66	2.17	-	-	0.23	99.15
	61.33	23.01	0.36	-	4.73	7.93	1.92	-	-	0.29	99.57
	61.26	22.27	0.36	-	4.41	7.97	2.08	-	-	0.21	98.56

Table 7 (cont'd.).

Field No.	SiO_2	Al_2O_3	FeO	MgO	CaO	Na_2O	K_2O	TiO_2	MnO	BaO	Total
CP3-1A											
	64.51	23.92	0.13	-	4.14	8.73	1.11	-	-	-	102.54
	63.55	24.04	0.16	-	3.83	9.11	1.23	-	-	-	101.92
	63.22	23.70	0.26	-	3.82	8.85	1.23	-	-	-	101.08
	63.18	23.29	0.19	-	3.69	9.02	1.26	-	-	-	100.63
	63.62	23.56	0.21	-	3.90	8.77	1.22	-	-	-	101.28
	64.76	23.37	0.19	-	3.73	8.75	1.21	-	-	-	102.01
	63.67	22.77	0.16	-	3.59	8.91	1.24	-	-	-	100.34
	58.62	26.74	0.10	-	7.73	7.18	0.44	-	-	-	100.81
	58.51	26.98	0.08	-	7.68	7.20	0.46	-	-	-	100.91
CP3-1B											
	57.57	26.84	0.05	-	7.80	7.09	0.47	-	-	0.11	99.93
	58.00	27.17	0.09	-	7.47	7.02	0.47	-	-	0.54	100.76
	63.52	23.21	0.20	-	3.68	8.91	1.23	-	-	-	100.75
	57.23	27.39	0.10	-	7.78	7.08	0.47	-	-	0.44	100.49
	58.08	27.26	0.11	-	7.37	7.12	0.48	-	-	-	100.42
	58.71	27.22	0.08	-	7.62	6.97	0.47	-	-	-	101.07
	58.27	26.66	0.18	-	7.38	7.24	0.47	-	-	-	100.20
	55.86	28.75	0.10	-	9.78	6.08	0.30	-	-	0.10	100.97
	55.35	29.04	0.19	-	9.76	5.82	0.33	-	-	-	100.49
	63.76	23.41	0.13	-	3.98	8.61	1.13	-	-	0.08	101.10
	63.31	23.97	0.16	-	3.97	8.64	1.19	-	-	0.46	101.70
	62.60	23.81	0.15	-	4.04	8.62	1.07	-	-	0.14	100.43
	63.55	23.41	0.08	-	3.46	8.85	1.31	-	-	0.32	100.98
	63.16	23.44	0.18	-	3.18	8.94	1.41	-	-	-	100.31
	63.25	23.90	0.13	-	3.30	8.54	1.34	-	-	-	100.46
	63.16	23.35	0.19	-	3.73	8.81	1.23	-	-	-	100.47
	63.79	23.59	0.12	-	3.65	8.74	1.34	-	-	-	101.23
	63.38	23.69	0.25	-	3.76	8.64	1.25	-	-	-	100.97
	63.62	23.81	0.14	-	3.71	8.75	1.25	-	-	0.13	101.41
	63.33	23.92	0.10	-	3.40	8.55	1.31	-	-	-	100.61
	63.55	23.13	0.13	-	3.78	8.67	1.11	-	-	0.31	100.68

Table 8. Microprobe Analyses of Sanidine.

Field No.	SiO_2	Al_2O_3	FeO	MgO	CaO	Na_2O	K_2O	TiO_2	MnO	BaO	Total
BB9-10C											
	61.21	20.68	0.25	-	0.80	1.49	8.53	0.08	-	3.41	96.45
	61.38	20.28	0.20	-	0.79	1.58	8.24	0.08	-	2.62	95.17
	63.39	20.17	0.18	-	0.82	2.36	8.55	-	0.68	-	96.15
	61.57	20.11	0.26	-	0.78	1.30	8.62	-	-	3.21	95.85
	62.75	20.45	0.27	-	0.94	5.04	7.36	0.13	-	3.50	100.44
	62.42	19.29	0.26	-	0.76	4.63	8.32	0.09	-	2.80	98.57
	62.43	19.60	0.31	-	0.82	4.45	8.17	0.13	-	3.55	99.46
	62.81	19.72	0.23	-	0.73	4.42	8.60	0.11	-	2.91	99.53
	64.42	19.41	0.21	-	0.72	4.59	8.51	0.10	-	1.96	99.92
	63.18	19.12	0.23	-	0.79	4.92	8.03	0.11	-	2.84	99.22
	63.89	19.69	0.21	-	0.72	4.48	8.56	0.11	-	2.36	100.02
	63.40	19.20	0.20	-	0.69	4.77	8.30	0.11	-	2.28	98.95
	63.25	19.42	0.27	-	0.76	4.63	8.39	0.09	-	2.20	99.01
	63.33	19.66	0.17	-	0.74	4.45	8.51	0.09	-	2.60	99.55
	63.52	20.02	0.23	-	0.88	4.60	8.59	0.11	-	3.21	101.16
	63.27	19.77	0.27	-	0.87	4.62	8.36	0.09	-	3.08	100.33
BB8-15B											
	64.96	18.89	0.09	-	0.25	4.52	10.17	-	-	-	98.88
	64.73	19.41	0.72	-	0.25	4.61	9.84	-	-	-	99.56
	66.20	18.47	0.16	-	0.26	4.10	10.29	-	-	0.12	99.60
	65.81	18.48	0.09	-	0.25	4.34	10.37	-	-	-	99.34
	66.92	18.53	0.14	0.06	0.31	6.07	6.50	-	-	-	98.53
	66.41	18.54	0.13	-	0.25	4.21	10.34	-	-	-	99.88
	65.83	18.46	0.11	-	0.29	4.69	9.31	-	-	-	98.69
	66.54	18.51	0.12	-	0.24	4.07	10.49	-	-	-	99.97
	66.56	18.35	0.11	-	0.24	5.48	8.49	-	-	0.11	99.34
	65.18	18.38	0.13	-	0.26	4.52	9.78	-	-	-	98.25
	65.89	18.33	0.11	-	0.33	4.39	9.87	-	-	-	98.92
	66.18	18.34	0.10	-	0.24	4.23	10.25	-	-	0.09	99.43
	67.99	17.82	0.07	-	0.28	4.29	9.63	-	-	-	100.08
	66.78	18.23	0.12	-	0.22	4.20	10.09	-	-	0.09	99.73
	66.88	18.31	0.08	-	0.21	4.14	10.30	-	-	0.11	100.03
	66.28	18.64	0.11	-	0.29	4.73	9.62	-	-	0.10	99.77
	65.88	18.42	0.11	-	0.24	4.18	10.05	-	-	0.11	98.99
	66.11	18.34	0.19	-	0.23	4.25	10.02	-	-	-	99.14
	67.14	18.49	0.14	-	0.26	4.14	10.04	-	-	0.14	100.35
	66.28	18.72	0.18	-	0.28	4.24	9.87	-	-	0.11	99.68
	65.57	18.46	0.14	-	0.21	3.98	10.03	-	-	0.09	98.48
	66.23	18.30	0.07	-	0.23	4.04	10.08	-	-	0.16	99.11
	64.36	18.75	0.18	-	0.35	4.54	9.91	-	-	-	98.09
	64.84	18.69	0.16	-	0.34	4.32	9.81	-	-	-	98.16
BB8-3B											
	66.17	19.74	0.16	-	0.29	4.98	9.97	-	-	-	101.31
	64.82	19.33	0.15	-	0.43	4.55	9.54	-	-	-	98.82

Table 8 (cont'd.).

Field No.	SiO_2	Al_2O_3	FeO	MgO	CaO	Na_2O	K_2O	TiO_2	MnO	BaO	Total
BB8-3B (cont'd.)											
	65.47	18.89	0.14	-	0.34	4.51	10.01	-	-	-	99.36
	66.82	19.94	0.13	-	0.36	5.56	9.07	-	-	0.08	101.96
	66.52	19.04	0.15	-	0.40	4.93	9.90	-	-	-	100.94
	64.67	19.36	0.61	-	0.30	4.75	9.99	-	-	-	99.68
	66.35	19.63	0.15	-	0.27	4.82	9.84	-	-	-	101.06
	64.51	18.95	0.18	-	0.43	4.85	9.64	-	-	-	98.56
	64.97	19.41	0.16	-	0.29	4.49	9.98	-	-	-	99.30
	66.00	19.31	0.16	-	0.29	4.71	9.93	-	-	-	100.40
	65.67	19.27	0.17	-	0.36	4.88	9.96	-	-	-	100.31
	64.80	18.60	0.10	-	0.30	4.55	9.92	-	-	-	98.27
	64.68	18.81	0.17	-	0.26	4.60	10.13	-	-	-	98.65
	64.79	18.80	0.15	-	0.25	4.75	9.79	-	-	-	98.53
	64.34	19.07	0.07	-	0.23	4.77	9.84	-	-	-	98.32
	64.11	18.90	0.19	-	0.29	4.40	9.91	-	-	-	97.80
	65.74	19.83	0.11	-	0.27	4.85	9.78	-	-	-	100.58
	65.38	19.23	0.14	-	0.26	4.55	9.94	-	-	-	99.50
	64.43	19.28	0.12	-	0.31	4.81	9.89	-	-	-	98.84
	64.07	19.18	0.16	-	0.30	4.42	9.99	-	-	-	98.12
	63.59	19.61	0.13	-	0.36	4.92	9.39	-	-	-	98.00
	64.25	19.19	0.17	-	0.32	4.75	9.75	-	-	-	98.43
	65.64	19.52	0.17	-	0.38	4.83	9.56	-	-	0.09	100.19
	64.30	18.89	0.19	-	0.28	4.58	10.02	-	-	-	98.26
BB8-1											
	66.61	19.58	0.11	-	0.24	4.71	10.34	-	-	0.18	101.77
	63.89	18.67	0.07	-	0.28	4.06	10.80	-	-	0.10	97.87
	62.48	18.99	0.13	-	0.21	4.14	10.66	0.05	-	0.11	96.77
	64.93	18.71	0.06	-	0.26	3.92	10.89	-	-	0.17	98.94
	64.91	19.02	0.17	-	0.30	4.15	10.70	0.05	-	0.14	99.44
	64.03	18.97	0.22	-	0.36	4.36	10.14	-	-	-	98.08
	64.81	18.98	0.10	-	0.30	4.17	10.64	-	-	-	99.00
	65.00	19.18	0.08	-	0.21	4.03	10.82	-	-	0.16	99.48
	65.59	18.88	0.08	-	0.28	4.04	10.56	-	-	0.08	99.51
LW1-A											
	64.22	20.35	-	-	0.66	4.97	9.14	-	-	0.08	99.42
	65.82	20.62	-	-	0.51	4.84	9.58	-	-	-	101.37
	65.28	19.99	-	-	0.53	4.65	9.35	-	-	-	99.80
	65.07	20.13	-	-	0.87	5.09	8.65	-	-	0.22	100.03
	64.29	20.08	-	-	0.65	4.79	9.24	-	-	-	99.05
	62.91	19.92	-	-	0.67	4.74	8.98	-	-	0.11	97.33
LW2-5											
	66.03	20.12	-	-	0.52	4.87	9.37	-	-	0.19	101.10
	64.00	20.03	-	-	0.53	4.76	9.10	-	-	-	98.42
	63.93	19.62	-	-	0.23	4.46	10.24	-	-	-	98.48
	63.66	20.26	-	-	0.52	4.81	8.99	-	-	-	98.24
	63.69	19.91	-	-	0.42	4.57	9.69	-	-	-	98.28
	62.98	19.80	-	-	0.32	4.46	9.45	-	-	-	97.01
	63.91	19.57	-	-	0.33	4.70	9.74	-	-	-	98.25
	63.68	18.71	0.15	-	0.53	4.52	9.26	-	-	0.21	97.06
	64.39	18.62	0.17	-	0.52	5.01	8.82	-	-	0.09	97.62

Table 8 (cont'd.).

Field No.	SiO_2	Al_2O_3	FeO	MgO	CaO	Na_2O	K_2O	TiO_2	MnO	BaO	Total
LW2-5 (cont'd.)											
	65.08	19.36	0.19	-	0.58	5.76	7.36	-	-	0.24	98.57
	63.24	18.68	0.17	-	0.57	4.35	9.34	-	-	0.25	96.60
	62.08	18.46	0.12	-	0.35	4.98	9.04	-	-	0.22	95.25
	61.72	19.24	0.24	-	0.64	5.20	8.25	-	-	0.28	95.57
	62.38	18.63	0.17	-	0.54	4.54	9.31	-	-	0.14	95.71
	64.41	19.04	0.16	-	0.63	4.70	9.05	-	-	0.25	98.24
	63.80	19.15	0.15	-	0.51	4.90	9.23	-	-	0.11	97.85
	64.09	18.78	0.17	-	0.61	5.64	7.60	-	-	0.19	97.08
	63.91	19.04	0.19	-	0.56	4.91	8.59	-	-	0.25	97.45
	63.12	18.76	0.19	-	0.62	5.38	7.39	-	-	0.16	95.62
	62.30	19.43	0.23	-	0.53	4.75	8.97	-	-	0.45	96.66
	63.78	18.99	0.25	-	0.55	5.03	8.32	-	-	0.25	97.17
	63.61	19.67	0.23	-	0.74	5.24	8.55	-	-	0.27	98.31
	65.08	18.39	0.10	-	0.50	8.50	2.53	-	-	-	95.10
	64.85	19.15	0.18	-	0.48	4.82	9.31	-	-	0.12	98.91
	63.33	18.84	0.18	-	0.73	5.41	7.93	-	-	0.22	96.64
LW4-1B											
	65.41	19.02	0.21	-	0.33	4.69	9.74	-	-	-	99.40
	66.25	18.79	0.20	-	0.31	5.14	9.50	-	-	0.16	100.35
	65.43	19.37	0.24	-	0.40	5.19	8.83	-	-	-	99.46
	65.26	18.77	0.23	-	0.35	4.93	9.50	0.06	-	0.11	99.21
	65.21	18.93	0.23	-	0.29	4.54	10.09	0.07	-	0.10	99.46
	63.32	19.35	0.21	-	0.25	4.64	10.12	0.06	-	0.11	98.06
	66.01	19.66	0.17	-	0.55	6.58	7.08	0.05	-	-	100.10
	65.41	19.10	0.24	-	0.39	4.59	9.81	0.06	-	-	99.60
	64.73	19.59	0.22	0.34	0.33	4.63	9.67	-	-	-	99.51
	65.56	19.56	0.25	-	0.35	4.50	10.16	-	-	0.10	100.48
	65.36	19.46	0.22	-	0.34	4.74	9.87	0.08	-	-	100.07
	63.53	18.67	0.21	-	0.33	4.70	9.76	0.07	-	-	97.27
	63.30	18.55	0.13	-	0.29	3.99	10.61	0.06	0.06	0.15	97.14
CP3-2A											
	62.73	21.80	0.30	0.05	0.81	4.85	8.51	-	-	2.86	101.91
	62.97	19.25	0.20	-	0.64	4.51	9.08	-	-	0.54	97.19
	61.81	19.41	0.72	-	0.96	4.69	8.08	-	-	0.52	96.19
	61.87	19.10	0.86	-	0.71	4.38	8.85	-	-	0.60	96.37
	63.72	19.05	0.94	-	0.63	4.37	9.10	-	-	0.39	98.20
	63.95	19.66	0.77	-	0.73	4.57	9.07	-	-	0.29	99.04
	63.78	20.21	0.78	-	0.88	4.81	8.37	-	-	0.84	99.67
	62.62	19.45	1.04	-	0.53	4.54	8.91	-	-	0.19	97.28
	63.72	19.78	0.97	-	0.54	4.43	9.49	-	-	0.26	99.19
	63.47	20.30	1.45	-	0.78	5.13	8.37	-	-	0.45	99.95
	62.68	19.61	0.78	-	0.74	4.40	8.61	-	-	1.02	97.84
	62.78	20.17	0.96	-	0.80	4.63	8.84	-	-	0.93	99.11
	61.44	19.36	0.20	-	0.75	4.27	8.76	-	-	0.46	95.24
	62.25	19.80	0.72	-	0.71	4.50	8.83	-	-	0.38	97.19
	64.31	20.88	0.76	-	0.71	4.67	8.84	-	-	1.32	101.49
	60.92	20.07	0.70	-	0.85	4.53	8.23	-	-	1.24	96.54
	61.57	19.42	0.69	-	0.82	4.28	8.39	-	-	0.87	96.04
	65.80	19.90	0.71	-	0.54	4.61	9.28	-	-	0.13	100.97

Table 8 (cont'd.).

Field No.	SiO_2	Al_2O_3	FeO	MgO	CaO	Na_2O	K_2O	TiO_2	MnO	BaO	Total
CP3-2A (cont'd.)											
	62.82	19.64	0.71	-	0.73	5.18	7.58	-	-	0.16	96.82
	61.90	19.71	0.75	-	0.79	4.42	8.48	-	-	1.04	97.09
	62.05	19.60	0.77	-	0.63	4.32	8.67	-	-	1.08	97.12
	62.85	20.05	0.74	-	0.96	4.75	8.11	-	-	0.11	97.57
	61.41	19.51	0.72	-	0.74	4.13	8.56	-	-	1.02	96.09
	64.44	20.33	0.70	-	0.75	4.56	8.79	-	-	1.06	100.63
	61.44	19.75	0.24	-	0.61	4.81	7.21	-	-	1.06	95.12
	62.39	20.14	0.69	-	0.72	4.43	8.67	-	-	0.96	98.00
	63.48	20.10	0.72	-	0.77	4.53	8.78	-	-	1.09	99.47
	63.85	19.56	0.78	-	0.71	4.65	8.60	-	-	0.56	98.71
	64.46	20.32	0.69	-	0.97	5.02	8.05	-	-	0.30	99.81
	60.95	19.67	1.89	-	0.88	4.41	8.23	-	-	1.09	97.12
	61.76	19.63	0.78	-	0.69	4.33	8.65	-	-	0.98	96.82
	62.11	20.30	0.80	-	0.98	4.70	7.96	-	-	1.33	98.18
	63.78	19.61	0.77	-	0.67	4.38	8.74	-	-	1.30	99.25
	63.02	19.44	0.72	-	0.60	4.35	8.99	-	-	0.30	97.42
	63.79	19.57	0.74	-	0.45	4.69	9.10	-	-	0.10	98.44
	64.44	20.12	0.75	-	0.55	4.75	6.74	-	-	0.32	97.67
	65.26	20.11	0.76	-	0.71	4.44	9.08	-	-	0.21	100.57
	64.08	19.42	0.66	-	0.70	4.55	8.99	-	-	0.16	98.56
	62.89	19.84	0.76	-	0.84	4.62	8.46	-	-	0.44	97.85
	61.90	19.46	0.78	-	0.75	4.42	8.55	-	-	0.75	96.61
	64.93	19.96	0.69	-	0.70	5.30	9.00	-	-	0.30	100.88
	62.73	19.97	0.50	-	0.80	4.57	9.27	-	-	0.52	98.36
	61.56	19.06	0.47	-	0.72	4.53	8.81	-	-	0.75	95.90
	62.88	20.59	0.43	-	0.80	5.20	8.49	-	-	0.94	99.33
	62.24	19.68	0.50	-	0.68	4.46	9.06	-	-	0.96	97.58
	64.17	19.79	0.44	-	0.73	4.73	9.13	-	-	0.38	99.37
	63.01	19.51	0.57	-	0.59	4.36	9.71	-	-	0.18	97.93
	63.06	20.78	0.52	-	0.71	5.16	8.39	-	-	0.80	99.42
	63.47	18.96	0.15	-	0.53	4.45	10.11	-	-	0.15	97.82
	63.06	18.58	0.60	-	0.68	4.69	9.22	-	-	0.24	97.07
	62.18	19.04	0.48	-	0.57	4.57	9.26	-	-	0.26	96.36
	61.45	19.29	0.42	-	0.73	4.69	8.57	-	-	0.38	95.53
	62.39	19.53	0.49	-	0.92	4.60	8.53	-	-	0.79	97.25
	62.97	19.96	0.15	-	0.83	4.69	8.56	-	-	1.23	98.39
	62.76	20.07	0.44	-	0.71	4.91	9.01	-	-	0.93	98.83
	59.70	19.63	0.27	-	0.75	4.13	8.66	0.07	-	2.41	95.62
	60.07	19.35	0.20	-	0.87	4.25	8.60	0.05	-	2.53	95.92
	63.39	20.47	0.20	-	0.83	4.53	8.92	0.06	-	2.55	100.95
	63.47	20.15	0.21	-	0.80	4.36	8.70	0.07	-	2.66	100.42
	62.46	20.70	0.25	-	0.82	4.28	8.65	0.05	-	2.59	99.80
	62.49	21.06	0.19	-	0.84	4.69	8.53	-	-	2.49	100.29
	63.76	20.55	0.24	-	0.75	4.90	8.67	0.07	-	2.51	101.45
	59.66	20.19	0.26	-	0.79	3.76	8.05	0.06	-	5.62	98.39
	61.49	19.39	0.24	-	0.74	4.44	8.66	0.06	-	2.50	97.52
	61.97	19.98	0.25	-	0.75	4.28	8.94	0.05	-	2.38	98.60
	62.67	19.93	0.23	-	0.68	4.54	9.00	0.06	-	2.25	99.36
	61.93	19.86	0.28	-	0.74	4.26	8.68	0.07	-	2.34	98.16
	61.31	19.67	0.20	-	0.76	4.40	8.62	0.11	-	2.65	97.72

Table 8 (cont'd.).

Field No.	SiO_2	Al_2O_3	FeO	MgO	CaO	Na_2O	K_2O	TiO_2	MnO	BaO	Total
CP3-2B											
	64.11	20.20	0.16	-	0.64	4.80	8.95	-	-	0.21	99.07
	66.44	18.87	0.21	-	0.50	4.76	8.93	-	-	0.12	99.83
	66.10	18.72	0.20	-	0.51	4.71	9.08	-	-	0.11	99.43
	66.34	18.74	0.23	-	0.70	4.85	8.43	0.09	-	0.84	100.22
	65.31	19.12	0.23	-	0.70	4.63	8.32	0.08	-	1.02	99.41
	64.31	19.00	0.27	-	0.87	4.98	7.93	0.07	-	1.17	98.60
	64.60	18.74	0.23	-	0.82	4.87	8.04	0.07	-	0.81	98.18
	66.33	18.33	0.20	-	0.47	4.43	9.17	-	-	0.06	98.99
	64.30	19.20	0.23	-	0.74	4.97	7.81	-	-	1.02	98.27
	64.51	18.94	0.21	-	0.74	4.92	7.89	-	-	1.09	98.30
	65.73	18.71	0.15	-	0.54	4.90	8.22	-	-	0.25	98.50
	66.38	18.65	0.19	-	0.61	4.83	8.31	-	-	0.26	99.23
	65.25	19.22	0.19	-	0.78	4.77	8.76	0.11	-	1.22	100.30
	65.90	18.73	0.24	-	0.62	4.73	9.39	-	-	0.36	99.97
	63.37	19.40	0.18	-	0.83	4.82	7.19	0.09	-	1.41	97.29
	64.68	19.04	0.20	-	0.76	4.87	8.66	0.10	-	1.26	99.57
	63.66	19.33	0.26	-	0.85	4.75	8.64	0.08	-	1.34	98.91
	64.06	19.15	0.29	-	0.85	4.89	8.57	0.07	-	1.23	99.11
	65.49	19.46	0.23	-	0.70	5.11	9.18	-	-	0.41	100.58
	64.49	19.17	0.23	-	0.77	4.98	8.58	0.08	-	1.23	99.53
	64.59	19.20	0.29	-	0.63	4.84	8.87	-	-	0.24	98.66
	64.24	19.06	0.19	-	0.66	4.90	9.14	-	-	0.39	98.58
	64.71	19.59	0.24	-	0.76	4.59	9.22	0.07	-	0.93	100.11
	64.48	18.73	0.23	-	0.74	4.88	8.96	0.08	-	0.43	98.53
	65.44	18.72	0.20	-	0.48	4.67	9.92	-	-	-	99.43
	64.61	19.11	0.28	-	0.75	4.62	9.10	0.08	-	1.08	99.63
	63.87	18.98	0.26	-	0.71	4.63	9.21	0.07	-	1.12	98.85
	65.11	18.71	0.24	-	0.74	4.94	9.43	0.07	-	0.49	99.73
	65.44	18.42	0.20	-	0.49	4.49	9.79	-	-	-	98.83
	64.27	19.76	0.28	-	1.28	5.43	8.23	-	-	0.83	100.08
	63.78	19.60	0.24	-	1.29	5.73	7.41	0.08	-	0.89	99.02
	64.41	19.36	0.25	-	0.89	5.20	8.32	0.07	-	1.35	99.85
	63.58	19.70	0.22	-	0.70	4.57	9.14	0.07	-	1.24	99.22
	63.94	19.40	0.26	-	0.73	4.46	8.94	0.07	-	2.03	99.83
	65.12	18.96	0.23	-	0.83	4.92	8.78	0.06	-	0.57	99.47
	64.15	19.09	0.20	-	0.80	4.57	9.15	0.07	-	0.91	98.94
	64.52	19.24	0.25	-	0.76	4.90	9.17	0.08	-	0.84	99.76
	65.29	18.20	0.19	-	0.35	4.29	10.31	-	-	-	98.63
	65.79	18.27	0.15	-	0.33	4.37	10.06	-	-	-	98.97
	65.16	18.45	0.21	-	0.43	4.82	9.41	-	-	-	98.48
	65.21	18.43	0.14	-	0.42	4.64	9.94	-	-	-	98.78
CP3-1A											
	66.11	20.69	0.07	-	0.21	3.99	11.02	-	-	0.08	102.17
	66.90	20.05	-	-	0.22	4.29	10.47	-	-	0.32	102.25
	66.50	19.90	0.10	-	0.22	3.91	11.07	-	-	0.18	101.88
	66.32	19.92	0.06	-	0.22	4.07	10.73	-	-	0.42	101.74
	65.97	19.54	0.07	-	0.21	4.07	10.96	-	-	0.10	100.92
	65.19	20.25	0.09	-	0.23	3.93	11.00	-	-	-	100.69
	65.86	20.35	0.13	-	0.22	4.66	10.77	-	-	-	101.99

Table 8 (cont'd.).

Field No.	SiO_2	Al_2O_3	FeO	MgO	CaO	Na_2O	K_2O	TiO_2	MnO	BaO	Total
CP3-1A (cont'd.)											
	66.24	19.99	0.10	-	0.21	4.03	11.05	-	-	0.27	101.89
	65.98	20.07	0.12	-	0.22	4.09	10.79	-	-	-	101.27
	66.28	20.21	0.11	-	0.22	4.03	10.98	-	-	0.19	102.02
	66.34	20.13	0.06	-	0.17	3.93	11.02	-	-	0.13	101.78
	66.17	20.17	0.07	-	0.22	4.22	10.91	-	-	0.58	102.34
CP3-1B											
	65.43	20.17	0.19	-	0.64	5.01	9.22	-	-	0.07	100.73
	64.60	20.33	0.22	-	0.62	5.02	9.27	-	-	0.10	100.16
	64.60	20.14	0.17	-	0.55	5.00	9.29	-	-	0.62	100.37
	65.43	19.73	0.24	-	0.30	6.81	6.80	-	-	-	99.31
	65.35	19.98	0.20	-	0.34	6.82	6.90	-	-	0.38	99.97
	67.02	20.59	0.14	-	0.33	6.68	6.97	-	-	-	101.73
	66.62	19.56	-	-	0.20	4.10	11.19	-	-	0.44	102.11
	65.52	20.13	0.09	-	0.19	3.96	11.01	-	-	0.10	101.00
	65.06	19.80	-	-	0.19	4.35	10.60	-	-	0.36	100.36
CP3-1D											
	64.99	19.88	0.14	-	0.67	5.05	9.02	-	-	0.44	100.19
	63.66	20.71	0.12	-	0.73	5.08	8.76	-	-	1.54	100.60
	64.26	20.02	0.25	-	0.69	4.87	9.28	-	-	0.43	99.80
	63.47	20.43	0.11	-	0.63	4.93	9.53	-	-	1.34	100.44
	64.60	20.14	0.28	-	0.59	4.87	9.37	-	-	0.25	100.10
	64.18	20.75	0.14	-	0.67	4.99	9.39	-	-	1.27	101.39
	64.26	20.26	0.16	-	0.76	5.07	9.09	-	-	0.31	99.91
	64.28	20.52	0.14	-	0.64	4.80	9.47	0.14	-	0.42	100.41
	65.12	20.31	0.42	-	0.70	5.02	9.10	-	-	0.24	100.91
	64.97	19.97	0.11	-	0.45	4.72	9.72	-	-	0.62	100.56
	65.26	19.95	0.12	-	0.53	4.80	9.78	-	-	0.11	100.55
	64.58	20.02	0.16	-	0.56	4.83	9.54	-	-	0.44	100.13
	65.38	20.08	0.14	-	0.44	4.76	9.58	-	-	0.12	100.50
	65.53	20.03	0.16	-	0.41	4.61	9.70	-	-	0.49	100.93
	64.75	20.11	0.13	-	0.50	4.67	9.71	-	-	0.33	100.20
	65.02	20.02	0.09	-	0.33	4.90	10.09	-	-	0.38	100.83
	64.55	20.20	0.16	-	0.40	4.85	10.05	-	-	0.09	100.30
	65.38	20.05	0.13	-	0.46	4.90	9.49	-	-	0.22	100.63
	64.40	20.32	0.26	-	0.54	4.82	9.57	-	-	0.16	100.07
	64.71	20.25	0.08	-	0.52	4.91	9.47	-	-	0.48	100.42
	64.60	20.32	0.14	-	0.62	4.89	9.37	-	-	0.23	100.17
CP1-3A											
	65.85	19.90	-	-	0.27	4.36	10.54	-	-	-	100.92

Table 9. Microprobe Analyses of Glass.

Field No.	SiO_2	Al_2O_3	FeO	MgO	CaO	Na_2O	K_2O	TiO_2	MnO	BaO	Total
BB9-5C											
	68.36	16.39	0.21	-	0.52	3.02	5.00	0.30	-	-	93.80
BB9-10C											
	68.96	15.80	0.24	-	0.73	1.87	6.16	0.21	-	-	93.97
	69.91	15.68	0.20	-	0.62	2.20	6.18	-	-	-	94.79
	70.03	15.98	1.10	-	0.56	2.77	6.28	0.44	-	-	97.16
	70.85	16.36	0.08	-	0.60	2.46	6.32	0.31	-	-	96.98
	70.76	16.20	0.39	-	0.63	2.54	6.17	0.18	-	-	96.87
	68.66	16.13	1.60	0.19	0.96	2.62	6.47	0.44	0.61	0.28	97.96
	69.67	16.46	1.54	-	0.64	2.47	6.31	0.31	0.53	0.31	98.24
	66.35	15.46	0.42	-	0.68	2.85	6.27	0.31	-	-	92.34
	70.51	14.97	0.49	0.04	0.44	2.37	6.83	0.20	0.07	-	95.92
	67.84	15.28	0.63	-	0.54	3.53	6.51	0.33	-	-	94.66
	65.50	16.01	0.18	-	0.63	3.45	6.39	0.34	-	0.17	92.67
	69.01	13.18	0.35	0.05	0.67	2.71	5.43	0.31	-	0.14	91.85
	66.78	14.50	0.85	-	0.59	3.57	6.37	0.28	-	-	92.94
	66.78	14.98	0.55	-	0.52	3.28	6.54	0.35	-	-	93.00
	69.48	15.22	0.35	-	0.67	3.48	6.11	0.36	-	0.15	95.82
	66.33	14.48	1.73	0.38	0.97	3.37	4.67	0.42	0.04	-	92.39
	67.44	14.97	0.79	0.03	0.73	3.90	5.30	0.37	-	0.16	93.69
BB8-15B											
	74.15	12.98	1.33	0.05	0.43	2.07	4.97	0.09	0.09	-	96.16
	73.83	12.98	0.13	-	0.37	2.33	5.03	0.07	0.08	-	94.82
	73.69	12.25	0.12	-	0.41	2.10	4.59	0.05	-	-	93.21
	73.55	12.42	0.23	-	0.50	1.83	5.09	0.04	-	-	93.66
	72.74	12.17	0.13	-	0.43	1.80	4.96	0.05	0.07	-	92.35
	72.36	11.43	0.52	0.03	0.51	2.81	4.47	0.04	0.07	-	92.24
	74.24	11.78	0.46	0.03	0.44	2.76	4.78	0.08	0.03	-	94.60
BB8-3B											
	74.37	12.13	0.76	-	0.51	2.08	5.02	0.11	0.09	-	95.07
	74.20	12.41	0.32	-	0.48	1.88	5.13	0.08	-	-	94.50
	73.40	12.40	0.41	-	0.42	1.89	5.06	0.10	-	-	93.68
	73.20	12.56	0.64	-	0.48	2.03	5.02	0.12	-	-	94.05
	73.74	12.72	0.74	0.05	0.55	1.71	4.79	0.08	0.07	-	94.45
	73.54	12.49	0.72	0.06	0.55	2.00	4.96	0.06	-	-	94.38
	72.35	12.28	0.70	0.05	0.57	1.91	4.96	0.09	-	-	92.91
	72.61	12.75	0.42	0.02	0.54	1.93	5.01	0.12	0.07	-	93.47
	70.47	17.41	0.61	-	0.26	3.25	6.54	0.07	-	-	98.61
	73.80	12.83	0.60	0.45	0.50	1.93	5.08	0.14	-	-	95.33
BB8-1											
	74.07	12.68	0.66	0.23	0.51	1.89	4.92	0.07	-	-	95.03
	74.08	12.54	0.52	-	0.51	2.14	4.85	0.10	0.09	-	94.83
	74.37	12.61	0.58	-	0.54	2.22	4.94	0.10	0.11	-	95.47
	75.33	12.91	0.30	-	0.47	2.30	5.02	0.06	-	-	96.39
	74.32	12.59	0.29	-	0.48	2.35	5.05	0.08	0.06	-	95.22

Table 9 (cont'd.).

Field No.	SiO_2	Al_2O_3	FeO	MgO	CaO	Na_2O	K_2O	TiO_2	MnO	BaO	Total
BB8-1 (cont'd.)											
	73.93	12.53	0.84	-	0.56	2.49	4.85	0.08	0.07	-	95.35
	73.30	12.47	0.59	-	0.54	2.25	5.11	0.08	0.08	-	94.42
	73.62	12.47	0.65	-	0.53	2.12	5.13	0.09	0.06	-	94.67
	73.63	12.53	0.58	-	0.54	2.34	4.95	0.10	0.09	-	94.76
LW2-5											
	66.94	14.80	0.36	-	0.38	2.44	6.91	0.12	-	-	91.95
	70.02	15.41	0.58	0.11	0.38	2.72	7.13	0.15	-	-	96.50
	67.31	14.01	0.57	0.11	0.50	2.76	6.85	0.24	0.07	-	92.42
	67.64	15.47	0.49	-	0.52	3.10	6.89	0.27	0.07	-	94.45
	67.55	14.31	0.34	-	0.45	2.85	7.23	0.27	0.08	-	93.08
	70.87	14.81	0.31	-	0.36	3.20	6.84	0.25	-	-	96.64
	70.22	15.19	0.42	-	0.46	3.43	6.75	0.31	-	-	96.78
	69.78	15.13	0.33	-	0.44	3.21	7.14	0.25	-	-	96.28
	70.18	14.47	0.48	-	0.47	3.15	7.08	0.24	-	-	96.07
	69.25	14.28	0.52	-	0.46	3.71	6.98	0.28	-	-	95.48
	69.05	14.06	0.30	-	0.44	3.10	6.99	0.26	-	-	94.20
	69.20	13.89	0.34	0.06	0.44	3.05	7.28	0.26	-	-	94.52
	68.39	13.66	0.60	-	0.60	2.77	6.60	0.24	-	-	92.86
	69.10	14.01	0.70	-	0.55	2.84	6.36	0.21	-	-	93.77
LW4-1B											
	71.76	13.23	0.85	0.06	0.28	2.64	6.14	0.19	-	-	95.15
	72.90	13.31	0.85	0.06	0.32	2.75	5.84	0.18	0.06	-	96.27
	73.47	13.47	0.61	0.06	0.38	2.32	6.81	0.16	-	-	97.28
	69.55	12.97	0.69	0.06	1.15	2.31	6.45	0.17	-	-	93.35
	69.85	13.26	0.92	0.07	0.39	2.98	5.79	0.16	0.14	0.09	93.65
	70.52	13.44	0.79	0.07	0.36	3.37	6.22	0.17	0.10	-	95.04
	70.92	13.34	0.76	0.07	0.41	3.06	6.49	0.17	0.09	0.13	95.44
CP3-2A											
	66.62	15.81	1.82	-	0.06	2.52	5.67	-	-	-	92.50
	69.79	12.54	0.53	-	0.03	1.85	5.45	-	-	-	90.19
	65.93	15.74	1.46	0.18	0.59	3.35	5.98	0.34	-	0.20	93.77
	67.88	15.70	1.68	0.06	0.34	3.22	6.04	0.36	-	0.13	95.41
	67.14	15.43	1.41	-	0.38	2.37	6.64	0.41	-	0.19	93.97
	73.31	12.24	0.71	-	0.15	1.82	6.68	0.09	-	0.10	95.10
	72.82	12.19	0.69	-	0.16	2.51	5.46	0.12	-	-	93.95
	71.88	12.52	0.69	-	0.14	2.53	5.50	0.08	-	0.14	93.48
	69.96	14.13	1.27	-	0.31	2.61	5.64	0.32	-	0.19	94.43
	65.23	16.80	1.37	-	0.66	2.87	5.86	0.36	-	0.27	93.42
	66.34	16.01	1.46	-	0.54	3.21	6.06	0.41	-	0.16	94.19
	64.51	15.67	1.52	0.07	0.39	3.20	6.00	0.41	-	0.18	91.95
	68.13	15.72	1.71	-	0.11	2.61	5.69	-	-	-	93.97
CP3-2B											
	66.63	14.55	1.07	-	-	4.13	5.92	0.37	0.01	-	92.68
	72.02	15.09	1.44	0.01	0.01	1.81	3.25	0.34	0.05	-	94.02
	68.50	14.69	1.30	0.02	-	4.65	5.41	0.36	-	-	94.93
	69.25	14.71	1.31	0.02	-	2.51	5.68	0.30	0.02	-	93.80
	67.97	14.43	1.01	0.02	-	3.87	6.07	0.26	-	-	93.63
	69.36	15.12	1.23	0.02	-	3.43	3.98	0.29	-	0.01	93.44
	67.95	14.51	1.24	-	-	4.17	5.97	0.28	0.02	0.04	94.18

Table 9 (cont'd.).

Field No.	SiO_2	Al_2O_3	FeO	MgO	CaO	Na_2O	K_2O	TiO_2	MnO	BaO	Total
CP3-2B (cont.)											
	68.26	14.65	1.21	-	-	4.35	5.78	0.28	0.03	0.03	94.59
	67.93	14.66	1.26	-	-	4.05	5.14	0.27	-	0.01	93.32
	67.65	14.74	1.26	0.04	0.01	4.27	6.01	0.32	-	-	94.30
	68.00	14.76	1.20	0.03	-	4.25	5.11	0.23	-	-	93.58
	66.74	14.62	1.27	-	-	4.21	5.84	0.22	0.02	-	92.92
	67.82	14.56	1.30	0.01	0.01	4.87	5.88	0.38	-	-	94.83
	67.56	14.76	1.26	0.01	-	3.24	5.88	0.33	0.06	0.03	93.13
	68.18	14.76	1.26	0.03	0.01	4.21	5.07	0.32	0.02	-	93.86
	67.41	14.49	1.34	0.02	0.02	3.62	6.36	0.34	0.04	0.06	93.70
	68.50	14.88	1.27	0.02	-	3.44	5.86	0.36	-	-	94.33
	68.25	14.86	1.27	0.04	0.01	4.60	5.97	0.37	-	0.02	95.39
CP3-1A											
	74.97	12.81	0.77	-	0.50	2.43	5.20	0.06	-	-	96.74
	75.15	12.92	0.78	0.03	0.49	2.32	4.98	-	-	0.07	96.74
	74.34	12.34	0.81	0.03	0.47	2.38	5.26	0.08	-	-	95.71
	74.43	12.80	0.73	0.03	0.41	2.32	5.15	0.11	-	-	95.98
	74.78	12.70	0.69	0.08	0.46	2.40	5.07	0.14	-	0.09	96.41
	75.72	12.64	0.80	0.04	0.43	2.38	5.22	0.13	-	0.06	97.42
	76.35	12.97	0.82	0.03	0.45	1.81	5.08	0.05	-	-	97.56
	75.84	12.45	0.81	0.04	0.49	2.32	5.07	0.06	-	-	97.08
	75.69	12.71	0.65	0.02	0.50	2.36	5.20	0.06	-	0.10	97.29
	73.14	12.75	0.82	0.03	0.50	2.45	5.03	0.07	-	-	94.79
	74.88	12.80	0.79	0.02	0.49	2.41	5.10	0.07	-	0.09	96.65

REFERENCES CITED

REFERENCES CITED

Abbey, S., Calibration standards, X-Ray Spectrometry, 7, 99-121, 1978.

Anderson, A. T., Oxidation of the La Blache Lake titaniferous magnetite deposit, Quebec, J. Geol., 76, 528-547, 1968.

Aramaki, S., and P. W. Lipman, Possible leaching of Na_2O during hydration of volcanic glasses, Japan Acad. Proc., 41, 467-470, 1965.

Bacon, C. R., Eruptive history of Mount Mazama and Crater Lake Caldera, Cascade Range, U.S.A., J. Volcanol. Geotherm. Res., 18, 57-115, 1983.

Bacon, C. R., R. Macdonald, R. L. Smith, and P. A. Baedecker, Pleistocene high-silica rhyolites of the Coso volcanic field, Inyo County, California, J. Geophys. Res., 86, 10223-10241, 1981.

Baker, B. H., and A. R. McBirney, Liquid fractionation. Part III: Geochemistry of zoned magmas and the compositional effects of liquid fractionation, J. Volcanol. Geotherm. Res., 24, 55-81, 1985.

Bence, A. E., and A. L. Albee, Empirical correction factors for the electron microanalyses of silicates and oxides, J. Geol., 76, 382-403, 1968.

Blake, S., Eruptions from zoned magma chambers, J. Geol. Soc. London, 138, 281-287, 1981.

Blake, S., and I. H. Campbell, The dynamics of magma-mixing during flow in volcanic conduits, Contrib. Mineral. Petrol., 94, 72-81, 1986.

Blake, S., and G. N. Ivey, Magma mixing and the dynamics of withdrawal from stratified reservoirs, J. Volcanol. Geotherm. Res., 27, 153-178, 1986.

Blake, S., and G. N. Ivey, Density and viscosity gradients in zoned magma chambers, and their influence on withdrawal dynamics, J. Volcanol. Geotherm. Res., 30, 201-230, 1986.

Broxton, D. E., D. Vaniman, F. Caporuscio, B. Arney, and G. Heiken, Detailed petrographic descriptions and microprobe data for drill holes USW-G2 and UE25b-1H, Yucca Mountain, Nevada, Rep. LA-9324-MS, 168 pp., Los Alamos Nat. Lab., Los Alamos, N. M., 1982.

Buddington, A. F., and D. H. Lindsley, Iron-titanium oxide minerals and synthetic equivalents, J. Petrol., 5, 310-357, 1964.

Byers, F. M., Jr., W. J. Carr, P. P. Orkild, W. D. Quinlivan, and K. A. Sargent, Volcanic suites and related cauldrons of Timber Mountain-Oasis Valley caldera complex, southern Nevada, U. S. Geol. Surv. Prof. Pap. 919, 70 pp., 1976.

Byers, F. M., Jr., P. P. Orkild, W. J. Carr, and W. D. Quinlivan, Timber Mountain Tuff, southern Nevada, and its relation to caldron subsidence, in Nevada Test Site, edited by E., B. Eckel, Mem. Geol. Soc. Am., 110, 87-97, 1968.

Campbell, I. H., and J. S. Turner, The influence of viscosity on fountains in magma chambers, J. Petrol., 27, 1-30, 1986.

Carmichael, I. S. E., The iron-titanium oxides of salic volcanic rocks and their associated ferromagnesian silicates, Contrib. Mineral. Petrol., 14, 36-64, 1967.

Chen, C. F., and J. S. Turner, Crystallization in a double-diffusive system, J. Geophys. Res., 85, 2573-2593, 1980.

Christiansen, R. L., P. W. Lipman, W. J. Carr, F. M. Byers, Jr., P. P. Orkild, and K. A. Sargent, Timber Mountain-Oasis Valley caldera complex of southern Nevada, Geol. Soc. Am. Bull., 88, 943-959, 1977.

Christiansen, R. L., P. W. Lipman, P. P. Orkild, and F. M. Byers, Jr., Structure of the Timber Mountain caldera, southern Nevada, and its relation to basin-range structure, U. S. Geol. Surv. Prof. Pap. 525-B, B43-B48, 1965.

Cox, K. G., J. D. Bell, and R. J. Pankhurst, The Interpretation of Igneous Rocks, 450 pp., George Allen & Unwin, London, 1979.

Crecraft, H. R., W. P. Nash, and S. H. Evans, Jr., Late Cenozoic volcanism at Twin Peaks, Utah; Part I: Geology and petrology, J. Geophys. Res., 86, 10303-10320, 1981.

Eichelberger, J. C., Vesiculation of mafic magma during replenishment of silicic magma reservoirs, Nature, 288, 446-450, 1980.

Ekren, E. B., C. L. Rogers, R. E. Anderson, and P. P. Orkild, Age of basin and range normal faults in Nevada Test Site and Nellis Air Force Range, Nevada, in Nevada Test Site, edited by E. B. Eckel, Mem. Geol. Soc. Am., 110, 247-250, 1968.

Flanagan, F. J., U. S. Geological Survey standards-II. First compilation of data for the new U. S. G. S. rocks, Geochim. Cosmochim. Acta, 33, 81-120, 1969.

Fridrich, C. J., and G. A. Mahood, Compositional layers in the zoned magma chamber of the Grizzley Peak Tuff, Geology, 15, 299-303, 1987.

Haggerty, S. E., Opaque mineral oxides in igneous rocks, in Oxide Minerals, edited by D. Rumble III, Mineral. Soc. Am. Short Course Notes, pp. Hg-101-300, 1976.

Haskin, L. A., M. A. Haskin, F. A. Frey, and T. R. Wildeman, Relative and absolute terrestrial abundances of the rare earths, in Origin and Distribution of the Elements, edited by L. H. Ahrens, pp. 889-912, Permagon Press, New York, 1968.

Hildreth, E. W., The magma chamber of the Bishop Tuff: Gradients in temperature, pressure, and composition, Ph.D. thesis, 328 pp., Univ. Calif., Berkely, 1977.

Hildreth, W., Gradients in silicic magma chambers: Implications for lithospheric magmatism, J. Geophys. Res., 86, 10153-10192, 1981.

Hildreth, W., The compositionally zoned eruption of 1912 in the Valley of Ten Thousand Smokes, Katmai National Park, Alaska, J. Volcanol. Geotherm. Res., 18, 1-56, 1984.

Huppert, H. E., and R. S. J. Sparks, The fluid dynamics of a basaltic magma chamber replenished by influx of hot dense ultrabasic magma, Contrib. Mineral. Petrol., 75, 279-289, 1980.

Huppert, H. E., and R. S. J. Sparks, Double-diffusive convection due to crystallization in magmas, Ann. Rev. Earth Planet. Sci., 12, 11-37, 1984.

Huppert, H. E., and J. S. Turner, A laboratory model of a replenished magma chamber, Earth Planet. Sci. Lett., 54, 144-152, 1981.

Huppert, H. E., R. S. J. Sparks, and J. S. Turner, Effects of volatiles on mixing in calc-alkaline magma systems, Nature, 297, 554-557, 1982a.

Huppert, H. E., J. S. Turner, and R. S. J. Sparks, Replenished magma chambers: Effects of compositional zonation and input rates, Earth Planet. Sci. Lett., 57, 345-357, 1982b.

Huppert, H. E., R. S. J. Sparks, and J. S. Turner, Some effects of viscosity on the dynamics of replenished magma chambers, J. Geophys. Res., 89, 6857-6877, 1984.

Kistler, R. W., Potassium-argon ages of volcanic rocks in Nye and Esmeralda Counties, Nevada, in Nevada Test Site, edited by E. B. Eckel, Mem. Geol. Soc. Am., 110, 251-263, 1968.

Lipman, P. W., Chemical comparison of glassy and crystalline volcanic rocks, U. S. Geol. Surv. Bull. 1201-D, 24 pp., 1965.

Lipman, P. W., Mineral and chemical variations within an ash-flow sheet from Aso caldera, southwestern Japan, Contrib. Mineral. Petrol., 16, 300-327, 1967.

Lipman, P. W., Iron-titanium oxide phenocrysts in compositionally zoned ash-flow sheets from southern Nevada, J. Geol., 79, 438-456, 1971.

Lipman, P. W., and I. Friedman, Interaction of meteoric water with magma: An oxygen-isotope study of ash-flow sheets from southern Nevada, Geol. Soc. Am. Bull., 86, 695-702, 1975.

Lipman, P. W., R. L. Christiansen, and J. T. O'Connor, A compositionally zoned ash-flow sheet in southern Nevada, U. S. Geol. Surv. Prof. Pap. 524-F, 47 pp., 1966.

Mahood, G. A., A summary of the geology and petrology of the Sierra La Primavera, Jalisco, Mexico, J. Geophys. Res., 86, 10137-10152, 1981

Marvin, R. F., F. M. Byers, Jr., H. H. Mehnert, P. P. Orkild, and T. W. Stern, Radiometric ages and stratigraphic sequence of volcanic and plutonic rocks, southern Nye and western Lincoln Counties, Nevada, Geol. Soc. Am. Bull., 81, 2657-2676, 1970.

McBirney, A. R., and R. M. Noyes, Crystallization and layering of the Skaergaard intrusion, J. Petrol., 20, 487-554, 1979.

McBirney, A. R., B. H. Baker, and R. H. Nilson, Liquid fractionation. Part I: Basic principles and experimental simulations, J. Volcanol. Geotherm. Res., 24, 1-24, 1985.

Noble, D. C., Ground-water leaching of sodium from quickly cooled volcanic rocks, (abstract), Am. Mineral., 50, 289, 1965.

Noble, D. C., Sodium, potassium, and ferrous iron contents of some secondarily hydrated natural silicic glasses, Am. Mineral., 52, 280-286, 1967.

Noble, D. C., and C. E. Hedge, Sr^{87}/Sr^{86} variations within individual ash-flow sheets, U. S. Geol. Surv. Prof. Pap. 650-C, 133-139, 1969.

Noble, D. C., J. C. Drake, and M. K. Whallon, Some preliminary observations on compositional variations within pumice- and scoria-flow deposits of Mount Mazama, Proc. Andesite Conf., State of Oregon Dept. Geol. Min. Ind., 157-164, 1969.

O'Connor, J. T., A classification for quartz-rich igneous rocks based on feldspar ratios, U. S. Geol. Surv. Prof. Pap. 525-B, B79-B86, 1965.

Rose, W. I., Jr., N. K. Grant, and J. Easter, Geochemistry of the Los Chocoyos Ash, Quezaltenango Valley, Guatamala, Geol. Soc. Am. Spec. Pap., 180, 87-99, 1979.

Rutherford, N. F., and R. F. Hemming, The volatile component of Quaternary ignimbrite magmas from the North Island, New Zealand, Contrib. Mineral. Petrol., 65, 401-411, 1978.

Schuraytz, B. C., T. A. Vogel, and L. W. Younker, Pumice heterogeneity in the Topopah Spring Member of the Paintbrush Tuff: Implications for ash-flow eruption dynamics (abstract), Eos Trans. AGU, 64, 896, 1983.

Schuraytz, B. C., T. A. Vogel, and L. W. Younker, Inflections in elemental and mineralogical gradients within the Topopah Spring Member of the Paintbrush Tuff: Evidence for the resolution of compositional and thermal properties across a magmatic interface, (abstract), Eos Trans. AGU, 66, 391, 1985.

Scott, R. B., F. M. Byers, Jr., and R. G. Warren, Evolution of magma below clustered calderas, southwest Nevada volcanic field (abstract), Eos Trans. AGU, 65, 1126-1127, 1984.

Smith, R. L., Ash flows, Geol. Soc. Am. Bull., 71, 795-842, 1960.

Smith, R. L., Ash-flow magmatism, Geol. Soc. Am. Spec. Pap., 180, 5-27, 1979.

Sparks, R. S. J., H. E. Huppert, and J. S. Turner, The fluid dynamics of evolving magma chambers, Phil. Trans. R. Soc. London, A 310, 511-534, 1984.

Spencer, K. J., and D. H. Lindsley, A solution model for coexisting iron-titanium oxides, Am. Mineral., 66, 1189-1201, 1981.

Spera, F. J., Simulations of magma withdrawal from crustal reservoirs (abstract), Eos Trans. AGU, 64, 876, 1983.

Spera, F. J., Some numerical experiments on the withdrawal of magma from crustal reservoirs, J. Geophys. Res., 89, 8222-8236, 1984.

Spera, F. J., D. A. Yuen, J. C. Greer, and G. Sewell, Dynamics of magma withdrawal from stratified magma chambers, Geology, 14, 723-726, 1986.

Stormer, J. C., Jr., The effects of recalculation on estimates of temperature and oxygen fugacity from analyses of multicomponent iron-titanium oxides, Am. Mineral., 68, 586-594, 1983.

Turner, J. S., and L. B. Gustafson, Fluid motions and compositional gradients produced by crystallization or melting at vertical boundaries, J. Volcanol. Geotherm. Res., 11, 93-125, 1981.

Turner, J. S., H. E. Huppert, and R. S. J. Sparks, An experimental investigation of volatile exsolution in evolving magma chambers, J. Volcanol. Geotherm. Res., 16, 263-277.

Vogel, T. A., F. J. Ryerson, D. C. Noble, and L. W. Younker, Limits to magma mixing based on chemistry and mineralogy of pumice fragments erupted from a chemically zoned magma body, J. Geol., 95, 659-670, 1987

Warren, R. G., F. M. Byers, Jr., and F. A. Caporuscio, Petrography and mineral chemistry of units of the Topopah Spring, Calico Hills, and Crater Flat tuffs, and older volcanic units, with emphasis on samples from drill hole USW G-1, Yucca Mountain, Nevada Test Site, Rep. LA-10003-MS, 78 pp., Los Alamos Nat. Lab., Los Alamos, N.M., 1984.

Weissberg, H. L., End correction for slow viscous flow through long tubes, Phys. Fluids, 5, 1033-1036, 1962.

Williams, H., Calderas and their origin, Univ. of California Publications in Geological Sciences, 25, 239-346, 1941.

Wohletz, K. H., T. R. Mcgetchin, M. T. Sanford II, and E. M. Jones, Hydrodynamic aspects of caldera-forming eruptions: Numerical models, J. Geophys. Res., 89, 8269-8285, 1984.

Wright, J. V., and G. P. L. Walker, The ignimbrite source problem: Significance of a co-ignimbrite lag-fall deposit, Geology, 5, 729-732, 1977.

MICHIGAN STATE UNIV. LIBRARIES
31293005363910